AD-A154 909 FIELD AND WIND TUNNEL TESTING ON NATURAL VENTILATION COOLING EFFECTS ON THREE NAVY BUILDINGS(U) NAVAL CIVIL ENGINEERING LAB PORT HUENEME CA S K ASHLEY DEC 84 1/2

UNCLASSIFIED NCEL-TR-912 F/G 13/1 NL

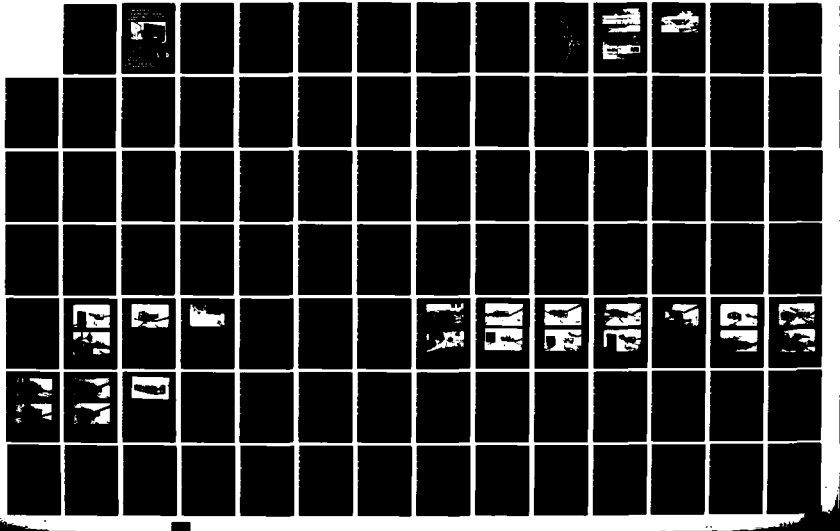

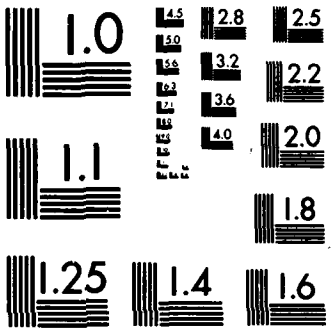

MICROCOPY RESOLUTION TEST CHART
NATIONAL BUREAU OF STANDARDS-1963-A

(2)

TECHNICAL REPORT R-912

Field and Wind Tunnel Testing on Natural Ventilation Cooling Effects on Three Navy Buildings

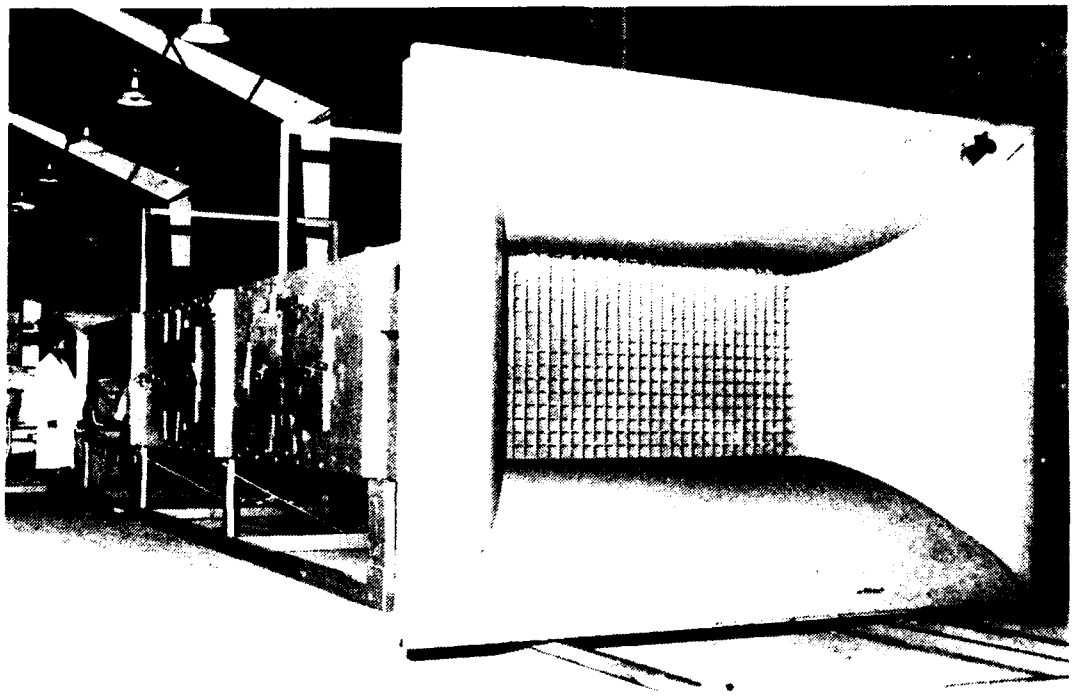

By Sophia K. Ashley

December 1984

Sponsored by
Chief of Naval Material
Washington, D.C. 20360

Naval Civil Engineering Laboratory
Port Hueneme, California 93043

METRIC CONVERSION FACTORS

Approximate Conversions to Metric Measures

Symbol	When You Know	Multiply by	To Find	Symbol
		LENGTH		
in	inches	*2.5	centimeters	cm
ft	feet	30	centimeters	cm
yd	yards	0.9	meters	m
mi	miles	1.6	kilometers	km
		AREA		
in^2	square inches	6.5	square centimeters	cm^2
ft^2	square feet	0.09	square meters	m^2
yd^2	square yards	0.8	square meters	m^2
mi^2	square miles	2.6	square kilometers	km^2
	acres	0.4	hectares	ha
		MASS (weight)		
oz	ounces	28	grams	g
lb	pounds	0.45	kilograms	kg
	short tons (2,000 lb)	0.9	tonnes	t
		VOLUME		
tsp	teaspoons	5	milliliters	ml
Tbsp	tablespoons	15	milliliters	ml
fl oz	fluid ounces	30	milliliters	ml
c	cups	0.24	liters	l
pt	pints	0.47	liters	l
qt	quarts	0.95	liters	l
gal	gallons	3.8	liters	l
ft^3	cubic feet	0.03	cubic meters	m^3
yd^3	cubic yards	0.76	cubic meters	m^3
		TEMPERATURE (exact)		
°F	Fahrenheit temperature	5/9 (after subtracting 32)	Celsius temperature	°C

*1 in = 2.54 (exactly). For other exact conversions and more detailed tables, see NBS Misc. Publ. 286, Units of Weights and Measures, Price $2.25, SD Catalog No. C13.10:286.

Approximate Conversions from Metric Measures

Symbol	When You Know	Multiply by	To Find	Symbol
		LENGTH		
mm	millimeters	0.04	inches	in
cm	centimeters	0.4	inches	in
m	meters	3.3	feet	ft
m	meters	1.1	yards	yd
km	kilometers	0.6	miles	mi
		AREA		
cm^2	square centimeters	0.16	square inches	in^2
m^2	square meters	1.2	square yards	yd^2
km^2	square kilometers	0.4	square miles	mi^2
ha	hectares (10,000 m^2)	2.5	acres	
		MASS (weight)		
g	grams	0.035	ounces	oz
kg	kilograms	2.2	pounds	lb
t	tonnes (1,000 kg)	1.1	short tons	
		VOLUME		
ml	milliliters	0.03	fluid ounces	fl oz
l	liters	2.1	pints	pt
l	liters	1.06	quarts	qt
l	liters	0.26	gallons	gal
m^3	cubic meters	35	cubic feet	ft^3
m^3	cubic meters	1.3	cubic yards	yd^3
		TEMPERATURE (exact)		
°C	Celsius temperature	9/5 (then add 32)	Fahrenheit temperature	°F

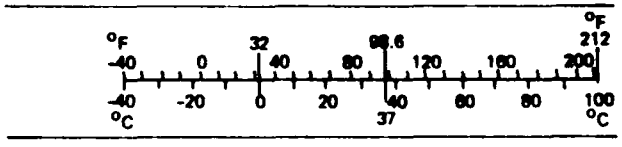

UNCLASSIFIED

SECURITY CLASSIFICATION OF THIS PAGE (When Data Entered)

REPORT DOCUMENTATION PAGE		READ INSTRUCTIONS BEFORE COMPLETING FORM
1 REPORT NUMBER TR-912	2 GOVT ACCESSION NO. DN987111 AD-A154 909	3 RECIPIENT'S CATALOG NUMBER
4 TITLE (and Subtitle) FIELD AND WIND TUNNEL TESTING ON NATURAL VENTILATION COOLING EFFECTS ON THREE NAVY BUILDINGS		5 TYPE OF REPORT & PERIOD COVERED Final; October 1982 - September 1983 6 PERFORMING ORG. REPORT NUMBER
7 AUTHOR(s) Sophia K. Ashley		8 CONTRACT OR GRANT NUMBER(s)
9 PERFORMING ORGANIZATION NAME AND ADDRESS NAVAL CIVIL ENGINEERING LABORATORY Port Hueneme, CA 93043		10 PROGRAM ELEMENT, PROJECT, TASK AREA & WORK UNIT NUMBERS SO829-01-132A 63724N
11 CONTROLLING OFFICE NAME AND ADDRESS Chief of Naval Material Washington, D.C. 20360		12 REPORT DATE December 1984 13 NUMBER OF PAGES 165
14 MONITORING AGENCY NAME & ADDRESS(if different from Controlling Office)		15 SECURITY CLASS. (of this report) Unclassified 15a DECLASSIFICATION DOWNGRADING SCHEDULE

16 DISTRIBUTION STATEMENT (of this Report)

Approved for public release; distribution is unlimited.

17 DISTRIBUTION STATEMENT (of the abstract entered in Block 20, if different from Report)

18 SUPPLEMENTARY NOTES

19 KEY WORDS (Continue on reverse side if necessary and identify by block number)

Natural ventilation, wind tunnel, scale models, humid climate, field measurements, comfort levels, computer model

20 ABSTRACT (Continue on reverse side if necessary and identify by block number)

Natural ventilation can reduce cooling loads and increase human comfort in buildings in hot, humid climates. Airflow rates are determined by wind pressure on the faces of buildings and the size of open areas. Wind pressures are calculated from the windspeed and the pressure coefficient. This report presents measurements of pressure coefficients of three buildings located at MCAS, Kaneohe Bay, Oahu, Hawaii, wind tunnel model tests, and comparisons of field tests, model tests, and existing data. This report establishes the validity of the NCEL

DD FORM 1 JAN 73 1473 EDITION OF 1 NOV 65 IS OBSOLETE

UNCLASSIFIED

SECURITY CLASSIFICATION OF THIS PAGE (When Data Entered)

20 Continued

computer model as an engineering tool to predict comfort levels within a building cooled by natural ventilation, and initiates a database of wind pressure coefficients for a variety of building forms. Keywords: Scale models, Human climates, Field measurements, Comfort levels

Library Card

Naval Civil Engineering Laboratory
FIELD AND WIND TUNNEL TESTING OF NATURAL VENTILATION COOLING EFFECTS ON THREE NAVY BUILDINGS (Final), by Sophia K. Ashley

TR-912 165 pp illus December 1984 Unclassified

1. Natural ventilation 2. Scale models I. SO829-01-132A

Natural ventilation can reduce cooling loads and increase human comfort in buildings in hot, humid climates. Airflow rates are determined by wind pressure on the faces of buildings and the size of open areas. Wind pressures are calculated from the windspeed and the pressure coefficient. This report presents measurements of pressure coefficients of three buildings located at MCAS, Kaneohe Bay, Oahu, Hawaii, wind tunnel model tests, and comparisons of field tests, model tests, and existing data. This report establishes the validity of the NCEL computer model as an engineering tool to predict comfort levels within a building cooled by natural ventilation, and initiates a database of wind pressure coefficients for a variety of building forms.

CONTENTS

INTRODUCTION

While Navy shore facilities have been able to reduce overall energy consumption in the past few years, electrical consumption and cost have increased.

In hot, humid climates the energy required to maintain an acceptably cool indoor environment can be a building's single largest energy cost. In many such climates cooling loads could be reduced or eliminated by using natural ventilation instead of mechanical cooling. Natural ventilation can replace mechanical cooling through two mechanisms: (1) air-flow rates through the building sweep away internal heat and moisture, bringing the indoor temperature and humidity closer to their outdoor counterparts, and (2) high indoor airspeed makes occupants feel cooler and more comfortable than they would in still air. Thus, there is a large potential for saving energy in climates where natural ventilation can be used.

If the concepts of natural ventilation are to be useful to the designer and/or architect, there must be some basic design tools that allow estimating the effects of natural ventilation. The development of these design tools requires field and laboratory measurements, as well as physical modeling. The most accurate method of measuring natural ventilation is to monitor an existing building; however, full-scale measurements can be both time consuming and costly. Accordingly, most wind-related design measurements are made on scale models in wind tunnels. As in any other kind of modeling, there is a need to make sure that the model behaves in the same manner as the real structure. Once the wind tunnel data has been confirmed, it can be used to predict the airflow and velocity distribution within the occupied space. This, in turn, leads to the calculation of the interior effective temperatures which is an indication of the thermal acceptability of the indoor environment and the usefulness of natural ventilation for that particular case.

This report presents the development and validation of a particular design tool used to estimate the effectiveness of natural ventilation in buildings in hot, humid climates. Full-scale tests were done at the Marine Corps Air Sation (MCAS) Kaneohe Bay, on the island of Oahu, Hawaii. This report compares wind tunnel data and full-scale field measurements for natural ventilation; establishes the validity of the NCEL computer model that can be used as an engineering tool to predict airflow rates and comfort levels within a building cooled by natural ventilation (by comparing it to full-scale measurements); and initiates a data base of wind pressure coefficients for a variety of building forms (to be used as input to NCEL's computer program).

FULL-SCALE MEASUREMENTS

Experimental Technique

The MCAS is an exposed site on the windward side of the island as seen in Figure 1; prevailing ENE winds are steady in the range of 3-6 m/s (6.7-13.4 mph) and usually within a narrow (20-degree) direction cone. During the period of this study, the outdoor temperature averaged approximately 25°C (77°F) with the extreme low about 20°C (68°F) and the extreme high about 30°C (86°F).

Three buildings were chosen (Figures 2, 3, and 4) for testing at MCAS during July 1982. The three buildings were a two-story visiting enlisted quarters (VEQ), a single-story duplex, and a two-story fourplex -- all with good wind exposure. Each building was tested 3 to 5 days. The tests included determining the exterior surface pressures on at least three sections of the windward and leeward faces and one section of the side face; pressures of accessible interior spaces were also measured. Windspeed and direction were measured with an on-site weather tower and the results were compared with those from the MCAS weather station. Interior and exterior dry bulb temperatures and relative humidities were also measured. From these measurements an estimate (or measurement) of the internal air velocity and effective temperatures was calculated and used as the comfort criterion.

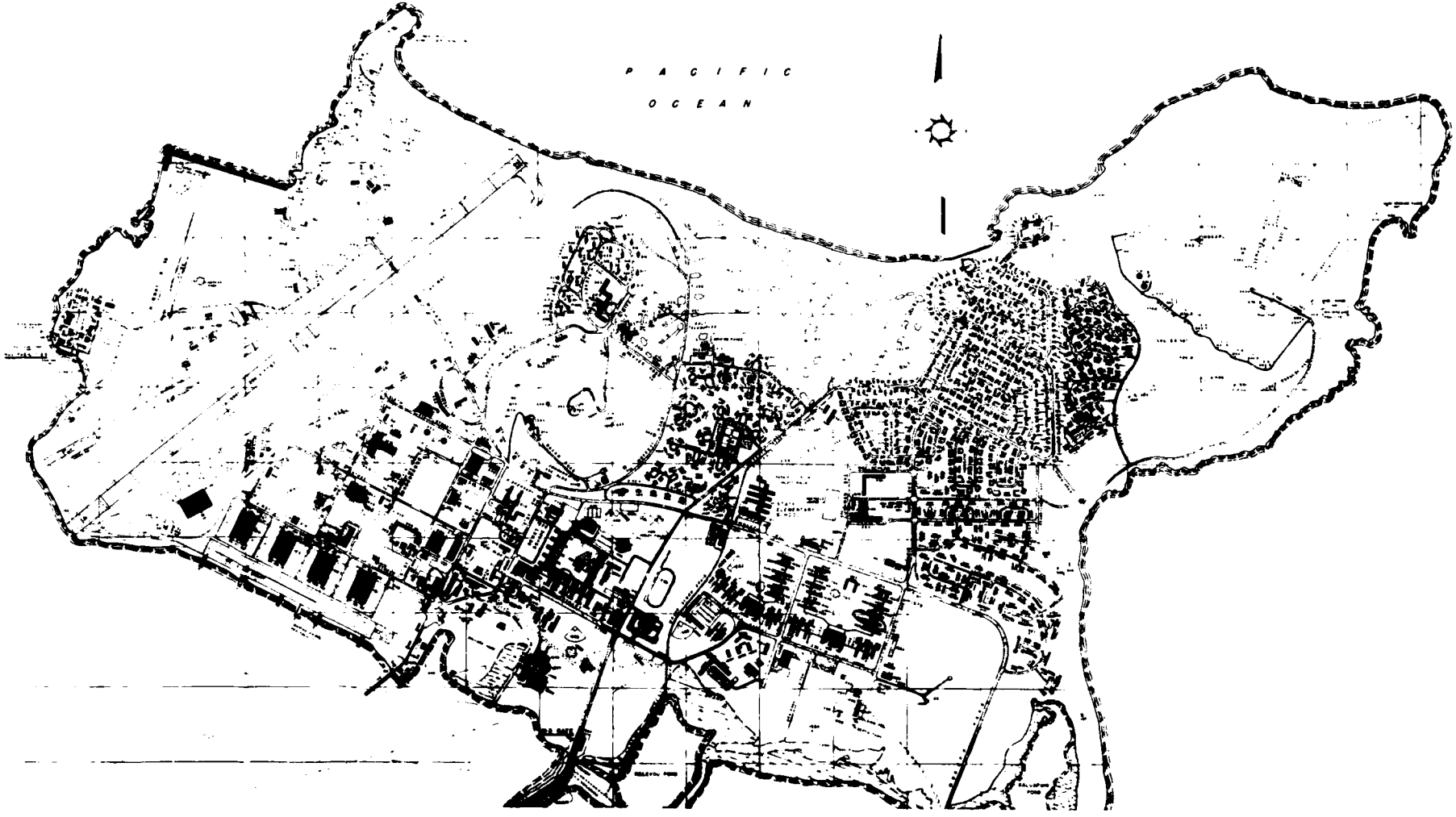

Figure 1. Marine Corps Air Station, Kaneohe Bay, Island of Oahu, Hawaii.

Figure 2. Test Building No. 1 - two-story VEQ.

Figure 3. Test Building No. 2 - single-story duplex.

Figure 4. Test Building No. 3 - two-story fourplex.

Frequent, time-series measurements of all relevant parameters were recorded in order for full-scale measurements to be useful for theoretical or wind-tunnel modeling. A microprocessor-based data acquistion system (Ref 1) was programmed to take frequent measurements and record half-hour averages and standard deviations. Data were stored on floppy disks for further analysis. This system has been used repeatedly in the mobile infiltration test unit (Ref 2), from which a great deal of information on infiltration, weather, and pressure correlations can be found (Ref 3 and 4). Individual components, as used in this project, are described in the following sections.

Pressure Measurements

The pressure measurements were done with six Validyne DP103 pressure transducers having a range of ±70 (0.28 inch of water) Pa full scale. The transducers were electronically connected to a demodulator box in the computer rack and the output voltages went directly to the

analog to a digital converter in the computer. The reference side of each Validyne measured the static pressure at the 6 meter height on the on-site weather tower.

The static pressure in the wind was measured using a static pressure probe that was designed, built, and calibrated by Dr. David Wilson from the Mechanical Engineering Department of the University of Alberta in Edmonton, Canada. The probe is relatively insensitive to horizontal wind direction, having a pressure coefficient of 0.07, and is insensitive to the vertical component of the wind within 10 degrees of the horizontal. It was possible to measure the external (and internal) building pressure coefficients as well as the outside/inside pressure differences with the static pressure probe.

The signal end of each pressure transducer was connected to a manifold of up to eight different pressure taps, which were located up to 300 feet from the transducers. Each pressure tap was a set of cross-shaped pipes that were tapped to the outside (or inside) of the building and connected to the manifold through a length of flexible tubing. (This tubing was covered in aluminum foil wherever it might be exposed to direct sunlight.) The tubing stopped at a solenoid valve connected to the manifold for each pressure transducer. The tap to be measured was selected by computer control of the solenoids; each connected tap was sampled repeatedly during each half-hour cycle and the results were stored individually. All six transducers and attendant solenoid valves were stored in one rack for easy transport and set-up.

Of the six transducers, three were used outside (levels 1, 2, 3) and three were used inside (levels 4, 5, 6).

Wind Measurements

Since pressure coefficients are the ratio of the absolute surface pressures to dynamic wind pressures, measuring the wind is very important. Windspeeds and directions at the sites were measured in two ways: (1) an on-site weather tower with weather heads at 10 meters (32.8 feet) and 7 meters (23 feet), and (2) weather information provided by the MCAS weather station. Each weather head, made by Weather Measure, measured

windspeed and direction relative to the building face. A weather tower was erected at each building and was aligned with the building face. The three test buildings were chosen because each front face had maximum exposure to the wind. Accordingly, the direction perpendicular to the front face of each building was designated as north and all directions are relative to that; the MCAS wind direction is relative to true north.

The static pressure probe was mounted at the 6 meter (19.7 feet) level to measure the static pressure in the wind. In addition to outdoor wind velocity, internal airspeed was measured for most of the time. An omni-directional velocity probe was used to measure the airspeed; its range is 0.05 to 2 m/s (9.84-393.7 fpm).

Psychrometric Measurements

Temperatures and humidities were measured for both the internal and external environment. Dry bulb temperatures were measured on the weather tower at 6.5 meters (21.3 feet), and air temperatures and relative humidity were measured at 2 meters (6.6 feet). Air temperatures and relative humidity were also measured at several locations throughout the interior of the test space. Daily measurements were made using a sling psychometer to measure dry bulb and wet bulb temperatures at all humidity measurement locations; these daily measurements served as a calibration for the humidity sensors. For comparison, dry bulb temperatures, dew point, and barometric pressures were recorded from the MCAS weather station.

Calibration

A full calibration of all sensors (i.e., pressure transducers, temperature probes, humidity sensors, and the computer) was done both before and after the test period. Quoted results were corrected for any change in the equipment calibration. The accuracies of the various sensors (calculated from the calibrations) are listed in Table 1. No measurement accuracies were supplied with the data from MCAS weather station.

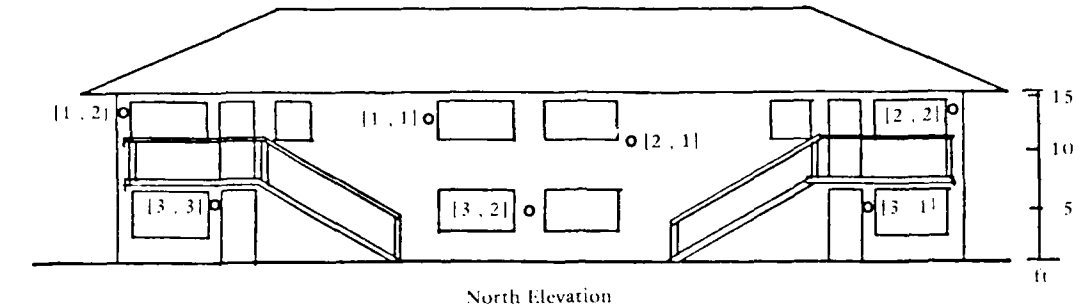

North Elevation
(Front)

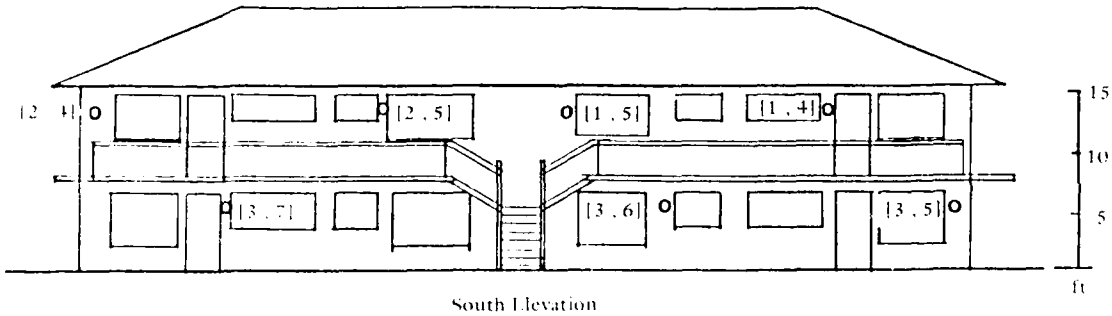

South Elevation
(Rear)

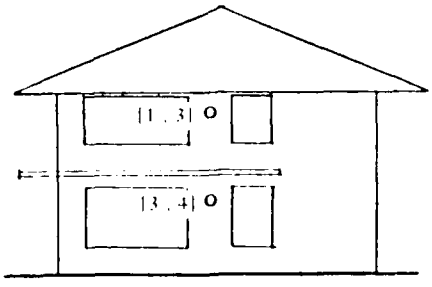

East Elevation

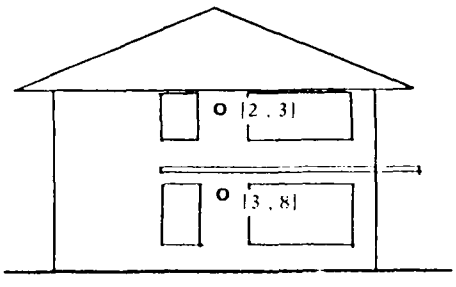

West Elevation

Figure 10. Elevation plan of Building No. 3 with the pressure taps locations shown.

Table 5. Data Log for Building No. 2

Date	Time	Windows	Comments
8 July	1930	---	Set up data taking systems
9 July	1130	Opened	Start data taking
9 July	1930	Closed	All pressures operational
10 July	1700	Closed	Air conditioner on
11 July	0830	Opened	Air conditioner off
11 July	2000	Closed	---
12 July	1100	Half opened	---
12 July	1930	Closed	---
13 July	0900	Half opened	---
13 July	1800	Closed	---
14 July	0830		End data taking

North is 68° east of true north.

Building No. 3 - Two-Story Fourplex. Building No. 3 was a two-story residence consisting of four units. Figures 10 and 11 are sketches of this building and include dimensions and the location of pressure taps over the surface of the building. The position of the computer and indoor climate measuring devices are also indicated. Table 6 shows the positions of the pressure taps and their numbers. The computer equipment was setup in the living room area of the upstairs east apartment. Initially, the internal temperature and airspeed were measured in the lanai (screen porch), both of which open into the living space. Each apartment had a lanai that had screen covers which should have been operable, but were not. Hence, during the measurements the screens on the lanais were loosely covered with cloth that served to keep the rain out, but allowed a fair amount of airflow through them.

Window schedule. Since the lower units were occupied by families, the status of these windows was not controlled and the internal pressure of these units was not measured. The windows configurations of the two test units are listed in Table 6.

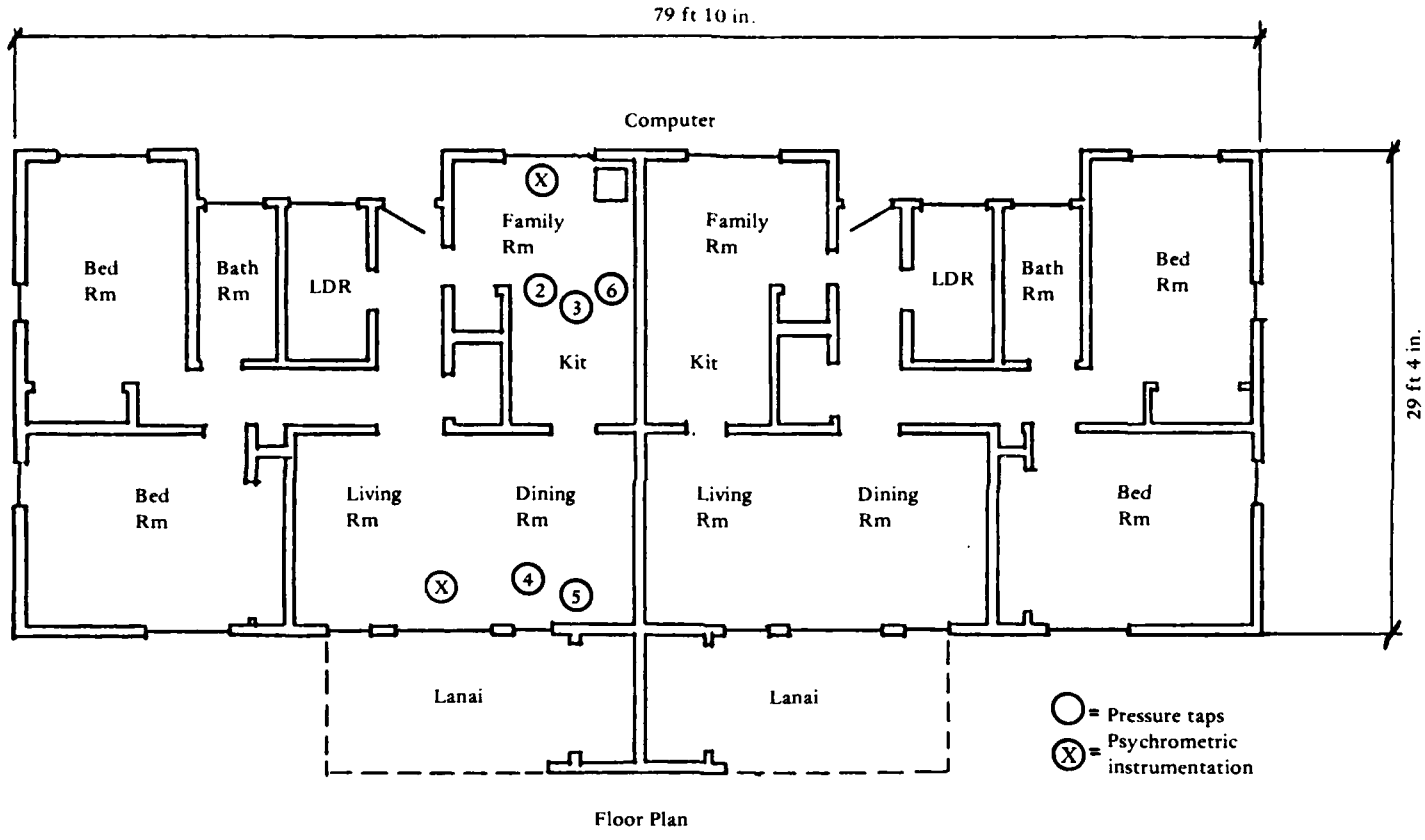

Figure 9. Floor plan of Building No. 2.

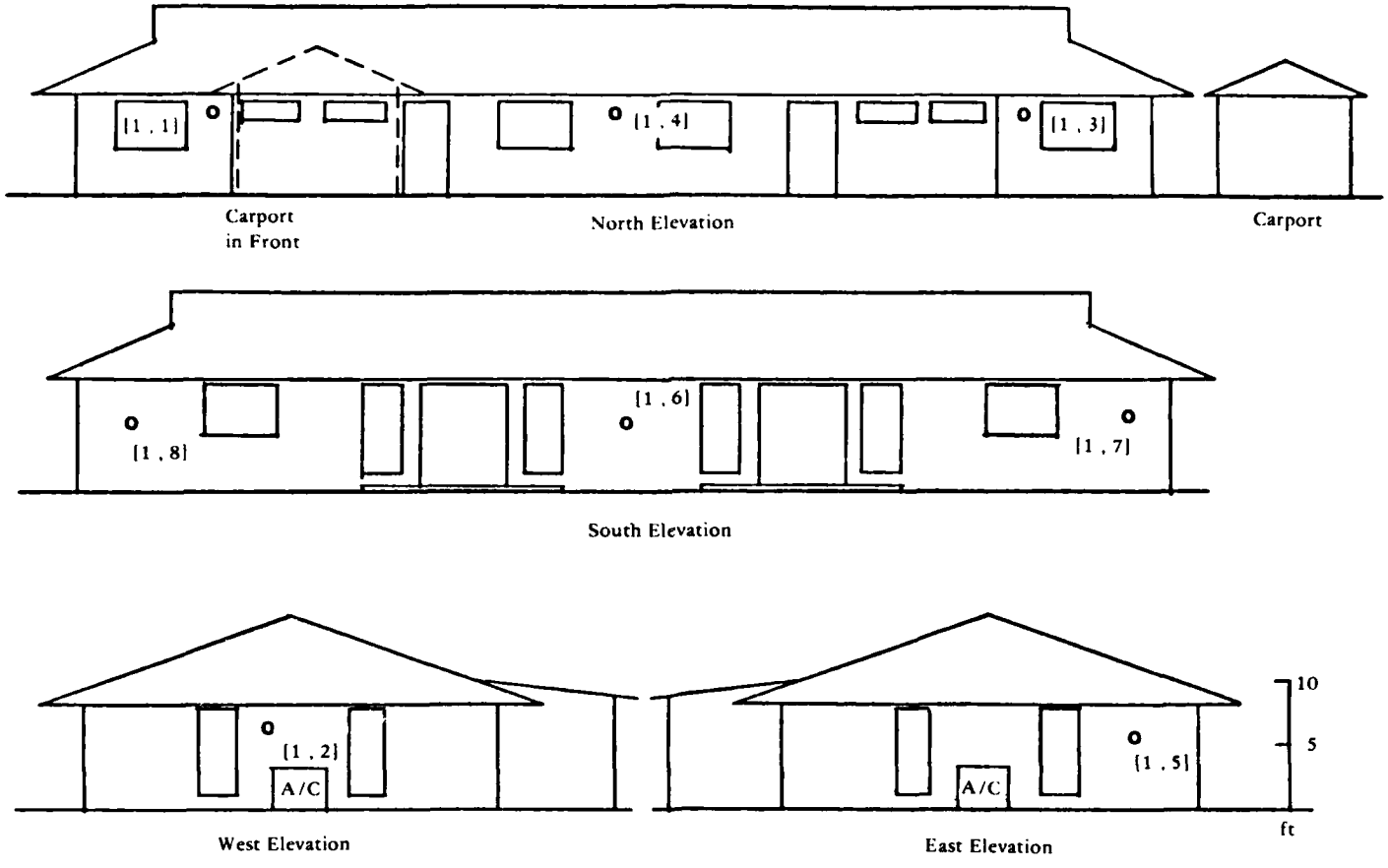

Figure 8. Elevation plan of Building No. 2 with the pressure taps locations shown.

computer equipment was setup in the kitchen/dining area and the internal pressure, temperature, and internal air velocity were measured in the central living room area.

Table 4. Location of Pressure Taps and Window Configuration of Building No. 2

Tap No.	Pressure Taps Location	Window Area, Full open (m^2)
1,1	North face east side	1.27
1,2	West face	1.51
1,3	North face west side	1.27
1,4	North face center	0.91
1,5	East face	1.51
1,6	South face center	1.05
1,7	South face east side	1.11
1,8	South face west side	1.11

Transducer 1: Exterior[a]
Transducer 2: Computer room (kitchen)
Transducer 3: Computer room (kitchen)
Transducer 4: Central space (living room)
Transducer 5: Central space (living room)
Transducer 6: Computer room (kitchen)

[a]X = 15% for open windows; X = 1% for closed windows.

Window schedule. Although the unit adjacent to the test unit was occupied by a family, and the status of the windows was not controlled; it was assumed that the windows were closed since the air conditioner was in operation most of the time. The internal pressure of that unit, furthermore, was not measured. The window configuration of the test unit is shown in the Table 5.

The air conditioner was operated in the test apartment from 1700 on 10 July to 0830 on 11 July and its operation effected both the internal and external pressures as measured by the nearby pressure tap.

Occupancy schedule. The test apartment was unoccupied except when the window configuration was changed.

Window schedule. Because of irregular occupancy on the first floor, the windows on that floor were opened and closed at irregular intervals, but were always closed at night for security reasons. The windows on the second floor were controlled and set according to the schedule presented in Table 3.

Table 3. Data Log for Building No. 1

Date	Time	Windows	Comments
1 July	1530	---	Set up data taking systems
4 July	1700	Closed	All systems functioning
5 July	0100	Closed	Weather tower down (approx.)
6 July	0930	Opened	Began using single weather head
7 July	1030	Half opened	---
8 July	0900	---	End data taking

North is 19° east of true north.

Occupancy schedule. The building was, in general, unoccupied from 1700 on 3 July on. There were a few officers and instructors, in addition to the testing team going in and out of the building at unscheduled times. For the most part these unscheduled entrances were in the eastern part of both floors. The testing team's occupancy schedule was:

Time	Date
1300 - 1700	4 July
0900 - 1030	6 July
1000 - 1030	7 July

Building No.2 - Single-Story Duplex. Building No. 2 was a single-story residence consisting of two mirror image units. Figures 8 and 9 are sketches of this building and include dimensions and the location of pressure taps over the surface of the building. The position of the computer and indooor climate measuring devices are also indicated. Table 4 shows the positions of the pressure taps and their numbers. The

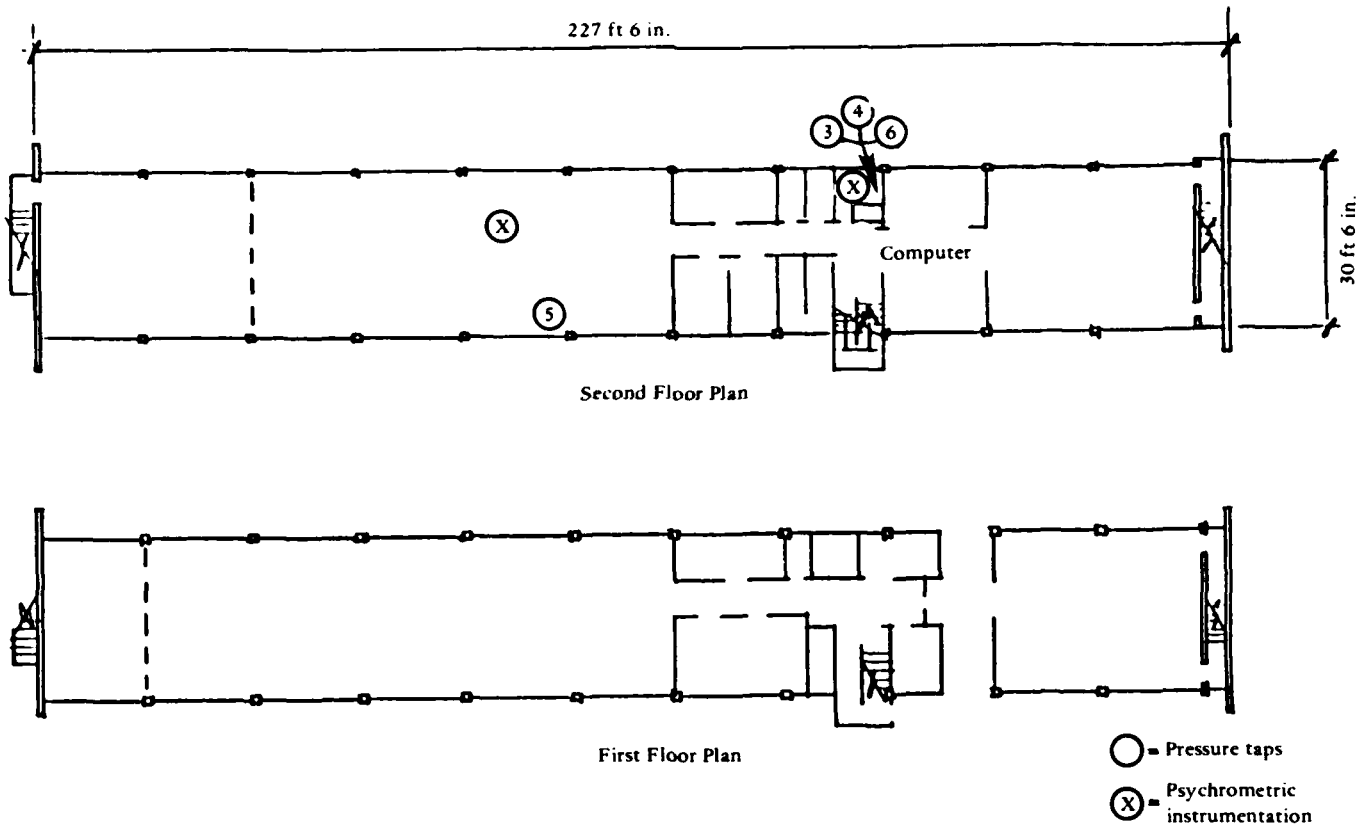

Figure 7. Floor plan of Building No. 1.

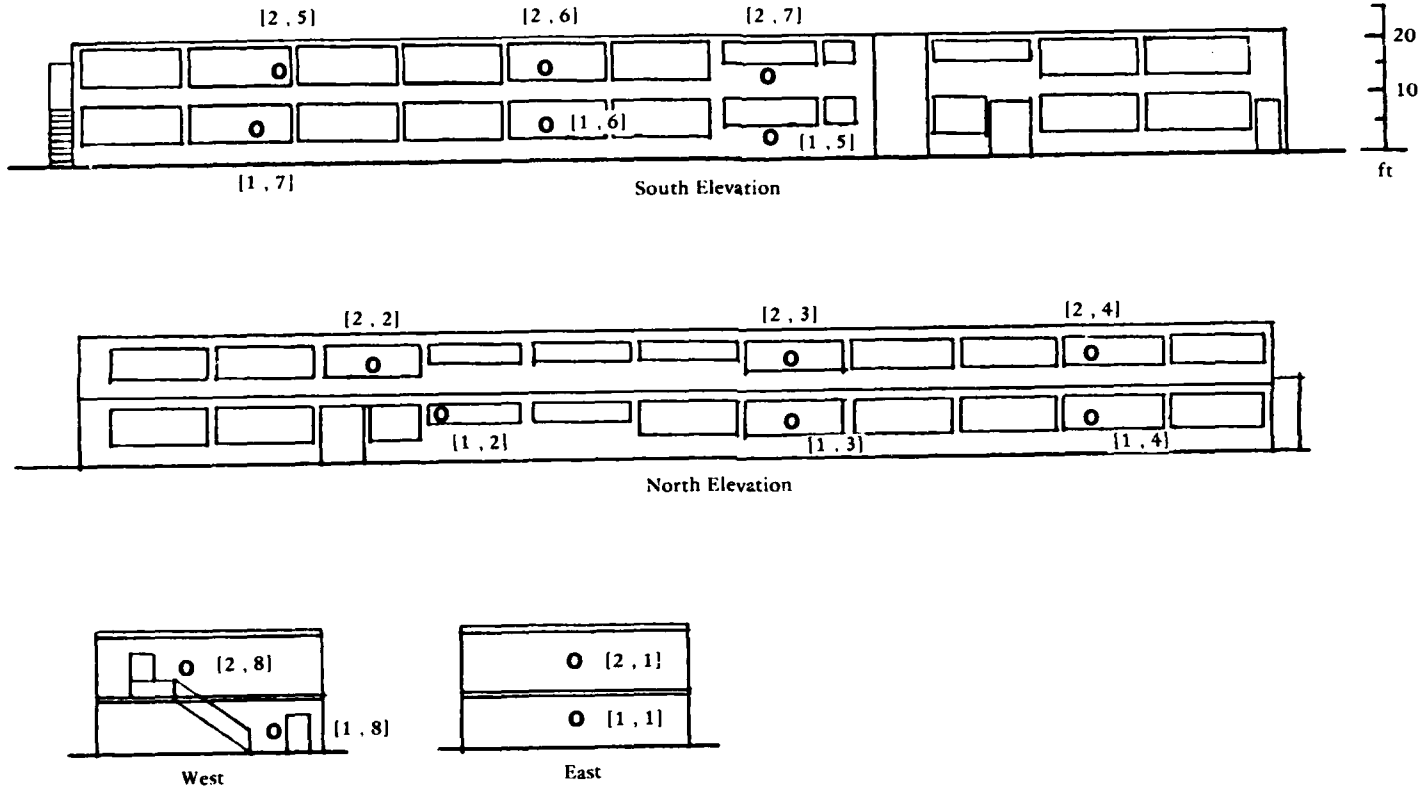

Figure 6. Elevation plan of Building No. 1 with the pressure taps locations shown.

Building No.1. Building No. 1 was a large two-story building used for the training and billeting of enlisted men. Figures 6 and 7 are sketches of this building and include dimensions and the location of pressure taps on the surface of the building. The position of the computer and indoor climate measuring devices are also indicated. Table 2 shows the positions of the pressure taps and their numbers. The equipment was setup on the second floor. Since there was no access to the inside of the first floor space, all differential pressures are relative to the second floor. Pressure transducers 3, 4, and 6 measured the pressure in the computer room, while transducer 5 measured the central area of the second floor.

Table 2. Location of Pressure Taps and Window Configuration of Building No. 1

Tap No.	Pressure Taps Location	Window Area, Full open (m^2)
1,1	East face	---[a]
1,2	North face east side	---
1,3	North face center	---
1,4	North face west side	---
1,5	South face west side	---
1,6	South face center	---
1,7	South face east side	---
1,8	West face	---
2,1	East face	0
2,2	North face east side	1.02
2,3	North face center	3.74
2,4	North face west side	4.08
2,5	South face west side	4.08
2,6	South face center	3.40
2,7	South face east side	1.36
2,8	West face	0

Transducer 1: First Floor
Transducer 2: Second Floor[b]
Transducer 3: Computer room
Transducer 4: Computer room
Transducer 5: Second floor central area
Transducer 6: Computer room

[a]Windows were opened and closed on an irregular basis but were closed at night for security reasons.
[b]X = 9.0% with open windows; X = 0.1% with closed windows.

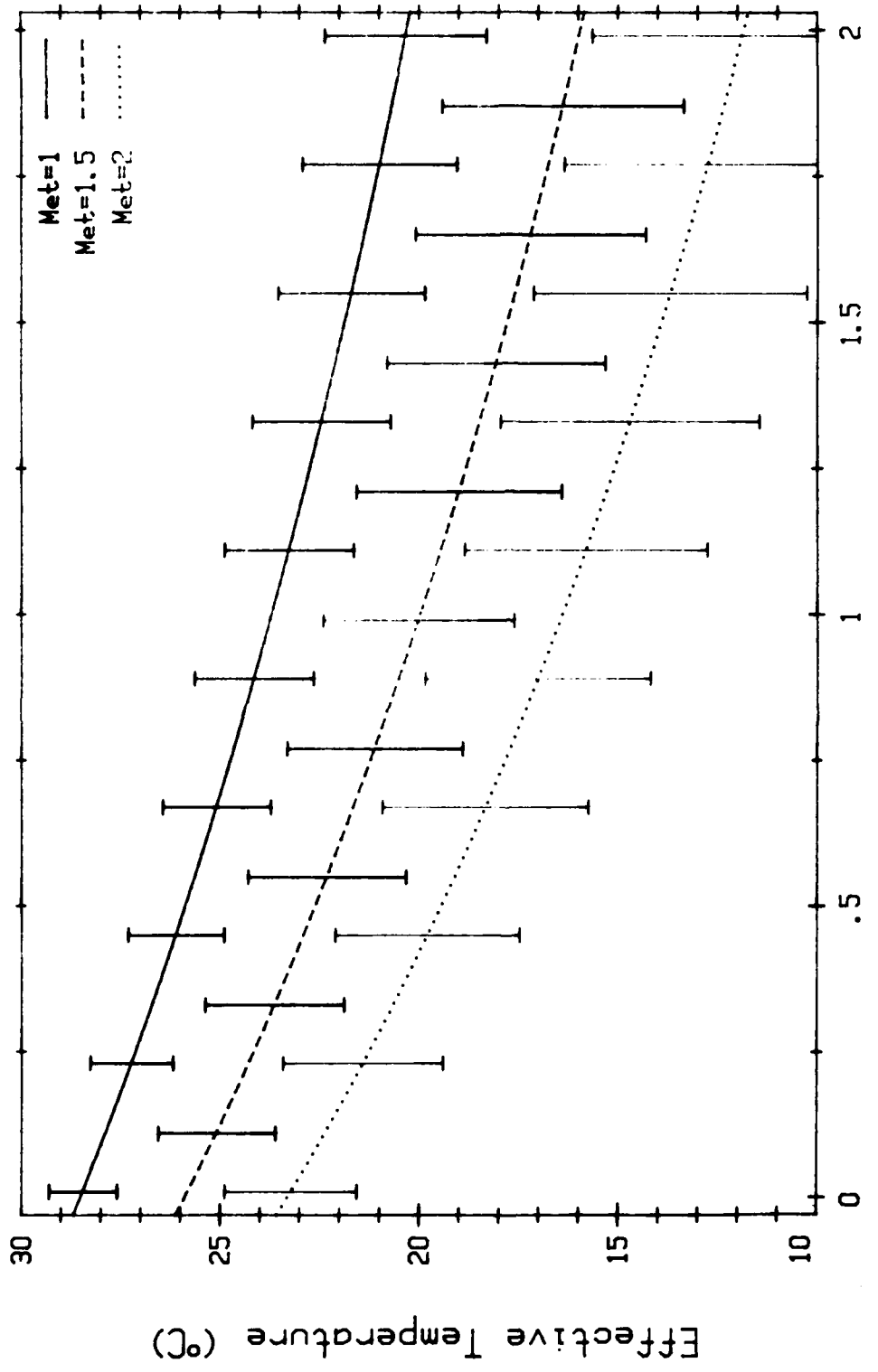

Figure 5. Acceptable values of effective temperatures (comfort temperatures).

The definition of the coefficients A, B, C, and D are given in Appendix A. The coefficients are functions of airspeed and the personal variables.

The effective temperature depends on the four environmental parameters: air temperature, mean radiant temperature, dew point, and windspeed, as well as the two personal parameters: clothing insulation levels and metabolic rate. All of the effective temperatures calculated from the field data use this definition for effective temperature.

The effective temperature alone does not indicate whether most individuals will find the conditions comfortable. In order to decide this, the comfort temperature range must be defined. Figure 5 displays the acceptable values of the effective temperature (i.e., the comfort temperature) for different combinations of personal variables. The formula for this comfort temperature as well as the acceptable range of effective temperature is also given in Appendix A.

Dry bulb and globe (mean radiant) temperatures were not always simultaneously measured. Because the inside-outside temperature difference was small and there was little direct sun on the wall surfaces, it was assumed that the internal mean radiant temperature was equal to the air temperature and, therefore, the dry bulb and globe temperatures are interchangeable. Dew point was not directly measured, but the relative humidity was measured. The standard psychrometric formulas (Ref 13) were used to convert the humidity from one form to another (e.g., dew point, relative humidity, wet bulb, etc.).

Building Descriptions

The recorded data contain all the information measured and calculated as described in the previous section. However, in order to use it for modeling purposes, a more detailed description of each building, including pressure tap configuration, open (window) area, occupancy schedule, etc., is needed. The following sections contain this information as well as any unusual happenings during the experimental runs.

Ideally, the infiltration, Q_+, and the exfiltration, Q_-, should balance; but, because of experimental uncertainties in the pressure measurements they are unlikely to. Previous studies (Ref 9) have shown that a small error in the internal pressure measurement can cause a large disagreement between infiltration and exfiltration. The best solution is to adjust the internal pressure (within experimental uncertainty) to minimize the difference between the two flows. Lacking this, a simple average of the two (unbalanced) flow rates is used. The LBL model does not use measured pressures or pressure coefficients but rather it internally estimates the pressures from the windspeed and terrain around the structure. Both estimates of the filtrations are presented in the data.

In order to estimate the usefulness of increasing interior airspeed and total ventilation, a simplified version of a comfort model (Ref 11 and 12) as the criterion for acceptable comfort was used. The concept of effective temperature was used to indicate the comfort level of the occupants. The effective temperature corrects the air temperature for the effects of radiant temperature, humidity, and air movement; as such it reflects any change in environmental conditions, including the increase in air exchange that natural ventilation causes.

In order to define a single variable, T_{eff}, as the comfort variable, a set of standard conditions was defined for the other environmental parameters. Under these standard conditions the effective temperature became equal to the air temperature. The standard conditions were low airspeed, air, and mean radiant temperature equal to the effective temperature and a standardized dew point.

The effective temperature is defined as follows:

$$T_{eff} = A + B\,T_r + C\,T_a + D\,T_d^2 \qquad (5)$$

where: T_{eff} = effective temperature, °C

T_r = mean radiant temperature, °C

T_a = ambient air temperature, °C

T_d = dew point temperature, °C

cross-section to determine the mean windspeed; this method is difficult because it is hard to determine the appropriate cross-section. An experimental relationship given in Reference 7 that relates the average indoor airspeed to the outdoor windspeed as a function of open area (the relationship assumes approximately equal windward and leeward openings with a square floor plan and no partitions) was used for the field test data analysis:

$$\bar{v} = 0.45 \left[1 - e^{-3.84X} \right] U_R \qquad (2)$$

where: $\bar{v}$ = mean internal airspeed, m/s

X = ratio of window area to wall area

U_R = windspeed at site at roof level, m/s

The airflow rate was estimated in two ways: (1) combining open areas and pressure coefficients with the windspeed, and (2) using the LBL infiltration model (Ref 6, 7 and 8). To use the open areas and pressure coefficients method, the orifice velocity of each opening was multiplied by its effective leakage area and the infiltration and exfiltration were totaled separately.

$$Q_+ = \sum_+ A_+ v_+ \qquad (3)$$

$$Q_- = \sum_- A_- v_- \qquad (4)$$

where: $Q_{+/-}$ = infiltration/exfiltration, m^3/s

$A_{+/-}$ = effective leakage area, m^2

$v_{+/-}$ = positive/negative orifice velocity, m/s

To estimate the leakage of the buildings with closed windows, a specific leakage of 4 cm^2/m^2 (i.e., 4 cm^2 for every m^2 of floor area) was used. To estimate the leakage with open windows, the open area was used and multiplied by an appropriate discharge coefficient (0.6 in most cases) (Ref 9 and 10).

Table 1. Sensor Accuracy

Sensor	Type	Units	Accuracy
Pressure	Differential	Pascals	0.5
Wind direction	Vane	deg LBL	1.0
Windspeed	Anemometer	m/s	0.1
Int. airspeed	Hot wire	m/s	0.02
Temperature	Globe	°C	0.5
Humidity	Relative	%	12.0

Data Reduction

Many of the quantities of interest for natural ventilation are derived ones: infiltration, dew point, mean internal airspeed, effective temperature, and comfort levels; and all of them can be derived or estimated from the measured data. There are several methods of estimating the mean interior airspeed. The most straightforward method is to use the spot measurement made by the airspeed probe; unfortunately there is no way of knowing whether a single probe is representative of the average windspeed in the space. Making the assumption that the occupants are seated directly in front of an open window, the orifice velocity of the window is used as the required airspeed (Ref 5 and 6).

$$v_o = \sqrt{\frac{2}{\rho} \Delta P} \qquad (1)$$

where: v_o = orifice velocity, m/s

ρ = density of air, 1.2 kg/m^3

ΔP = pressure drop across the window, Pa

But, this is not useful for finding the average effective temperature in the entire space. Another method that is used in the NCEL computer model is to estimate the airflow rate and divide it by an appropriate

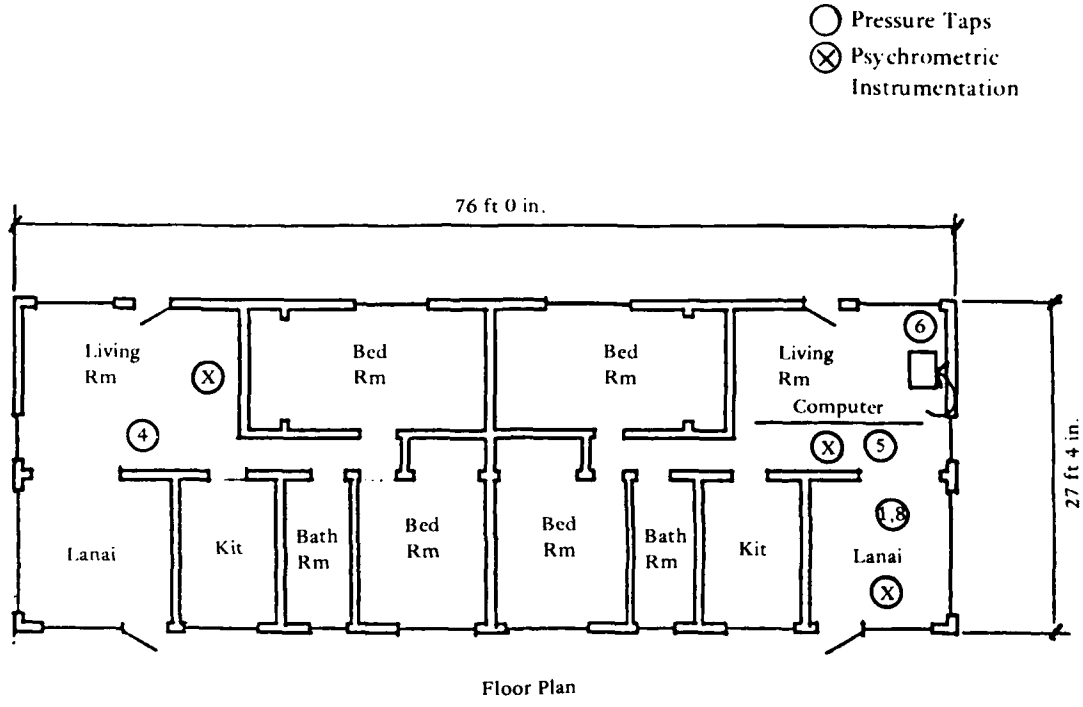

Figure 11. Upstairs floor plan of Building No. 3.

Table 6. Location of Pressure Taps and Window Configuration of Building No. 3

Tap No.	Pressure Taps Location	Window Area, Full open (m^2)
1,1	North face west side	1.95
1,2	North face east side	1.21
1,3	East face[a]	1.43/0.56[b]
1,4	South face east side[a]	1.95/1.34
1,5	South face west side	1.38
1,8	Lanai	0.02
2,1	North face east side	1.95
2,2	North face west side	1.21
2,3	West face[a]	1.43
2,4	South face west side[a]	1.95
2,5	South face east side	1.38
3,1	North face west side	---
3,2	North face center	---
3,3	North face east side	---
3,4	East face	---
3,5	South face east side	---
3,6	South face center	---
3,7	South face west side	---
3,8	West face	---

Transducer 1: East Apt[c] Upstairs Exterior
Transducer 2: West Apt[c] Upstairs Exterior
Transducer 3: Downstairs Exterior
Transducer 4: Internal Upstairs East Apartment (central area)
Transducer 5: Internal Upstairs West Apartment (central area)
Transducer 6: Internal Upstairs West Apartment (near equipment)

[a]The lanai windows had a discharge coefficient of 0.25.

[b]The numbers after the "/" refer to the lanai isolated configuration.

[c]X = 9.9%/16.2% with open windows; X = 3.7%/.05% with closed windows.

Sometime during the night of 15 July to 16 July taps 1,1; 1,4; 1,5; 2,1; and 3,1 fell during a rain storm. The taps were repaired and replaced on 16 July and did not fall again. On 18 July the lanai in the

east upstairs apartment (the one with the computer) was isolated from the living space by closing all connecting doors. At that time the internal temperature and windspeed sensors were moved from the lanai to the central living space, and an additional pressure tap 1,8 was installed in the lanai to record the internal pressure.

Occupancy schedule. Since the apartments were occupied, the downstairs apartments were not monitored for occupancy or window configuration. The upstairs west apartment was occupied only at the times indicated in Table 7. In addition to those times, the occupants of the upstairs east apartment were in the building as follows:

Time	Date
2100 - 2130	15 July
2000 - 2030	17 July
0700 - 0715	19 July
1830 - 1900	20 July
2330 - 2400	20 July
0001 - 0640	21 July

Table 7. Data Log for Building No. 3

Date	Time	East Windows	West Windows	Comments
15 July	1300	---	---	Set up data taking systems
15 July	1700	Closed	Closed	Started taking data
16 July	0930	Opened	Opened	Repaired fallen taps
16 July	2000	Closed	Closed	---
18 July	0800	Half opened	Half opened	Isolated east lanai
18 July	2000	Closed	Closed	---
19 July	1000	Opened	Half	---
19 July	2130	Closed	Closed	---
20 July	0800	Closed	Opened	---
21 July	0900	---	---	End data taking

North is 57° east of true north.

Field Test Results

The data from these tests were recorded on over 700 pages. Each page represents a particular half-hour set of data from one of the three buildings. On each page are the averages and standard deviations (indicated by parentheses) of the following measured quantities: differential pressure and pressure coefficient for each pressure tap; mean radiant temperature and relative humidity for the active temperature/humidity probes; windspeed and direction from the on-site weather tower, as well as the MCAS weather station; and internal air velocity as measured by the omni-directional probe. Several quantities derived from measured data were also displayed for each half-hour: dew point, estimated internal airspeed, effective temperature, wind-driven exfiltration and infiltration, and total infiltration as estimated from the LBL model.

At scattered times throughout the data some of the sensors (temperature, humidity, windspeed, or pressure) were not working or not working correctly. This was handled in one of two ways: (1) if only a few sensors gave bad readings, the data was included, but the bad measurements were marked; (2) if a large portion of the data (e.g., all of the pressures or all of the weather, etc.) was bad, the data were eliminated. The first method was used on the temperature and humidity sensors that were outside. On occasion rain would get into the sensors and caused them to give faulty readings until they dried out. Faulty temperature and humidity readings are indicated by a negative value. Faulty (off-scale) pressure measurements are indicated by an asterisk, "*", next to the entry. Some readings were suspicious but possible readings; these were indicated by negative standard deviations. Due to start-up delays and the weather tower crash, most of the data prior to 5 July were bad and were eliminated.

Figures 12, 13 and 14 are samples of the output data, one half-hour of data for Buildings 1, 2, and 3, respectively. The data are available on magnetic tape and include data taken on the following dates:

Building No.	Dates
1	5 - 8 July
2	9 - 14 July
3	15 - 21 July

The exact environmental conditions during the test, the calculated surface pressure coefficients, the estimated airflow rates, and the estimated and measured interior airspeed were plotted for all the buildings. Figure 15a, b, and c show the windspeeds and directions; Figures 16a, b, c, and d show the indoor and outdoor air temperatures; Figures 17a, b, and c show the indoor and outdoor dew points; Figures 18a, b, c, and d show the estimated airflow rates; Figures 19a and b, show the measured and estimated interior airspeeds; and Figures 20a, b, and c show calculated effective temperatures. Field test pressure coefficients for all the buildings are given in Appendix B.

NCEL WIND TUNNEL TESTS

Wind Tunnel Configuration

The wind engineering study was performed in the NCEL boundary layer wind tunnel, which is partially shown in Figure 21. The wind tunnel is an open circuit facility driven by a 45-horsepower vaneaxial propeller, with a test cross-sectional area of 0.762 by 1.524 meters (2.5 by 5 feet) (test section height and width) and a 7.315 meter (24-foot) length. The free stream velocity in the wind tunnel ranges from 3.5 to 20 m/s (11.48-65.62 f/s). The general characteristics of the wind tunnel are shown in Figure 22.

BUILDING 1

TIME = 14.07 DATE = 07/07

TAP	PRESSURE (PA) DIFFERENCE	PRESSURE COEFFICIENT	TAP	PRESSURE (PA) DIFFERENCE	PRESSURE COEFFICIENT
1 , 1	11.35 (5.50)	2.70 (1.51)	4 , 1	1.88 (4.70)	0.27 (0.27)
1 , 2	5.41 (2.02)	1.28 (0.68)	4 , 2		
1 , 3	3.25 (1.70)	0.75 (0.50)	4 , 3		
1 , 4	3.07 (1.67)	0.67 (0.43)	4 , 4		
1 , 5	1.64 (1.41)	0.36 (0.33)	4 , 5		
1 , 6	1.57 (1.54)	0.37 (0.37)	4 , 6		
1 , 7	0.00 (1.44)	-0.02 (0.37)	4 , 7		
1 , 8	-1.49 (1.36)	-0.38 (0.38)	4 , 8		
2 , 1	11.48 (5.85)	2.76 (1.57)	5 , 1	1.11 (5.26)	0.32 (0.27)
2 , 2	5.47 (2.47)	1.30 (0.78)	5 , 2		
2 , 3	3.29 (1.94)	0.76 (0.58)	5 , 3		
2 , 4	3.08 (1.81)	0.70 (0.53)	5 , 4		
2 , 5	0.59 (1.41)	0.11 (0.32)	5 , 5		
2 , 6	-0.16 (1.57)	-0.05 (0.37)	5 , 6		
2 , 7	-1.04 (1.52)	-0.27 (0.38)	5 , 7		
2 , 8	-2.39 (1.29)	-0.61 (0.38)	5 , 8		
3 , 1	4.38 (2.60)	1.03 (0.76)	6 , 1	0.07 (0.18)	1.00 (0.75)
3 , 2			6 , 2		
3 , 3			6 , 3		
3 , 4			6 , 4		
3 , 5			6 , 5		
3 , 6			6 , 6		
3 , 7			6 , 7		
3 , 8			6 , 8		

WIND DATA

	VELOCITY (M/S)		DIRECTION (DEG)	
LBL	3.5	(0.7)	8	(2)
MCAS	2.5		8	

LOCATION	AIR TEMPERATURE (C)		DEW POINT	RELATIVE HUMIDITY (%)		EFFECTIVE TEMPERATURE (C)
2 COMPUTER ROOM	29.9	(0.7)	22.3	64	(1.1)	27.0
0 20 METERS NORTH	30.7	(1.4)	-1.0	-1	(19.5)	-1.0
2 DORM ROOM	29.1	(1.6)	22.2	66	(0.8)	26.4
0 WEATHER TOWER	-1.0	(-.9)	-1.0	78	(0.7)	-1.0
2 COMPUTER ROOM	29.4	(1.5)				
MCAS	23.3		21.8	91		22.5

ESTIMATED INSIDE AIR VELOCITY (M/S)

LOCATION	CALCULATED	ORIFICE
SECOND FLOOR	0.25	2.18

ESTIMATED NATURAL VENTILATION RATES (M^3/HR)

LOCATION	INTO BUILDING	OUT OF BUILDING	LBL INFILTRATION
SECOND FLOOR	38065	31340	32408

BAROMETRIC PRESSURE (KPA)

MCAS	101.43

Figure 12. Data sample from Building No. 1.

TIME = 2.82 DATE = 07/11

TAP	PRESSURE (PA) DIFFERENCE	PRESSURE COEFFICIENT	TAP	PRESSURE (PA) DIFFERENCE	PRESSURE COEFFICIENT
1 , 1	1.57 (1.60)	0.62 (0.69)	4 , 1	0.57 (1.46)	0.42 (0.41)
1 , 2	0.56 (1.22)	0.28 (0.66)	4 , 2	-0.55 (0.87)	0.50 (0.59)
1 , 3	2.35 (1.48)	1.18 (1.66)	4 , 3	1.33 (1.22)	0.49 (0.73)
1 , 4	3.21 (1.95)	1.40 (1.22)	4 , 4	2.26 (1.54)	0.40 (0.51)
1 , 5	-0.49 (1.03)	-0.21 (0.49)	4 , 5	-1.51 (1.07)	0.40 (0.42)
1 , 6	0.18 (0.95)	0.05 (0.43)	4 , 6	-0.80 (0.80)	0.39 (0.41)
1 , 7	0.41 (0.89)	0.13 (0.48)	4 , 7	-0.53 (0.67)	0.38 (0.45)
1 , 8	0.02 (1.05)	-0.02 (0.54)	4 , 8	-0.85 (0.78)	0.36 (0.41)
2 , 1			5 , 1		
2 , 2			5 , 2		
2 , 3			5 , 3		
2 , 4			5 , 4		
2 , 5			5 , 5		
2 , 6			5 , 6		
2 , 7			5 , 7		
2 , 8	1.18 (0.91)	0.52 (0.55)	5 , 8	-0.04 (0.11)	0.53 (0.55)
3 , 1			6 , 1		
3 , 2			6 , 2		
3 , 3			6 , 3		
3 , 4			6 , 4		
3 , 5			6 , 5		
3 , 6			6 , 6		
3 , 7			6 , 7		
3 , 8	1.24 (0.92)	0.54 (0.56)	6 , 8	-0.07 (0.14)	0.57 (0.58)

WIND DATA

	VELOCITY (M/S)	DIRECTION (DEG)
LBL	2.6 (0.7)	-3 (2)
MCAS	3.1	7

LOCATION	AIR TEMPERATURE (C)	DEW POINT	RELATIVE HUMIDITY (%)	EFFECTIVE TEMPERATURE (C)
1 KITCHEN	27.3 (0.4)	12.5	40 (0.5)	26.1
0 UNDER CARPORT	24.7 (0.9)	20.0	75 (1.5)	22.2
1 LIVING ROOM	26.5 (1.0)	12.7	42 (0.5)	25.4
0 WEATHER TOWER	23.7 (1.2)	21.0	84 (0.7)	22.3
1 LIVING ROOM	23.1 (0.9)			
MCAS	26.9	23.7	83	25.2

ESTIMATED INSIDE AIR VELOCITY (M/S)

LOCATION	CALCULATED	DISA	ORIFICE
WEST APARTMENT	0.00	0.13 (0.02)	1.76

ESTIMATED NATURAL VENTILATION RATES (M^3/HR)

LOCATION	INTO BUILDING	OUT OF BUILDING	LBL INFILTRATION
WEST APARTMENT	127	133	46

BAROMETRIC PRESSURE (KPA)

MCAS	101.27

Figure 13. Data sample from Building No. 2.

TIME = 3.58 DATE = 07/16

TAP	PRESSURE (PA) DIFFERENCE	PRESSURE COEFFICIENT	TAP	PRESSURE (PA) DIFFERENCE	PRESSURE COEFFICIENT
1 , 1	6.26 (4.40)	1.16 (0.91)	4 , 1	9.67 (5.62)	-0.63 (0.47)
1 , 2	5.96 (4.34)	1.13 (0.95)	4 , 2	9.36 (5.62)	-0.60 (0.50)
1 , 3	-6.20 (4.71)	-1.11 (0.86)	4 , 3	-3.06 (3.30)	-0.59 (0.52)
1 , 4	-3.99 (2.53)	-0.78 (0.58)	4 , 4	-0.59 (1.17)	-0.63 (0.49)
1 , 5	-2.87 (2.20)	-0.57 (0.54)	4 , 5	0.55 (1.78)	-0.61 (0.51)
1 , 6			4 , 6		
1 , 7			4 , 7		
1 , 8			4 , 8		
2 , 1	5.17 (3.28)	1.00 (0.74)	5 , 1	6.81 (3.74)	-0.31 (0.45)
2 , 2	4.46 (3.10)	0.90 (0.85)	5 , 2	6.14 (3.58)	-0.29 (0.54)
2 , 3	-3.00 (2.72)	-0.57 (0.55)	5 , 3	-1.79 (1.32)	-0.22 (0.41)
2 , 4	-1.69 (2.45)	-0.33 (0.47)	5 , 4	-0.36 (0.78)	-0.25 (0.42)
2 , 5	-1.67 (1.94)	-0.35 (0.49)	5 , 5	-0.34 (1.19)	-0.25 (0.48)
2 , 6			5 , 6		
2 , 7			5 , 7		
2 , 8			5 , 8		
3 , 1	1.20 (3.13)	0.25 (0.61)	6 , 1	4.49 (3.32)	-0.62 (0.44)
3 , 2	5.39 (3.36)	0.98 (0.69)	6 , 2	8.74 (4.10)	-0.58 (0.49)
3 , 3	7.07 (5.23)	1.37 (1.01)	6 , 3	10.37 (6.16)	-0.65 (0.58)
3 , 4	-5.85 (4.36)	-1.04 (0.77)	6 , 4	-2.64 (2.66)	-0.59 (0.57)
3 , 5	-4.01 (2.80)	-0.77 (0.53)	6 , 5	-0.66 (1.56)	-0.61 (0.48)
3 , 6	-2.17 (2.88)	-0.39 (0.53)	6 , 6	0.98 (1.83)	-0.54 (0.48)
3 , 7	-1.29 (2.33)	-0.26 (0.45)	6 , 7	1.91 (1.96)	-0.60 (0.47)
3 , 8	-2.75 (2.22)	-0.51 (0.50)	6 , 8	0.40 (2.12)	-0.58 (0.45)

WIND DATA

	VELOCITY (M/S)		DIRECTION (DEG)	
LBL	3.9	(1.0)	1	(2)
MCAS	8.6		7	

LOCATION	AIR TEMPERATURE (C)		DEW POINT	RELATIVE HUMIDITY (%)		EFFECTIVE TEMPERATURE (C)
2 EAST LIVING ROOM	26.4	(0.5)	23.2	83	(0.7)	25.2
0 SOUTH BALCONY	24.8	(1.0)	20.2	76	(40.4)	22.3
2 WEST LIVING ROOM	25.2	(1.2)	20.7	76	(0.5)	23.5
0 WEATHER TOWER	23.9	(1.3)	19.3	76	(1.0)	21.4
2 WEST LIVING ROOM	25.9	(1.2)				
MCAS	28.5		17.5	51		22.2

ESTIMATED INSIDE AIR VELOCITY (M/S)

LOCATION	CALCULATED	DISA		ORIFICE
EAST APARTMENT	0.23	0.13	(0.01)	2.31
WEST APARTMENT	0.23			1.85

ESTIMATED NATURAL VENTILATION RATES (M^3/HR)

LOCATION	INTO BUILDING	OUT OF BUILDING	LBL INFILTRATION
EAST APARTMENT	259	12129	5622
WEST APARTMENT	205	9688	5622

BAROMETRIC PRESSURE (KPA)

MCAS	101.24

Figure 14. Data sample from Building No. 3.

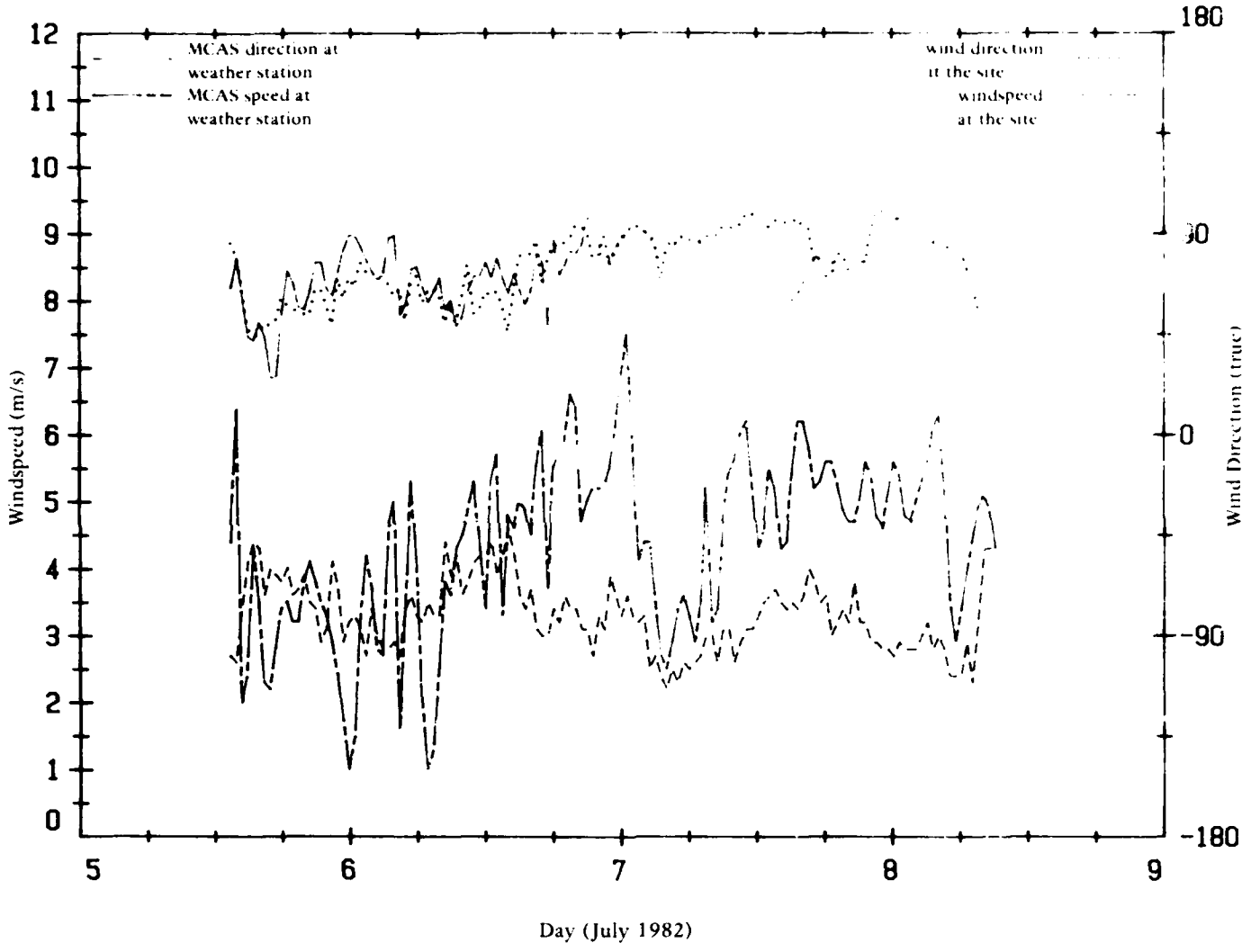

(a) Building No. 1, VEQ.

Figure 15. Windspeeds and directions.

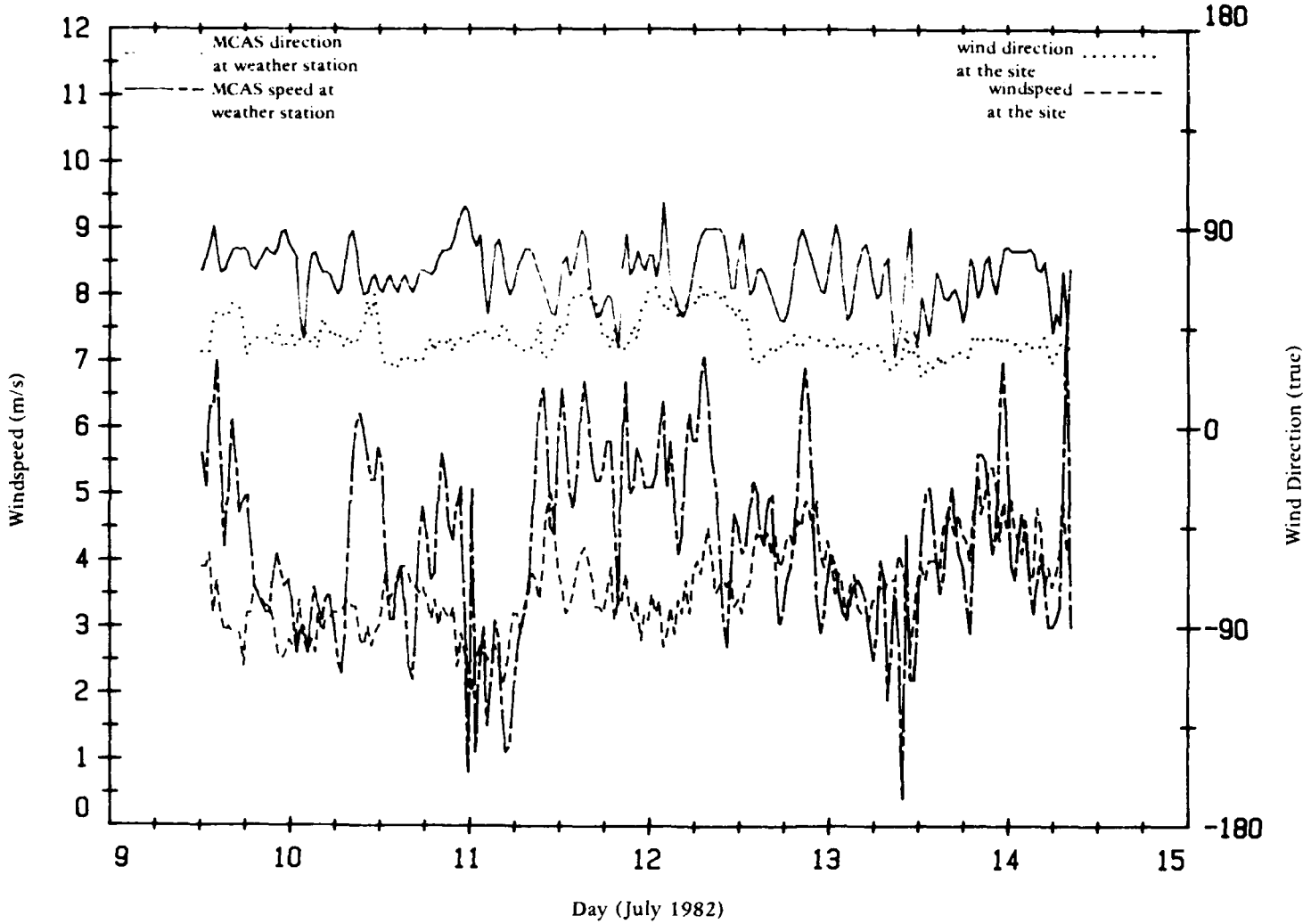

(b) Building No. 2, single-story duplex.

Figure 15. Continued.

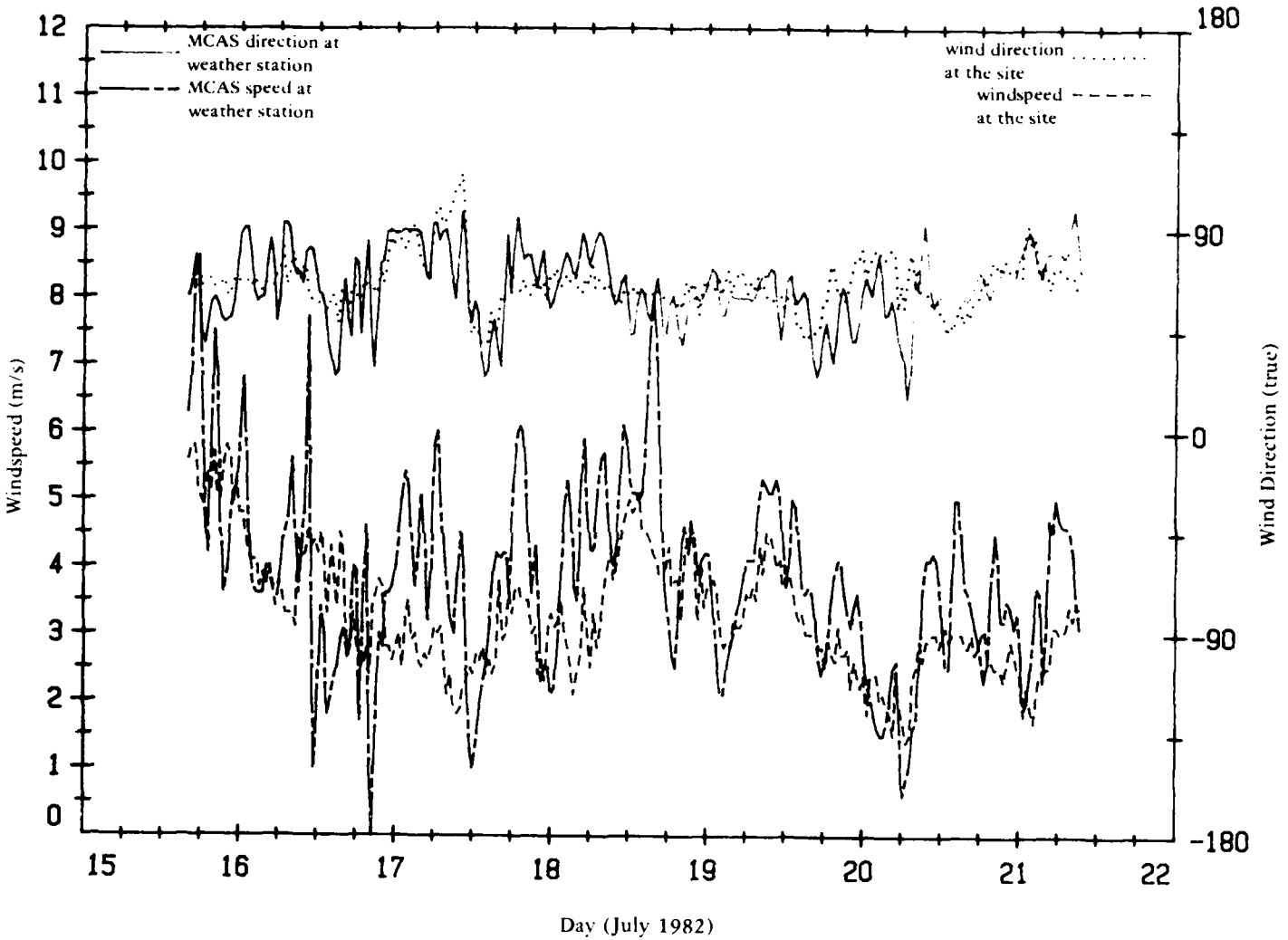

(c) Building No. 3, two-story fourplex.

Figure 15. Continued.

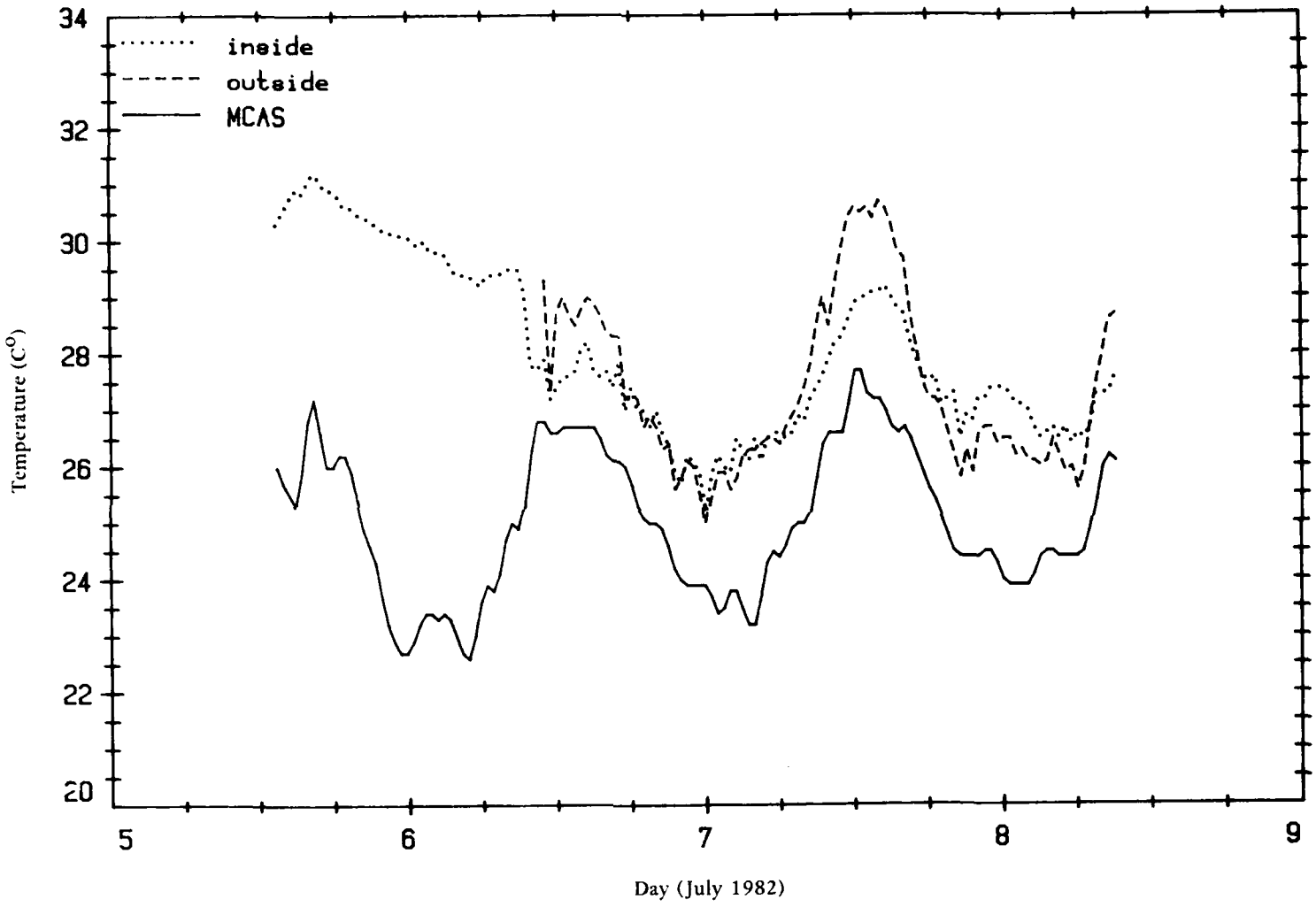

(a) Building No. 1, VEQ.

Figure 16. Dry bulb air temperatures.

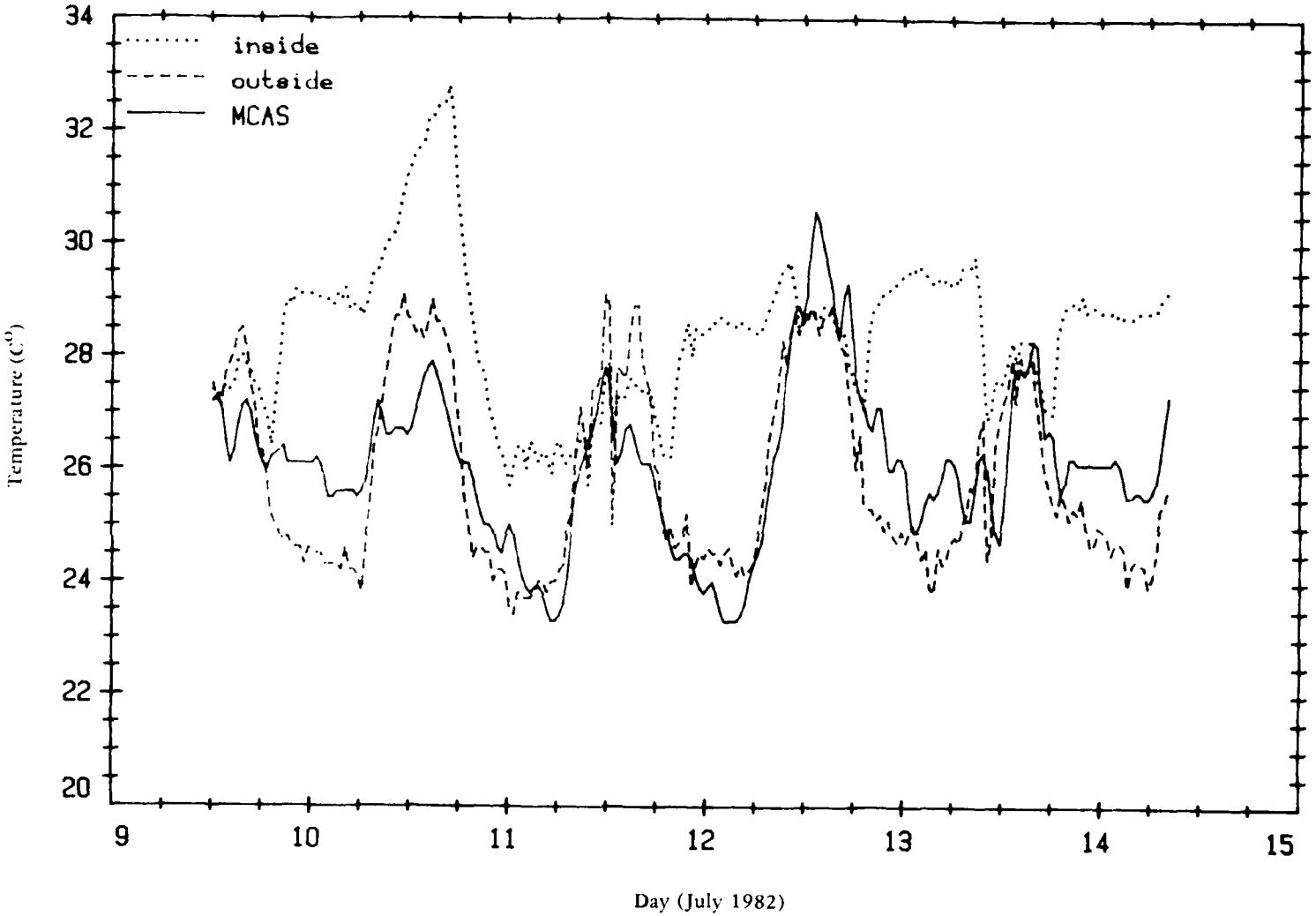

(b) Building No. 2, single-story duplex.

Figure 16. Continued.

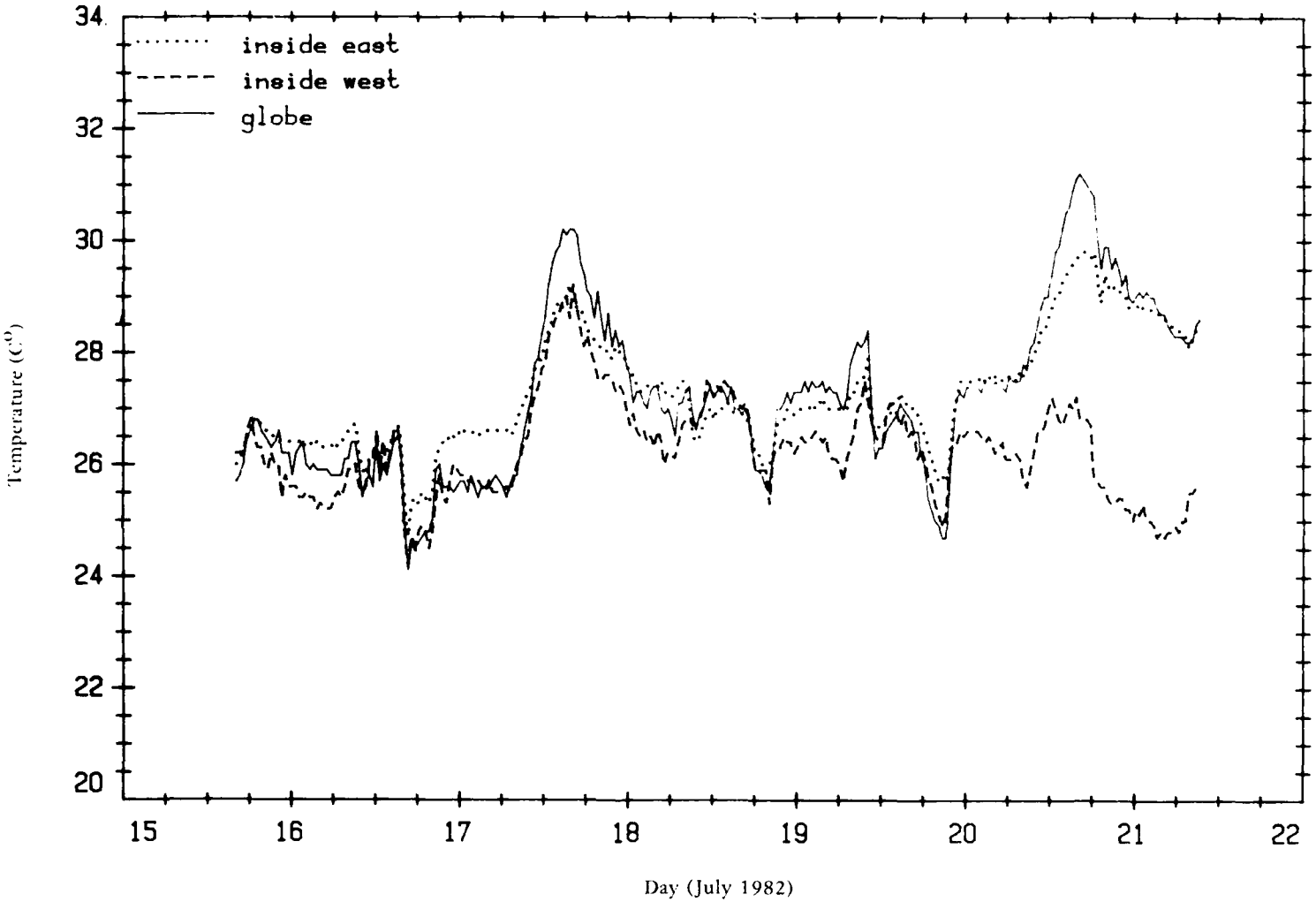

(c) Building No. 3, two-story fourplex (inside temperatures).

Figure 16. Continued.

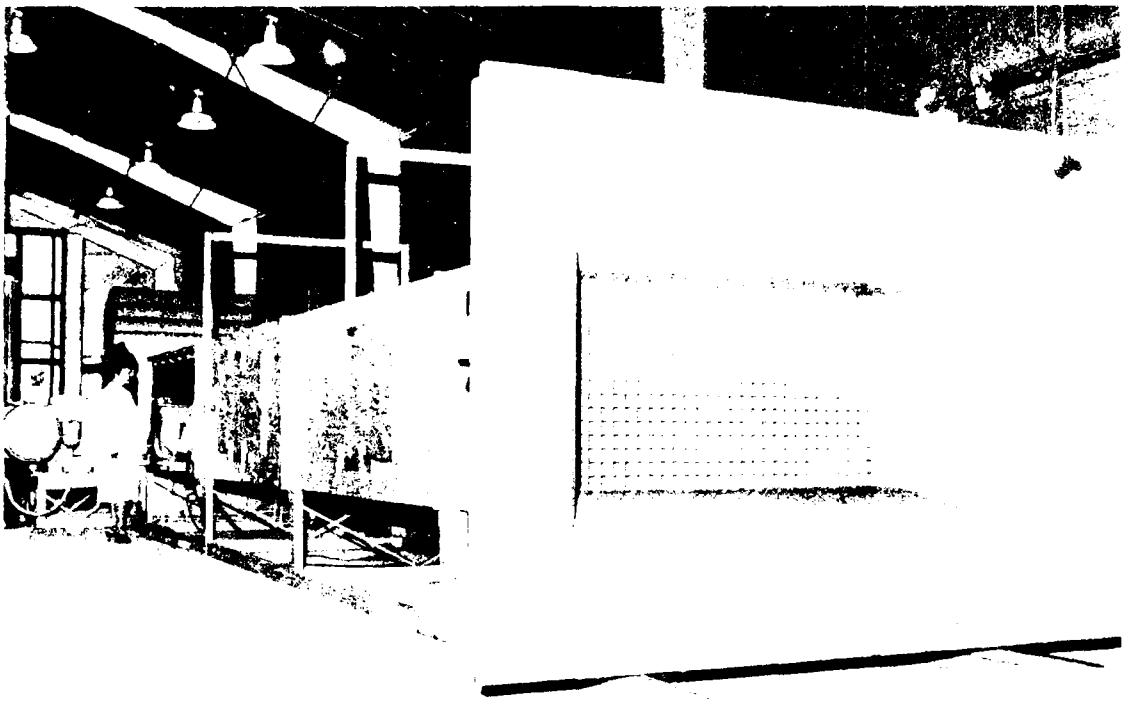

Figure 21. NCEL boundary layer wind tunnel.

Wind Tunnel Test Models

Modeling the aerodynamic loading on a structure requires special consideration of airflow conditions in order to guarantee similitude between the model and prototype. In general, the requirements are that the model and the prototype be geometrically similar (Ref 14, 15 and 16), that the approach mean wind velocity at the building site have a vertical profile shape similar to the full-scale airflow, that the turbulence characteristics of the airflows are similar, and that the Reynolds number for the model and the prototype are equal. The criteria were satisfied by constructing scale models of the buildings tested in Hawaii. The building geometry is described by two ratios: the side ratio (length/width) and the aspect ratio (width/height). The side ratios of 0.125, 0.3 and 0.35 were tested over a range of aspect ratios from 0.3 to 0.5. Model 1, Figure 23, was made of plexiglass and instrumented at 20 locations with pressure taps. Models 2 and 3, Figures 24 and 25, were made of plywood and instrumented at 20 locations at mid-height with pressure taps. Maximum model blockage was limited up to 5% of the cross-sectional test area (Ref 14). Scale of models ranged from 1:46 to 1:80.

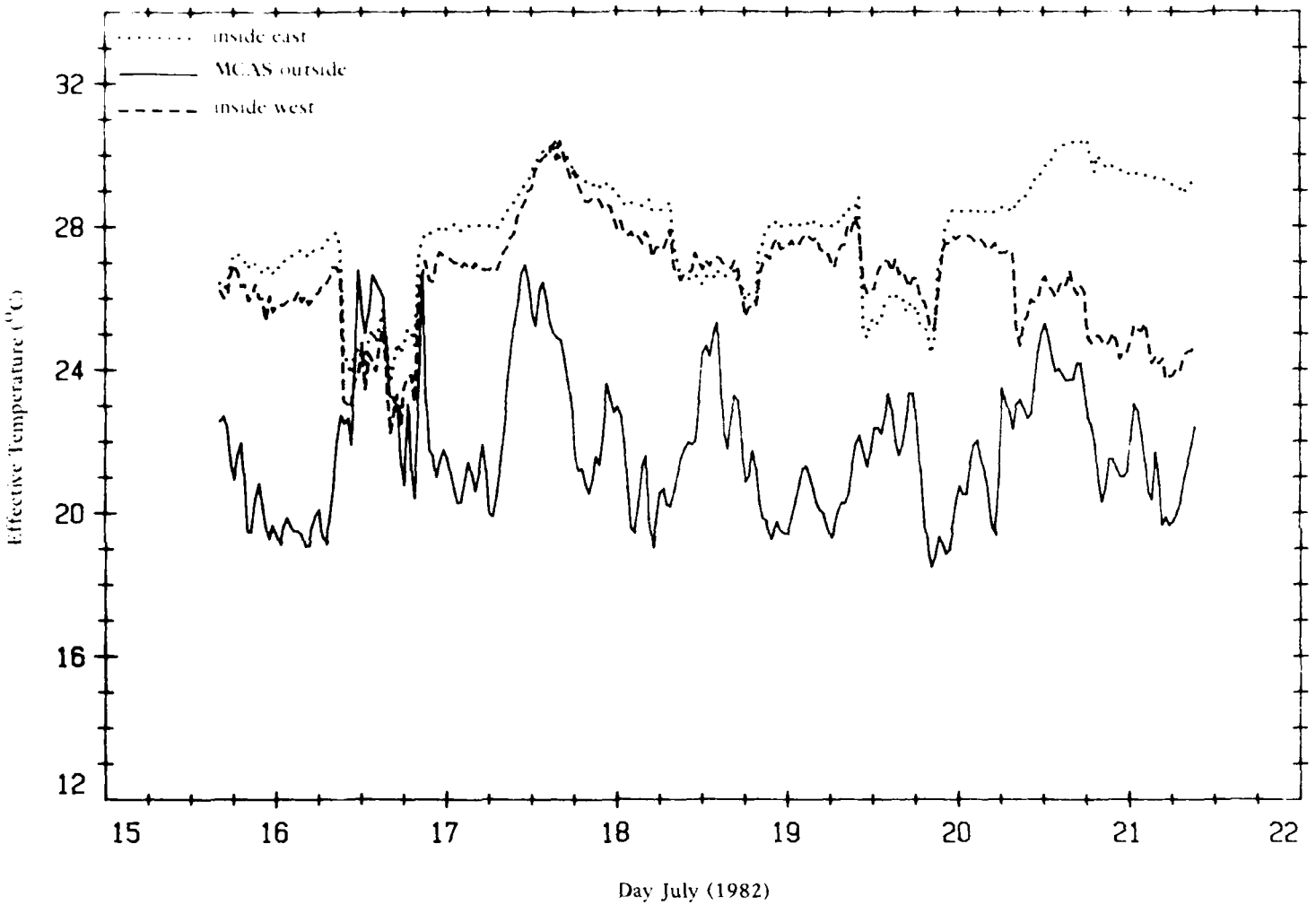

(c) Building No. 3, two-story fourplex.

Figure 20. Continued.

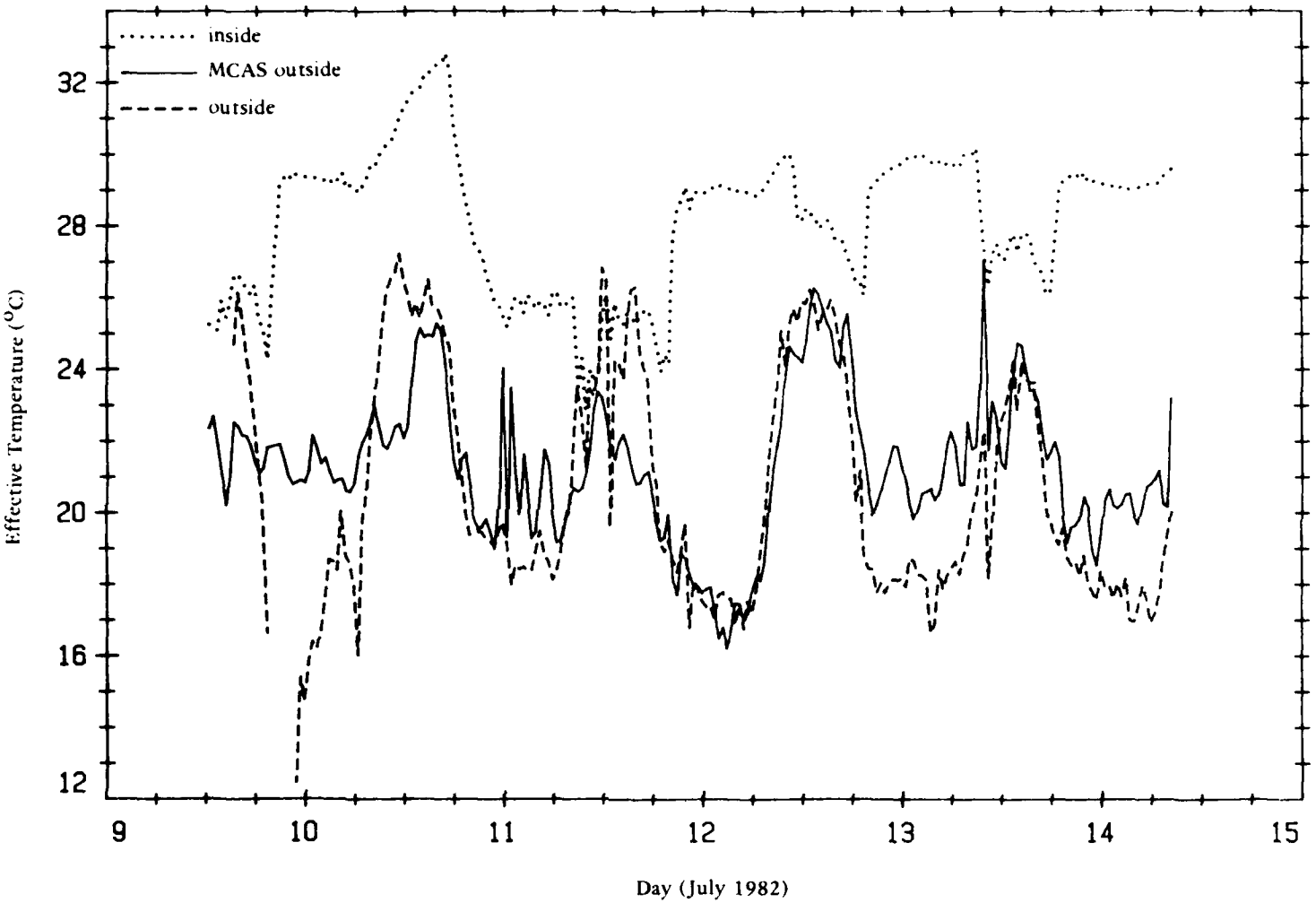

(b) Building No. 2, single-story duplex.

Figure 20. Continued.

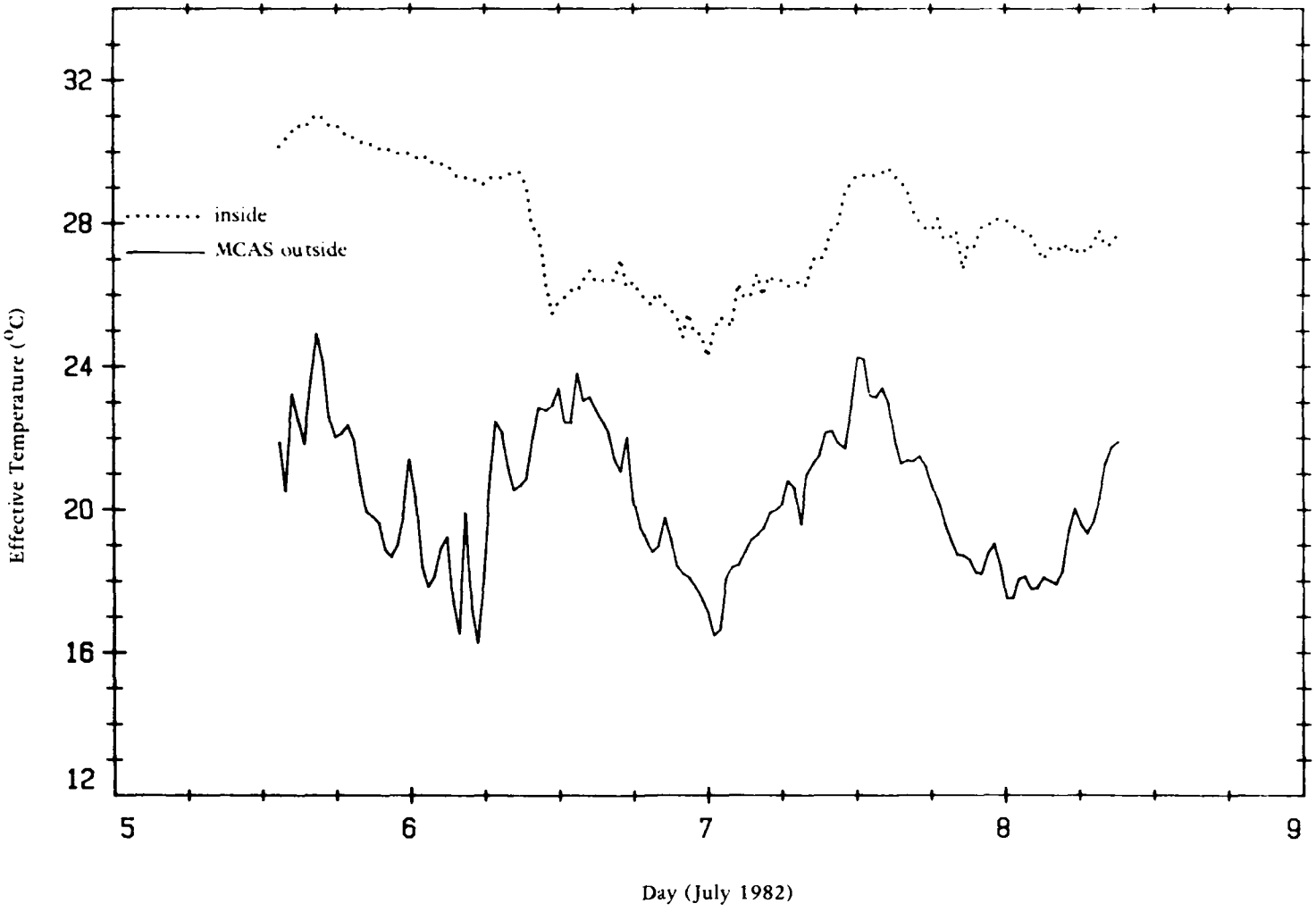

(a) Building No. 1, VEQ.

Figure 20. Effective temperatures.

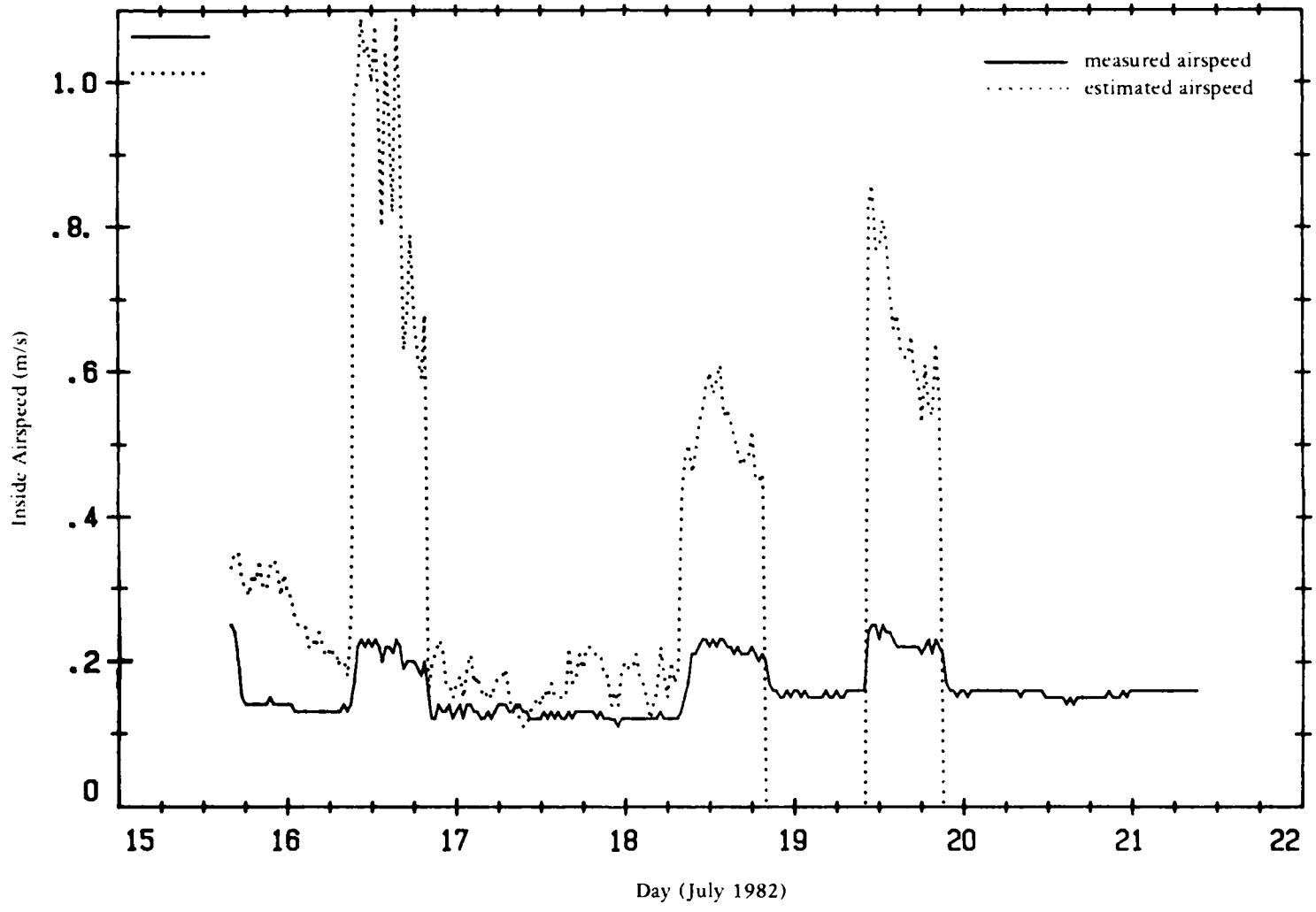

(b) Building No. 3, two-story fourplex (east apartment).

Figure 19. Continued.

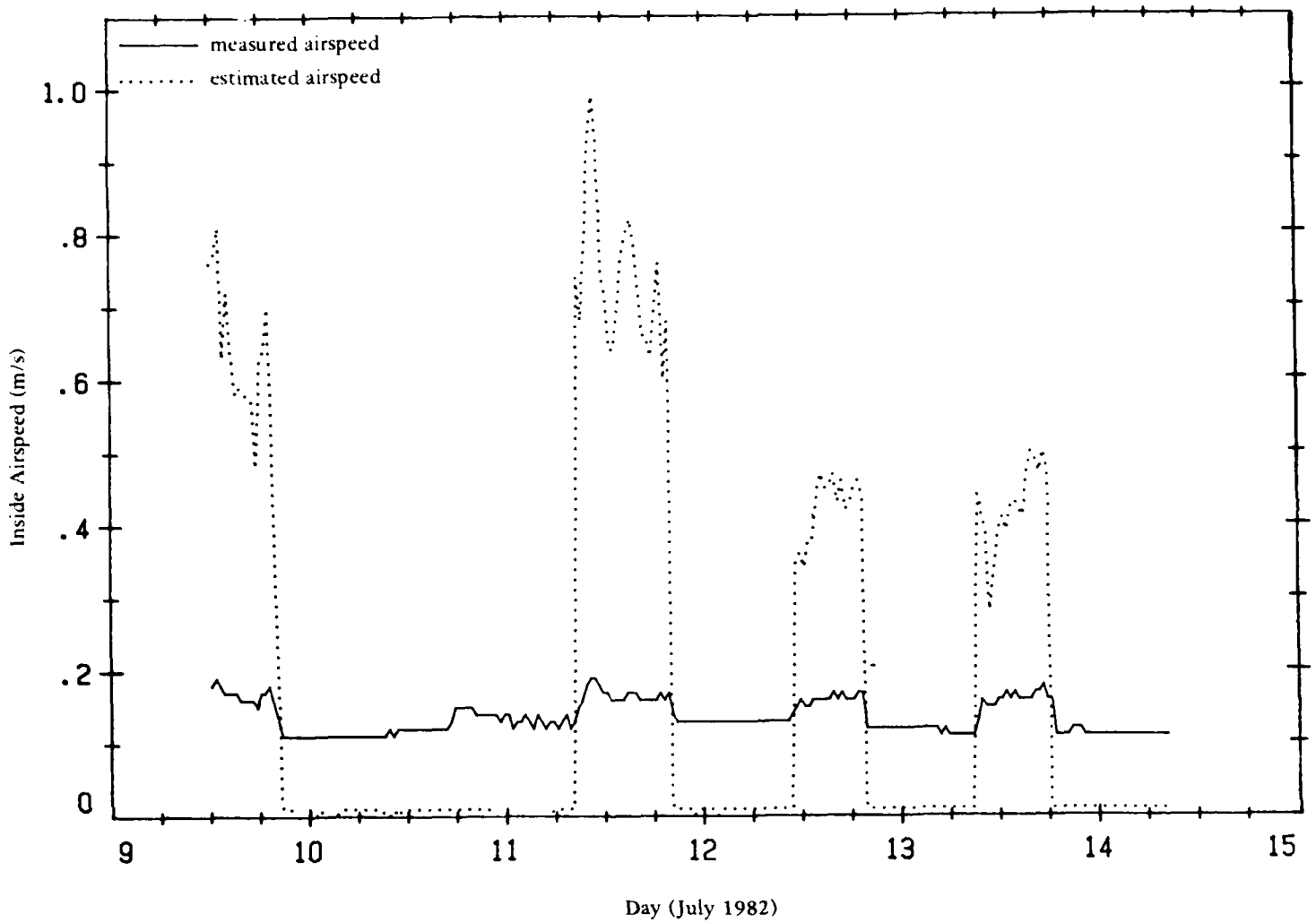

(a) Building No. 2, single-story duplex.

Figure 19. Interior airspeeds.

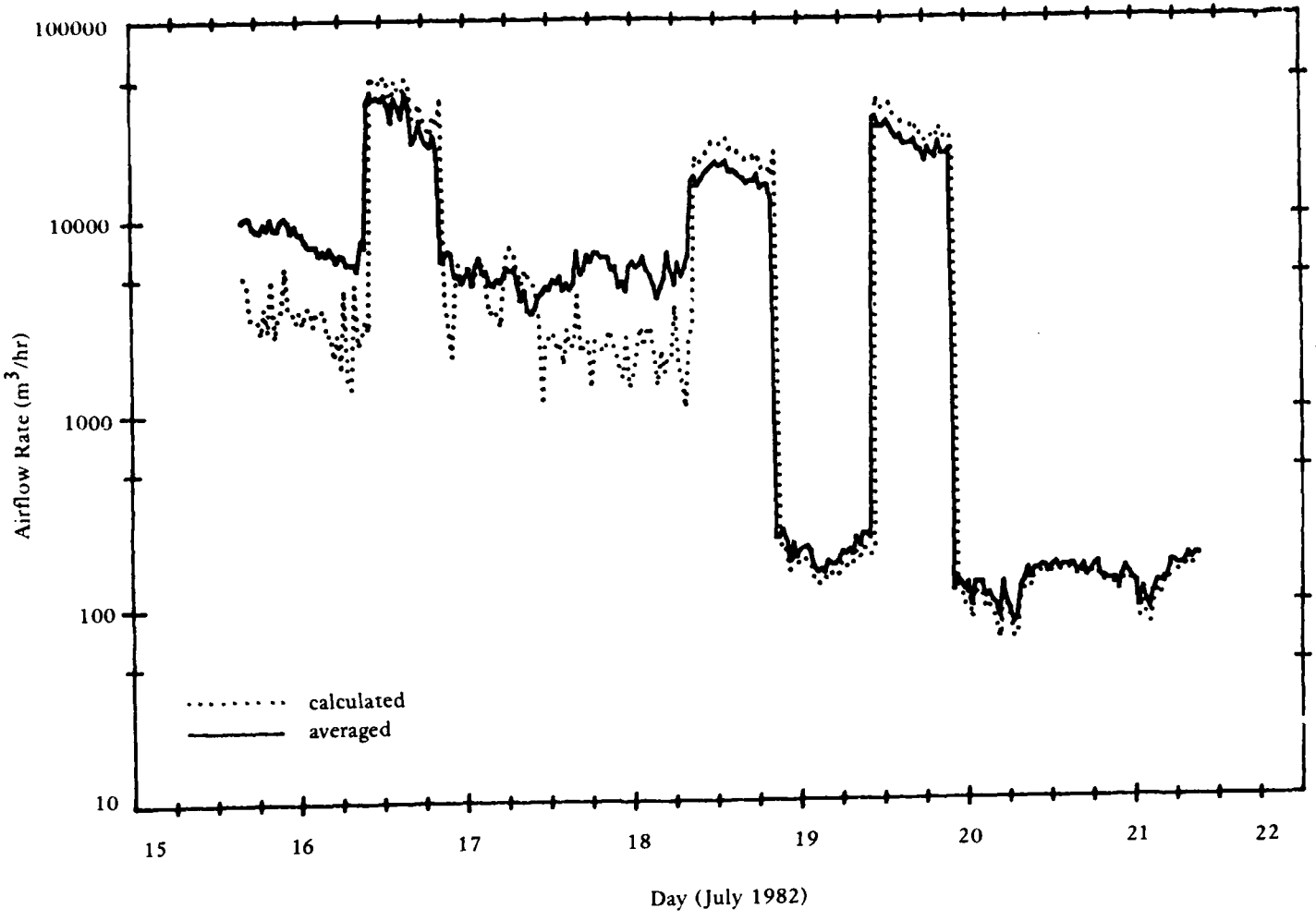

(d) Building No. 3, two-story fourplex (east apartment).

Figure 18. Continued.

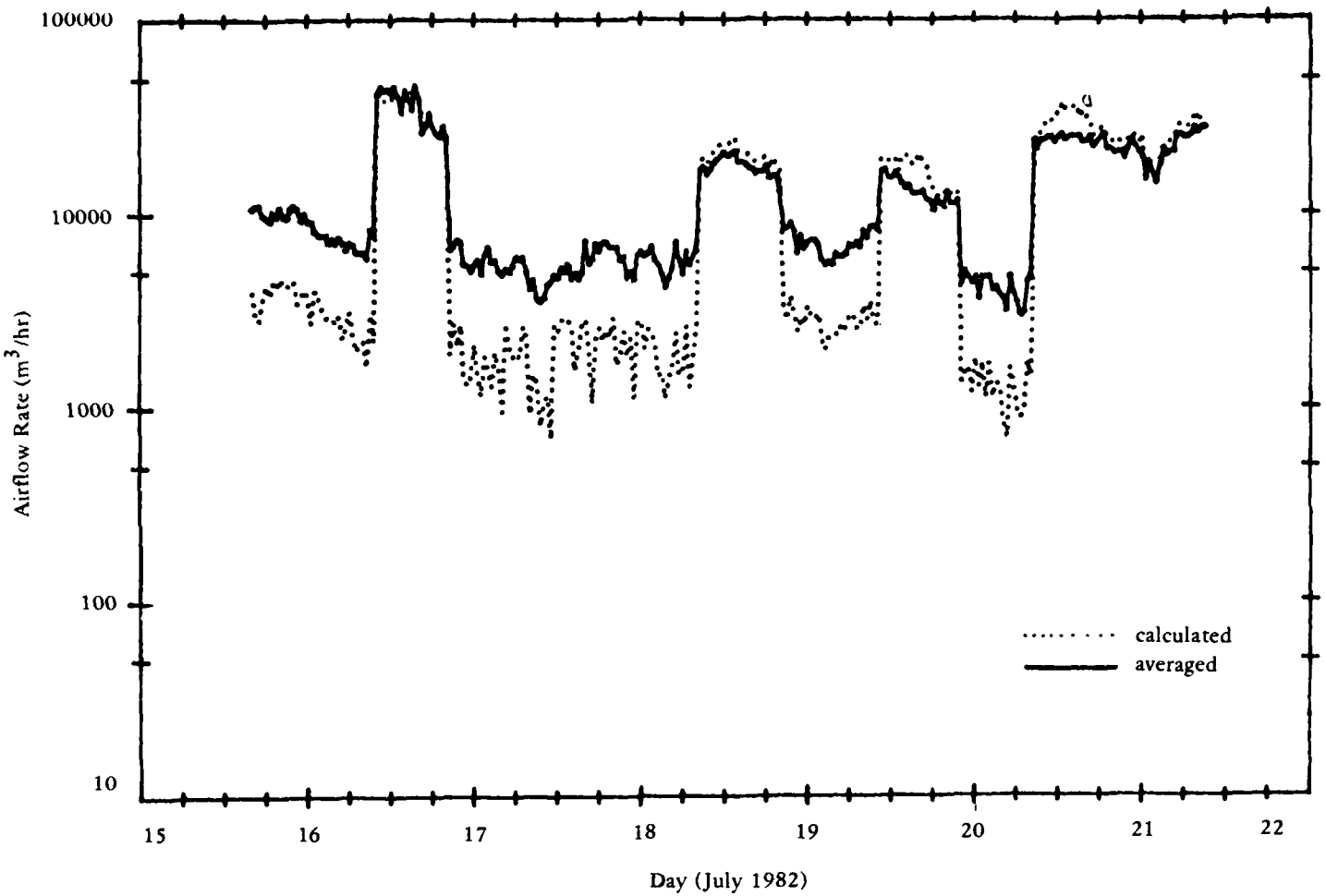

(c) Building No. 3, two-story fourplex (west apartment).

Figure 18. Continued.

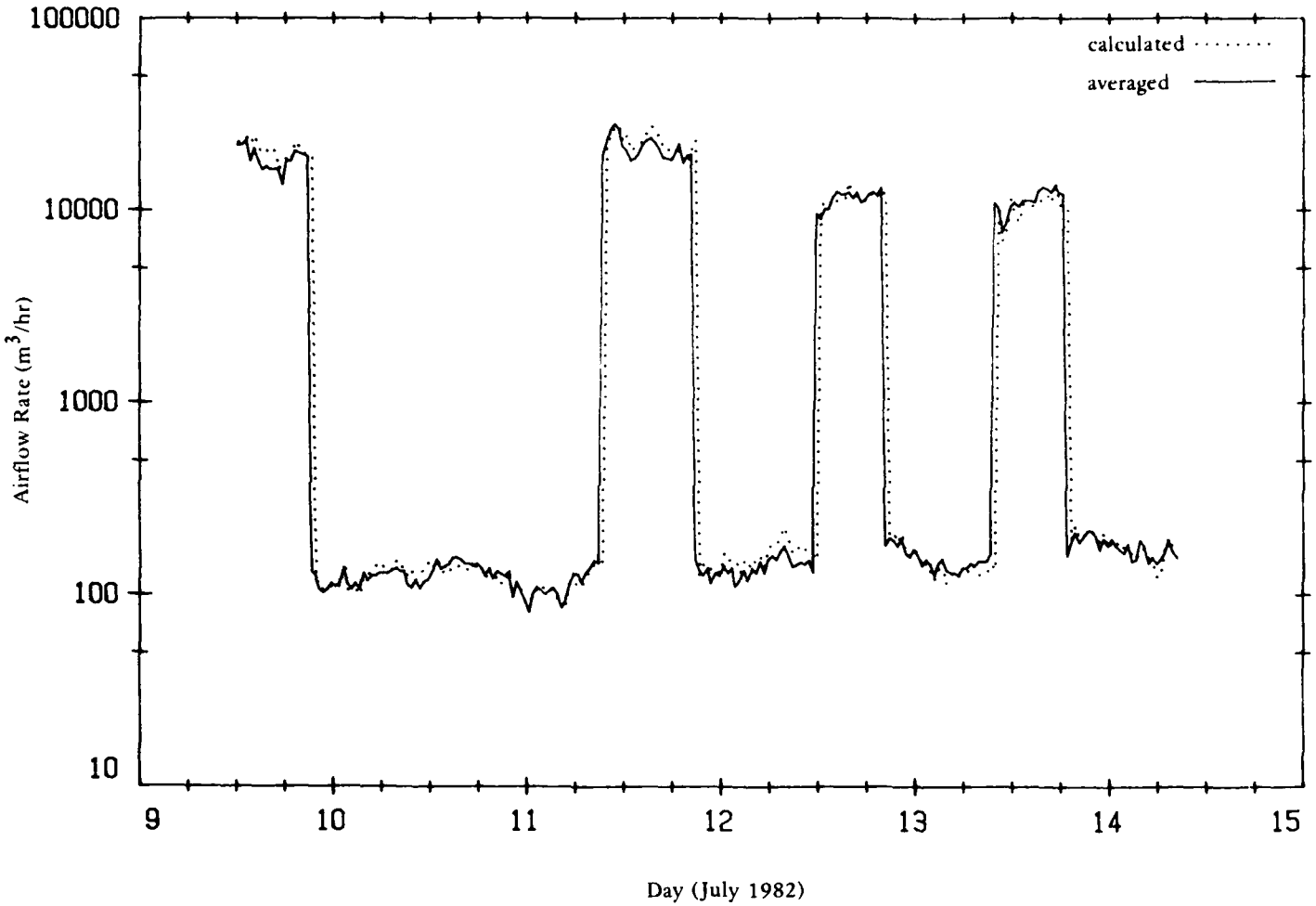

(b) Building No. 2, single-story duplex (west apartment).

Figure 18. Continued.

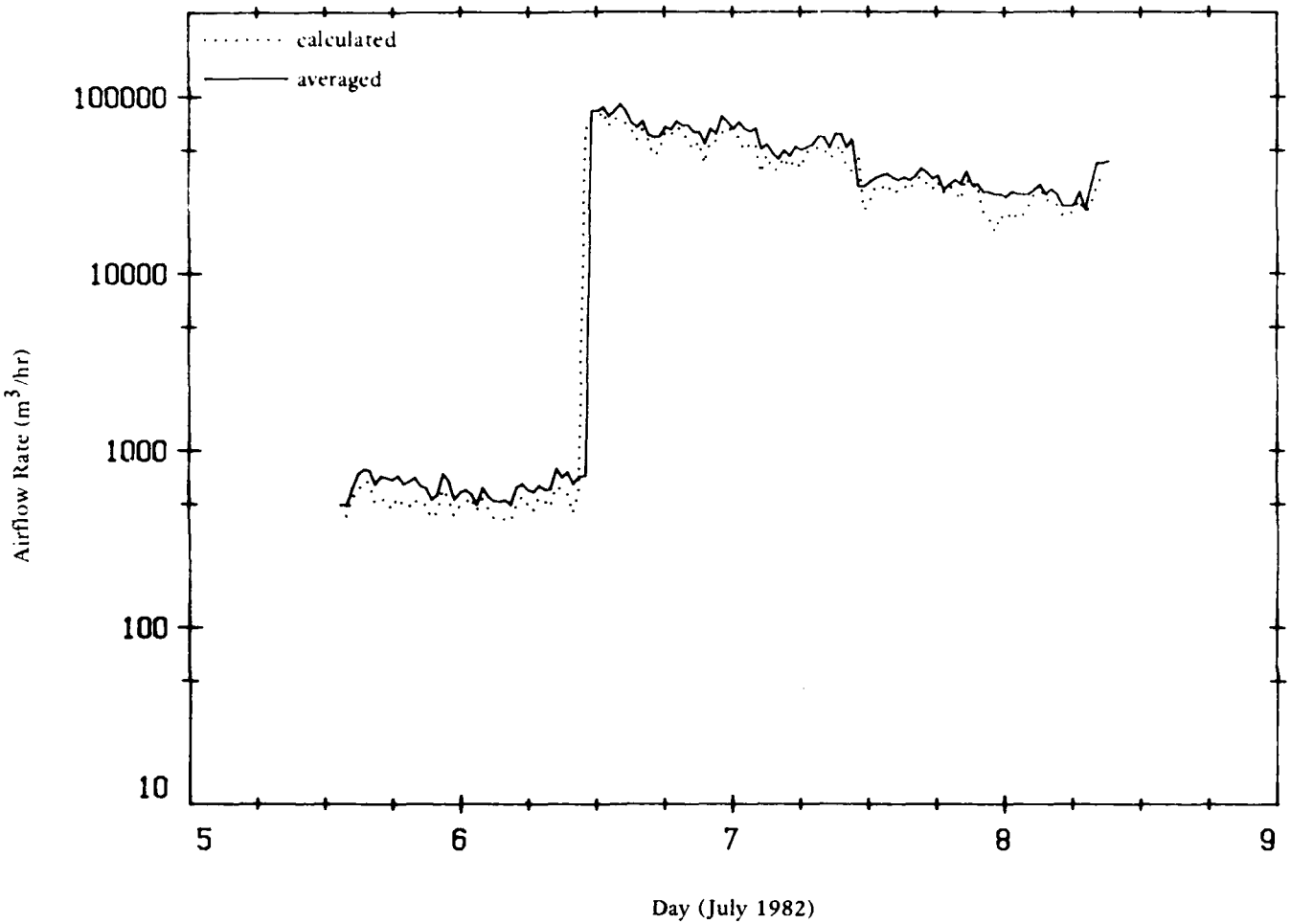

(a) Building No. 1, VEQ (second floor).

Figure 18. Estimated airflow rates.

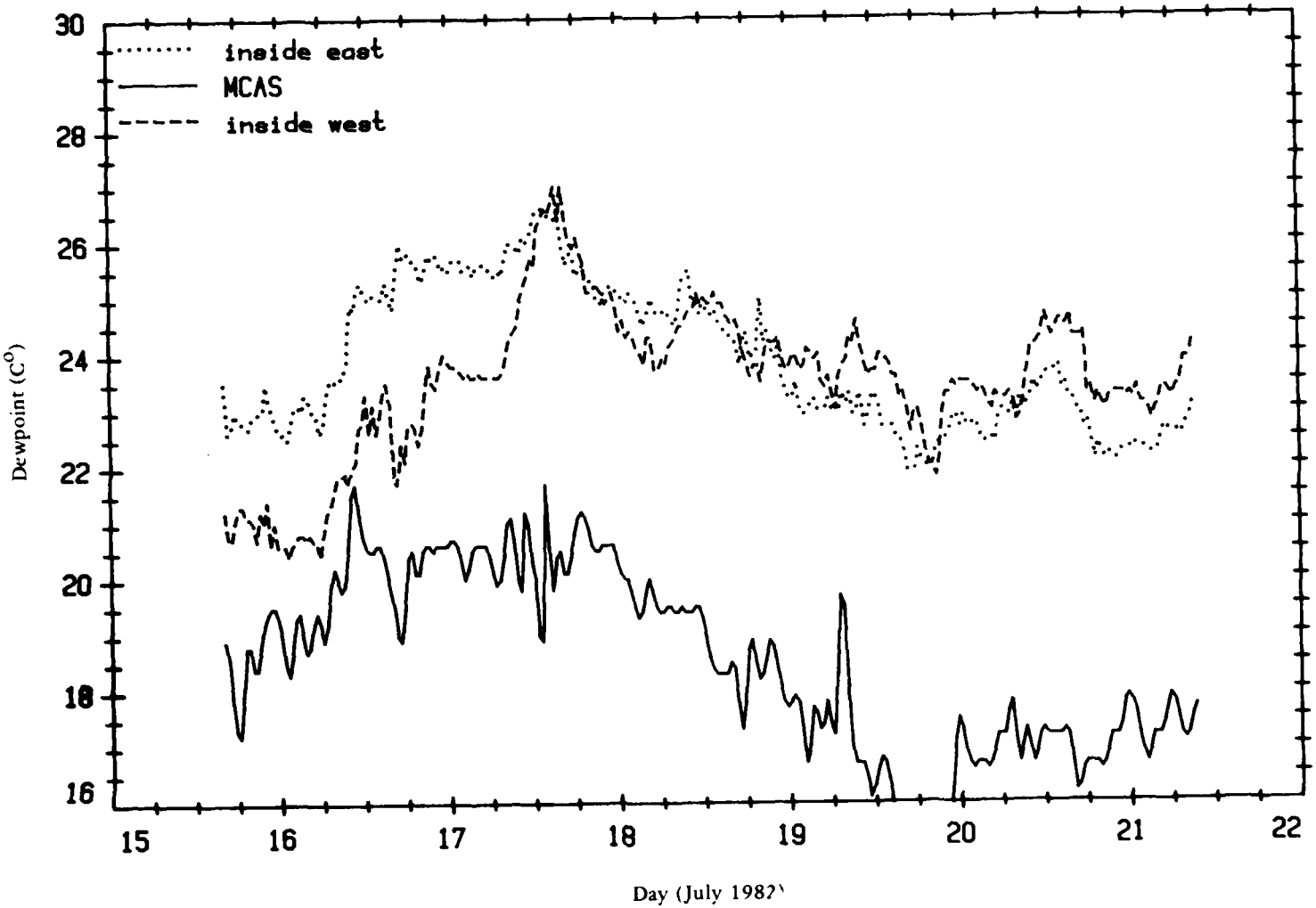

(c) Building No. 3, two-story fourplex.

Figure 17. Continued.

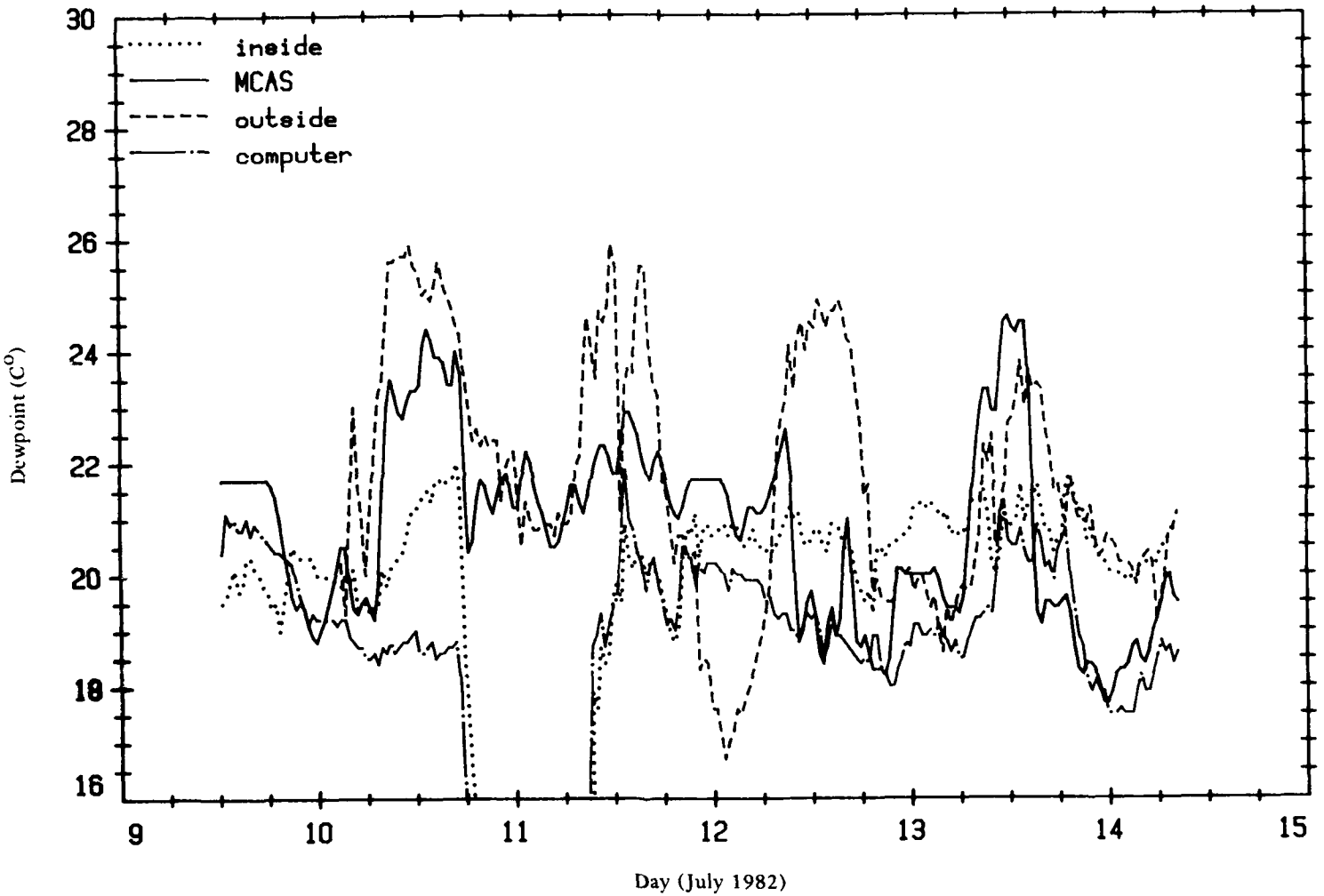

(b) Building No. 2, single-story duplex.

Figure 17. Continued.

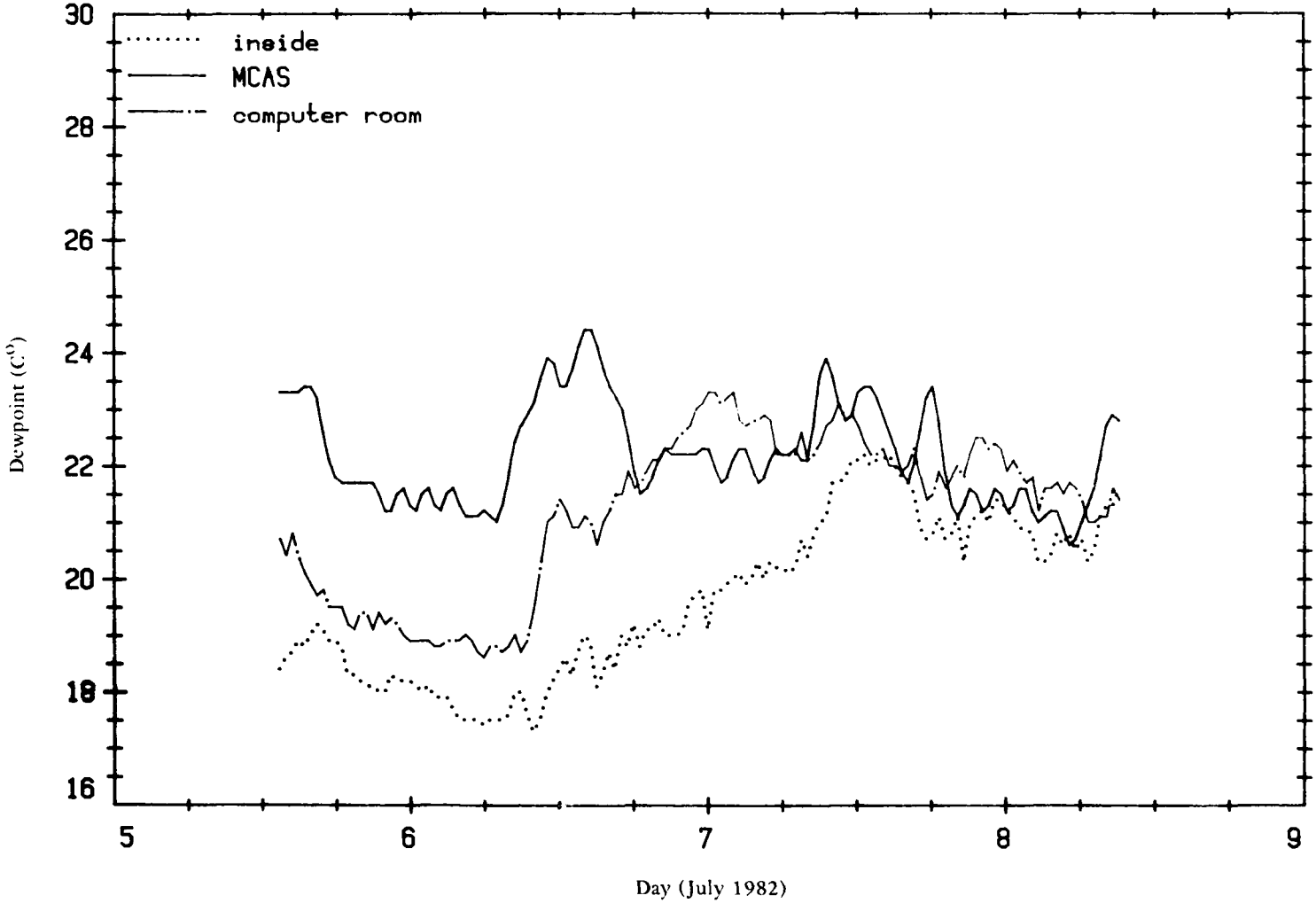

(a) Building No. 1, VEQ.

Figure 17. Dew point temperatures.

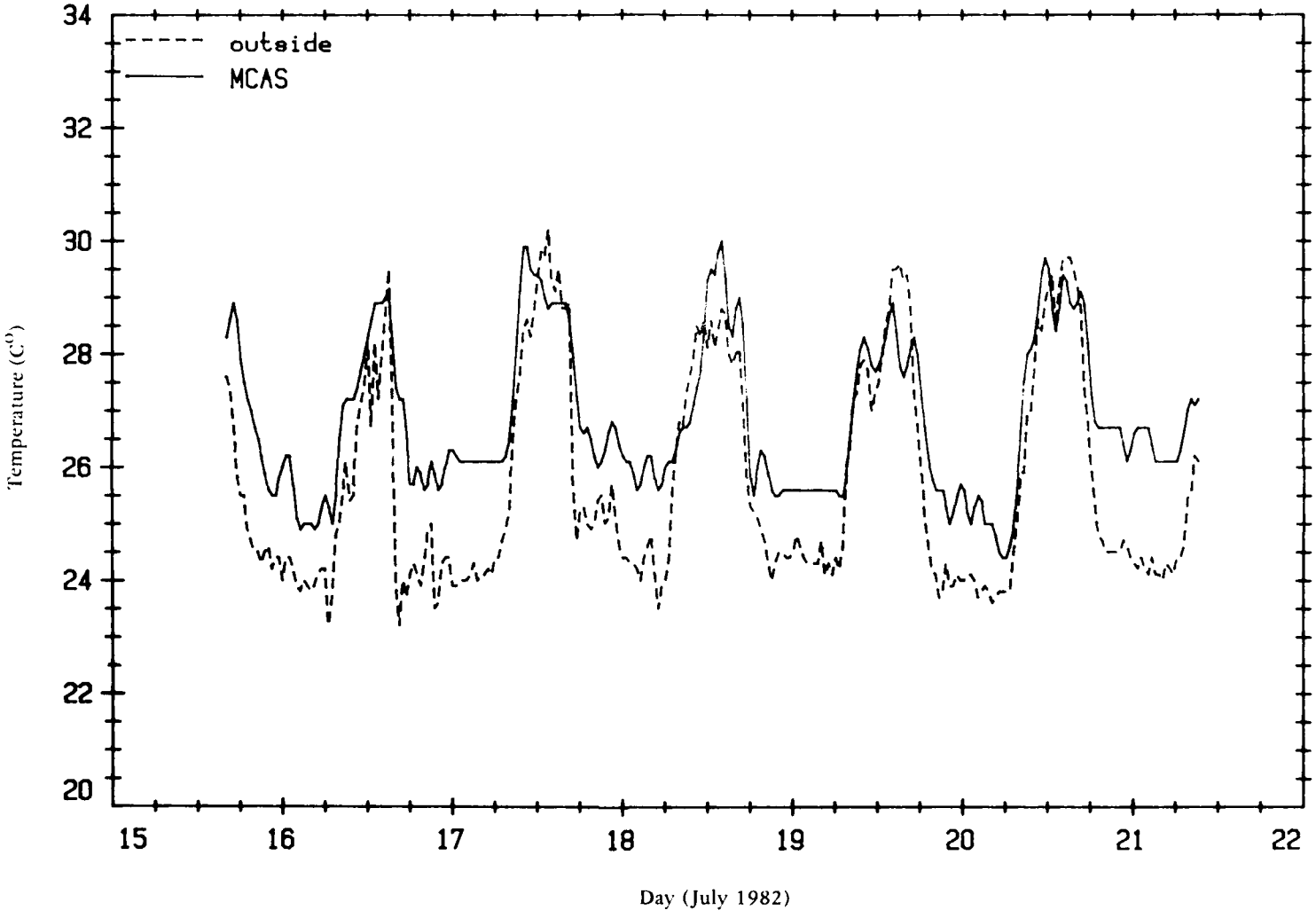

(d) Building No. 3, two-story fourplex (outside temperature).

Figure 16. Continued.

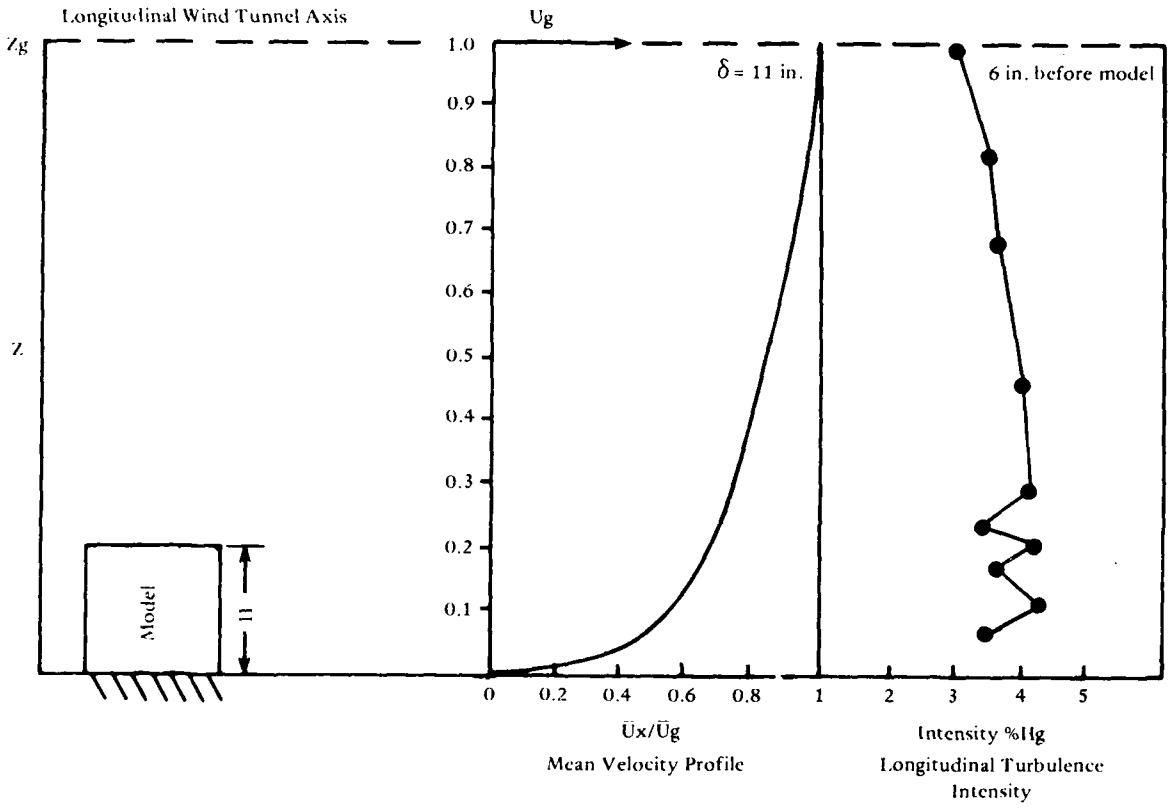

Figure 22. General characteristics of the NCEL wind tunnel.

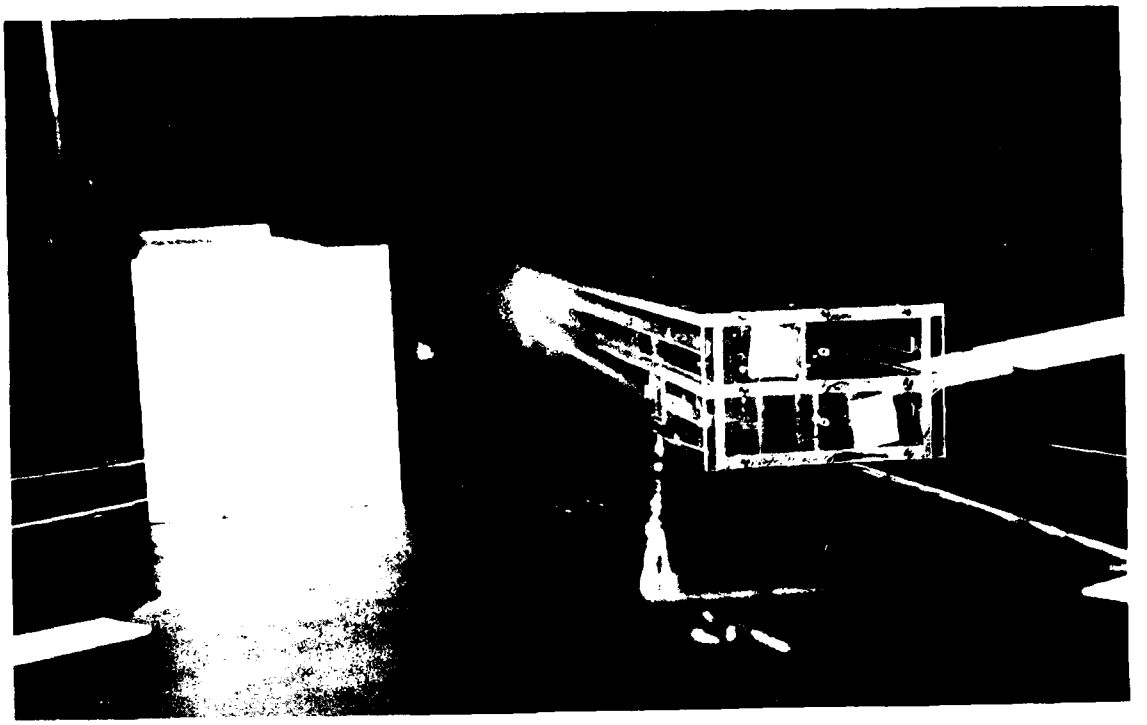

Figure 23. Model 1.

Figure 24. Model 2.

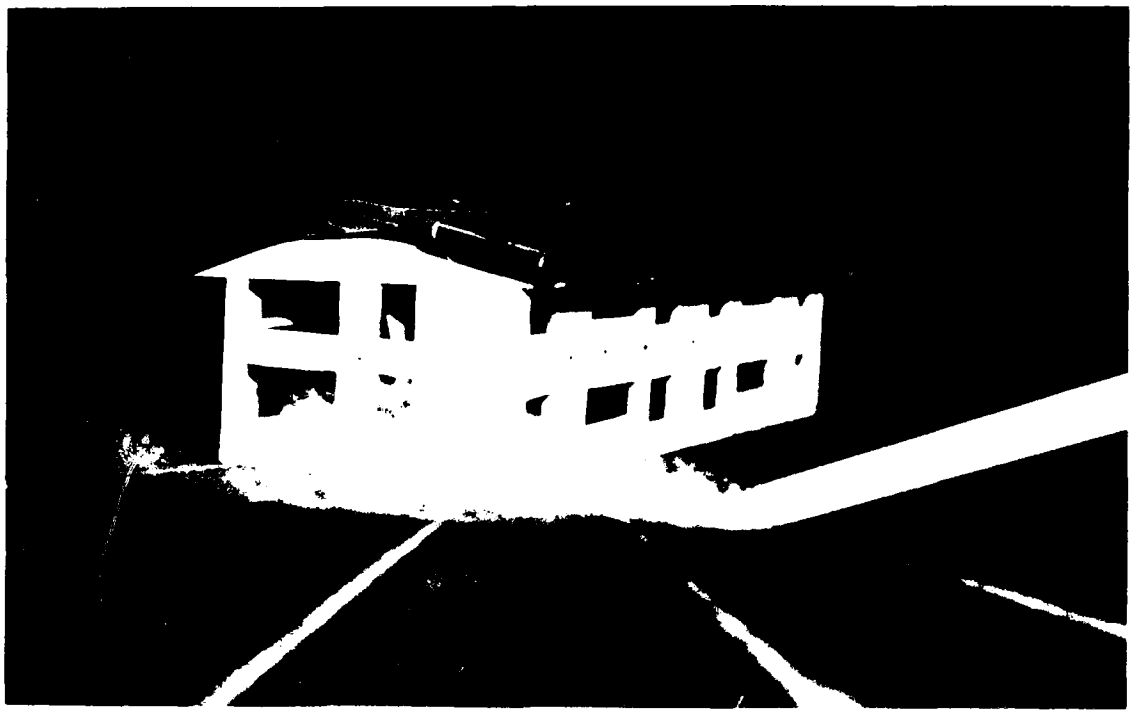

Figure 25. Model 3.

A combination of wire mesh (Figure 26), and a step board positioned at 0.914 and 5.5 meters (3 feet and 18 feet), respectively, upwind of the model produced a mean wind velocity profile (power law exponent 0.20) (Figure 27a and b). From the windspeed data taken at the site and data recorded by the MCAS weather station, the terrain seem to have characteristics of a country with scattered windbreaks. For the distribution of mean windspeed with height, the power law expression (Ref 15) of the form:

$$\bar{U}_z / \bar{U}_g = (z/\delta)^a \qquad (6)$$

where: $\bar{U}_z$ = mean wind velocity at height z
$\bar{U}_g$ = gradient wind volocity in the free stream
a = power law exponent
δ = boundary layer thickness
z = height

was used to represent the mean wind velocity profiles; the exponent α was set about 0.20.

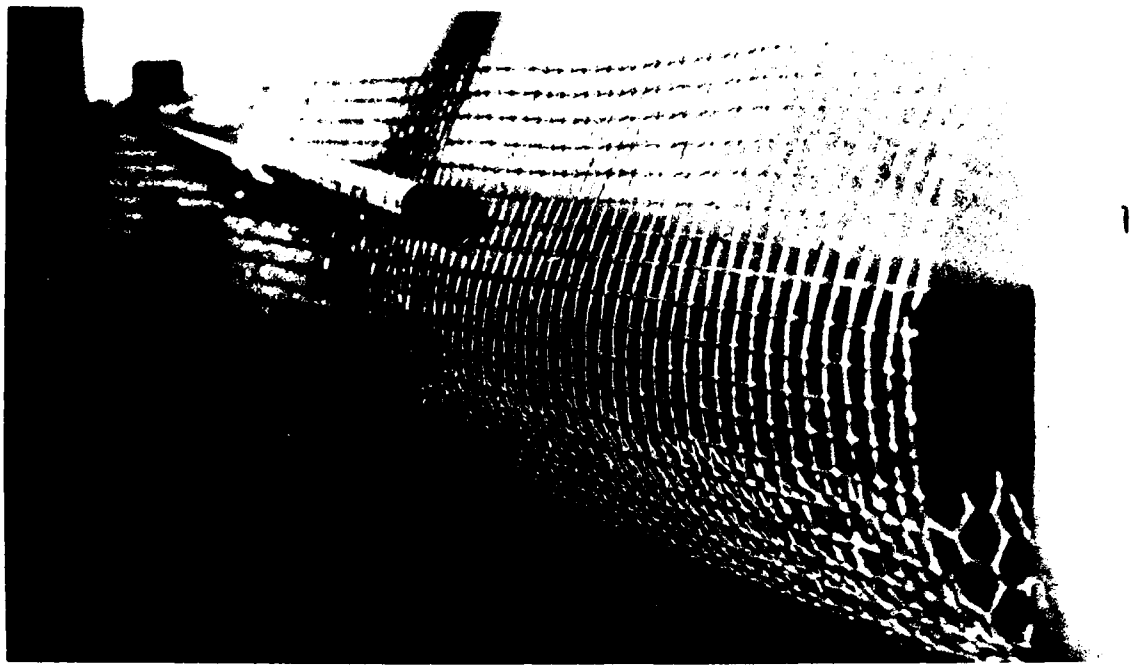

Figure 26. Wire mesh used in NCEL wind tunnel tests.

The windspeed used in the wind tunnel ranged from 14.8 f/s to 17.1 f/s (4.5 m/s to 5.2 m/s) above the boundary layer and 10.8 f/s (3.3 m/s) at the 2-1/2-inch height.

The turbulence intensity, I, into the shear layer was not subjected to as stringent requirements as was the mean wind velocity profile. This was because full-scale data of turbulence intensity for sites with specific terrain characteristics are extremely limited. However, tests conducted in the NCEL wind tunnel and at other facilities show that an increase in turbulence intensity will cause a change on base pressures, and the pressure coefficient at the center of the windward wall increases while the coefficients at the periphery of the windward wall decreases. Overall it was found that a 90-100% increase in turbulence intensity caused an overall decrease in pressure difference coefficient of 10% at wind incidence perpendicular to the windward wall. Further studies are required to assess the effect of rapid pressure fluctuations with turbulence on natural ventilation rates. It is believed that these pressure fluctuations may be important for special situations, for example, where buoyancy is dominant and pressure difference across the building is comparatively small. The turbulence intensity in the wind tunnel ranged from 3.5 to 4.2% along the vertical axis (Figure 22).

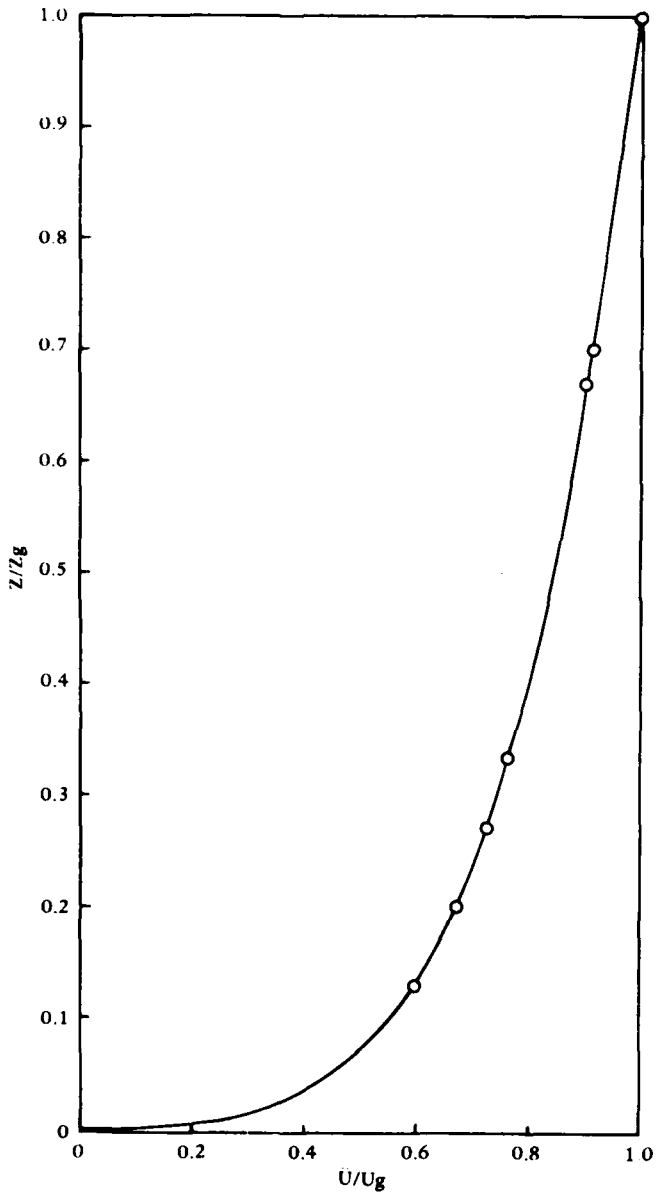

(a) Velocity profile at test section of the NCEL wind tunnel.

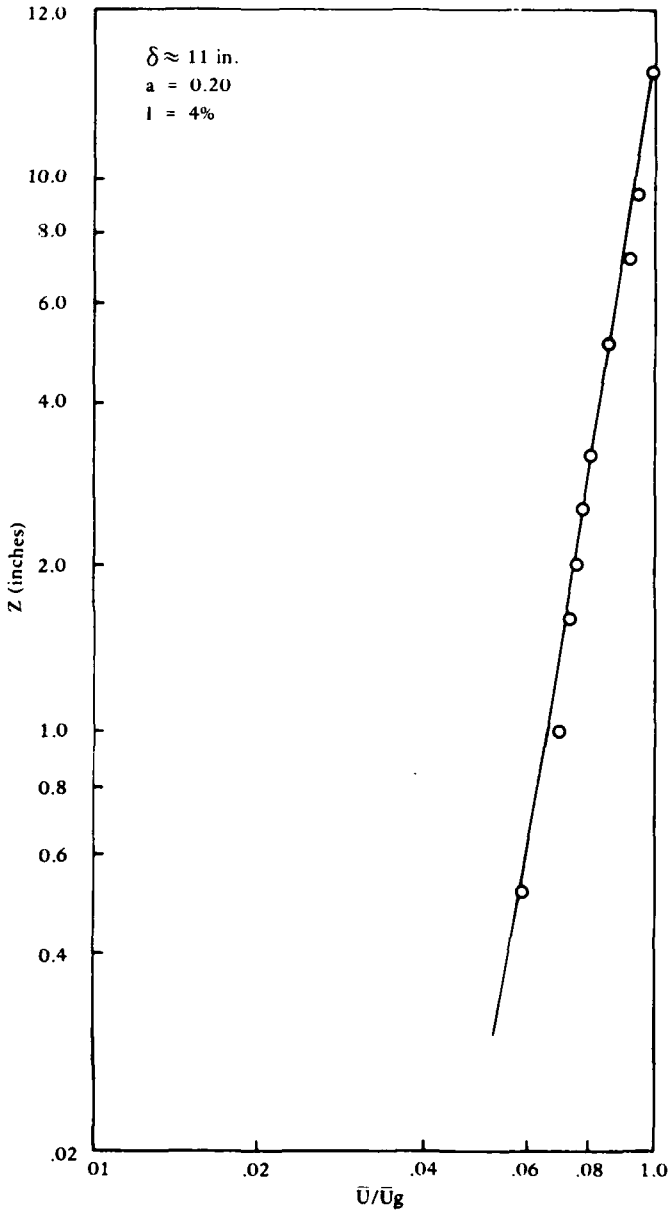

(b) Determination of boundary layer thickness.

Figure 27. Wind velocity profiles.

Reynolds number similarity requires that the quantity UD/ν (wind speed x diameter/kinematic viscosity) be similar for model and prototype. Since ν is identical for both, the Reynolds number cannot be made precisely equal with reasonable wind velocities. Wind velocity in the wind tunnel would have to be the model scale factor times the prototype wind. However, for a high Reynolds number ($> 10^5$) a pressure coefficient at any location on the structure will be essentially constant with Reynolds number. A value $\bar{>} .011 \times 10^6$ in the wind tunnel (Ref 16) will meet the requirement.

The building Reynolds number for all models ranged from $.03 \times 10^6$ to $.14 \times 10^6$ with a boundary layer thickness of at least twice the building model height.

Instrumentation and Data Acquisition

Airflow Visualization. Airflow visualization in the vicinity of the model is helpful in understanding and interpreting mean and fluctuating pressures, in defining zones of separated airflow, and reattachment where pressure coefficients can be expected to be high. Mineral oil smoke was produced by a smoke generator, Figure 28, and was released from a source near the model. Video tape records and photographs were made. Conclusions obtained from these smoke studies are discussed later.

Pressures. Pressure and interior and exterior windspeed measurements were measured by strain gage pressure transducers, hot-wire anemometers, and a 32-channel intelligent data logger (Figure 29). The pressures measured were the difference between instantaneous local pressure at a location on a building and the static pressure in the ambient airflow over the models. Mean pressure coefficients were averaged over an entire side of a model. The average pressure coefficient used was defined by:

$$\bar{C}_p = \frac{\overline{P-P_o}}{0.5\,\rho\,U_R^2} \qquad (7)$$

where: $\bar{C}_p$ = average pressure coefficient

P = pressure at location on the building

P_o = local static pressure

ρ = density of air

U_R = windspeed at site at roof level

The average pressure difference coefficient, $\Delta\bar{C}_p$ calculated as follows:

$$\Delta\bar{C}_{p_{J-i}} = \bar{C}_{p_J} - \bar{C}_{p_i} \quad (8)$$

where: i, J = subscripts for opposite sides of the model

$\bar{C}_{p_i}, \bar{C}_{p_J}$ = average pressure coefficient for each side

Data were obtained from six to nine different wind directions from 0 to 90 degrees. Model 1, Building No. 1 at MCAS, Hawaii, was placed in an isolated and sheltered environment with and without wall openings. Model 2, Building No. 2 at MCAS, Hawaii, was placed in an isolated environment with no adjacent structures present, with and without wall openings and carports and was elevated. Model 3, the two-story home at MCAS, Hawaii, was placed in an isolated environment with and without wall openings. Interior airspeeds and pressures were measured for each wind direction for Models 2 and 3.

Wind Tunnel Test Results

Airflow Visualization. Smoke was used to make the airflow visible. The characteristics of the airflow around and through the models are shown in Figures 30 through 32.

With the airflow approaching 32 degrees to the east side of Model 1, Figure 30a, the high velocity airflow passed around the corner. The effect of a two-story building located behind Model 1 is shown in Figures 30b through 30g. The airflow between the two buildings was turbulent and a slightly positive pressure on the upper east side of the leeward long side was observed. This caused a reduction on ventilation rates through Model 1.

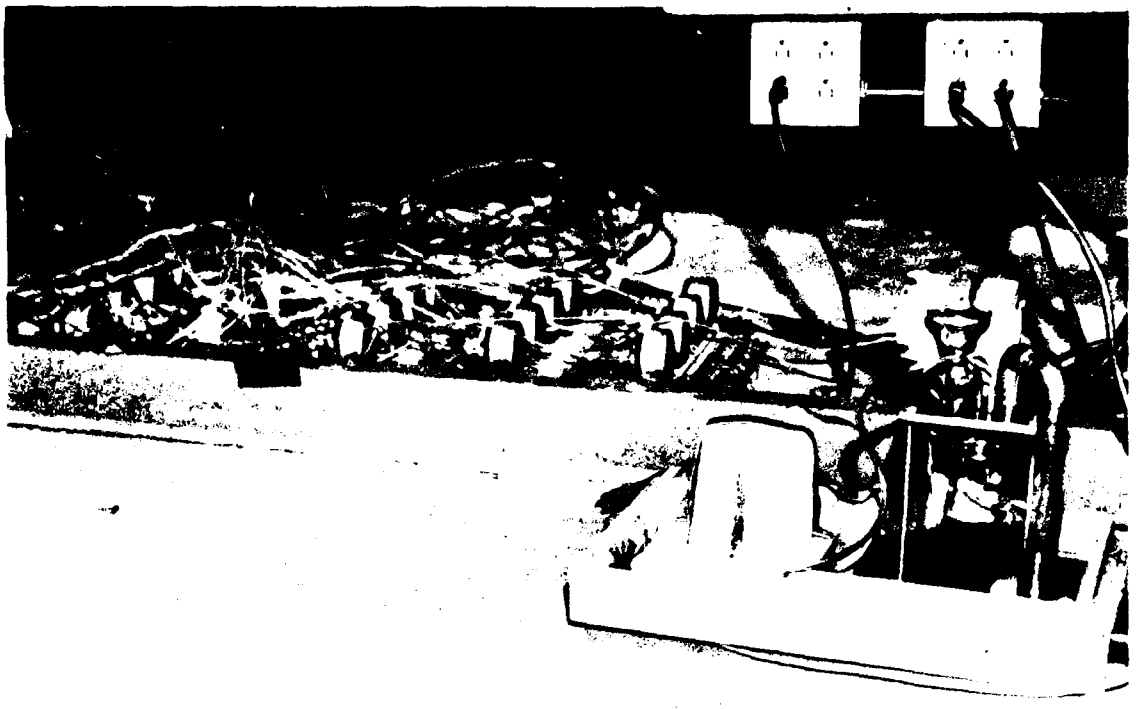

Figure 28. Smoke generator and strain gage pressure transducers.

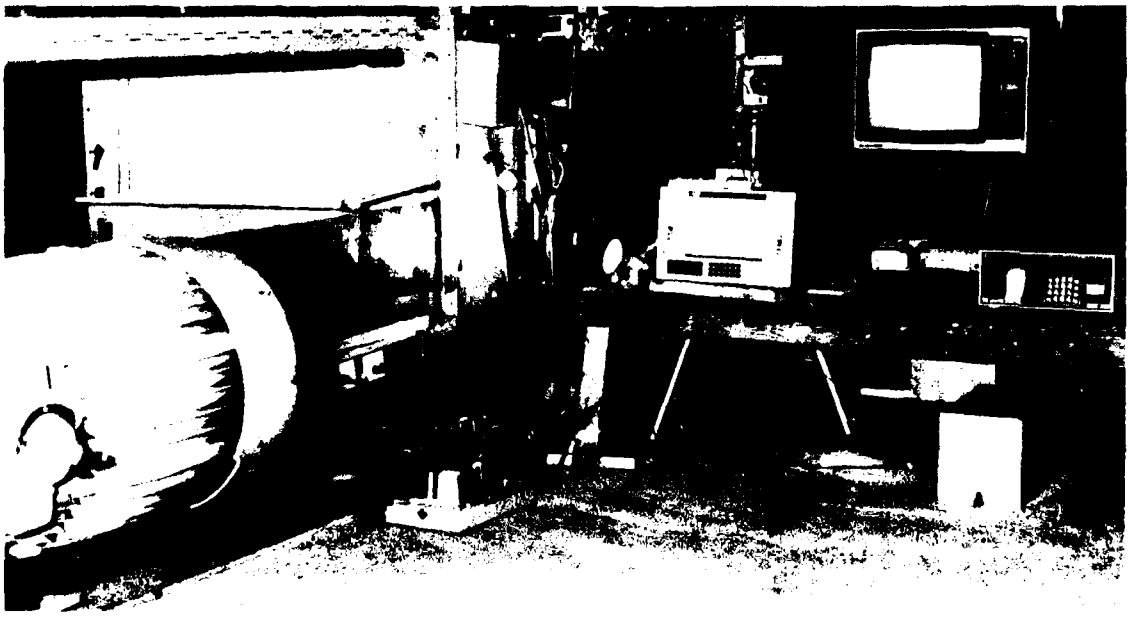

Figure 29. K-data logger, JVC color video camera, cassette recorder, and TV monitor used to measure pressure and inside and outside windspeeds.

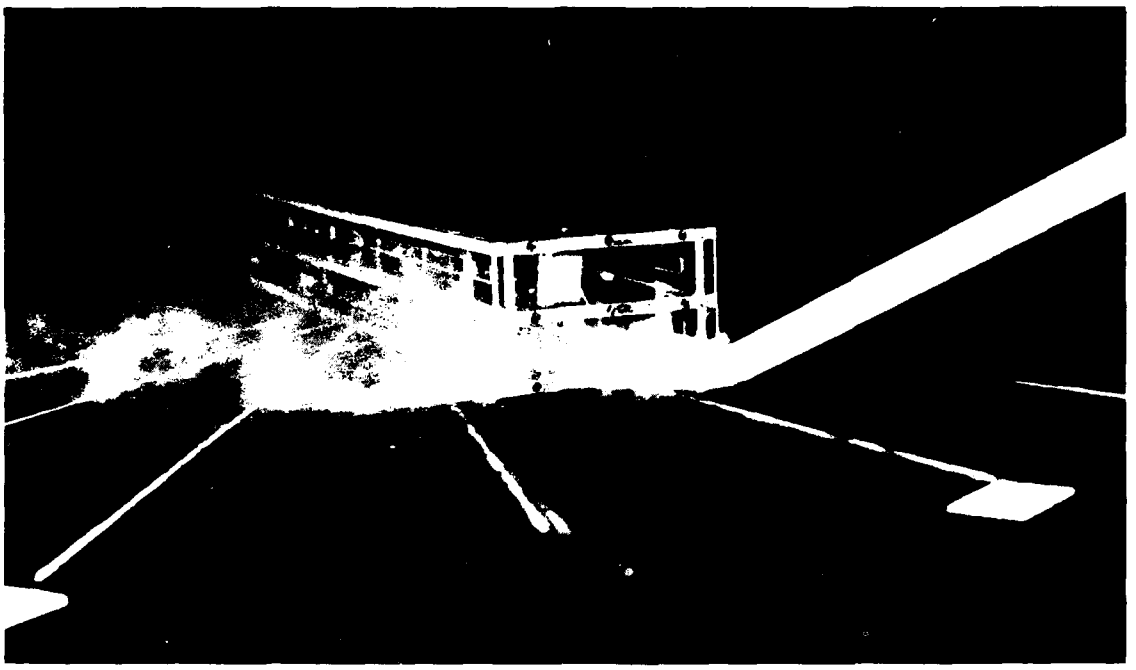

(a) Airflow around Model 1, isolated (windows opened).

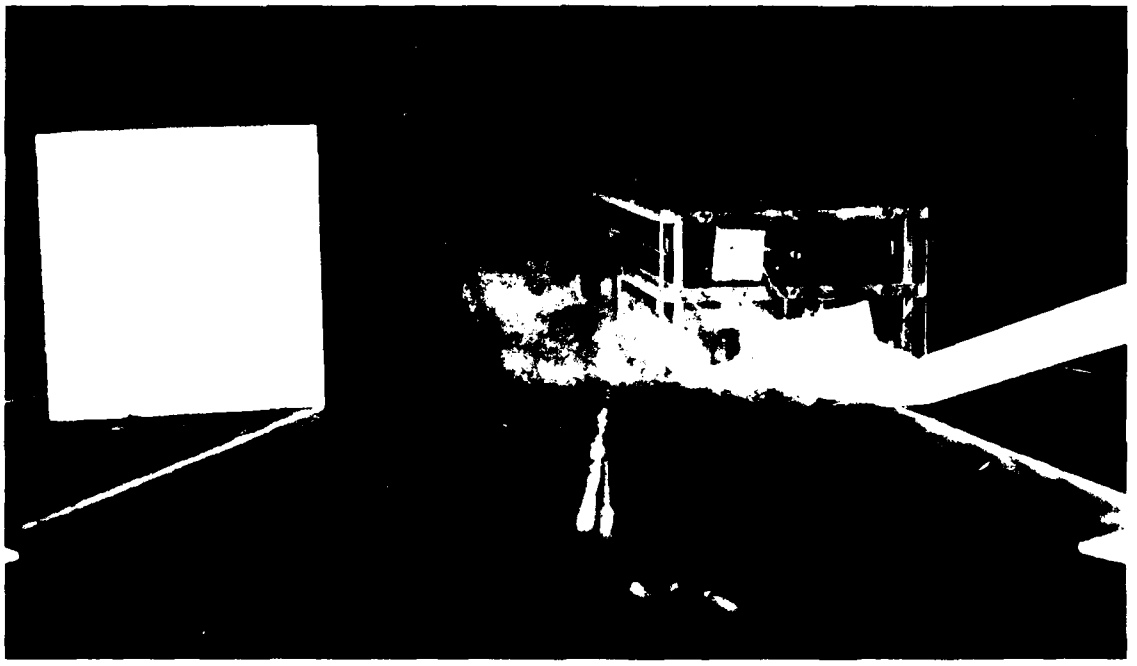

(b) Effect of neighboring building on the airflow around Model 1. Distance between models is 2-1/2 the height of Model 1 (windows opened).

Figure 30. Smoke tests of Model 1. Model 1 was tested with windows opened and closed, isolated and sheltered, with wind incidence of 60 degrees to long wall (α = 30 degrees).

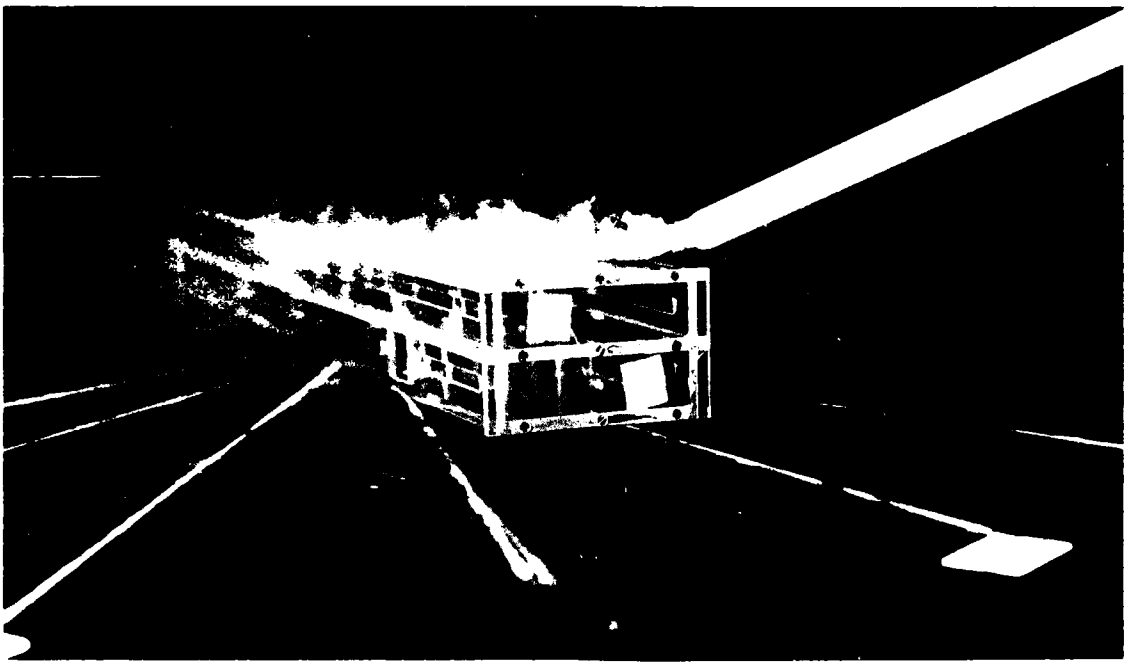

(c) Airflow over the roof of Model 1, isolated (windows opened).

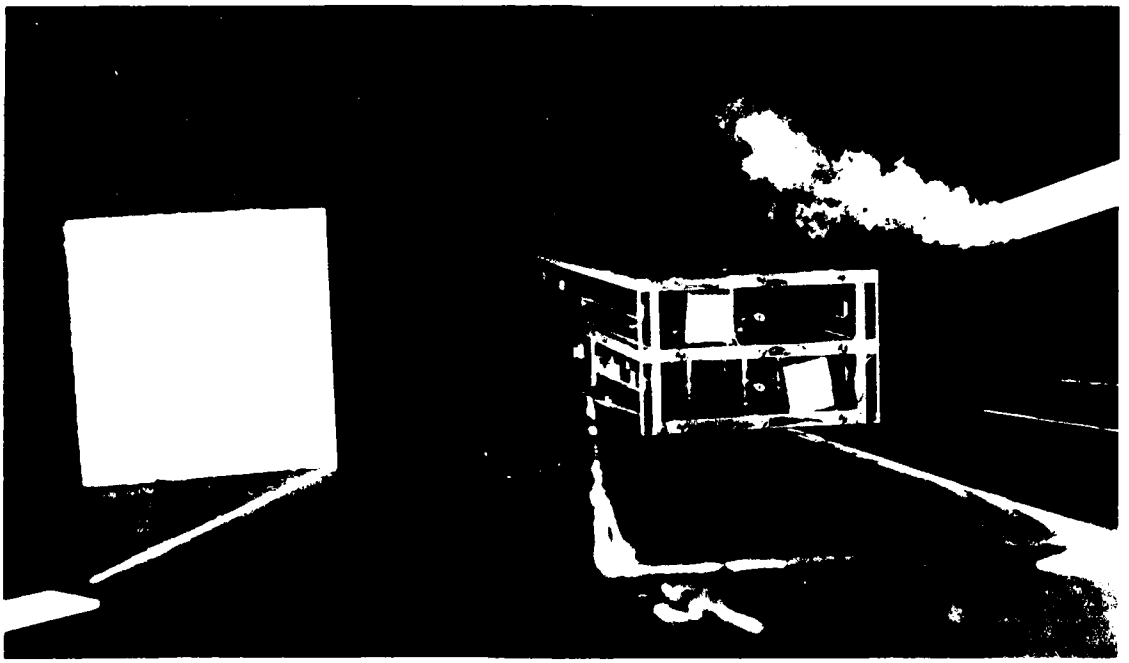

(d) Effect of neighboring building on airflow over the roof of Model 1 (windows opened).

Figure 30. Continued.

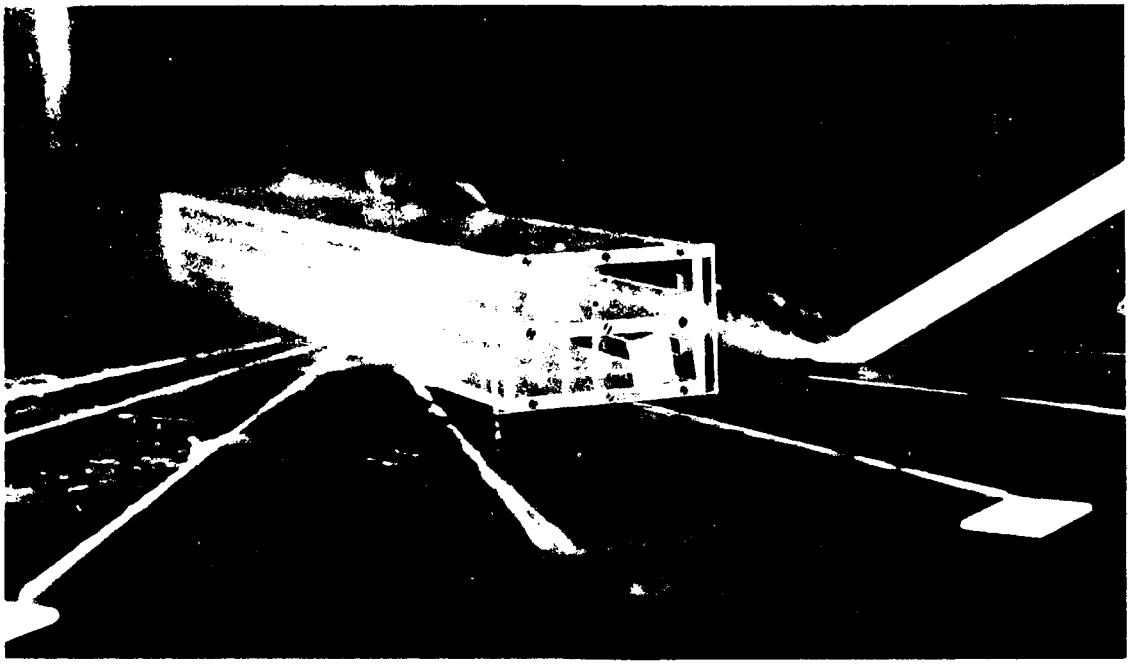

(e) Airflow around Model 1 from long windward side, isolated (windows opened).

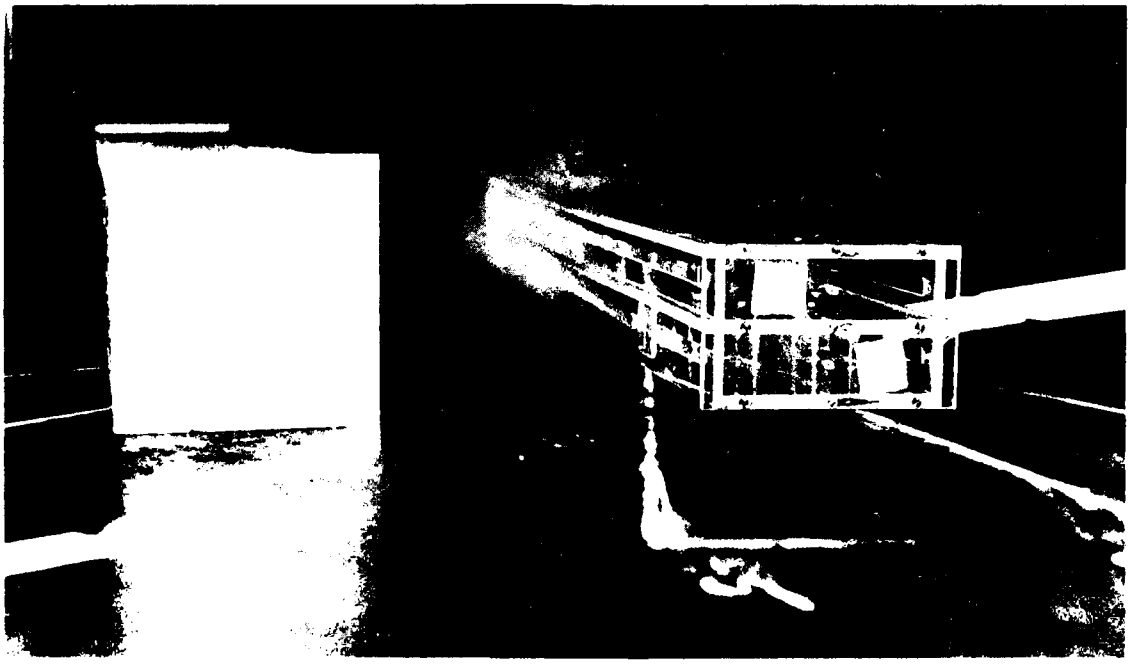

(f) Effect of neighboring building on airflow over Model 1, (windows opened).

Figure 30. Continued.

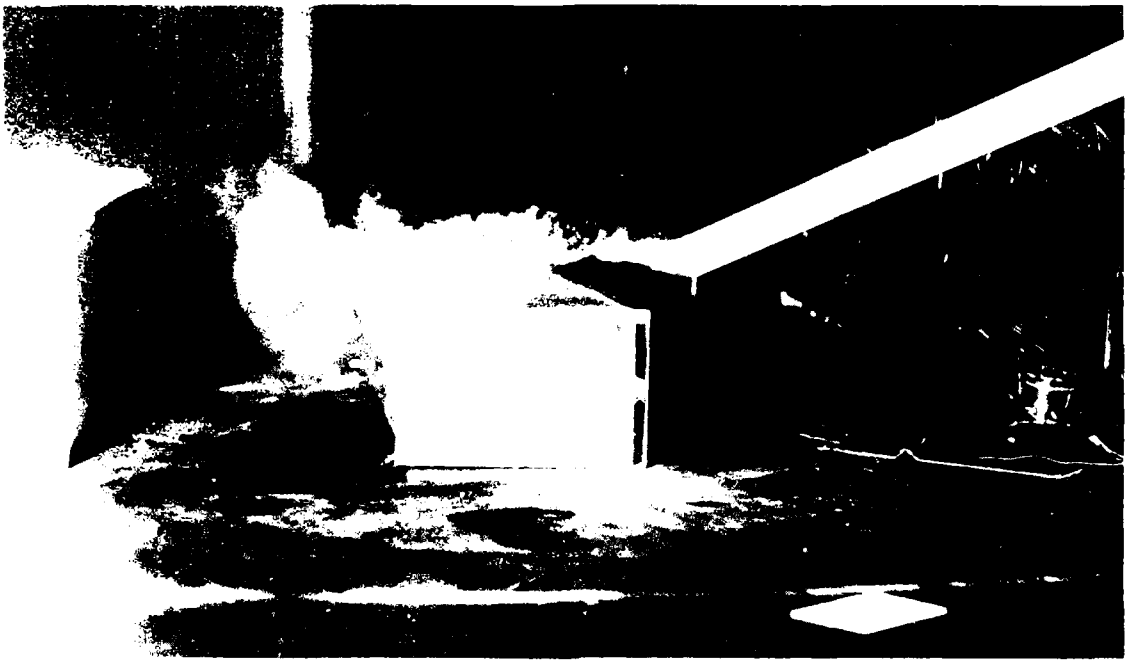

(g) Airflow over the roof of Model 1, sheltered (windows closed).

Figure 30. Continued.

Model 2 smoke test showed that the airflow was attached on the windward side of the roof and separated on the leeward side as seen in Figures 31a, b, c, and d. Also, the effects of carports on airflow was small, which indicates that the ventilation rates were not greatly affected. The airflow around Model 3 was generally well behaved. The reattachment zone occurred over the small living room window on the east side; hence, it tended to increase the ventilation rates of the upper and lower east apartments, as seen in Figures 32a through e. In general the model tests agreed with the field tests.

Pressure. For each of the pressure ports examined, the data recorded were analyzed and a mean pressure coefficient, $\bar{C}_p$ was obtained. This coefficient represents the mean of the instantaneous pressure difference between building pressure ports and static pressure in the wind tunnel outside the boundary layer nondimensionalized by the dynamic pressure, $0.5\ \rho\ U_R^2$, ahead of the model and at roof level, and averaged over a period of 30 minutes, with three instantaneous readings per minute.

(a) Airflow over Model 2 without carports, windows opened, and windward side.

(b) Airflow over Model 2 without carports, windows opened, and leeward side.

Figure 31. Smoke tests of Model 2. Model 2 was tested with windows opened, with and without carports, and with the wind incidence of 30 degrees to long windward wall (α = 60 degrees).

(c) Airflow over Model 2 with carport on windward side with windows opened (side view of Model 2).

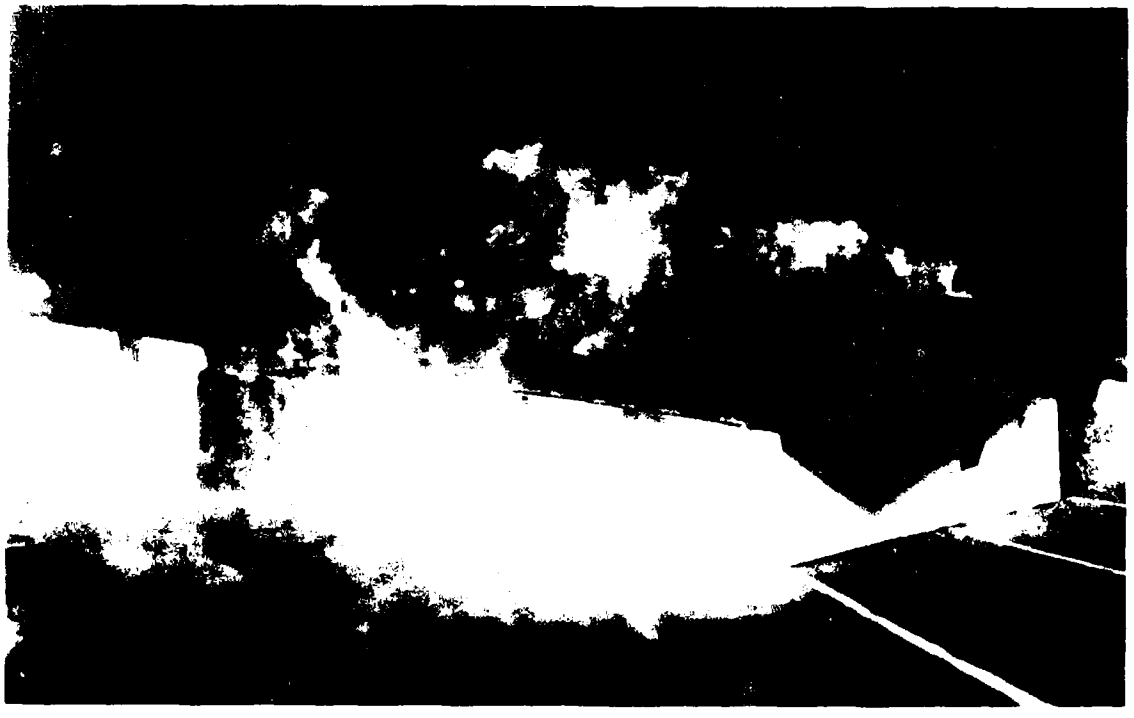

(d) Airflow over Model 2 with carport on windward side with windows opened (leeward view of Model 2).

Figure 31. Continued.

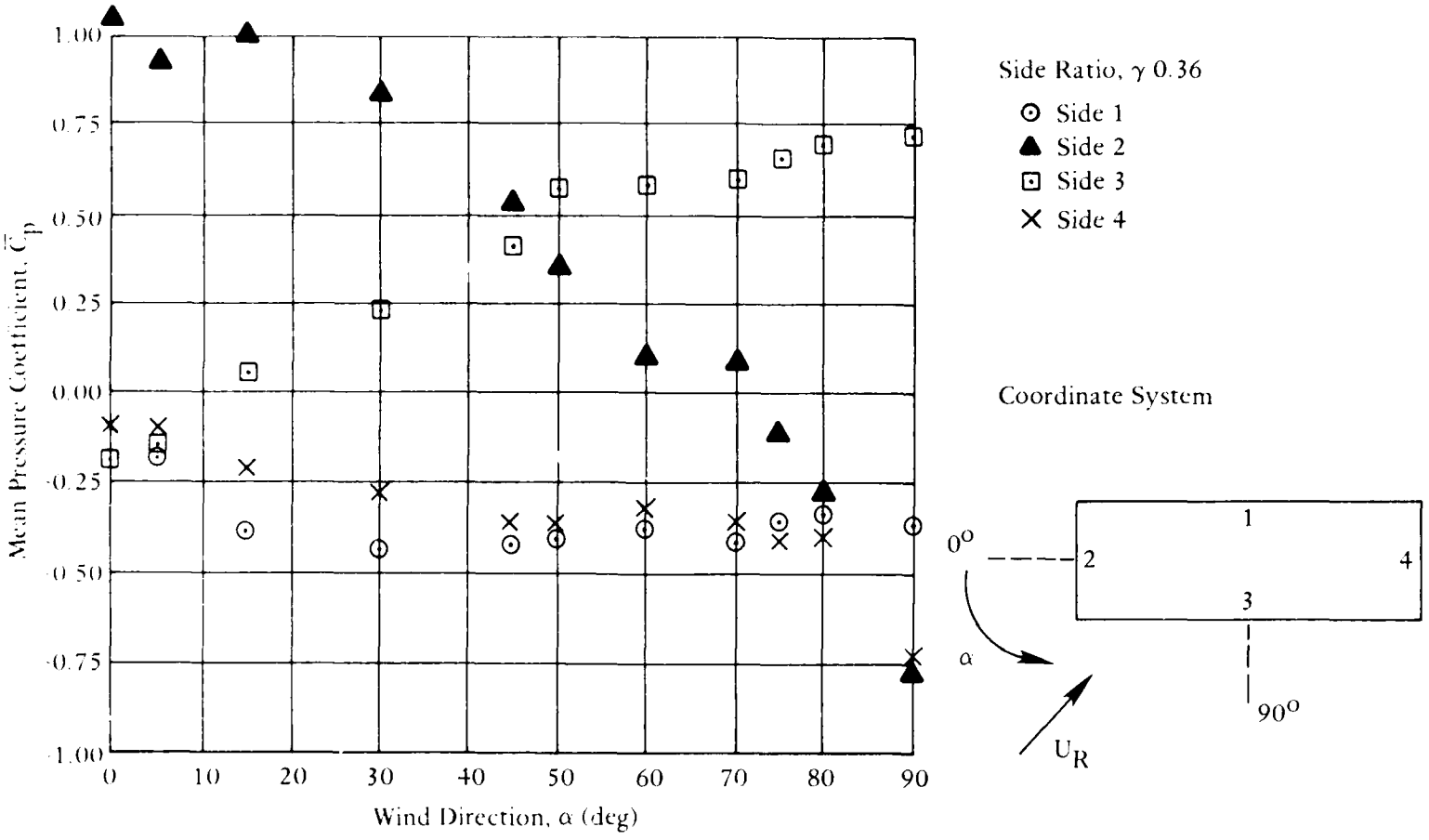

Figure 43. Mean pressure coefficient for all sides of Model 3 with the windows closed. Reference windspeed was measured at roof level.

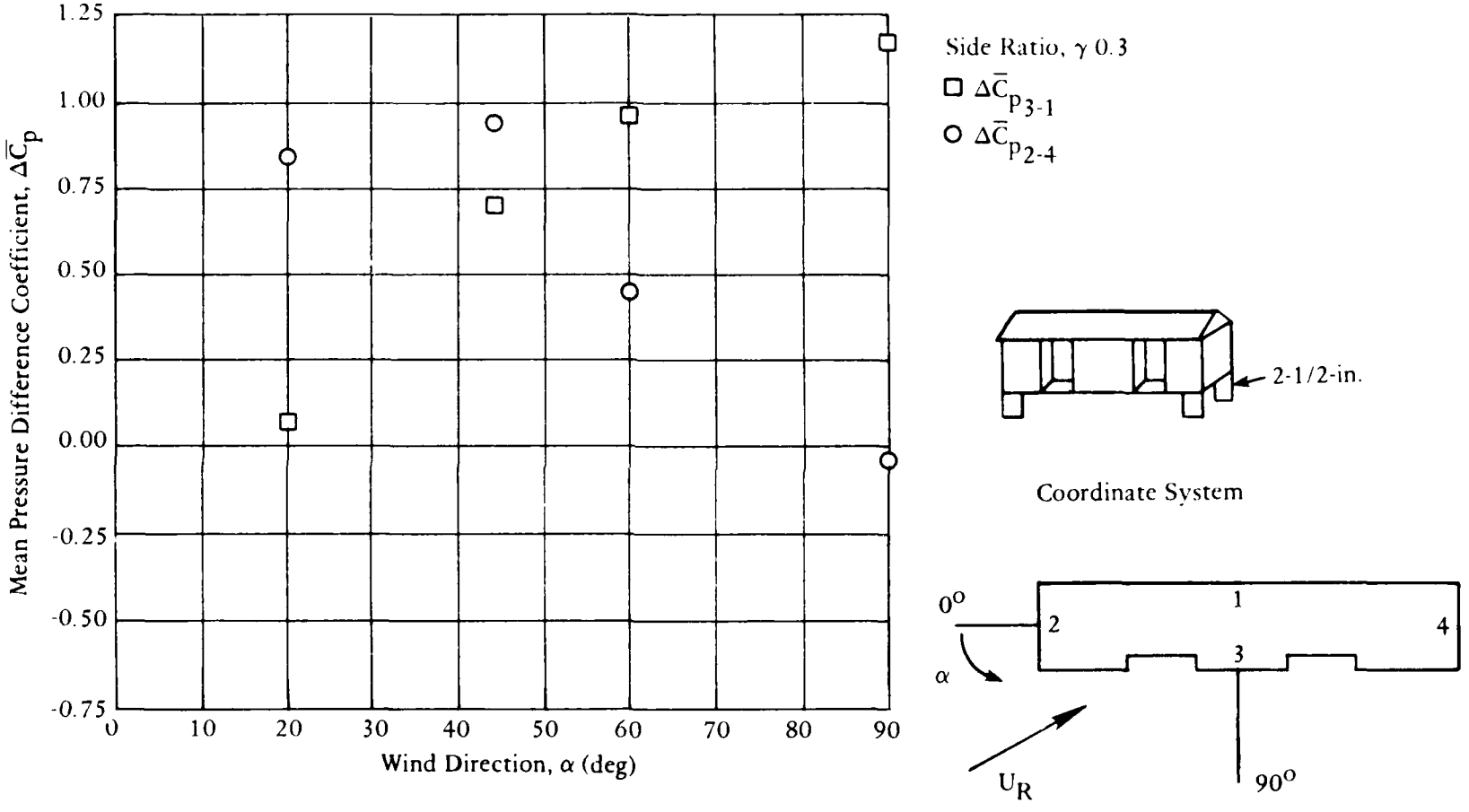

Figure 42. Mean pressure coefficient between windward and leeward sides of Model 2. Model 2 was isolated, elevated, and the windows were opened.

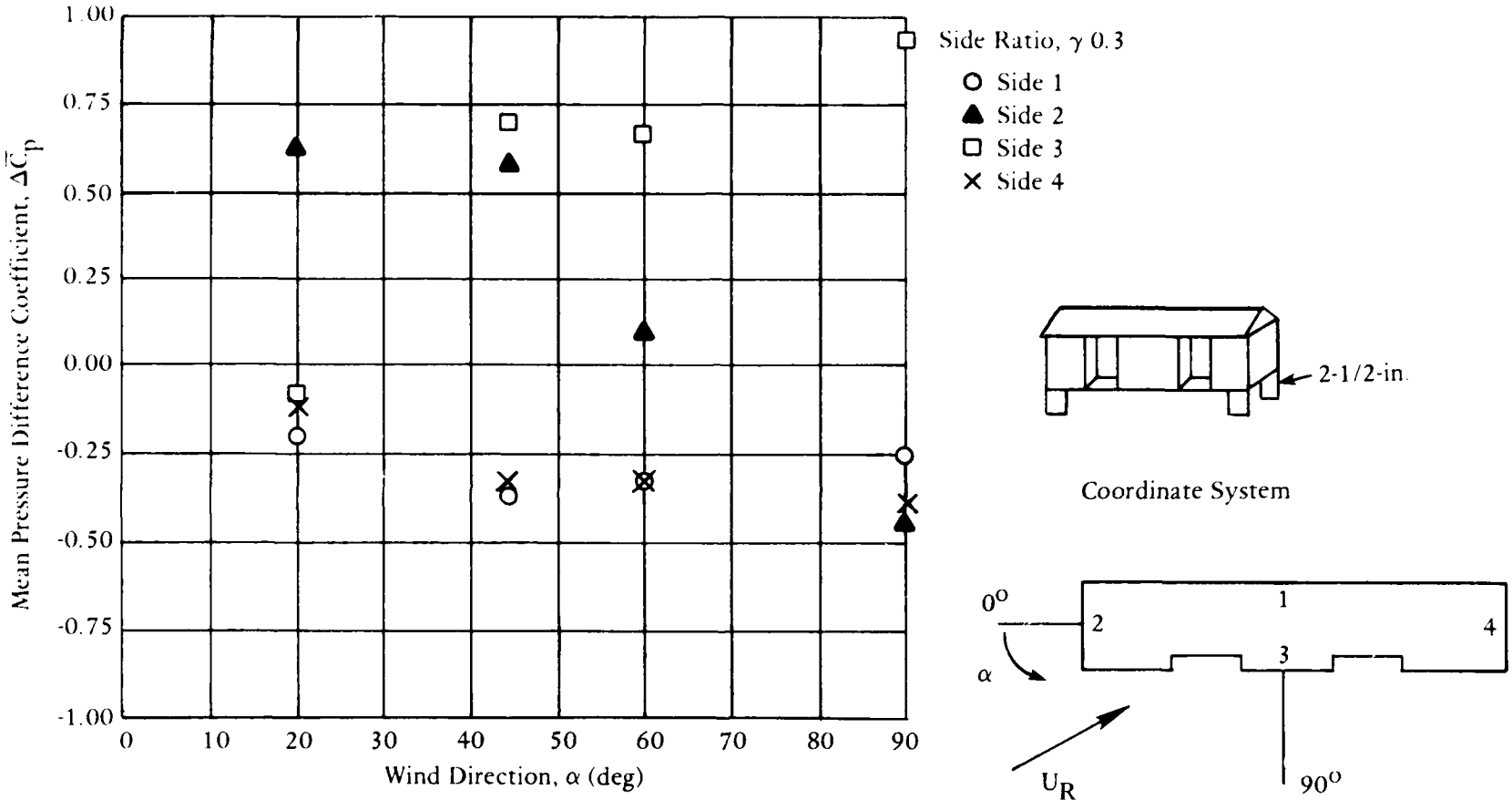

Figure 41. Mean pressure coefficient for all sides of Model 2, isolated, elevated and windows opened. Reference windspeed was measured at roof level.

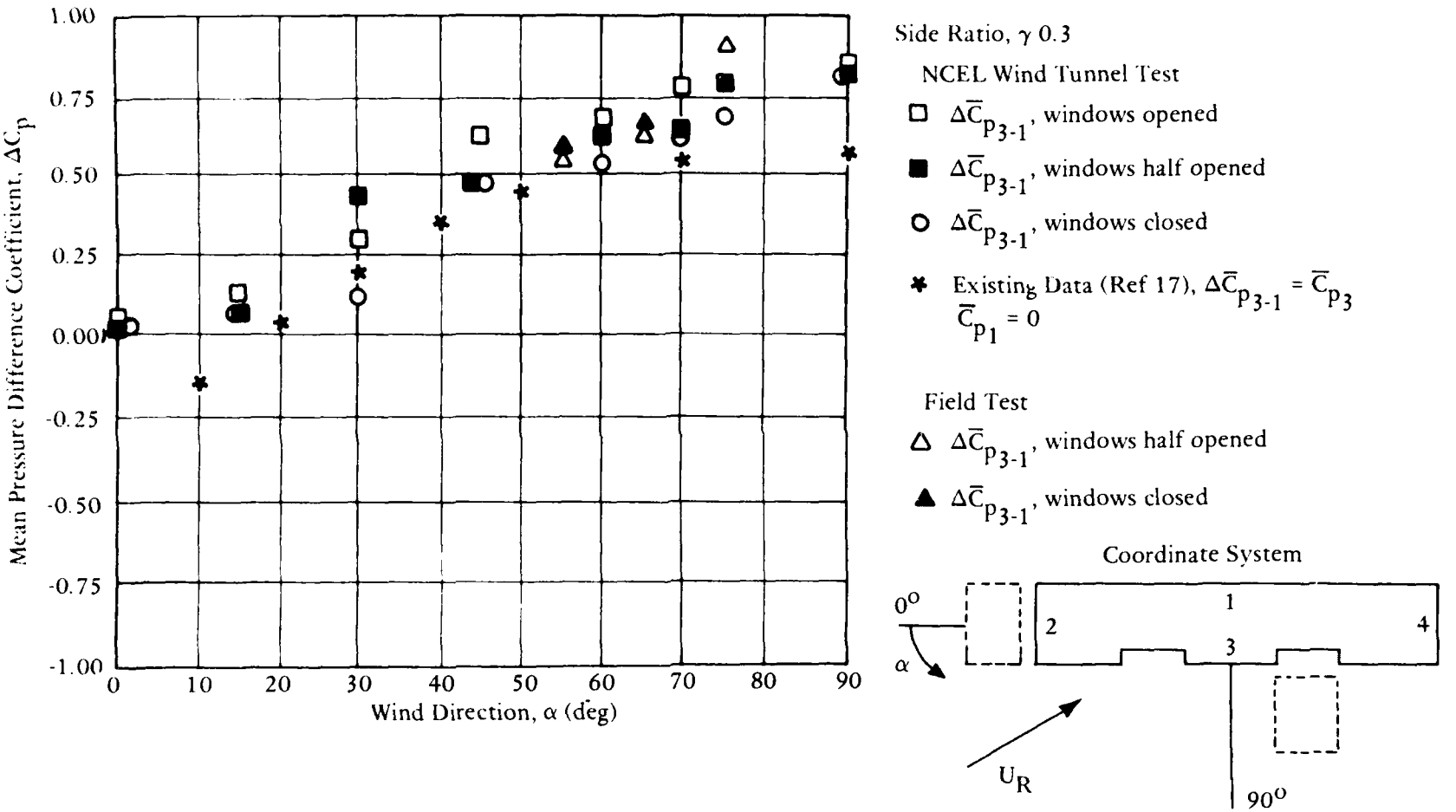

Figure 40. Comparison of wind tunnel, field test, and existing data of mean pressure coefficient between windward and leeward sides of Model 2.

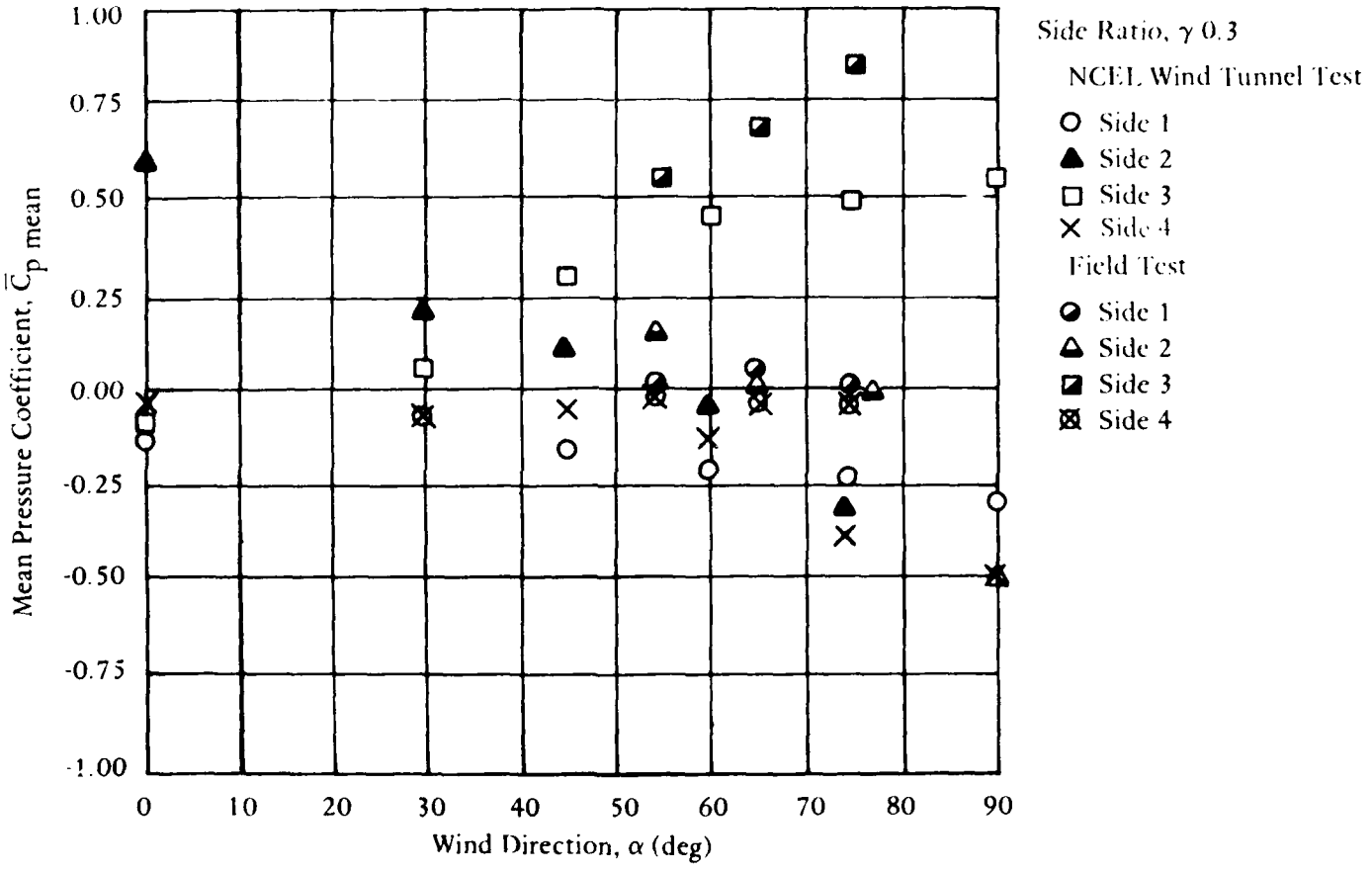

Figure 39. Comparison of wind tunnel and field test data of mean pressure coefficient based on reference windspeed measured at roof level for Model 2, the windows were opened (15%).

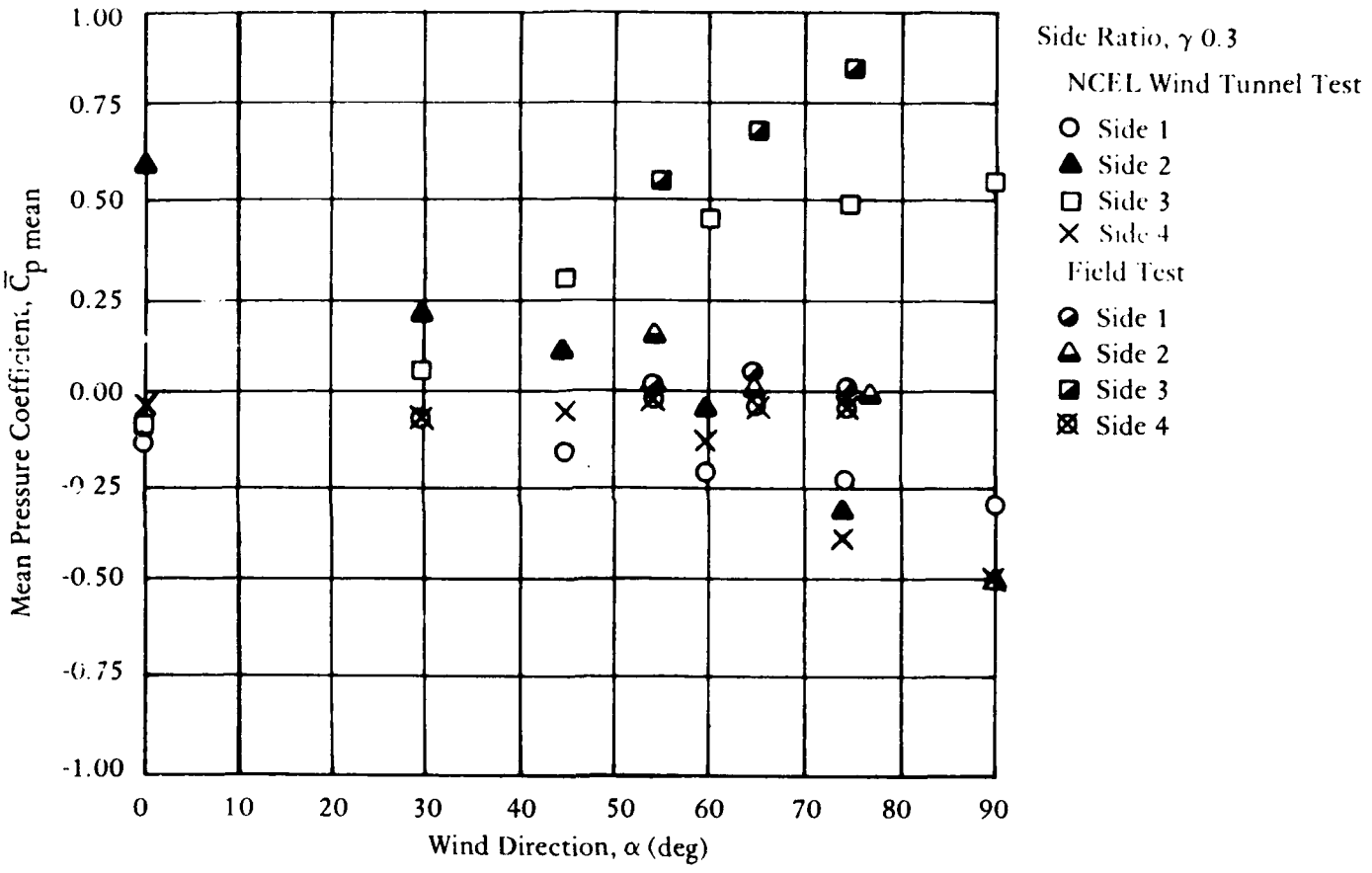

Figure 38. Comparison of wind tunnel and field test/data of mean pressure coefficient based on reference windspeed measured at roof level for Model 2, the windows were half opened (7.5%).

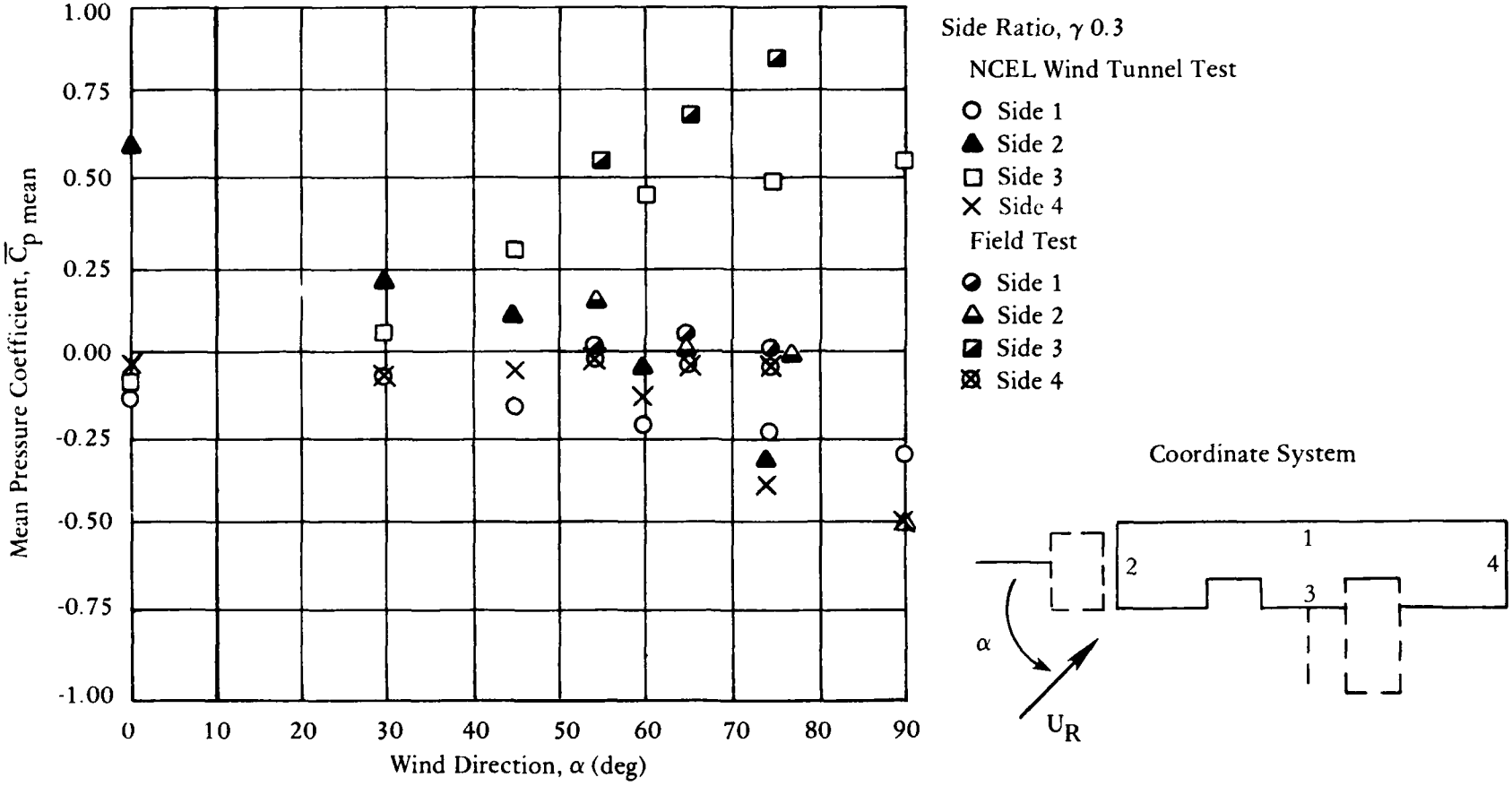

Figure 37. Comparison of wind tunnel and field test/data of mean pressure coefficient based on reference windspeed measured at roof level for Model 2, the windows were closed.

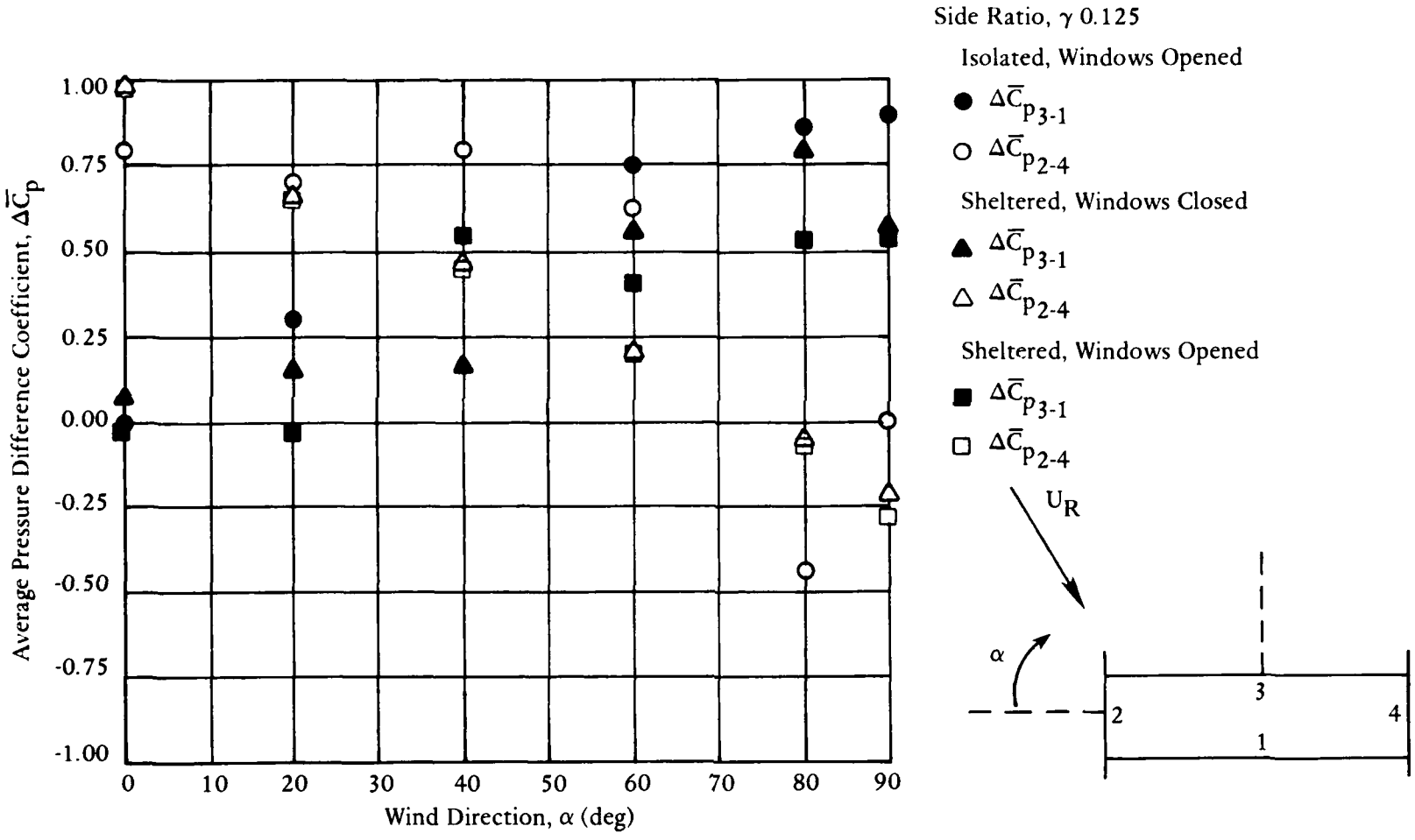

Figure 36. Average pressure difference coefficient between opposite sides of Model 1 (reference windspeed measured at roof level).

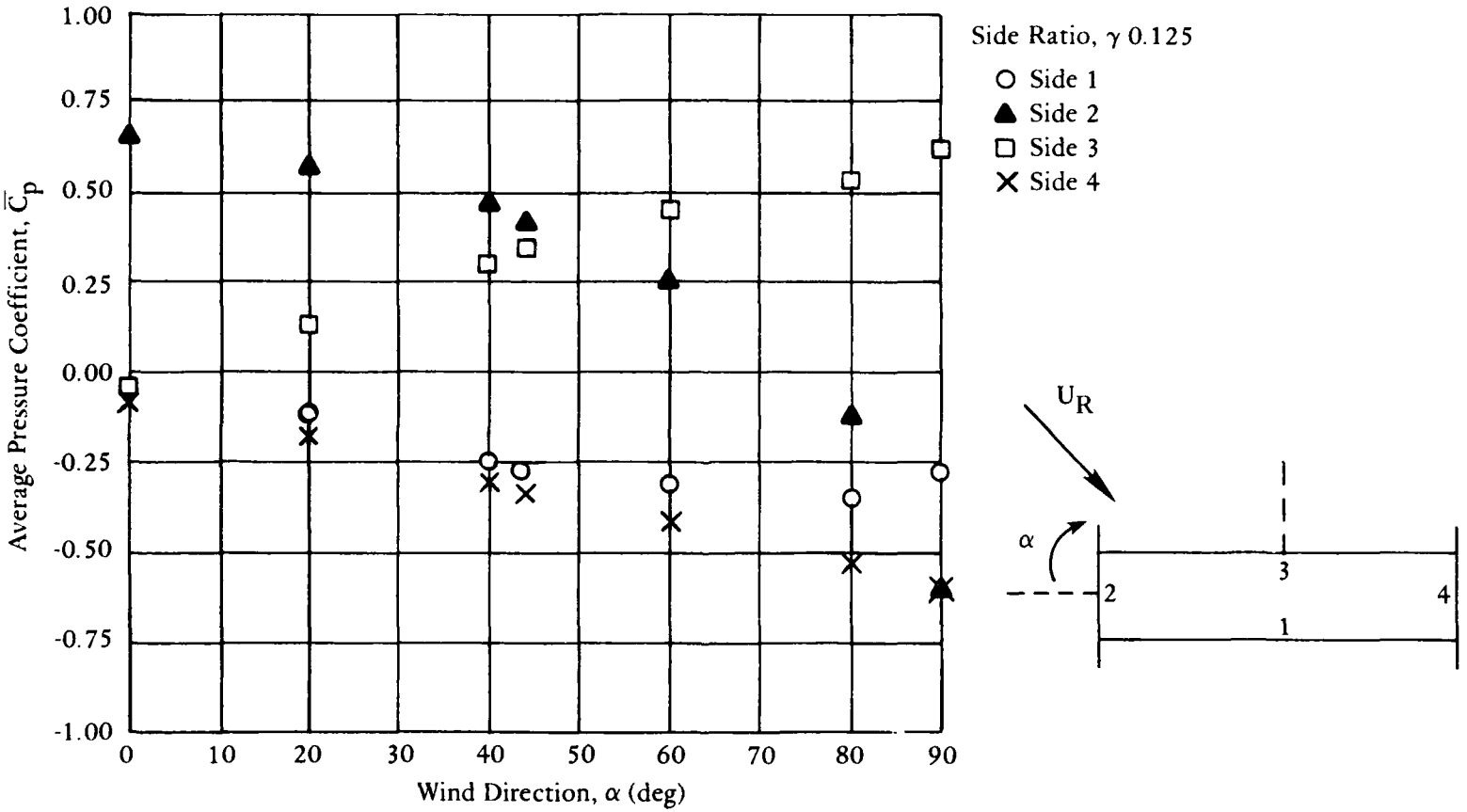

Figure 35. Average pressure coefficient of Model 1 with windows opened (opening size 40% of windward long wall, side 3) in an isolated environment (reference windspeed measured at roof level).

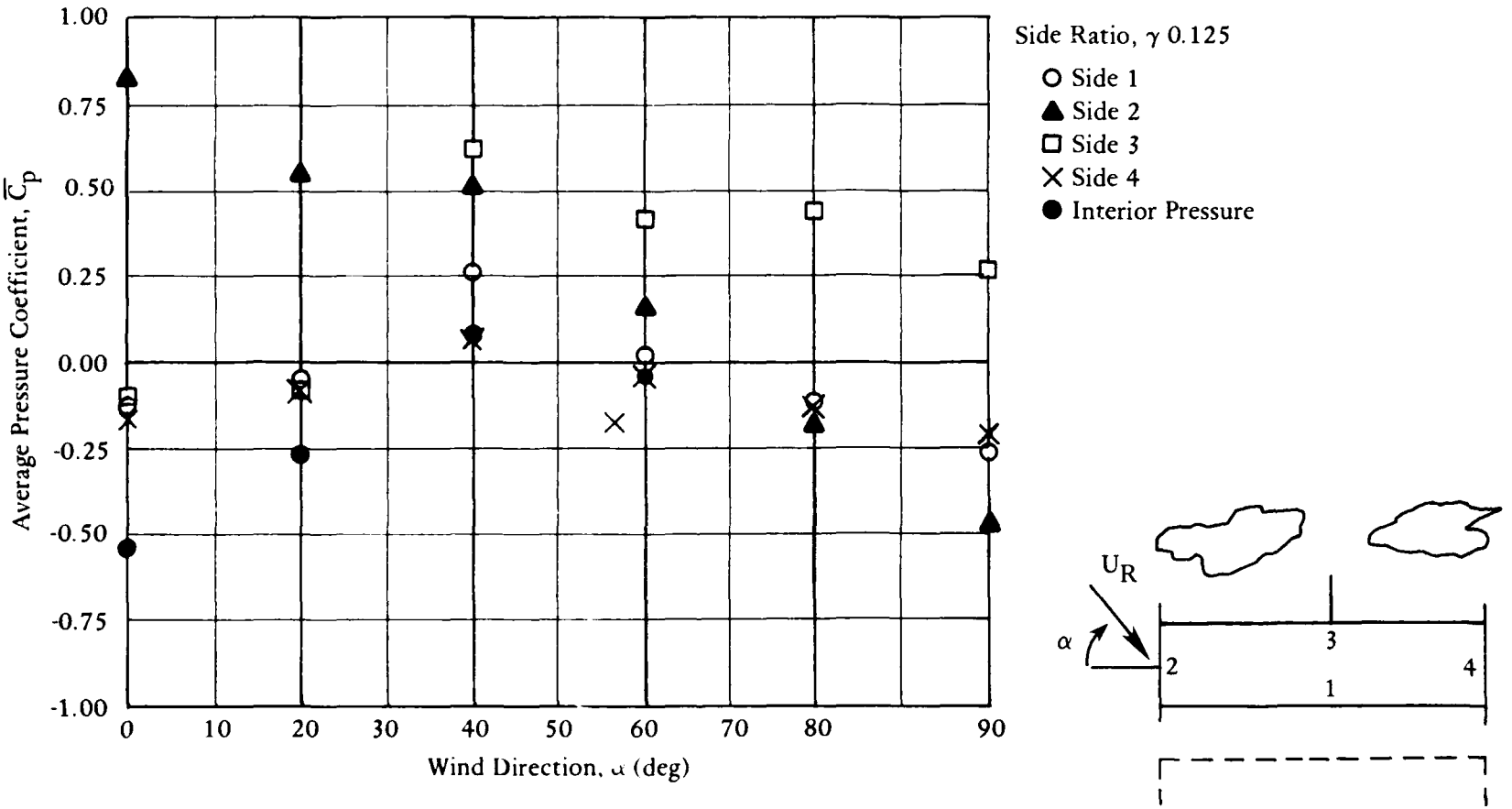

Figure 34. Average pressure coefficient of Model 1 with windows opened (opening size 40% of windward long wall, side 3) and in a sheltered environment (reference windspeed measured at roof level).

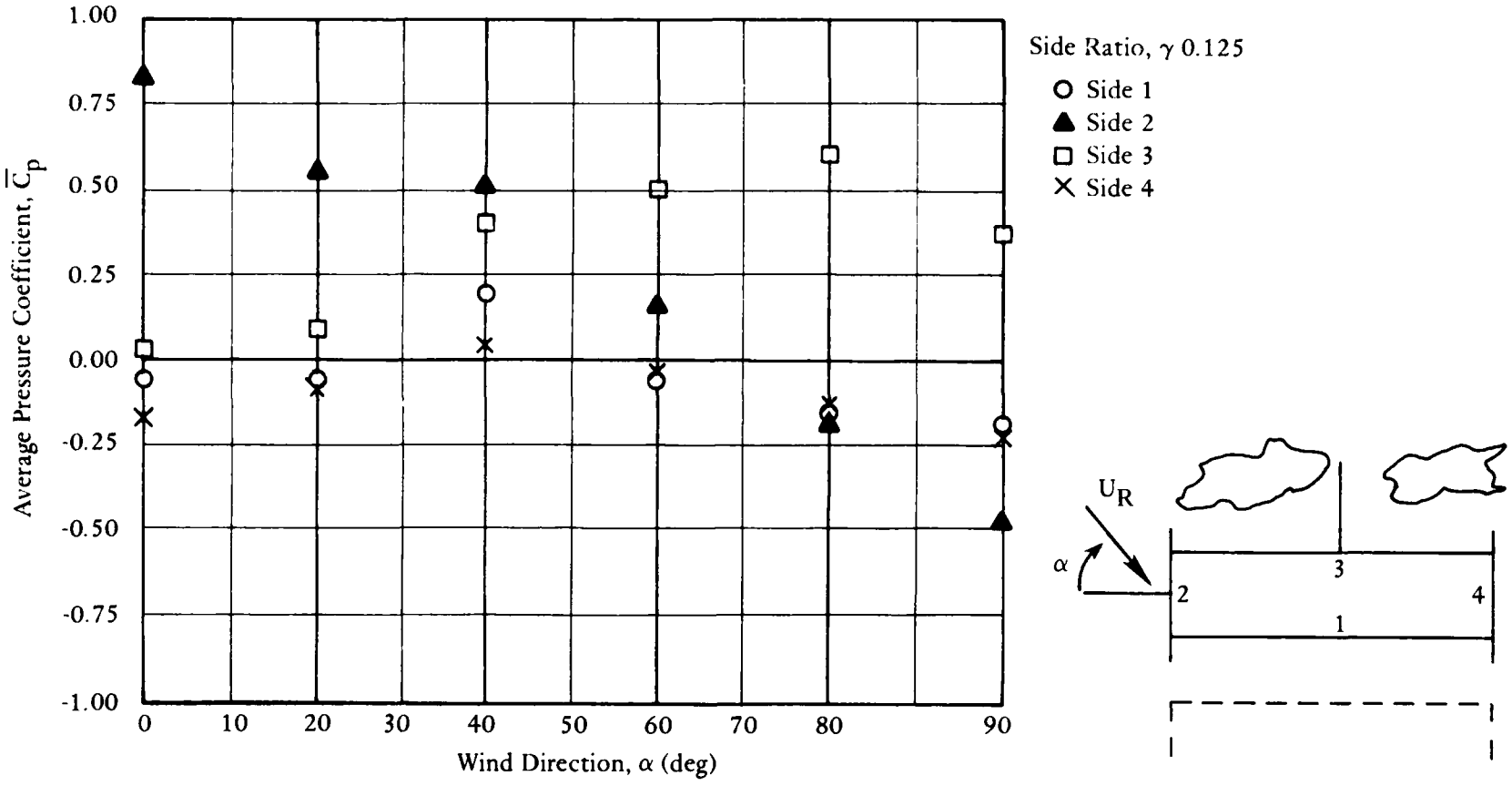

Figure 33. Average pressure coefficient for Model 1 with windows closed and in a sheltered environment (reference windspeed measured at roof level).

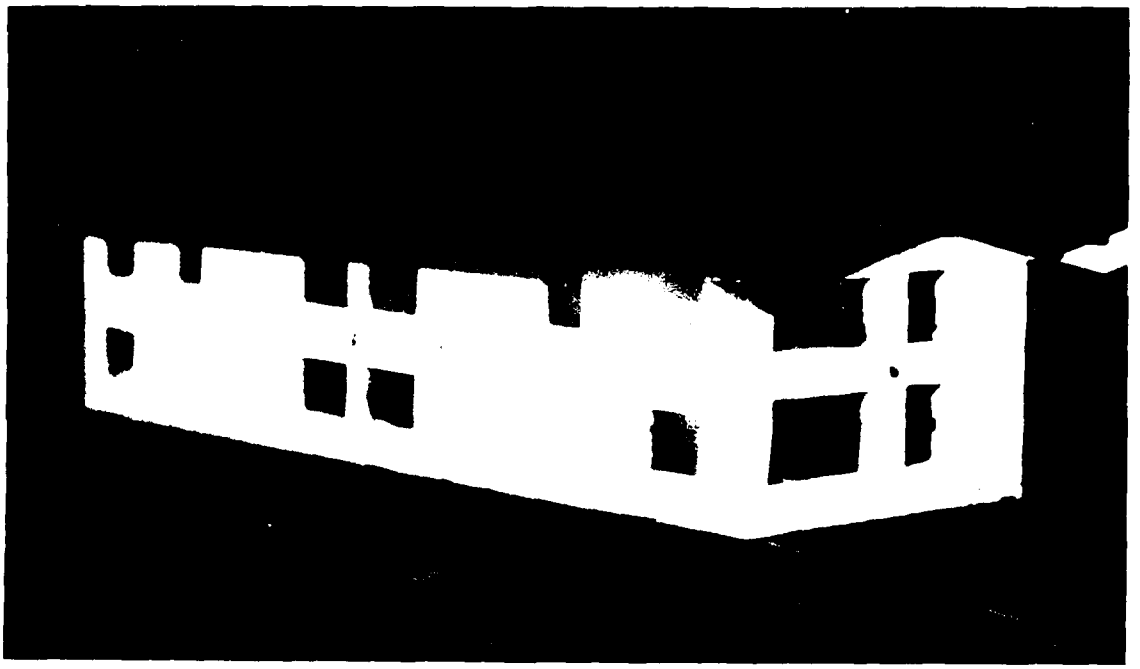

(e) Airflow over and through Model 3 (leeward side view of second floor).

Figure 32. Continued.

Mean pressure coefficients for each port, $\bar{C}_p$, were averaged for each side at mid-height, and an average pressure coefficient, $\bar{C}_p$, was obtained. These values were used to calculate the average pressure difference coefficient, $\Delta\bar{C}_{pi,j}$, between oppsite sides of the model, and for all cases.

A graphic representation of the wind tunnel test results is given in Figures 33 through 45 for all models and all cases. In addition to the wind tunnel results, results of existing data (Ref 17) and field test data are also included in some of the figures and Appendix B.

COMPARISON OF WIND TUNNEL TESTS, FIELD TESTS, AND EXISTING DATA

Since adequate wind tunnel modeling should reproduce the important aspects of the field data, the full-scale data were compared with the scale model measurements. The average pressure coefficient, $\bar{C}_p$, and the average pressure difference coefficient, $\Delta\bar{C}_p$, between opposite sides of the models as measured in the wind tunnel, are shown in Figures 37, 38, 39, 40, 45, 46, 47, and 48. The values were compared to the experimental values obtained from field tests.

(c) Airflow over Model 3 (windward view of second floor).

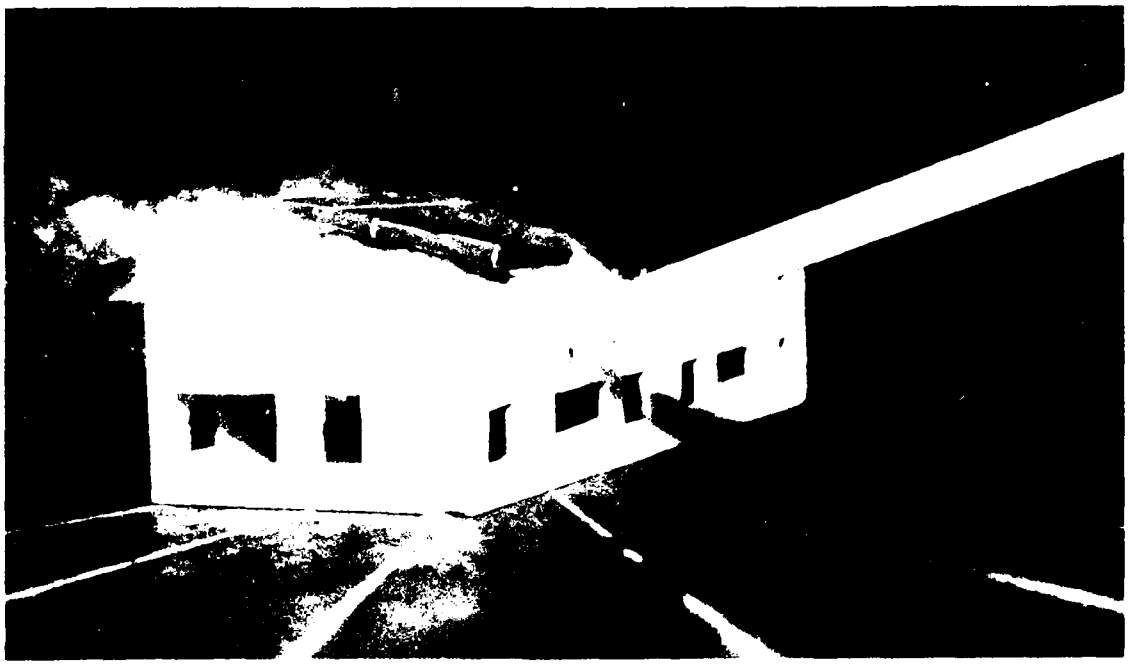

(d) Airflow over and through Model 3 (side view of second floor).

Figure 32. Continued.

(a) Airflow over and through Model 3 (windward view of first floor).

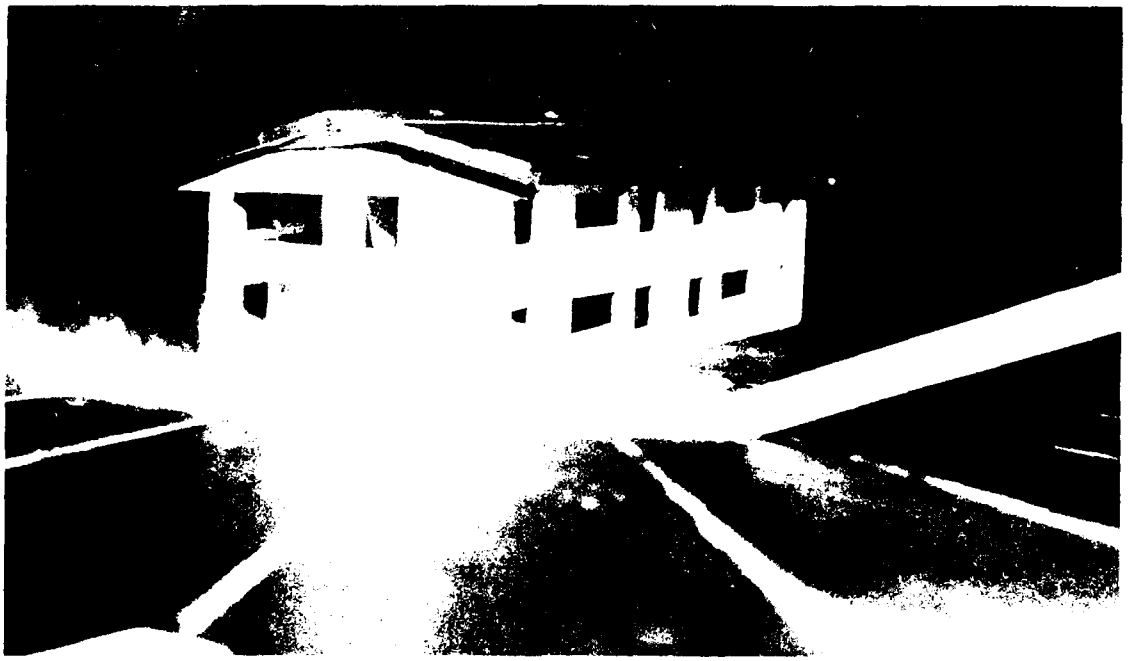

(b) Airflow around and through Model 3 (side view of first floor).

Figure 32. Smoke tests of Model 3. Model 3 was tested with windows opened. Wind incidence was 20 degrees to long windward wall (α = 70 degrees).

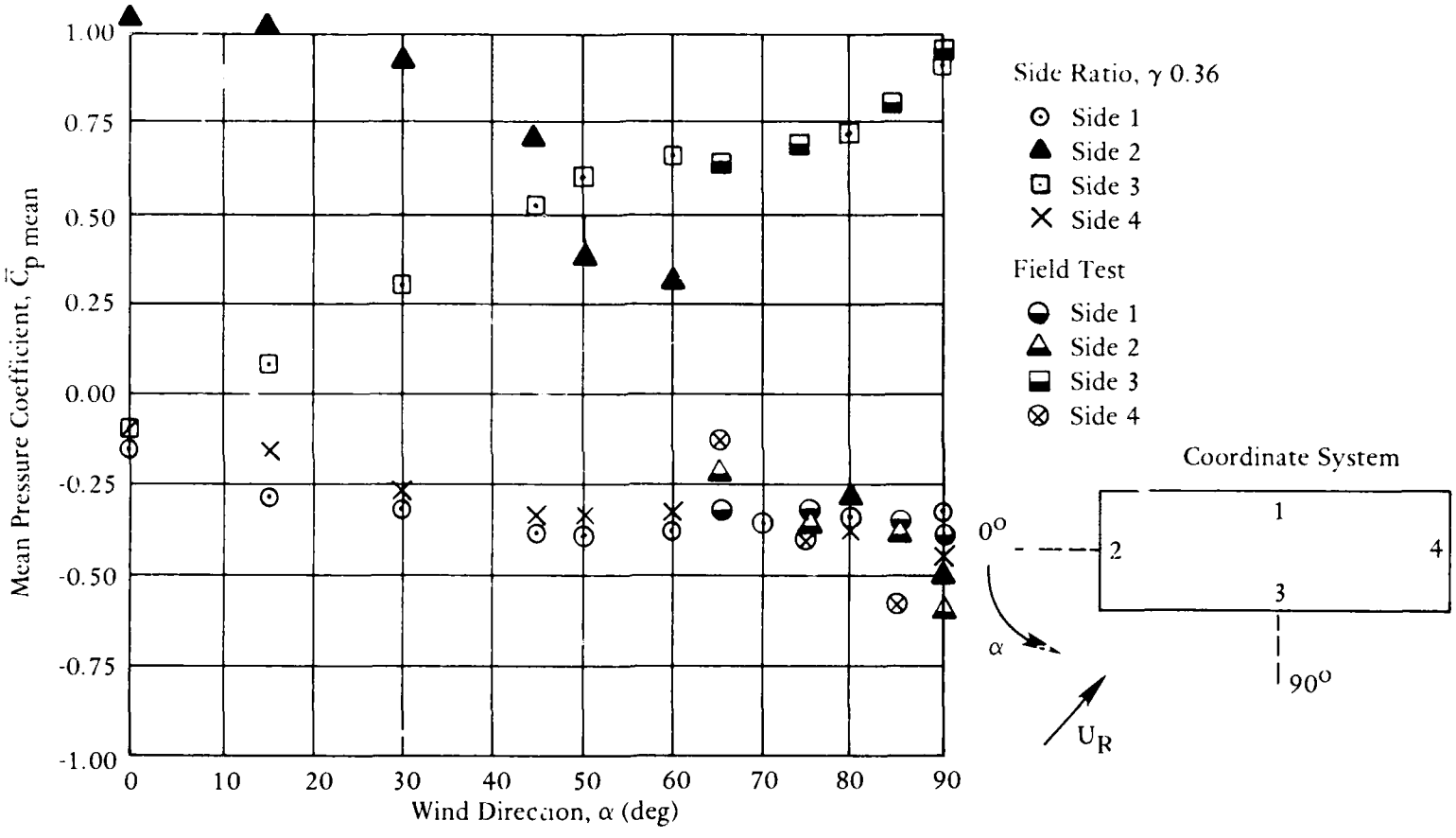

Figure 44. Mean pressure coefficient for all sides of Model 3 with windows opened. Reference windspeed was measured at roof level.

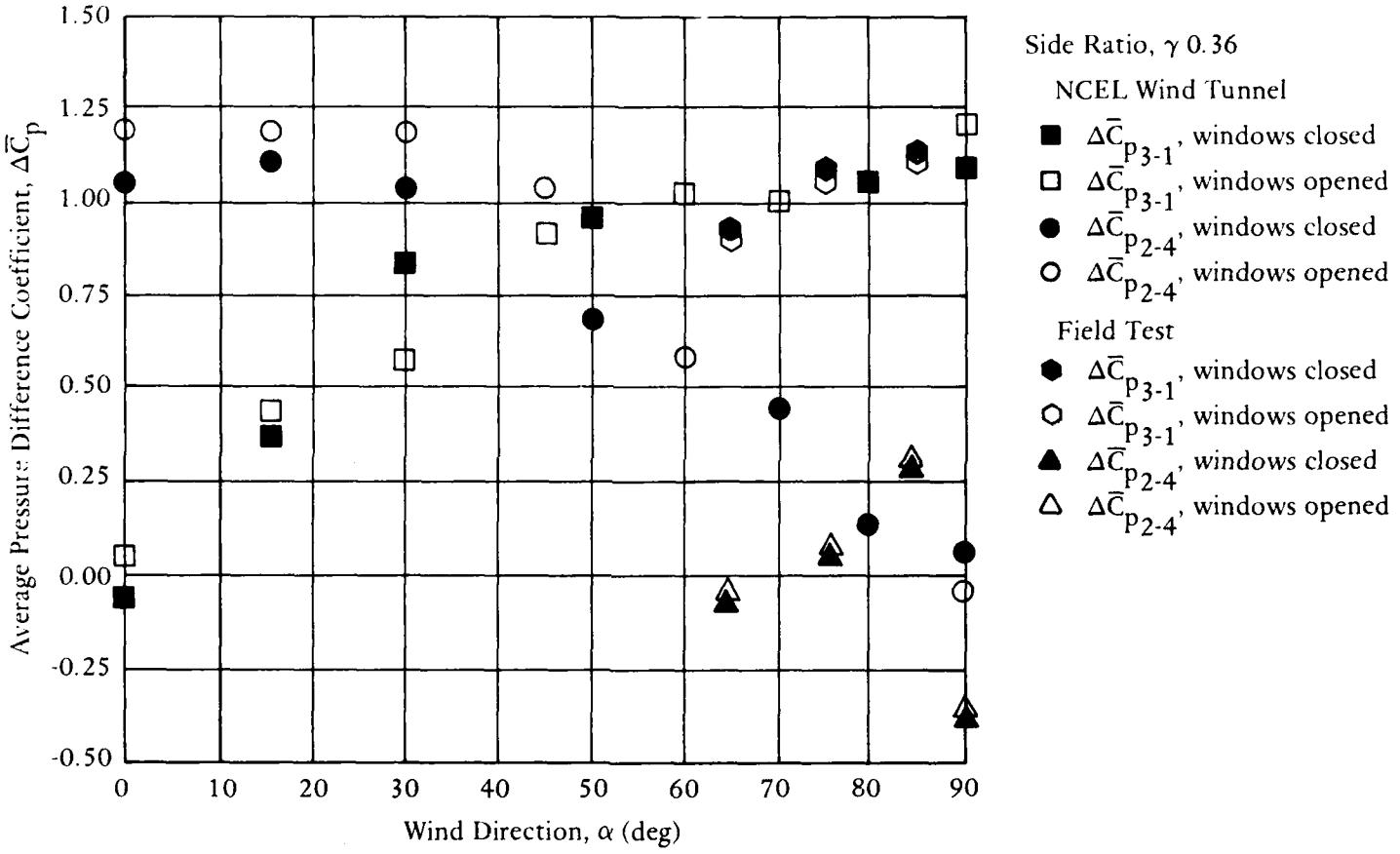

Figure 45. Comparison of wind tunnel and field test data of average pressure difference coefficient between windward and leeward sides of Model 3.

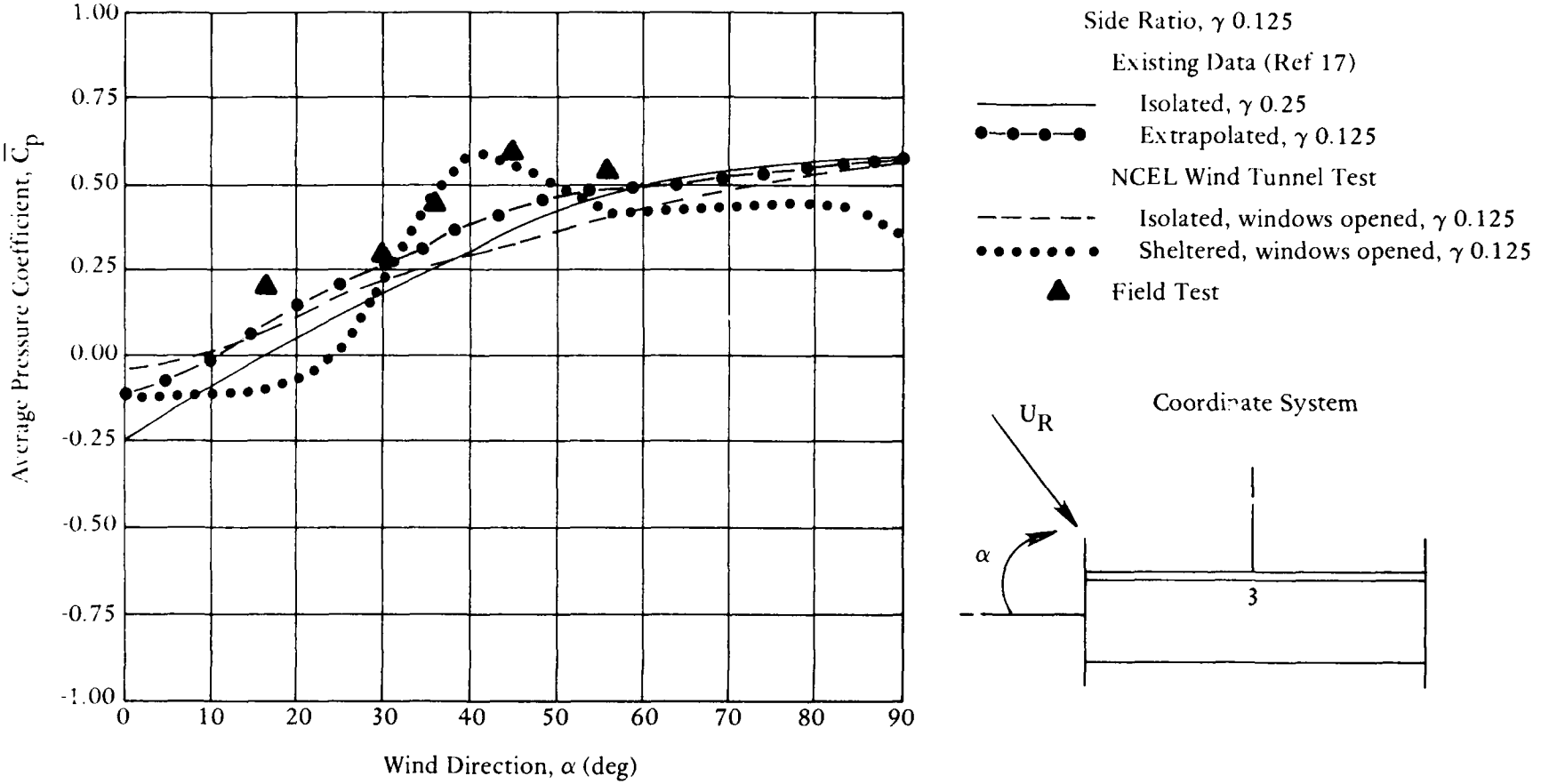

Figure 46. Comparison of wind tunnel tests, field tests, and existing data of average pressure coefficients of Model 1 (windward side).

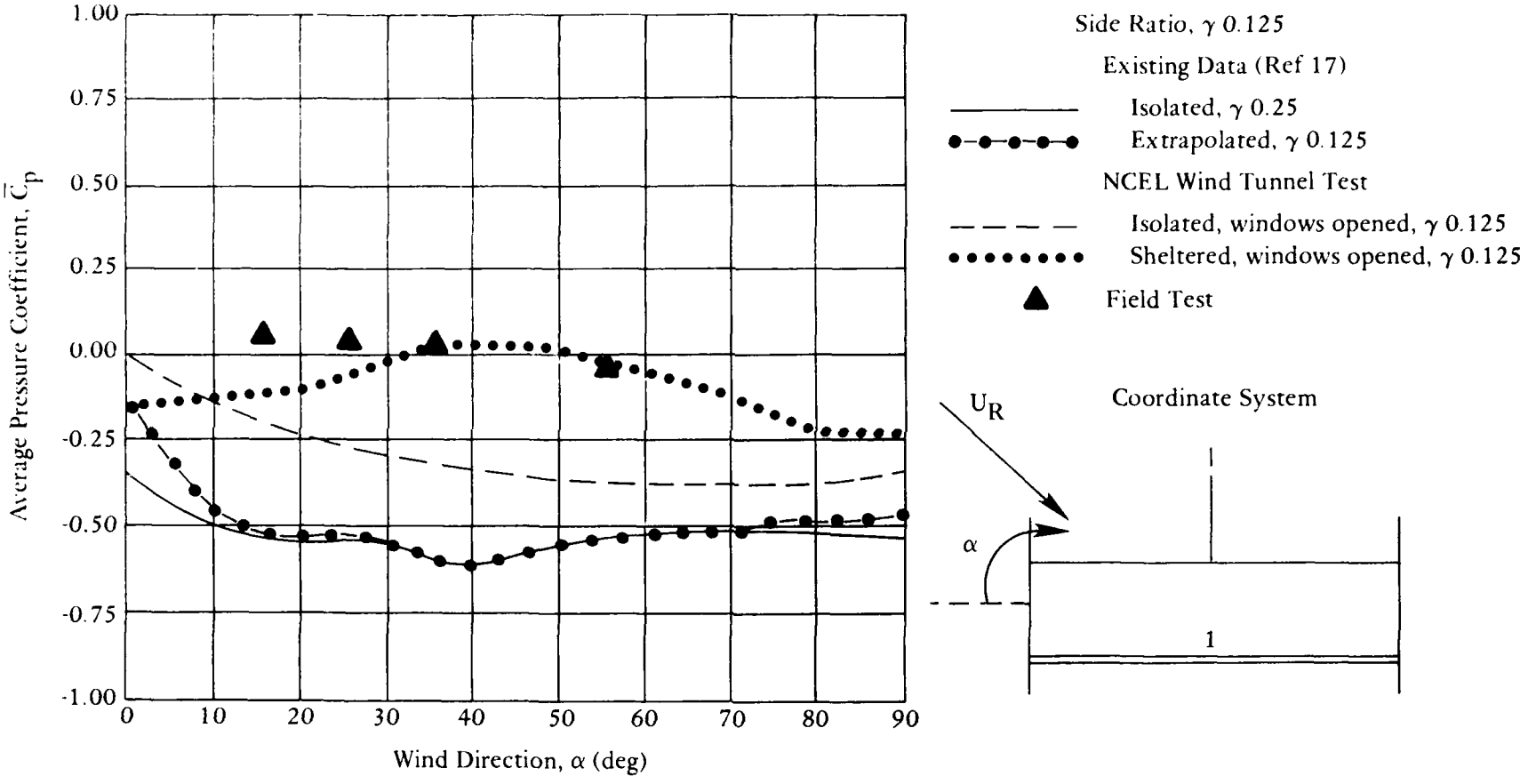

Figure 47. Comparison of wind tunnel tests, field tests, and existing data of average pressure coefficient of Model 1 (leeward side).

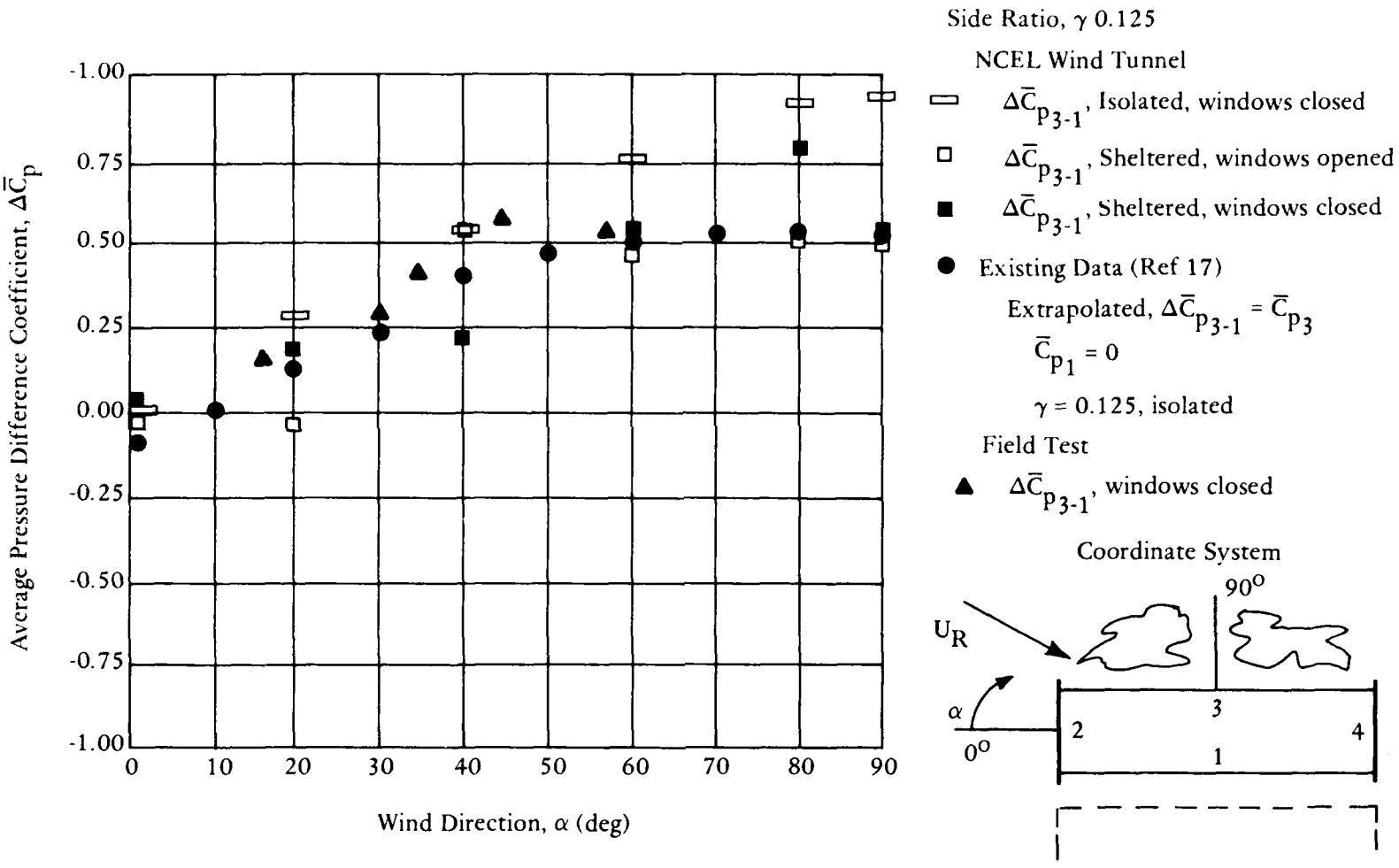

Figure 48. Comparison of wind tunnel tests, field tests, and existing data of average pressure difference coefficient between windward and leeward sides of Model 1.

Values of $\Delta\bar{C}_p$ between the short walls of the models for angle of incidence 79-90 degrees do not correlate well with field test data due to fluctuating wind and two malfunctioning pressure taps as mentioned earlier in the text. Model 2's pressure coefficient for side 1 (see Figure 39) went positive and the coefficient for the short sides are less negative for the field test. It is believed that the hill, located directly behind Model 2, had an effect on the leeward side. In the wind tunnel the hill was not modeled on the downwind side. Modeling the hill would have had a much smaller model scale of Building 2.

Values of the $\Delta\bar{C}_p$ between the long walls of the field test data are in close agreement with the NCEL wind tunnel test data for all models (Figures 40, 45 and 48). Figures 36, 40, 45, and 48 show the effect of window openings on the $\Delta\bar{C}_p$. Wind tunnel measurements of Model 1 show that a wall opening area equivalent to 40% of windward and leeward wall area (inlet openings equal to outlet openings) caused an estimated 33% decrease in the $\Delta\bar{C}_p$ at high wind incidence.

For Models 2 and 3, the wall openings ranged from 0 to 15% of windward and leeward walls and slightly increased the $\Delta\bar{C}_p$. The sheltering effect of trees and buildings located close to the building (Model 1) is also shown in Figure 48. A 30% decrease of $\Delta\bar{C}_p$ was noted for various wind incidences (45 - 90 degrees). Figure 49 shows the average pressure difference coefficients for Model 2 on-grade and elevated. For the elevated case the $\Delta\bar{C}_p$ is greater for α>45 degrees.

Since only an average pressure difference coefficient $\Delta\bar{C}_p$, is needed to estimate the airflow in a building (and in the design criteria for natural ventilation), only an $\Delta\bar{C}_p$ is needed to predict the comfort limits. Therefore, basic data are needed to supply the $\Delta\bar{C}_p$ within a 20% error.

Existing data (Ref 17 and Appendix C, Figures C-1 through C-8) of $\bar{C}_p$ for flat-roofed, rectangular buildings tend to overestimate the pressure coefficients (Figures 47 and 48) and, consequently, overestimate the $\Delta\bar{C}_p$ for different side ratios. Since most of the buildings have some form of shelter (trees, buildings, etc.), the leeward pressure coefficient was forced to zero and the windward pressure coefficient,

$\bar{C}_{p_3}$, set represent $\Delta\bar{C}_{p_{3-1}}$ for long walls. These values were compared to the experimental values from field and wind tunnel tests. Figures 40 and 48 show that at high wind incidence the $\Delta\bar{C}_p$ (as assumed) is underestimated for most of the models but is in close agreement at the lower wind incidence. At 0- to 20-degree wind incidence, a $\Delta\bar{C}_p$ to ±0.15 is assumed due to the fluctuation of the wind direction. Since architectural features of a building (Figures 41 and 42) tend to increase the $\Delta\bar{C}_p$ the existing data ($\Delta\bar{C}_p$ is set to the windward pressure coefficient with the leeward pressure coefficient set to zero) can be used as basic data (no special architectural features) in conjunction with other existing data (Ref 14, 18, and 19), and Appendix C, Figure C-9 and Tables C-1 and C-2.

Since most of the buildings had a pitched roof or were flat-roofed and rectangular, a basic set of $\Delta\bar{C}_p$ curves was developed (Figures 50, and 51). These curves were developed by combining existing wind tunnel and field test data. The observed and expected changes in $\Delta\bar{C}_p$ due to architectural changes in the basic building design are summarized in Table 8. More testing is needed in order to further validate these curves. The proposed curves reflect the $\Delta\bar{C}_p$ expected for a basic one-story building. Any deviation from the basic design will cause a change in the $\Delta\bar{C}_p$.

Figure 52 compares wind tunnel data of $\Delta\bar{C}_p$ and the estimated pressure difference coefficient, $\Delta\bar{C}_{p_e}$ (Figure 51 and Table 8). There is a close agreement between the $\Delta\bar{C}_{p_e}$ value and the $\Delta\bar{C}_p$ value measured in the wind tunnel for Models 1 and 2. For Model 3 there is a close agreement at high wind incidence (60 degrees < α < 90 degrees), but a difference at the lower wind incidence (Figure 52).

Figures 50 and 51, and Table 8 form the start of a data base of pressure difference coefficients for a variety of buildings with specific architechtural features. Values from this data base can be used to calculate the expected airflow rates through the building using the following equation:

$$Q = C_D A U_R (\Delta\bar{C}_p)^{1/2} \qquad (9)$$

where: Q = airflow rate, m^3/hr (cfm)

C_D = nondimensional discharge coefficient, usually 0.6

A = effective inlet area, m^2 (ft^2)

U_R = approach windspeed at the site of roof level, m/hr (fpm)

$\Delta\bar{C}_p$ = nondimensional average pressure difference coefficient between opposite walls of building

Once the airflow rates have been determined, the values can be used for estimating the acceptable comfort levels (effective temperatures) within the building.

Table 8. Effect of Architectural Characteristics on Pressure Difference Coefficients[a]

Architectural Characteristic	$\Delta\bar{C}_p$ (% increase)
Basic design (one story)	0
Two or more stories	40
Single story (elevated above ground)	30
Single story with extended eaves and end walls	25
Single story elevated above ground with extended verandas and end walls	50
Single story with windward wall projections or insets	25

[a]If two or more architectural characteristics are combined, the average of the percent increase is taken with a maximum of 50% total increase. These corrections should be used only for the calculation of natural ventilation.

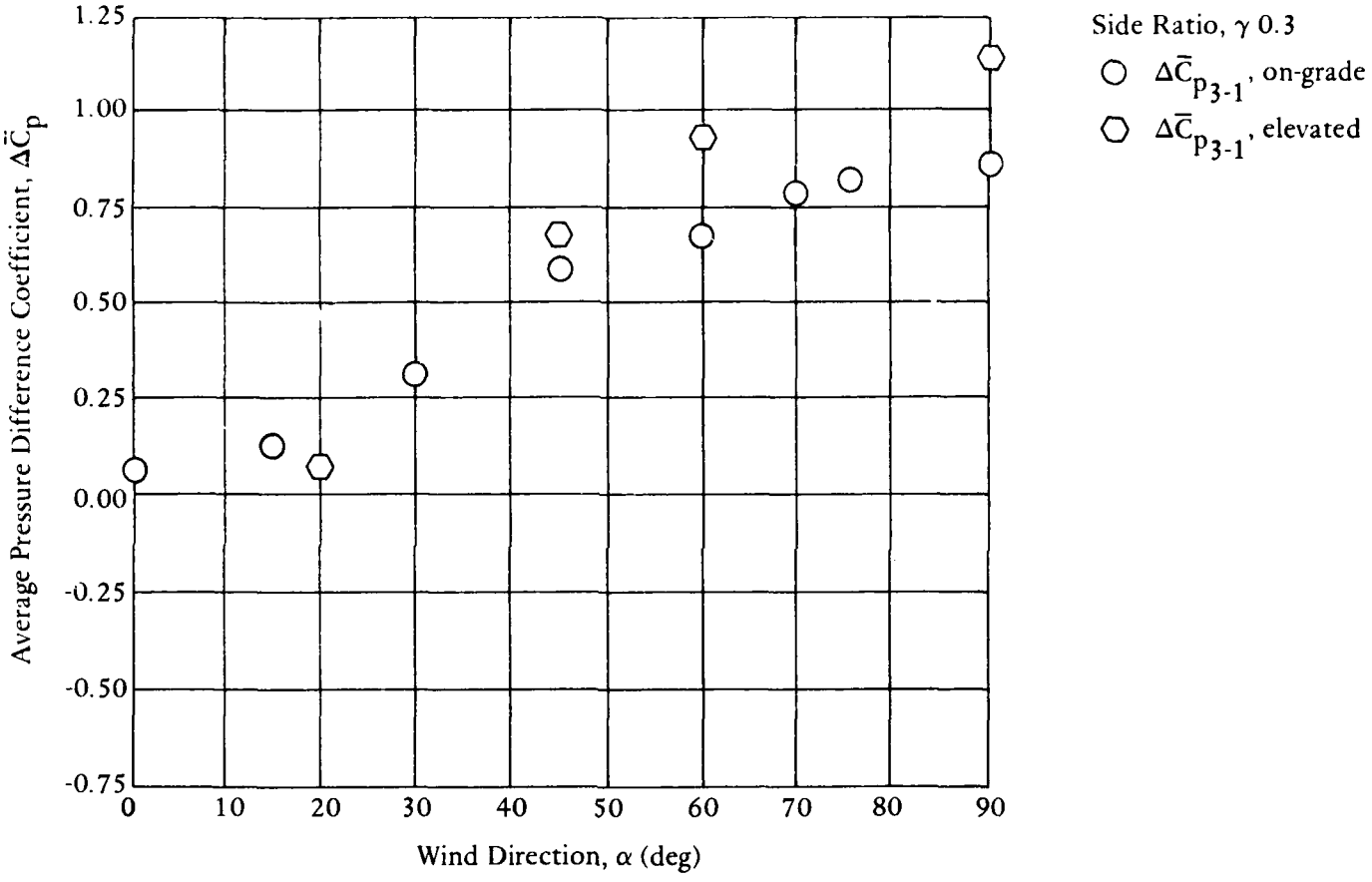

Figure 49. Comparison of average pressure difference coefficient between long walls for Model 2 (on-grade, elevated, and windows opened).

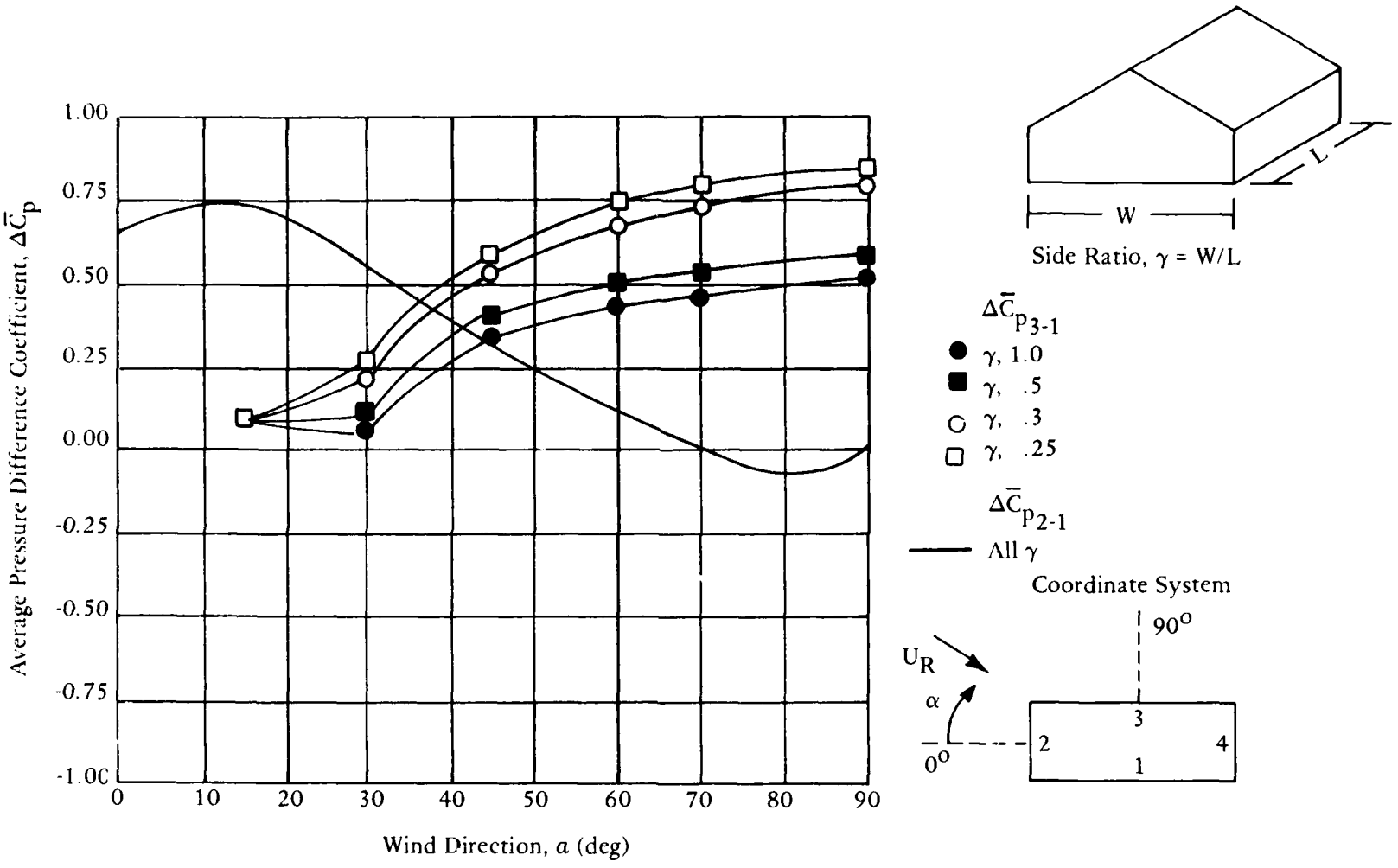

Figure 50. Average pressure difference coefficient for a single-story, on-grade, pitched-roof rectangular building. $\Delta\bar{C}_{p_{3-1}}$ and $\Delta\bar{C}_{p_{2-1}}$ is the pressure difference coefficient between long and short walls of the building.

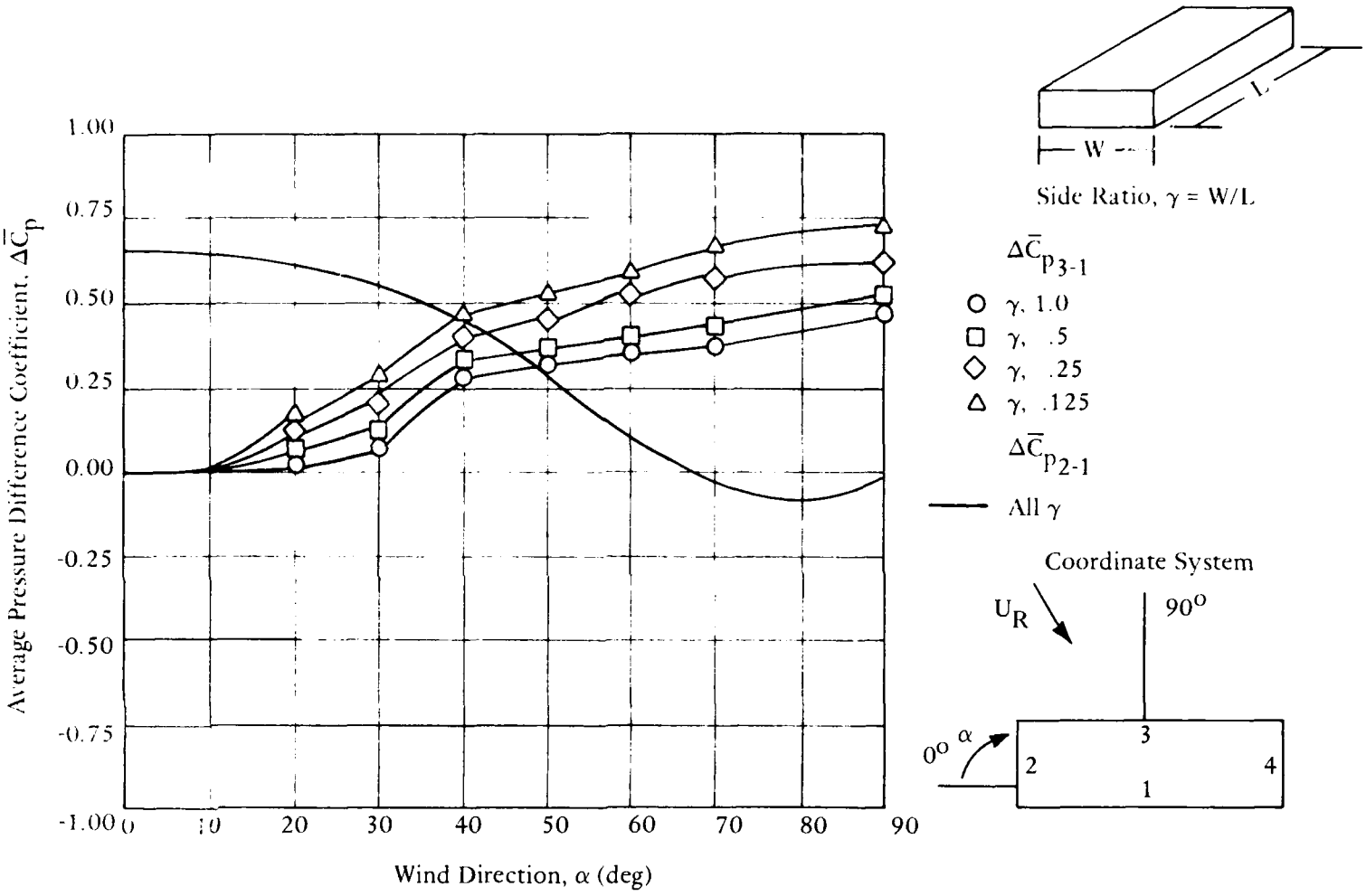

Figure 51. Average pressure difference coefficient for a single-story, on-grade, flat-roof rectangular building. $\Delta\bar{C}_{p_{2-1}}$ and $\Delta\bar{C}_{p_{2-1}}$ is the pressure difference coefficient between long and short walls of the building.

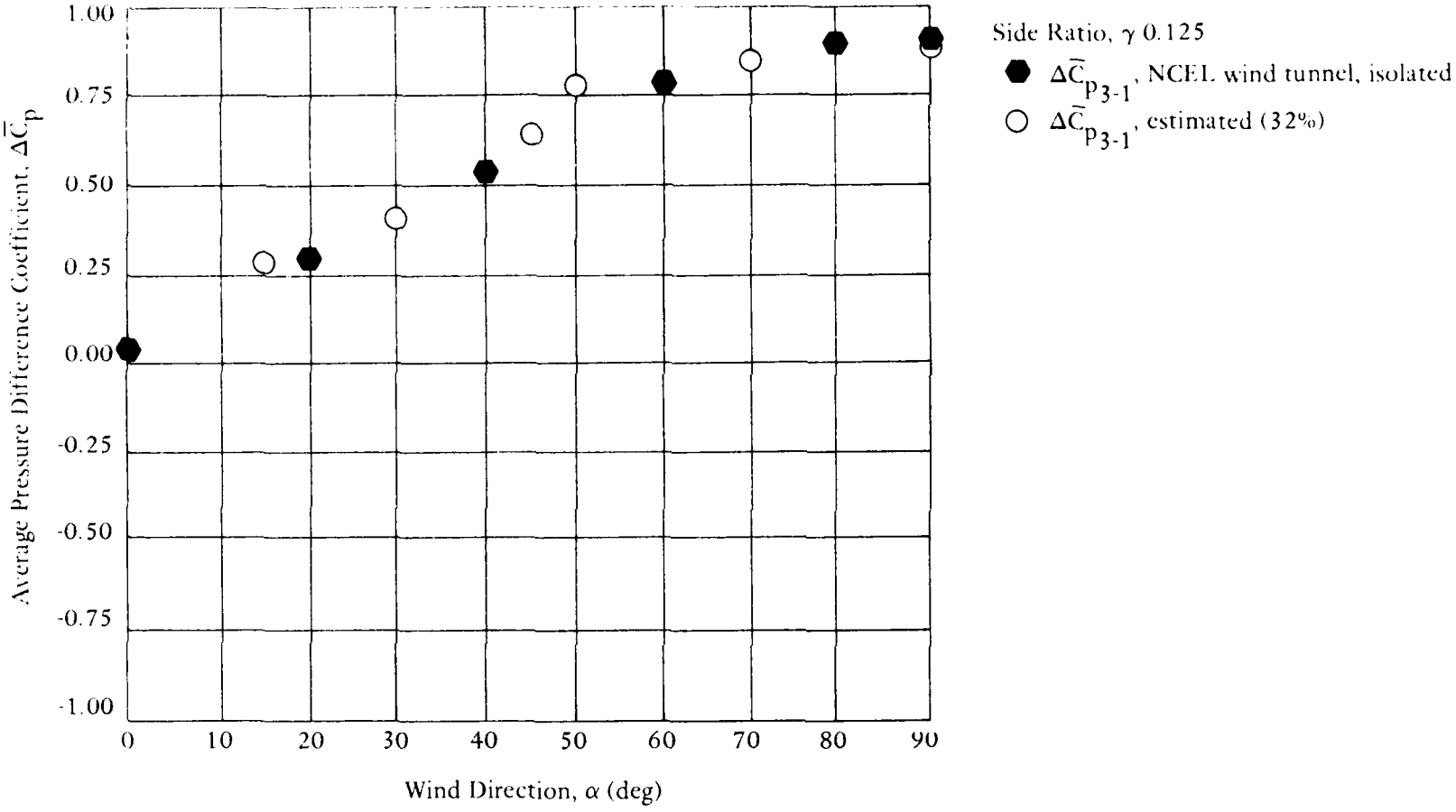

(a) Model 1, isolated.

Figure 52. Comparison of measured average pressure difference coefficient and estimated pressure difference coefficient of Models 1, 2, and 3.

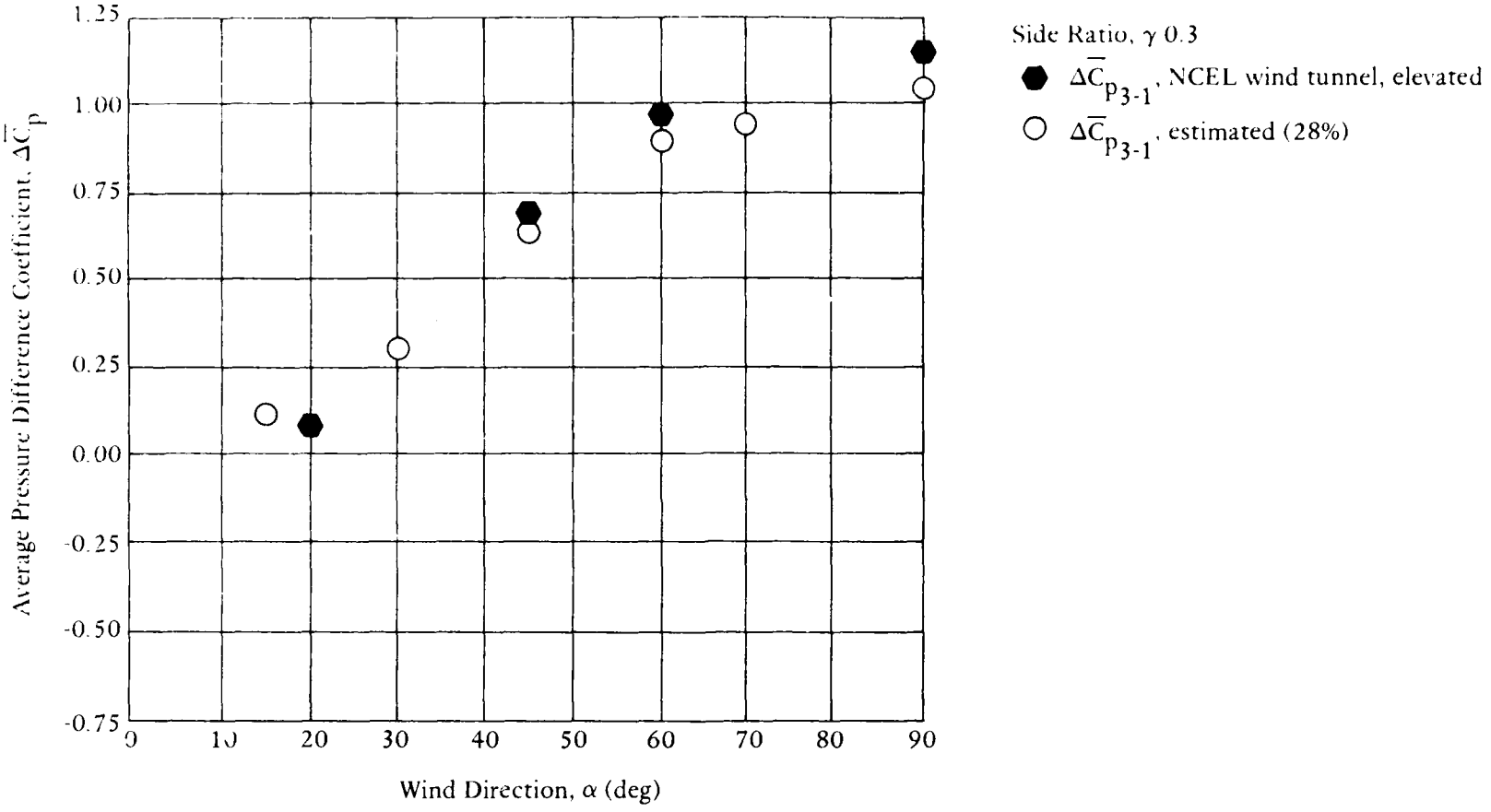

(b) Model 2, elevated.

Figure 52. Continued.

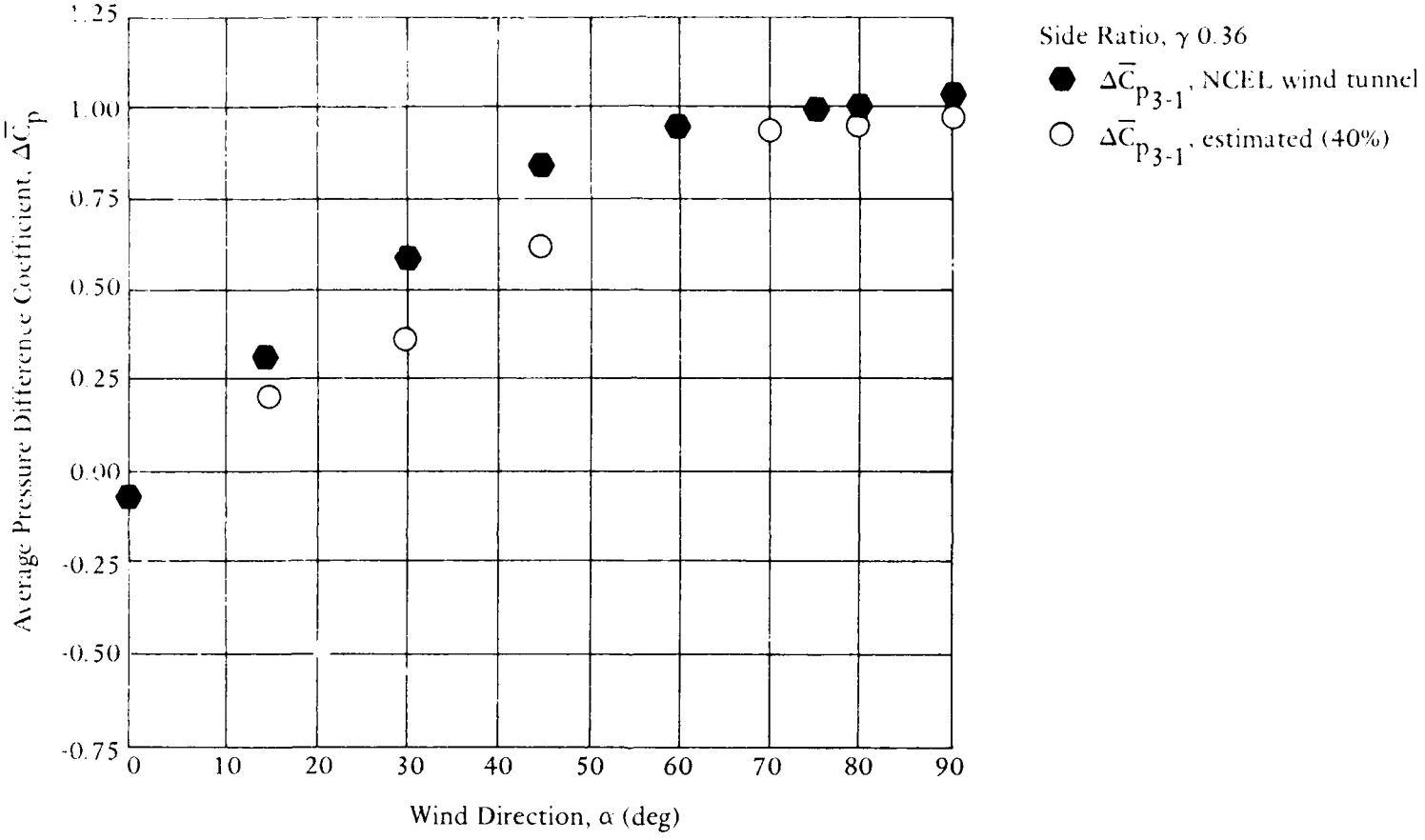

(c) Model 3, isolated.

Figure 52. Continued.

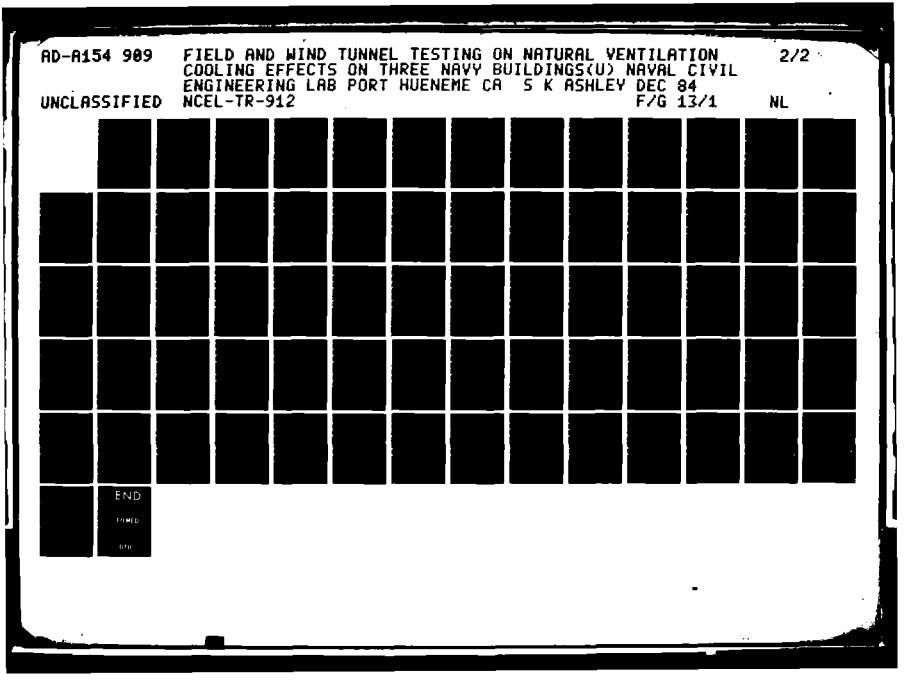
AD-A154 909
FIELD AND WIND TUNNEL TESTING ON NATURAL VENTILATION COOLING EFFECTS ON THREE NAVY BUILDINGS(U) NAVAL CIVIL ENGINEERING LAB PORT HUENEME CA S K ASHLEY DEC 84
2/2
UNCLASSIFIED
NCEL-TR-912
F/G 13/1
NL
END
FILMED
DTIC

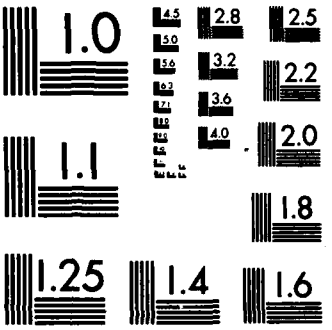

COMPARISON OF THE NCEL COMPUTER MODEL AND FIELD TEST RESULTS

Both field and wind tunnel studies are expensive and time consuming ways to investigate natural ventilation. A computer program is a more satisfactory method for the designer to use as a design tool. Such computer programs require information about the weather and pressure coefficient, and information about wind/building/occupant interactions including airflows and comfort levels. Although pressure difference coefficient information can come from field or wind tunnel measurements, a catalog of typical coefficients for different building designs is more convenient.

The NCEL computer program (Ref 20) is such a program. The program consists of two main routines: (1) the airflow routine calculates airflow through the building, and (2) another routine estimates temperatures based on results of airflow routine. The program calculates expected windspeed at site, airflow rates and direction, internal pressure, air changes, interior and exterior effective temperatures, interior dry and wet bulb temperatures, and humidity ratios. (The effective temperatures calculated in the computer program do not use exactly the same algorithms as presented in the effective temperature section; but rather use the values from the ASHRAE Handbook of Fundamentals.) Corresponding input are weather data by region, pressure coefficients, size of openings (exterior and interior, such as windows, doors, etc.), and building heat loads.

Figures 50 and 51 show the average pressure difference coefficients for each building type for various wind directions. The program can use this value as the windward pressure coefficient by setting the leeward value to zero. If it is used then the pressures printed at the end of the programs will be essentially incorrect, however, the air volume flow rates and direction of airflow will be correct.

For validating the computer program, pressure coefficients from the field test were used as data. The daily weather reports were from: the MCAS weather tower (MCAS data), the National Climatic Center*, Asheville, N.C. (ASHV data) and the corresponding effective temperatures and airflows calculated for each building site. Figures 53a, b, and c compare computer program results of airflow into each building with field test results. The results are within a ±10% accuracy for a closed building (no openings) and ±15% for buildings with openings. For Model 3 (Figure 53c) a considerable difference in airflow was observed due to the inability to control the opening of the lanai. Ambient and interior effective temperature comparisons between field tests and the computer model results are shown in Figure 54a, b, c, and d. For Figure 54d the two effective temperature algorithms (one used in the NCEL computer program and the one presented earlier) were used on the inside and outside weather data for Building 3. The differences observed from the plot range from 1-2°C, and are indicative of the fact that the effective temperature model presented earlier takes into account activity, clothing, etc.; while the NCEL computer model is based on average metabolic heat rate, and does not take clothing into account. For the full, open inlet area, there is close agreement between field test and computer test results; but there is some deviation for the closed condition.

Discussion

The comparison of the laboratory measurements with the field measurements is encouraging. The use of wind tunnel data can be substituted for full-scale data on pressure coefficients. From the existing data of wind tunnel measurements, average pressure difference coefficients can be cataloged for a variety of buildings with specific architectural features. Computer programs that use this information, such as the NCEL program, can be used as design tools to estimate the effectiveness of natural ventilation for cooling.

*Standard weather data representative for this region for the month of July.

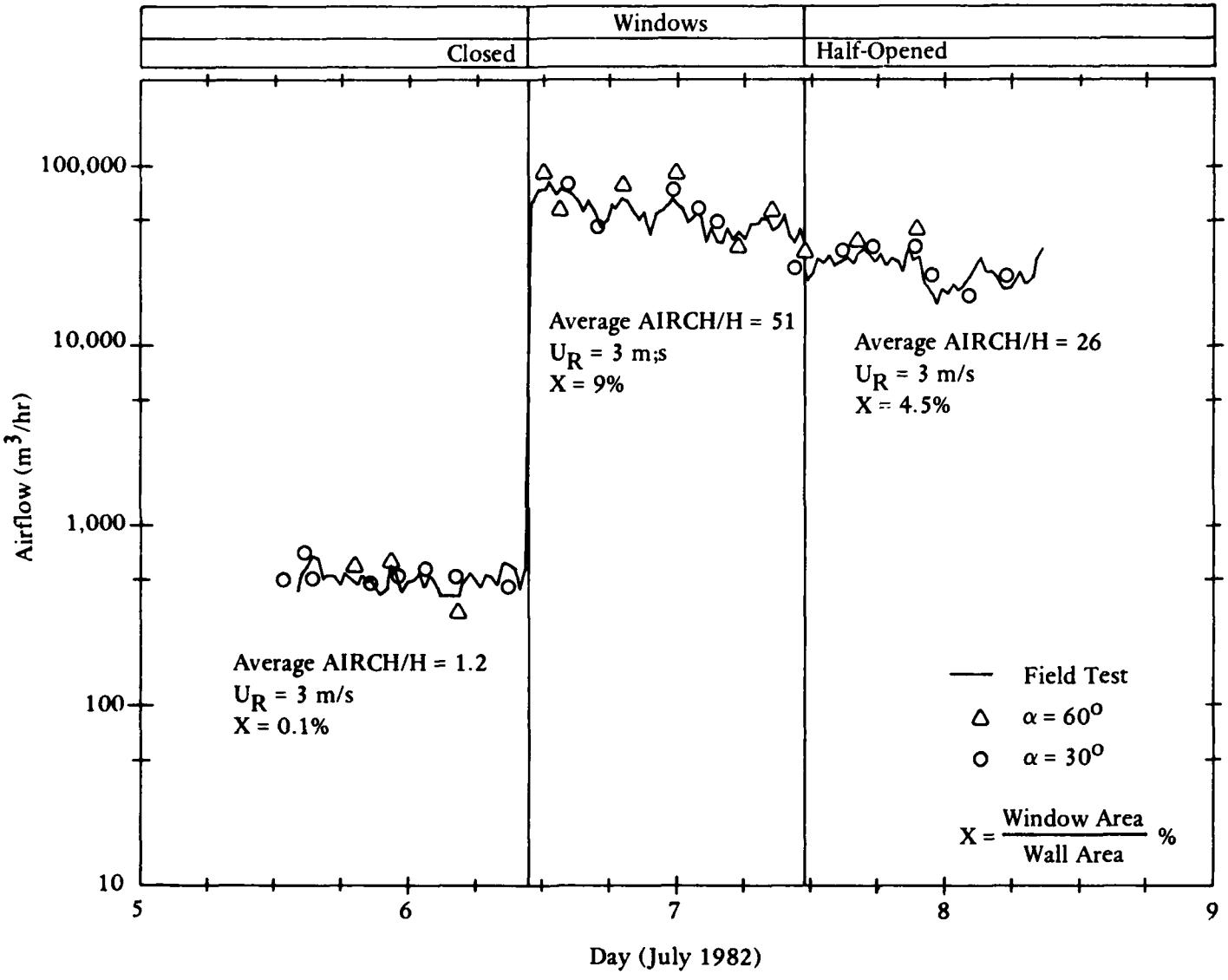

(a) Building No. 1, second floor.

Figure 53. Comparison of computer model and field test results of airflows into Buildings No. 1, 2, and 3.

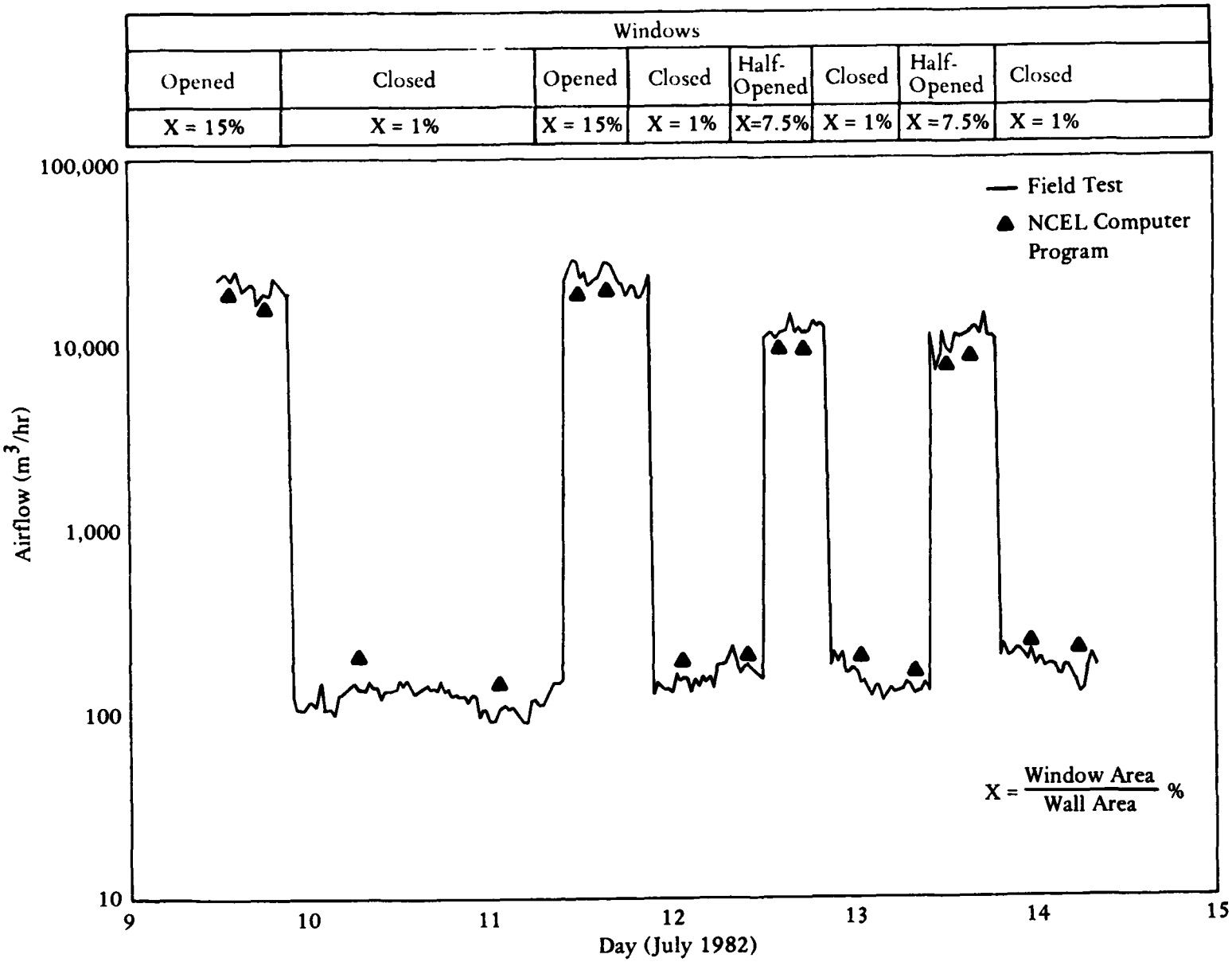

(b) Building No. 2, west apartment.

Figure 53. Continued.

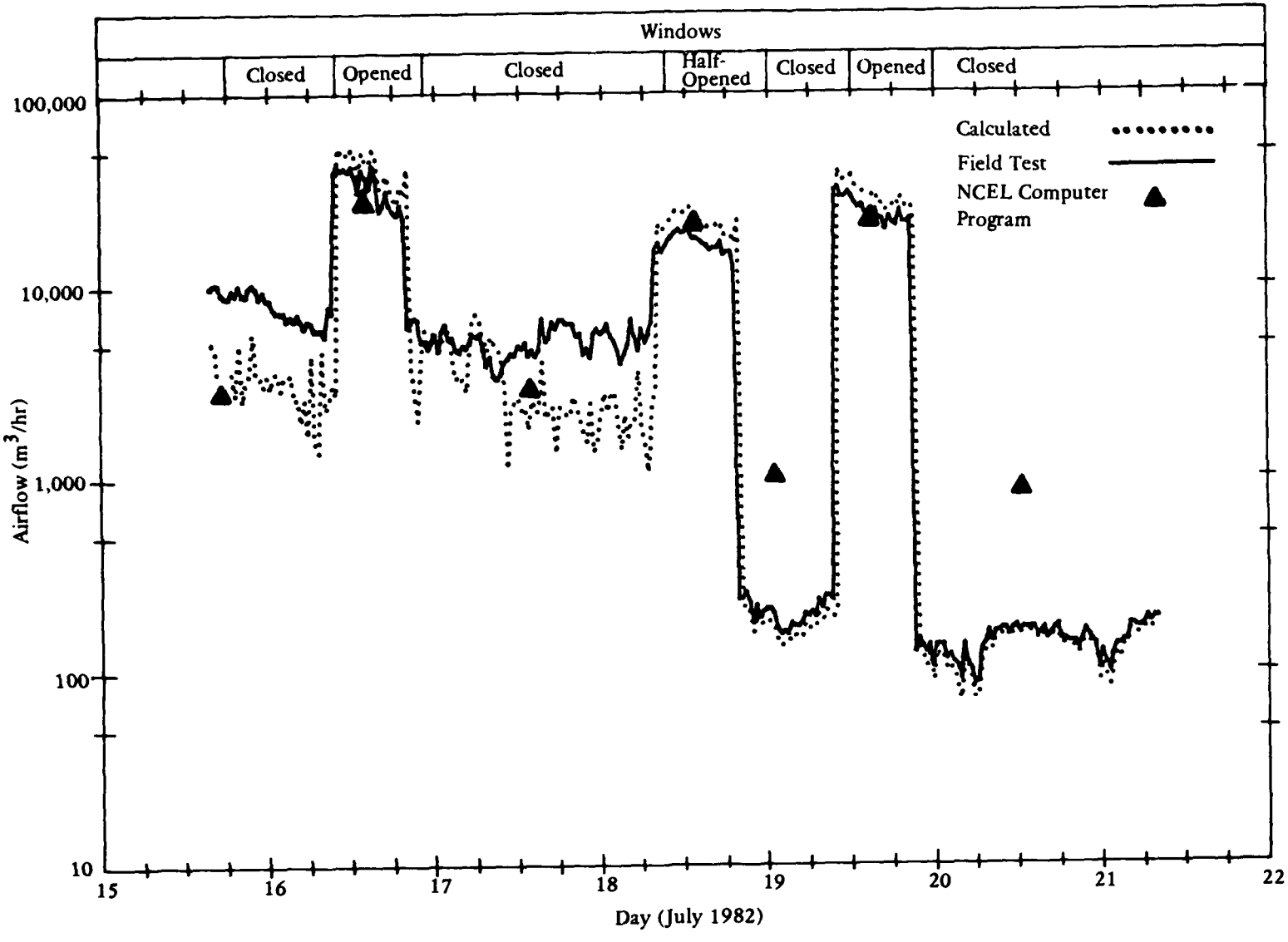

(c) Building No. 3, east apartment.

Figure 53. Continued.

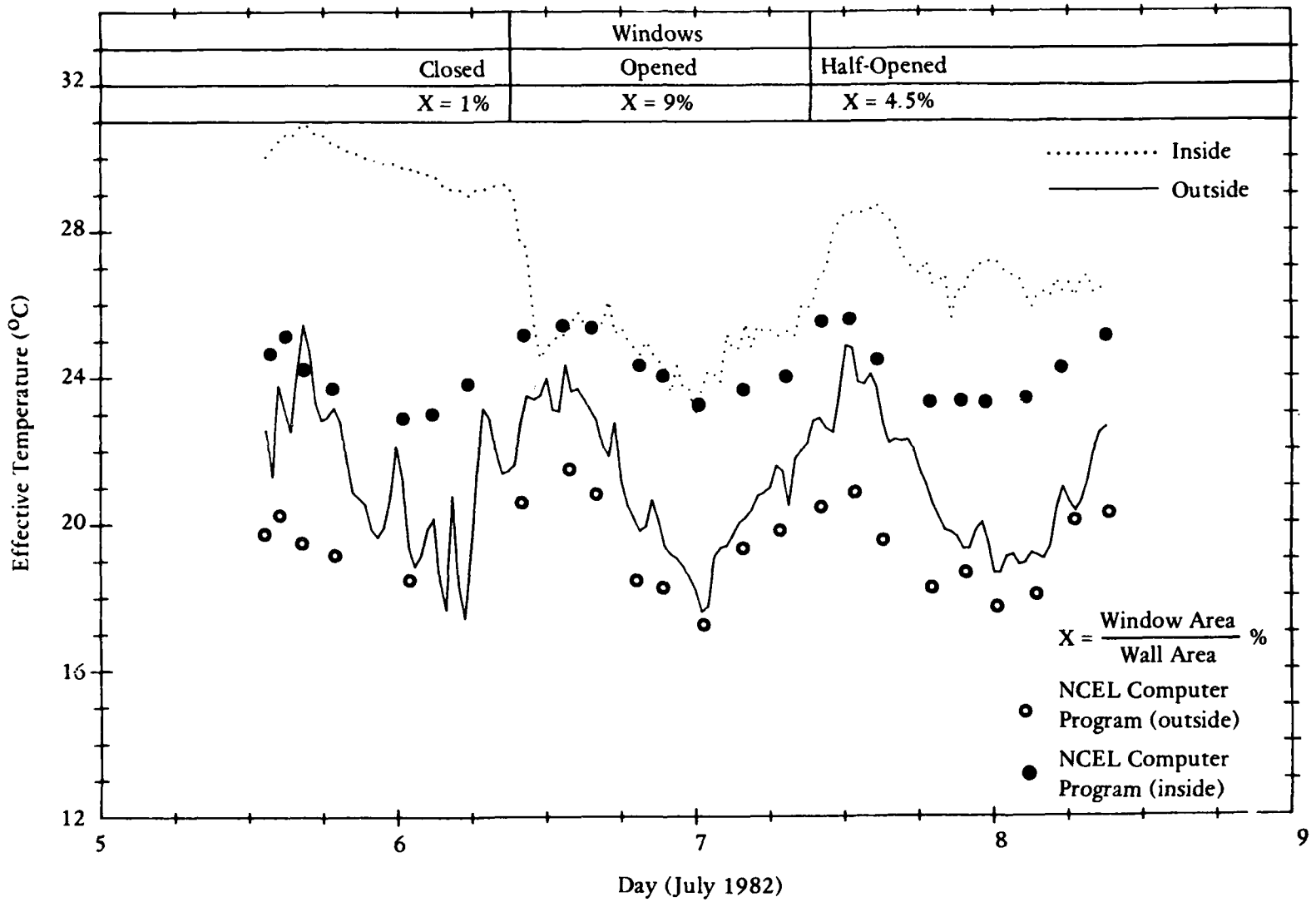

(a) Building No. 1, second floor.

Figure 54. Effective temperatures for Buildings No. 1, 2, and 3.

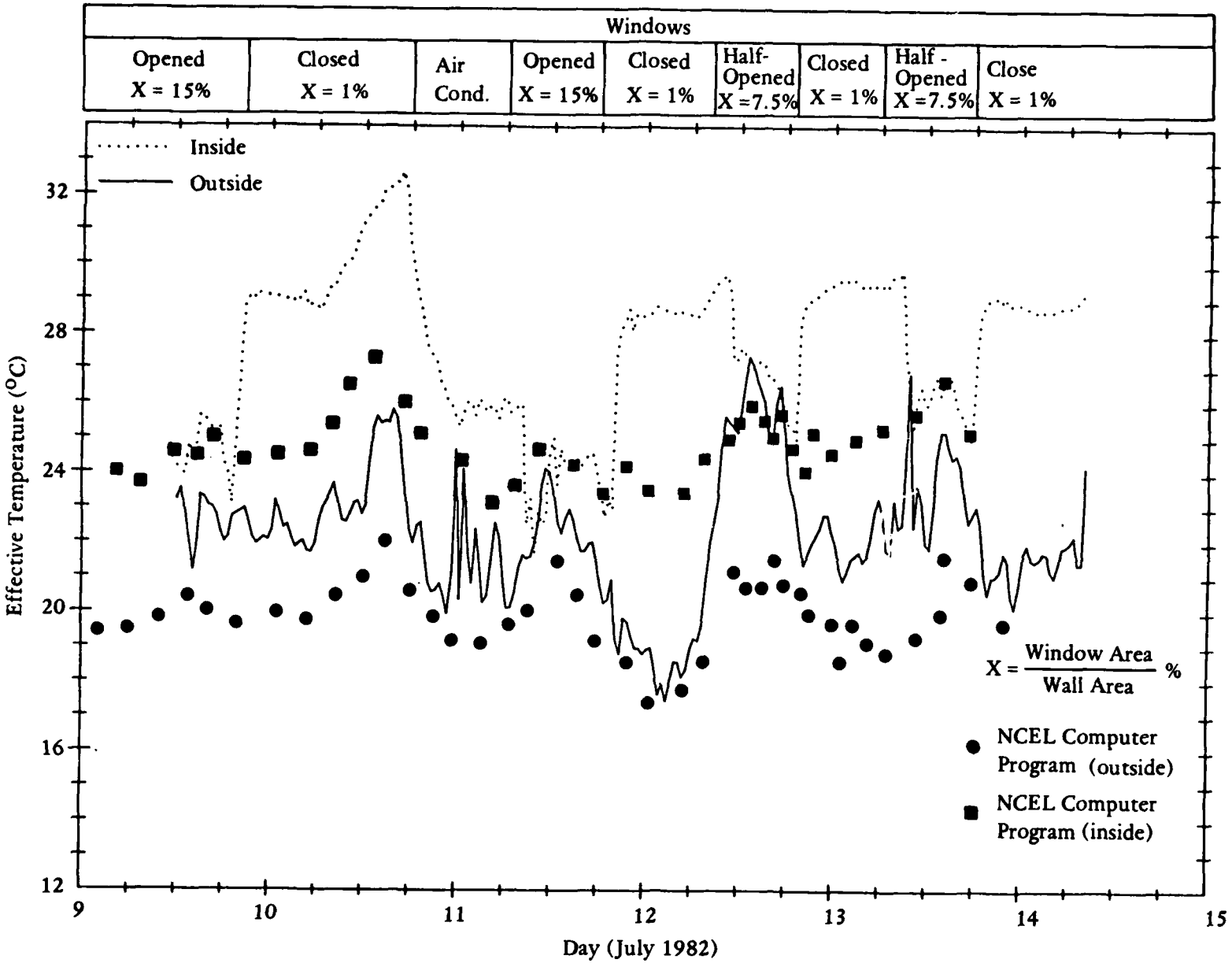

(b) Building No. 2, west apartment.

Figure 54. Continued.

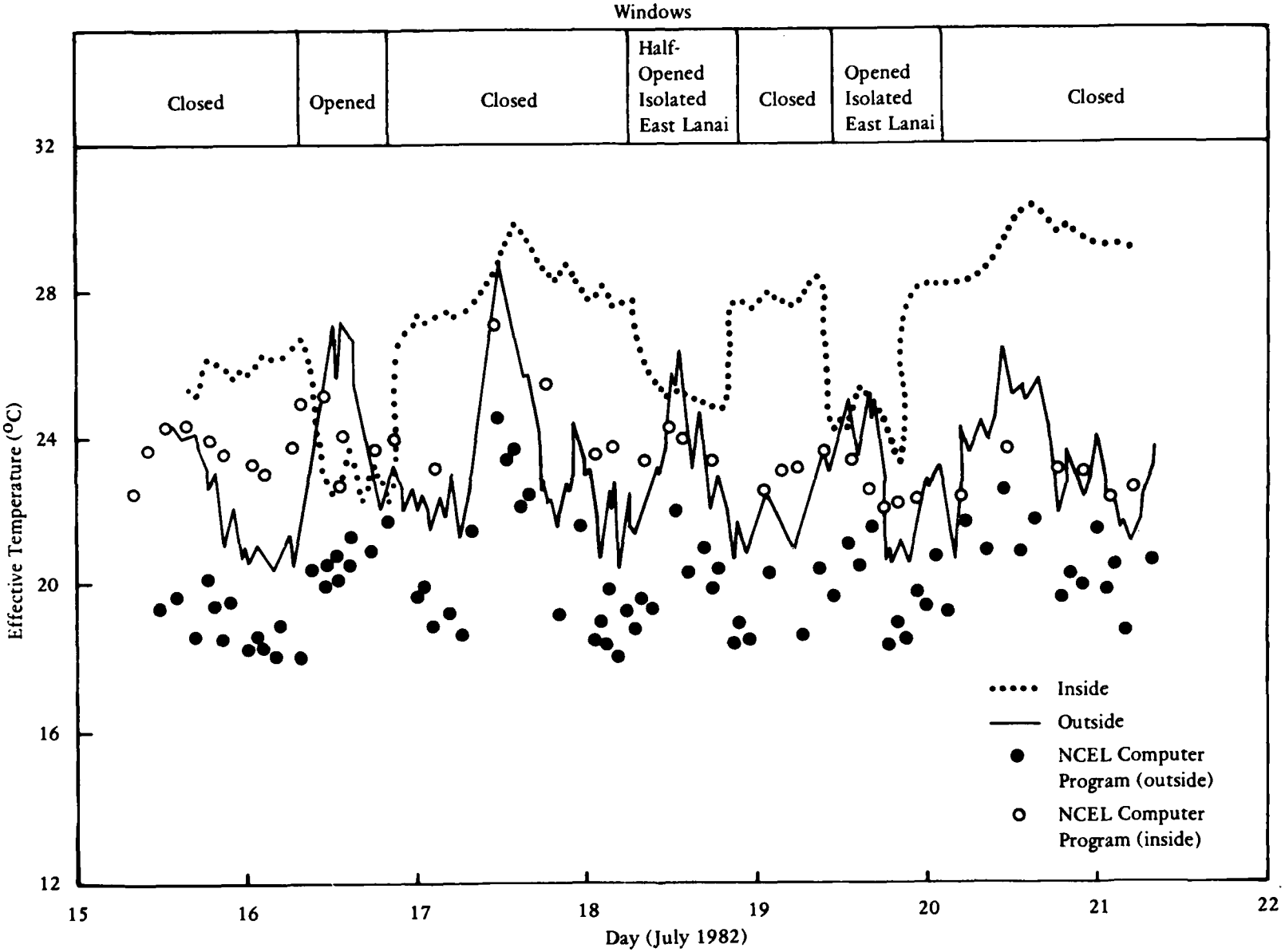

(c) Building No. 3, east apartment.

Figure 54. Continued.

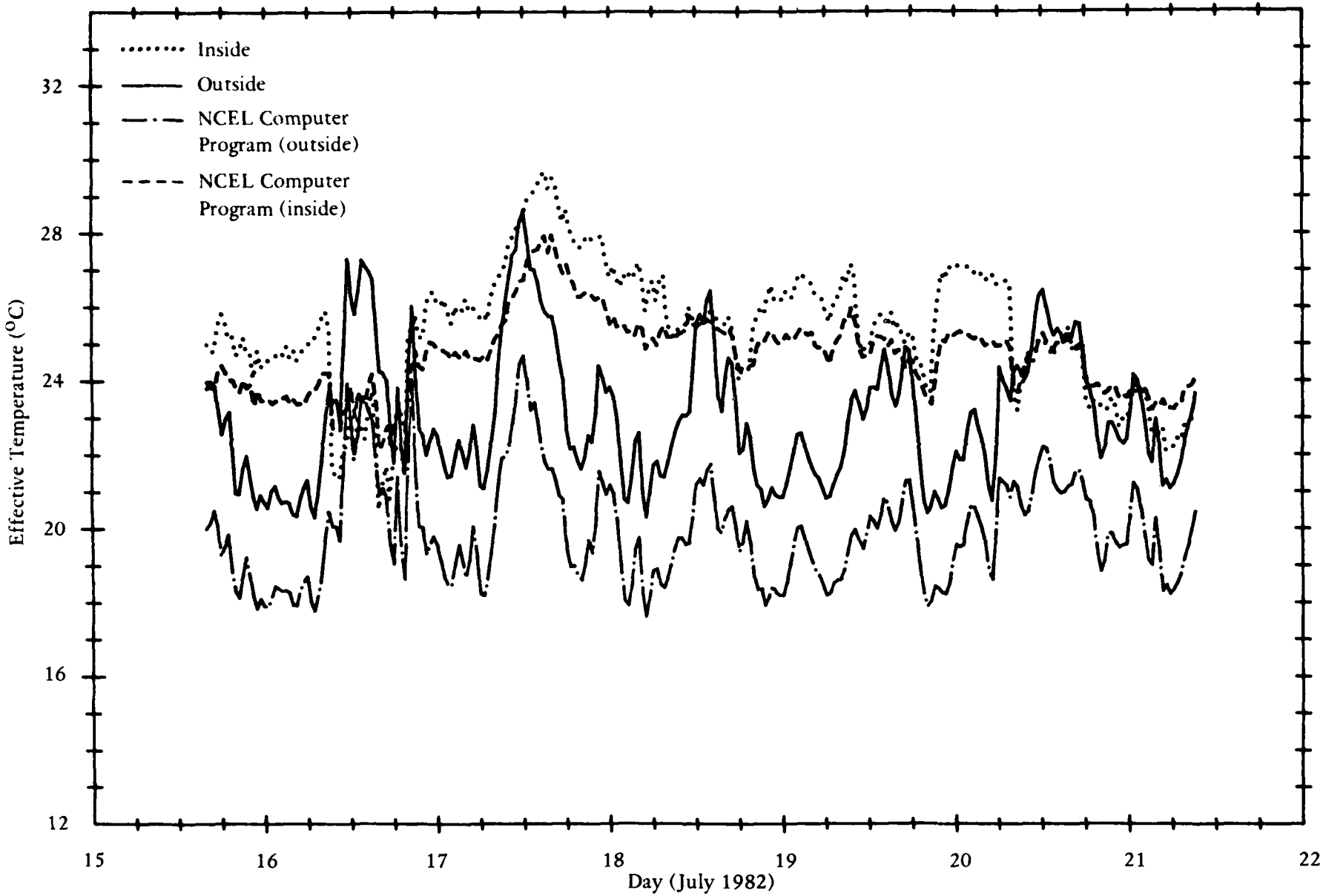

(d) Building No. 3, west apartment.

Figure 54. Continued.

In order to use the NCEL computer model as a design tool for natural ventilation, two sets of data are needed: (1) surface pressure coefficients and (2) weather data (information on surface wind velocities and psychometric summaries). For typical calculations, average weather data (e.g. TRY tapes) may be used for determining extreme conditions, the maximum temperature data or weather data recorded for the past 5 years can be used. The final output of the computer model is the predicted time series data for the effective temperature the occupants would experience. For Figure 55a, b, and c, two different sources of weather data were used: (1) the daily weather station and (2) the average weather reports published by the Naval Oceanography Command (designated by ASHV). The expected effective temperatures were calculated. From these effective temperatures the designer can then decide what natural ventilation strategies are acceptable and effective. The NCEL computer program can be used with a high level of confidence to establish a particular region and a specific building design suitable for natural ventilation cooling.

Conclusions

Field tests, wind tunnel tests, and computer simulation of buildings cooled by natural ventilation (Ref 20) show that for hot, humid climates:

1. The minimum required effective inlet area should not be less than 15 - 20% of the windward wall area (assuming the inlet area is equal to the outlet area). The effective inlet area is the actual free opening area after window dressings (screens, louvers, etc.) have been taken into consideration.

2. When certain architectural characteristics are used (extended eaves and end walls, elevation, etc.), the required inlet area decreases due to the increase in wind pressure.

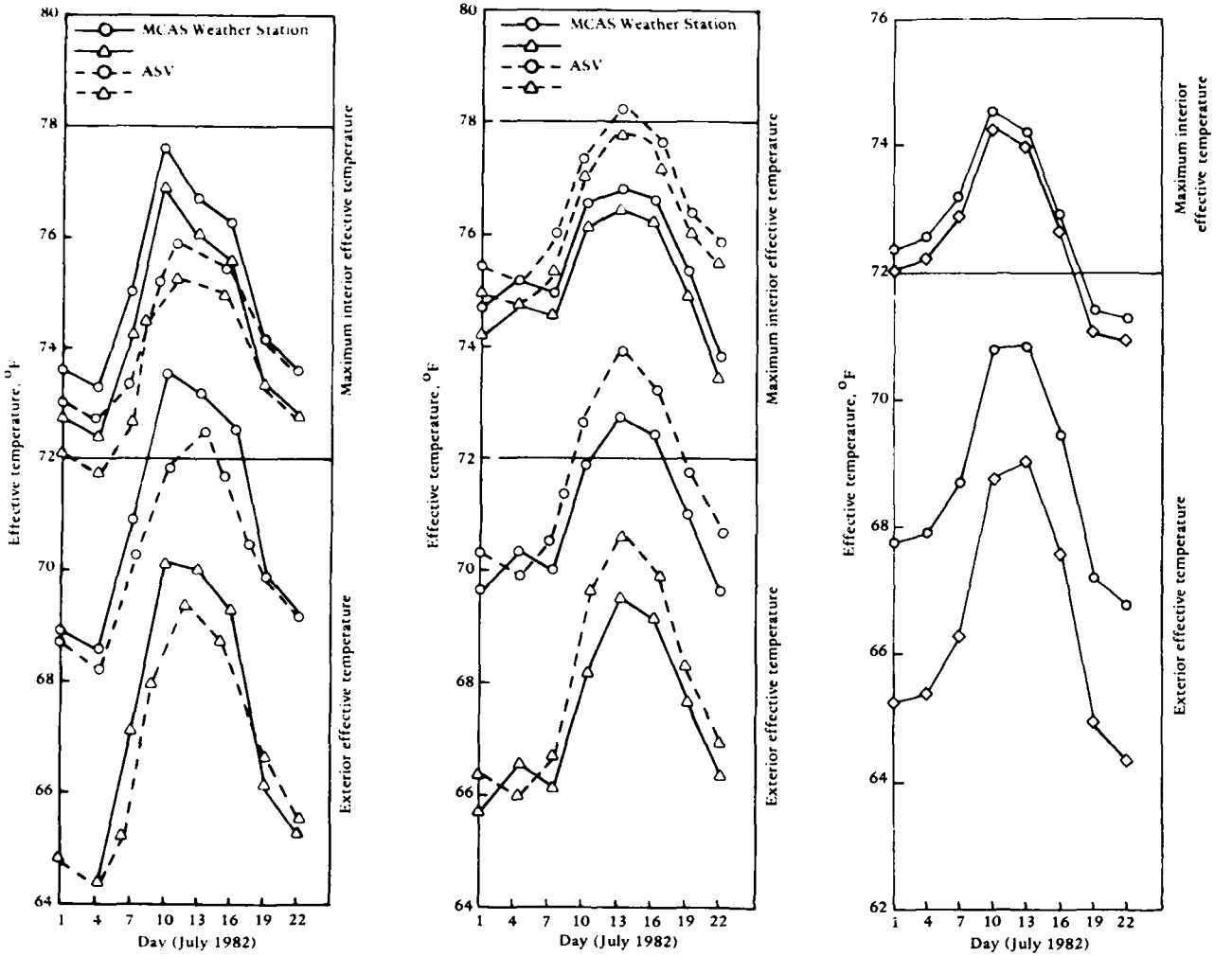

(a) Building No. 1, dorm room.

(b) Building No. 2, living room.

(c) Building No. 3, lanai isolated (MCAS weather hourly data was used on 19 July 1982).

Figure 55. NCEL computer model results of exterior and interior effective temperatures for Buildings No. 1, 2, and 3.

3. Opening and closing of windows does not affect the average pressure coefficient when the effective inlet opening area is less than 20% of the wall area. When the effective inlet area is over 40% of the windward wall area the average pressure coefficient decreases.

4. Assuming orifice flow, a sensitivity analysis shows that an increase or decrease of 25 to 60% of the pressure difference coefficient will cause an increase or decrease in the airflow rate into the building of 10 to 22%, assuming that the effective inlet area and wind velocity at the site remain constant.

5. The NCEL computer program can be used to estimate: (a) airflow rate through the building, (b) the number of air changes per hour, and (c) internal and external building environmental conditions.

RECOMMENDATIONS

The development of Figures 50 and 51 was based on existing data. Pressure coefficient data for buildings with various side ratios are limited. More wind tunnel testing of various building configurations is needed. The development of such pressure coefficient data will be valuable not only for the natural ventilation cooling of buildings, but for projects such as: air infiltration, indoor air quality, or casualty assessment in Navy shore facilities and installations in case of biological warfare.

REFERENCES

1. B.V. Smith and P.E. Condon. LBL/EPB data acquisiton system: Description and user instructions, Lawrence Berkeley Laboratory, Report LBL 11739 (unpublished). Berkeley, Calif., 1980.

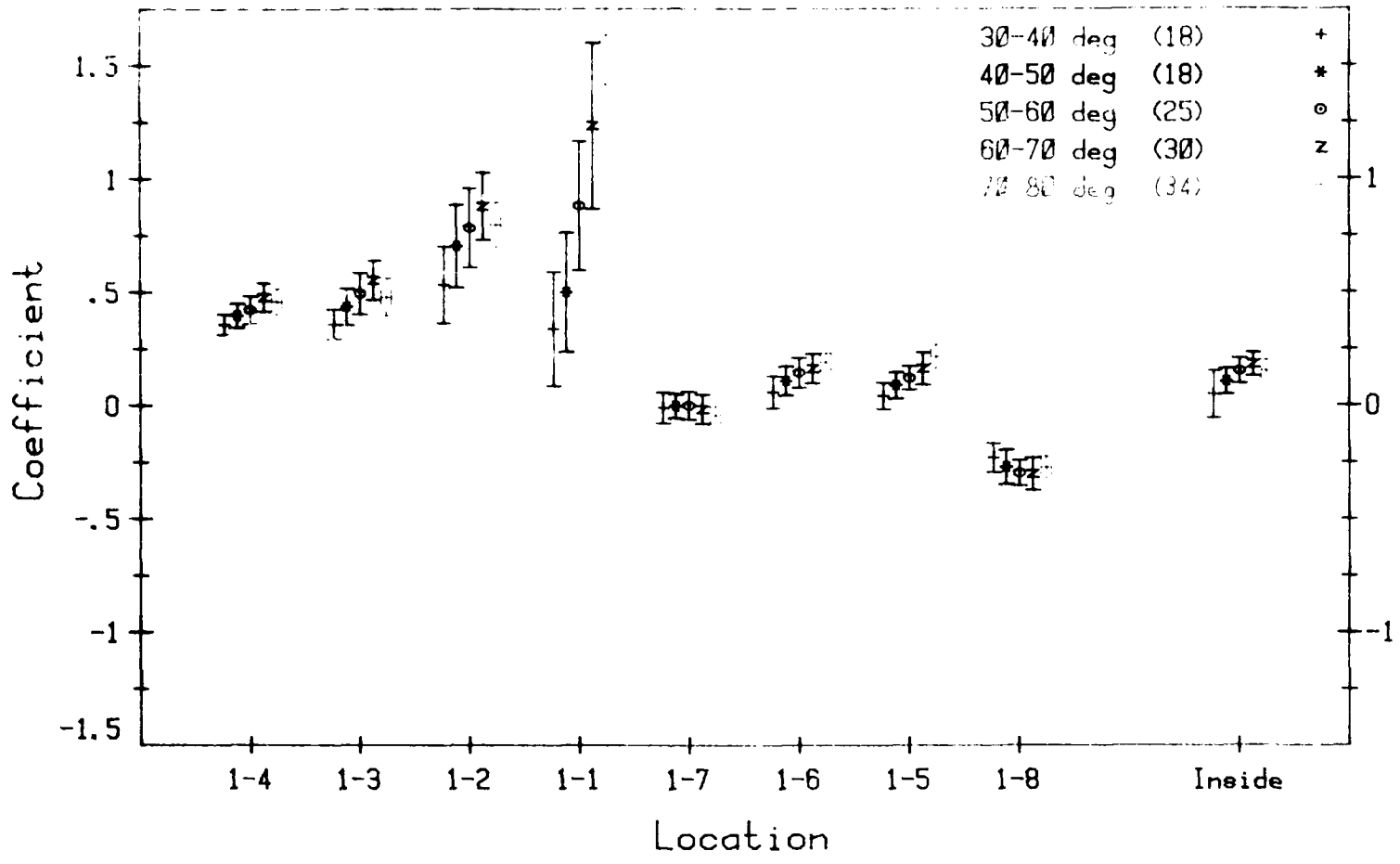

(a) Building No. 1, ground floor.

Figure B-1. Average pressure coefficients for Building No. 1. Angles are relative to building north. Numbers in parenthesis are points in that angle bin. Ordinate indicators refer to taps in the main text.

Appendix B

FIELD TEST PRESSURE COEFFICIENTS DATA

$$\Delta T_{comf} = \frac{T_s}{Y_t^*} \qquad \text{(A-20)}$$

The comfort band range begins at approximately 2°C for lightly clothed, sedentary situations and increases with both the clothing level and metabolic rate (e.g., clo = 2, met = 2 implies a comfort band of 7°C or over).

As an alternative, the last two expressions can be used to rewrite the effective temperature equation in terms of the comfort temperature and comfort band:

$$T_{eff} = T_{comf} + Y_o \, \Delta T_{comf} \qquad \text{(A-21)}$$

These same two equations can be used to eliminate all comfort coefficients terms in the standard condition from the definitions of the temperature coefficients:

$$A = T_{comf} + Y_o \, \Delta T_{comf} \qquad B = Y_r \frac{\Delta T_{comf}}{T_s} \qquad \text{(A-22)}$$

$$C = Y_c \frac{\Delta T_{comf}}{T_s} \qquad D = Y_e \frac{\Delta T_{comf}}{2}$$

Metabolic Rate. The activity level of the body is given in units of met, m. One met is equal to the basic metabolic rate, M_o, and has a value of:

$$M_o = 58.1 \ [W/m^2] \qquad \text{(A-18)}$$

This value incorporates a mechanical efficiency of work (i.e., the amount of body energy that is converted into useful work), which for the activities considered here is a very small effect.

COMFORT TEMPERATURES

The effective temperature gives a corrected temperature value for the existing conditions but does not directly indicate the comfort level. However, since there is an expression that calculates the effective temperature as a function of predicted mean vote, the expression can be used to find the effective comfort temperatures. These comfort temperatures then become functions of the personal variables alone - they are independent of environmental conditions.

The optimal value of the effective temperature must occur for comfortable conditions and is given by the following expression:

$$T_{comf} = \frac{T_s}{Y_t^*}(1/2 \ Y_e^* - Y_o^*) \qquad \text{(A-19)}$$

Because both the personal and environmental parameters are variable, a comfort value alone is often insufficient; a range of acceptable temperatures is required. Even at the comfort temperature no more than 95% of individuals will report that they are comfortable. A comfort band has been defined in a range of effective temperatures where at least 90% of the individuals will report that they are comfortable:

Radiative Heat Transfer Coefficient. A linearized form of the radiation equations was used. This implies that the heat transfer coefficient will depend on the surface temperature of the body. However, for the normal range of environmental conditions a constant value of 4.8 ($W/m^2{}^\circ C$) for the coefficient can be assumed:

$$h_r = 4.8 \quad \frac{W}{m^2{}^\circ C} \tag{A-14}$$

Effective Thermal Efficiency of Clothing. The effective thermal efficiency of clothing, F_{cle}, is a measure of the effectiveness of clothing at insulating the skin surface from heat exchange:

$$F_{cle} = \frac{1 + 0.23\ I_{cle}}{1 + 0.178\ I_{cle}\ (h_c + h_r)} \tag{A-15}$$

Permeation Efficiency of Clothing. The permeation efficiency, F_{pcl}, is a measure of the ability of clothing to allow the transfer of moisture from the skin surface:

$$F_{pcl} = \frac{1}{1 + 0.143\ I_{cle}\ h_c} \tag{A-16}$$

Clo Value. The insulation value of clothing is given in units of clo. One clo is equal to 0.155 ($m^2{}^\circ C/W$) or (0.88 hr · ft^2/Btu). Clo values are usually quoted as either a basic clo value, I_{cl}, or an effective clo value, I_{cle}. The average relationship between these two values is as follows:

$$I_{cl} = 1.16\ I_{cle} \tag{A-17}$$

Basic comfort coefficient,

$$Y_o = \left[0.42 + 0.58\ m\right] \times \left[1.6 + 17.6\ e^{-2.1\ m}\right] - Y_r - Y_c - Y_e \quad \ldots\ldots\ldots \quad (A\text{-}10)$$

For convenience the total comfort coefficient is defined as follows:

$$Y_t = Y_r + Y_c + Y_e \quad (A\text{-}11)$$

The standard comfort coefficients (Y_x^*) are calculated using the same formulas as the comfort coefficients versions, except that the low airspeed value of the convection coefficient is used.

Basic Definitions

The equations below are useful definitions that are required for the previous set of equations.

Skin Temperature. In the comfort range the skin temperature, T_s, is only a function of the activity level, m.

$$T_s = 35.7 - 2.16\ m \quad (A\text{-}12)$$

Convective Heat Transfer Coefficient. The convective heat transfer coefficient, h_c, can either be dominated by airspeed or by thermal buoyancy. The larger of the two values for h_c should be used.

$$h_c = 8.3\ v^{0.53}$$

$$h_c = 5.66\ (m - 0.85)^{0.39} \quad (A\text{-}13)$$

Note that very similar forms for the wind-dominated convection coefficient have been found by others (Ref 13 and 14).

EFFECTIVE TEMPERATURE

The following simple expression was used for the effective temperature as a function of the environmental variables:

$$T_{eff} = A + B\,T_r + C\,T_a + D\,T_d^2 \qquad \text{(A-5)}$$

whose constants are a function of airspeed and the personal variables.

The temperature coefficients used above are defined as follows:

$$A = \frac{T_s}{Y_t^*}(1/2\,Y_e^* + Y_o - Y_o^*) \qquad B = \frac{Y_r}{Y_t^*}$$

$$C = \frac{Y_c}{Y_t^*} \qquad D = \frac{1}{T_s}\frac{Y_e}{Y_t^*} \qquad \text{(A-6)}$$

Comfort Coefficients

The comfort coefficients, (Y_x), (as used in this paper) are defined as follows:

Radiative comfort coefficient,

$$Y_r = \left[F_{cle}\,\frac{h_r\,T_s}{M_o}\right] x \left[1.6 + 17.6\,e^{-2.1\,m}\right] \qquad \text{(A-7)}$$

Convective comfort coefficient,

$$Y_c = \left[0.0014\,T_s\,m + F_{cle}\,\frac{h_c\,T_s}{M_o}\right] x \left[1.6 + 17.6\,e^{-2.1\,m}\right] \qquad \text{(A-8)}$$

Evaporative comfort coefficient,

$$Y_e = \left[0.0024\,I_s\,m + .132\,F_{pcl}\,\frac{h_c\,T_s}{M_o}\right] x \left[1.6 + 17.6\,e^{-2.1\,m}\right] \qquad \text{(A-9)}$$

Appendix A

DEFINITION OF EFFECTIVE TEMPERATURE

Definitions involved in calculating the effective temperature are stated below. In order to define effective or comfort temperatures a set of standard conditions* must be defined to which the actual conditions must be corrected. The asterisk in the equations indicate that the quantity is in the standard condition and is defined as follows:

zero airspeed,

$$v^* = 0 \tag{A-1}$$

air temperature is equal to the effective temperature,

$$T_a^* = T_{eff} \tag{A-2}$$

mean radiant temperature is equal to the effective temperature,

$$T_r^* = T_{eff} \tag{A-3}$$

standardized dew point

$$(T_d^*)^2 = T_s \left(T_{eff} - \frac{T_s}{2}\right) \tag{A-4}$$

This definition leads to approximately 50% (±5%) relative humidity for the normal range of indoor temperatures and activity levels.

*A standard value for the clothing and metabolic values was not assumed and, therefore, comfort coefficients will depend on the actual values of the personal variables.

ΔP = pressure drop across the window, Pa

ΔT_{comf} = comfort band

ρ = density of air, 1.2 kg/m^3

T_d = dew point temperature, °C

T_{eff} = effective temperature, °C

T_r = mean radiant temperature, °C

T_s = skin temperature

$\bar{U}_g$ = gradient wind velocity in the free stream

U_R = windspeed at site at roof level, m/s

$\bar{U}_z$ = mean wind velocity at height z

v = zero airspeed

$\bar{v}$ = mean internal airspeed, m/s

v_o = orifice velocity, m/s

$v_{+/-}$ = positive/negative orifice velocity, m/s

X = ratio of window area to wall area

Y_c = convective comfort coefficient

Y_e = evaporative comfort coefficient

Y_o = basic comfort coefficient

Y_r = radiative comfort coefficients

Y_t = total comfort coefficient

Y_x = comfort coefficients

Y_x^* = standard comfort coefficients

z = height

α = wind incidence angle measured from short side of model

δ = boundary layer thickness

$\Delta\bar{C}_p$ = nondimensional average pressure difference coefficient between opposite walls of building

$\Delta\bar{C}_{p_e}$ = estimated pressure difference coefficient

$\Delta\bar{C}_{p_{J-i}}$ = average pressure difference coefficient between opposite sides of building

LIST OF SYMBOLS

A = effective inlet area, m^2

$A_{+/-}$ = effective leakage area, m^2

a = power law exponent

C_D = nondimensional discharge coefficient, usually 0.6

$\bar{C}_{p_i}$, $\bar{C}_{p_J}$ = average pressure coefficient for each side, example: $\bar{C}_{p_1}$, $\bar{C}_{p_2}$, $\bar{C}_{p_3}$, etc.

$\bar{C}_p$ = average pressure coefficient

clo = unit insulation value of clothing, one clo = 0.155 ($M^2 °C/W$) or (.088 hr ft^2/Btu)

F_{cle} = effective thermal efficiency of clothing

F_{pcl} = permeation efficiency of clothing

h_c = convective heat transfer coefficient, $W/m^2 °C$

h_r = radiative heat transfer coefficient, $W/m^2 °C$

I = turbulence intensity

I_{cl} = basic clo value

I_{cle} = effective clo value

i,J = subscripts indicating sides of model

M_o = basic metabolic rate

m = unit of activity level of the body, met

P = pressure at location on the building

P_o = local static pressure

Q = airflow rate, M^3/hr

$Q_{+/-}$ = infiltration/exfiltration, M^3/s

T_a = ambient air temperature, °C

T_{comf} = comfort temperature

18. R.M. Aynsley. Wind-generated natural ventilation of housing for thermal comfort in hot humid climates, University of Sydney. Sydney, Australia, 1979.

19. N. Chien, Y. Fong, W. Wang, and T. Siao. Wind-tunnel studies of pressure distribution on elementary building forms, Iowa Institute of Hydraulic Research, State University of Iowa. Iowa City, Iowa, 1951.

20. S.K. Ashley. Computer simulation of buildings cooled by natural ventilation, Naval Civil Engineering Laboratory, Technical Note N-1666. Port Hueneme, Calif., May 1983.

10. M.H. Sherman, and D.T. Grimsrud. "The measurement of infiltration using fan pressurization and weather data," in Proceedings of 1st Air Infiltration Center Conference, London, England. Also published as Lawrence Berkeley Laboratory Report LBL 10852, 1980.

11. M.H. Sherman. A simplified model of thermal comfort, Lawrence Berkeley Laboratory Report LBL 159923 (unpublished). Berkeley, Calif., 1983.

12. S.K. Ashley. Basic design criteria for natural ventilation cooling of buildings, Naval Civil Engineering Laboratory, Technical Memorandum 63-82-08. Port Hueneme, Calif., Nov 1982.

13. M.P. Modera, M.H. Sherman, and D.T. Grimsrud. "Long-term infiltration measurements in a full-scale test structure," in Proceedings of Air Infiltration Center Conference on Building Design for Minimum Air Infiltration, Sep 1981. Also published as Lawrence Berkeley Laboratory Report LBL 13504, 1981.

14. M. Jensen and N. Frank. Model-scale tests in turbulent wind part I and II, The Danish Technical Press. Copenhagen, Denmark, 1963.

15. A.G. Davenport. "1963 proceedings of the conference on wind effects on buildings and structures," vol 1, HMSO, 1965.

16. J.A. Paterka and J.E. Cermak. Wind engineering study of One Williams Center, Tulsa. Colorado State University, Fort Collins, Colo., Dec 1974.

17. R.E. Akins, J.A. Paterka, and J.E. Cermak. Average pressure coefficients for rectangular buildings, Colorado State University. Fort Collins, Colo., 1979.

2. A.K. Blomsterbert, M.P. Modera, and D.T. Grimsrud. The mobile infiltration test unit - its design and capabilities: Preliminary experimental results, Lawrence Berkeley Laboratory, Report LBL 12259. Berkeley, Calif., 1981.

3. M.H. Sherman, M.P. Modera, and D.T. Grimsrud. "A predictive air infiltration model - Field validation and sensitivity analysis," in Proceedings of Third (CIB) International Symposium on Energy Conservation in the Built Environment, 6.A.1, March 1982. Also published as Lawrence Berkeley Laboratory Report LBL 13520. Berkeley, Calif., 1981.

4. M.P. Modera, M.H. Sherman, and D.T. Grimsrud. "A predictive air infiltration model - long-term field test validation," American Society of Heating, Refrigerating and Air Conditioning Engineers Transcripts, vol 88, part I, 1982. Also published as Lawrence Berkeley Laboratory Report LBL 13509, Berkeley, Calif., 1981.

5. Handbook of fundamentals. American Society of Heating, Refrigerating and Air Conditioning Engineers, Chapter 8, 1981.

6. Handbook of fundamentals. American Society of Heating, Refrigerating and Air Conditioning Engineers, Chapter 5, 1981.

7. B. Givoni. Man, climate, and architecture. Applied Science Publishers, London, England, p 293, 1976.

8. M.H. Sherman, R.C. Sonderegger and D.T. Grimsrud. The LBL infiltration model (unpublished). Berkeley, Calif.

9. M.H. Sherman. Air infiltration in buildings, Ph.D. Thesis, University of California, Lawrence Berkeley Laboratory LBL 10712, Berkeley, Calif., 1980.

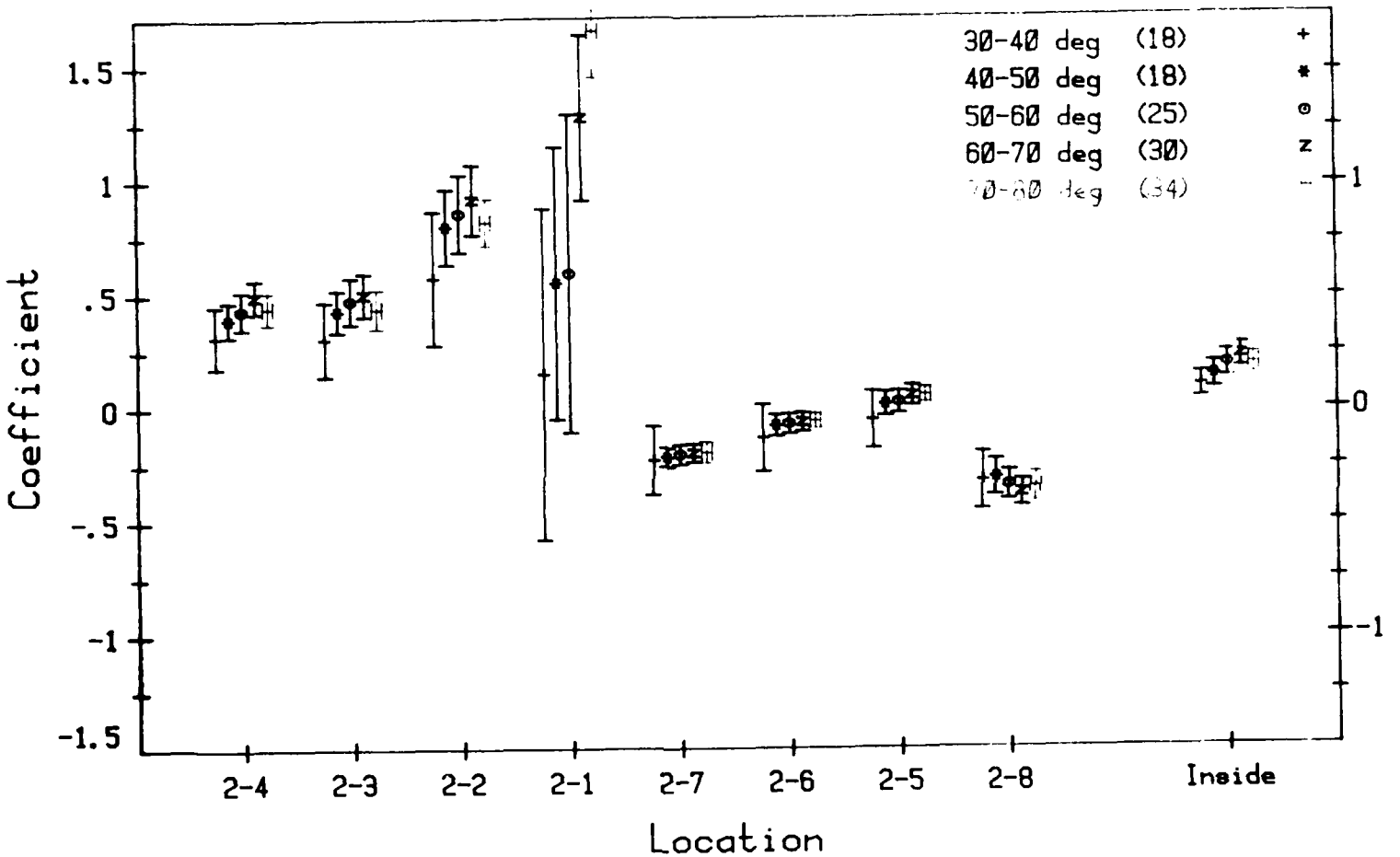

(b) Building No. 2, second story.

Figure B-1. Continued.

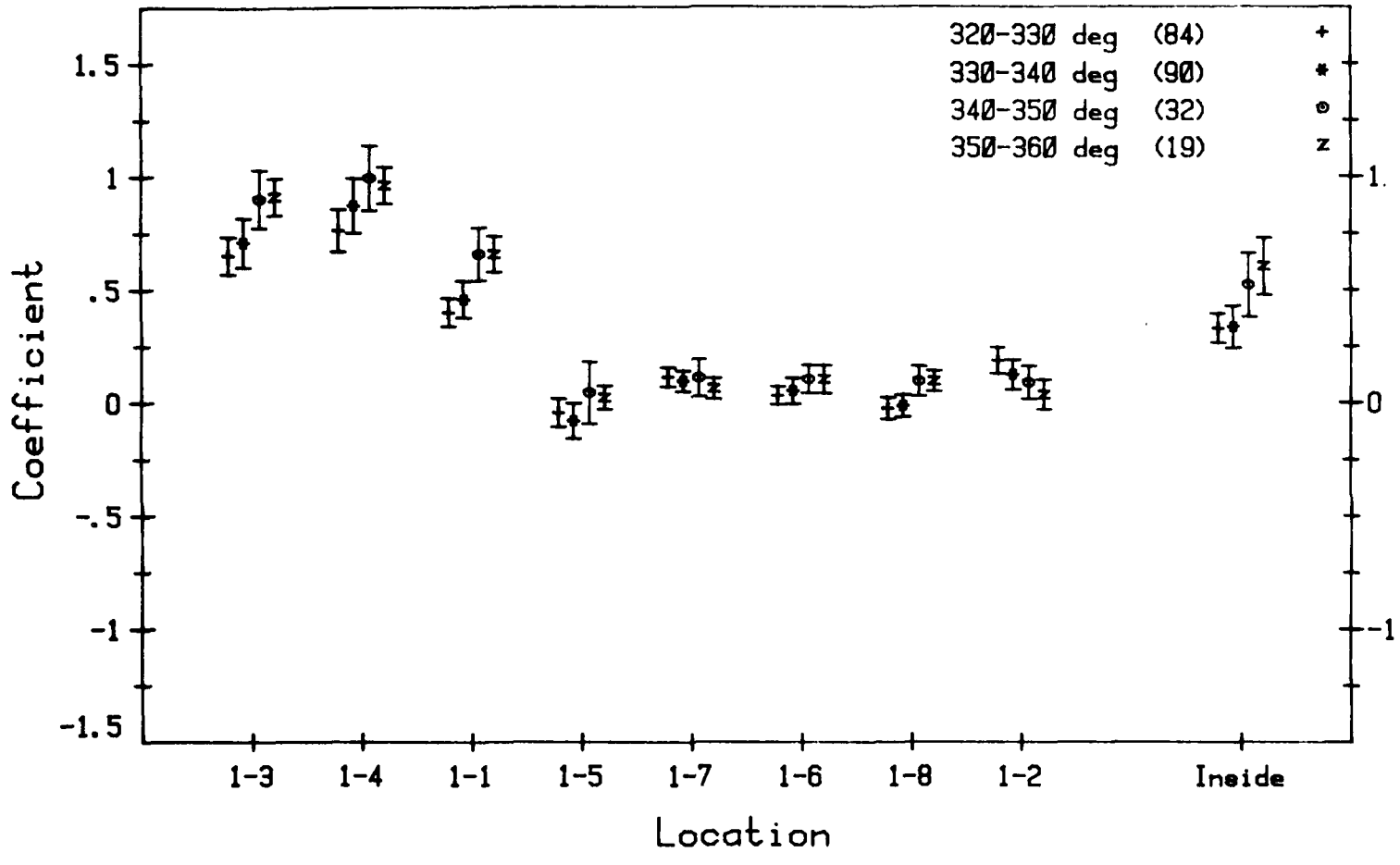

Figure B-2. Average pressure coefficients for Building No. 2 (single-story). Angles are relative to building north. Numbers in parenthesis are points in that angle bin. Ordinate indicators refer to taps in the main text.

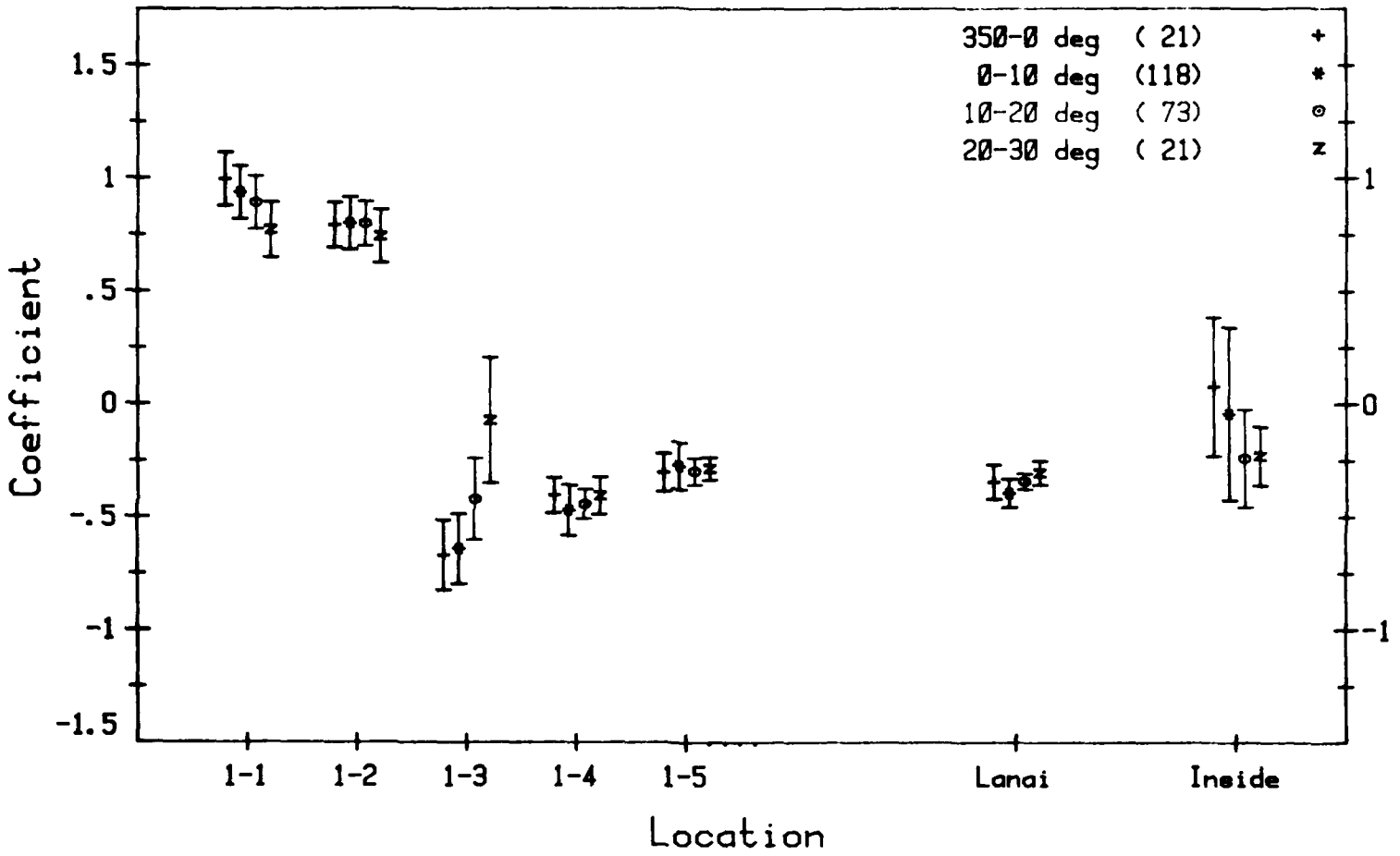

(a) Building No. 3, east apartment.

Figure B-3. Average pressure coefficients for Building No. 3. Angles are relative to building north. Numbers in parenthesis are points in that angle bin. Ordinate indicators refer to taps in the main text.

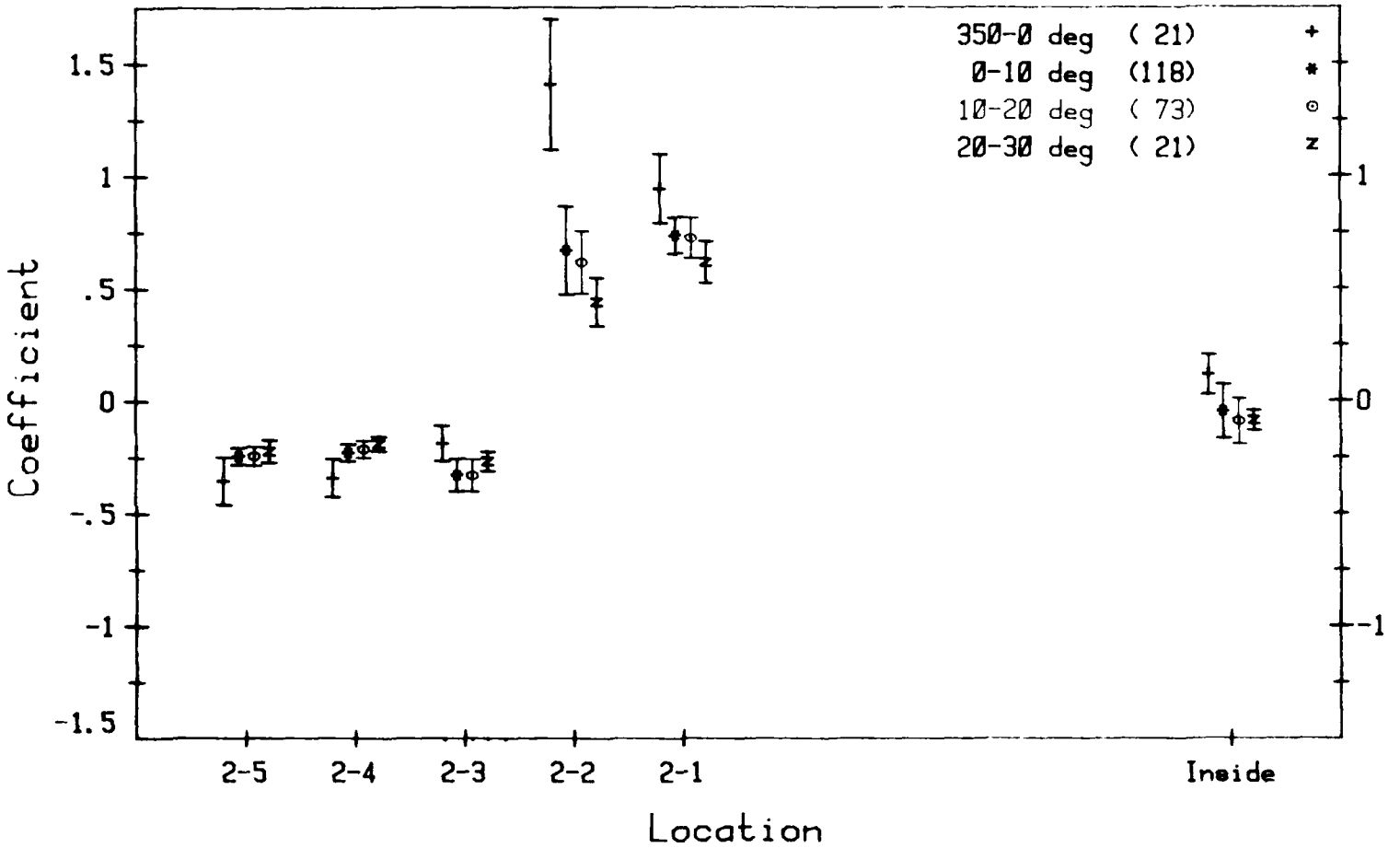

(b) Building No. 3, west apartment.

Figure B-3. Continued.

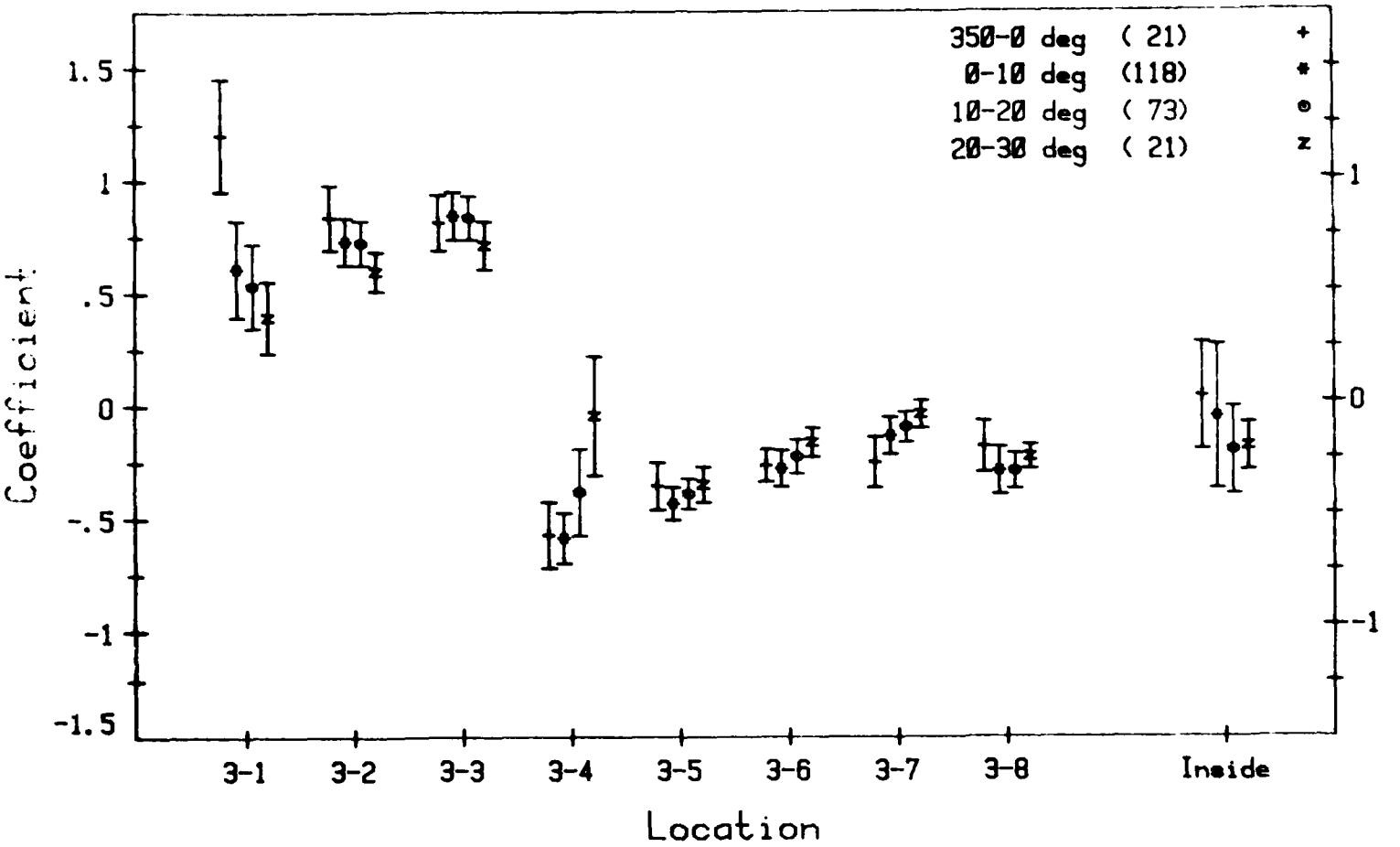

(c) Building No. 3, ground floor.

Figure B-3. Continued.

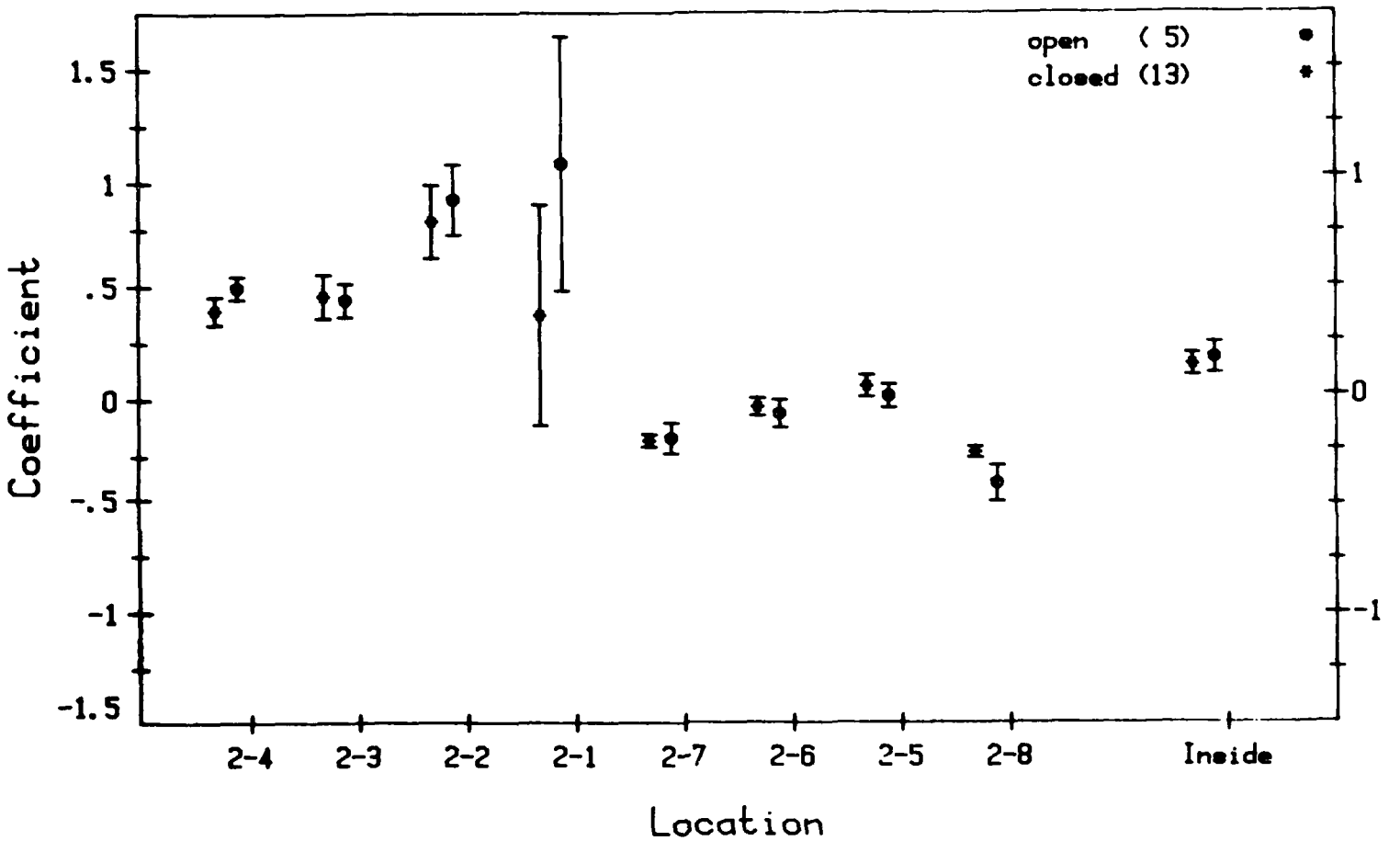

(a) Building No. 1, second story, 40-50 degrees.

Figure B-4. The effect on Building No. 1 (second story) pressure coefficients due to open windows. Angles are relative to building north. Numbers in parenthesis are points in that angle bin. Ordinate indicators refer to taps in the main text.

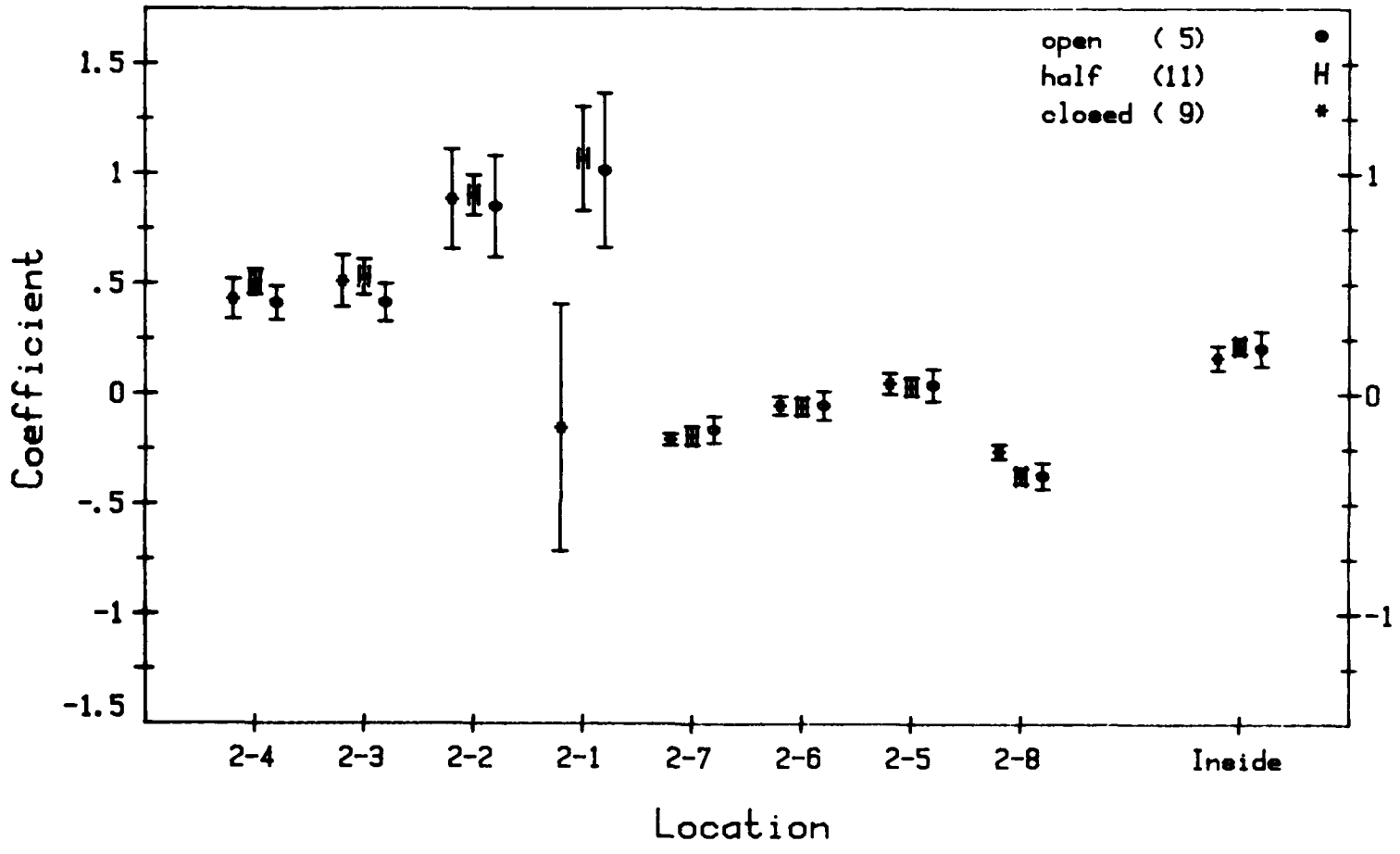

(b) Building No. 1, second story, 50-60 degrees.

Figure B-4. Continued.

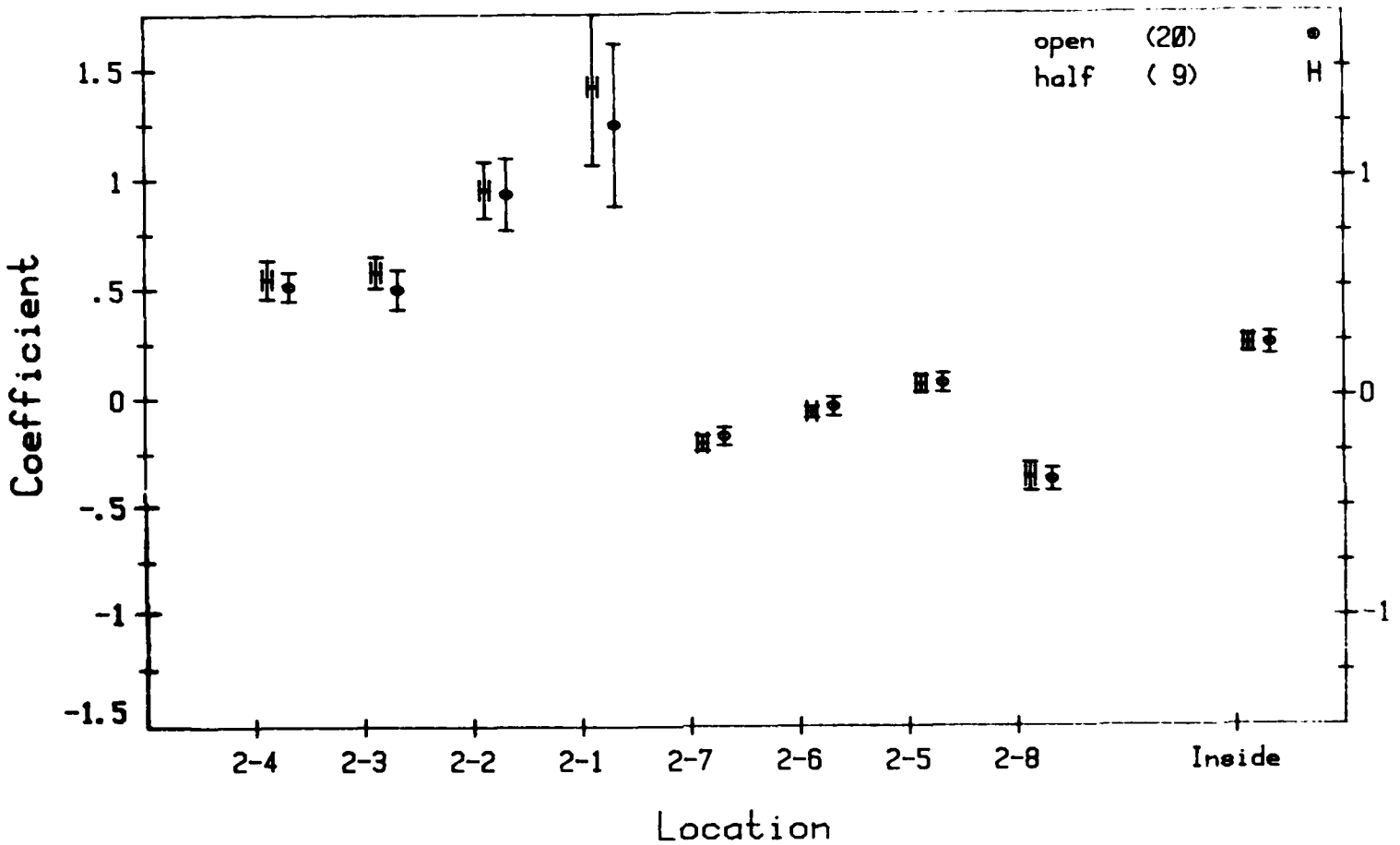

(c) Building No. 1, second story, 60-70 degrees.

Figure B-4. Continued.

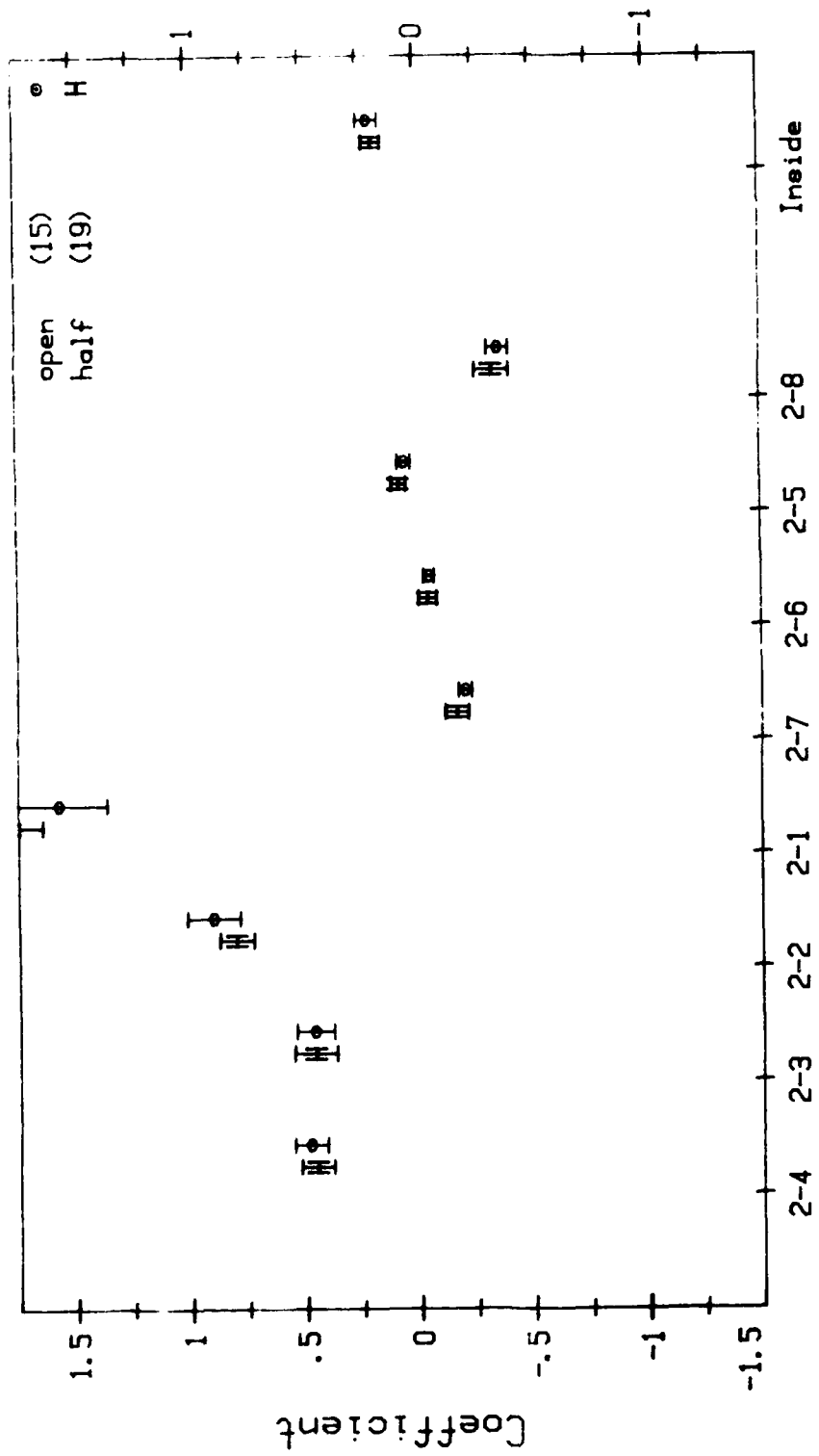

(d) Building No. 1, second story, 70-80 degrees.

Figure B-4. Continued.

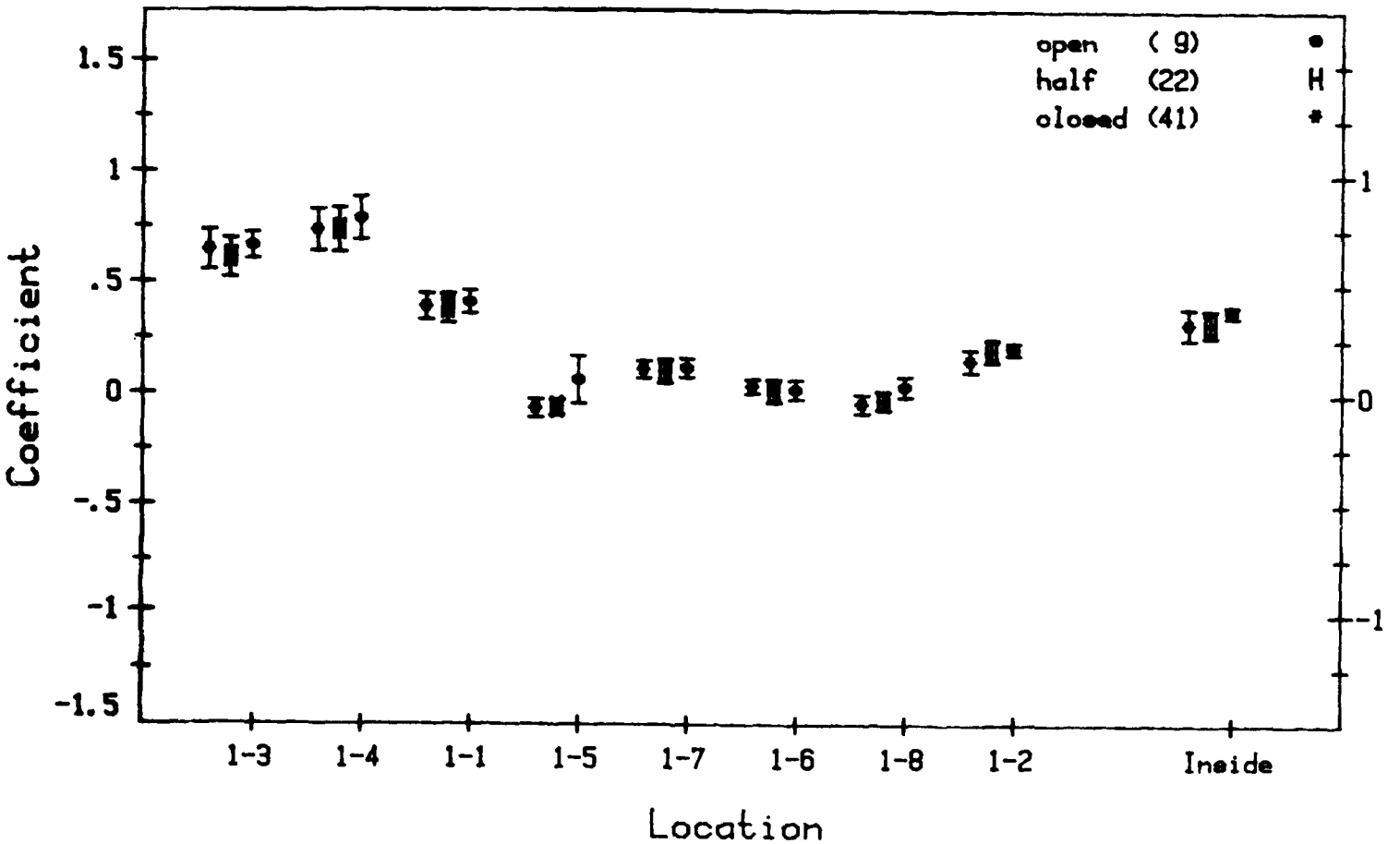

(a) Building No. 2, 320-330 degrees.

Figure B-5. The effect on Building No. 2 pressure coefficient due to open windows. Angles are relative to building north. Number in parenthesis are points in that angle bin. Ordinate indicators refer to taps in the main text.

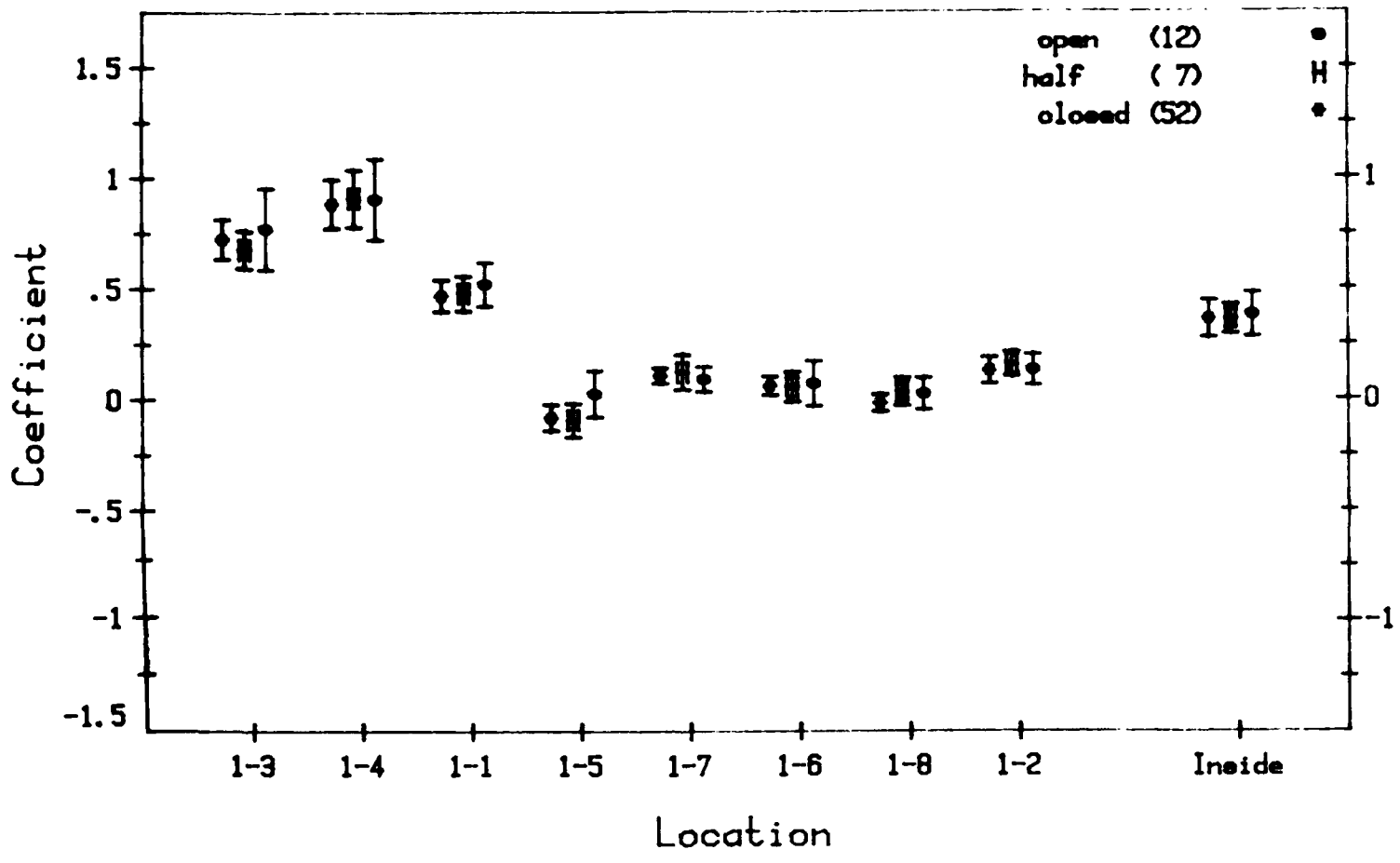

(b) Building No. 2, 330-340 degrees.

Figure B-5. Continued.

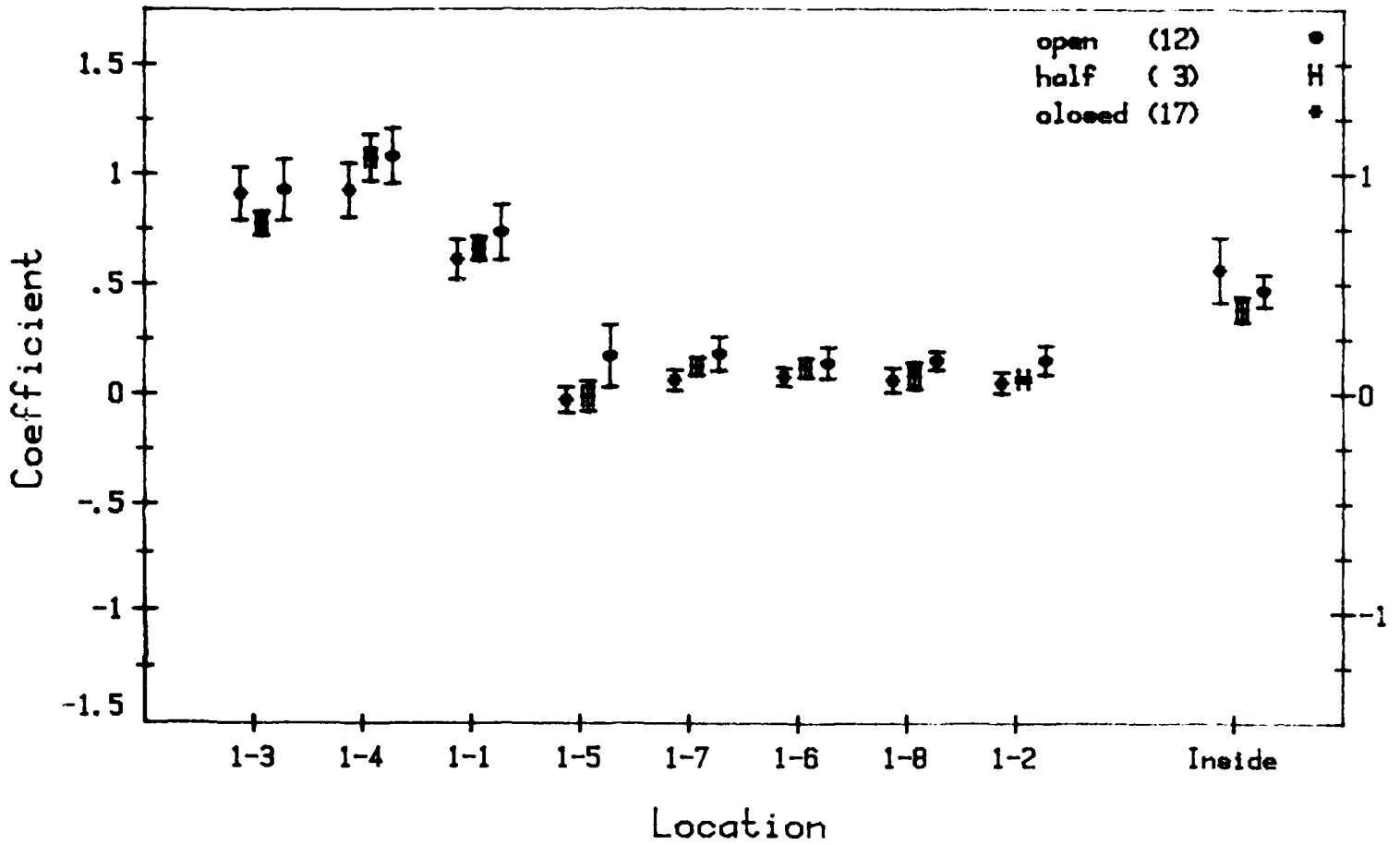

(c) Building No. 2, 340-350 degrees.

Figure B-5. Continued.

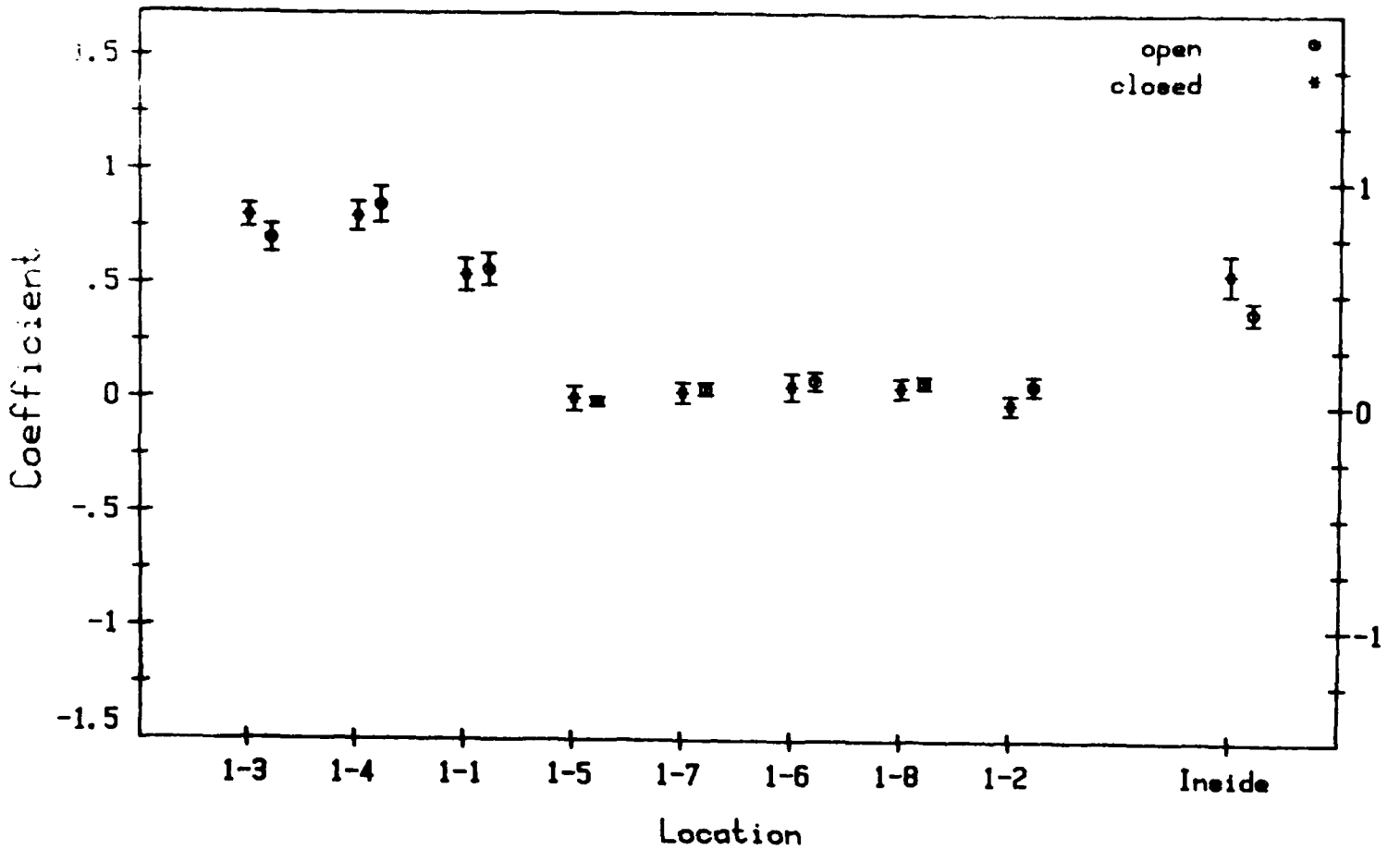

(d) Building No. 2, 350-0 degrees.

Figure B-5. Continued.

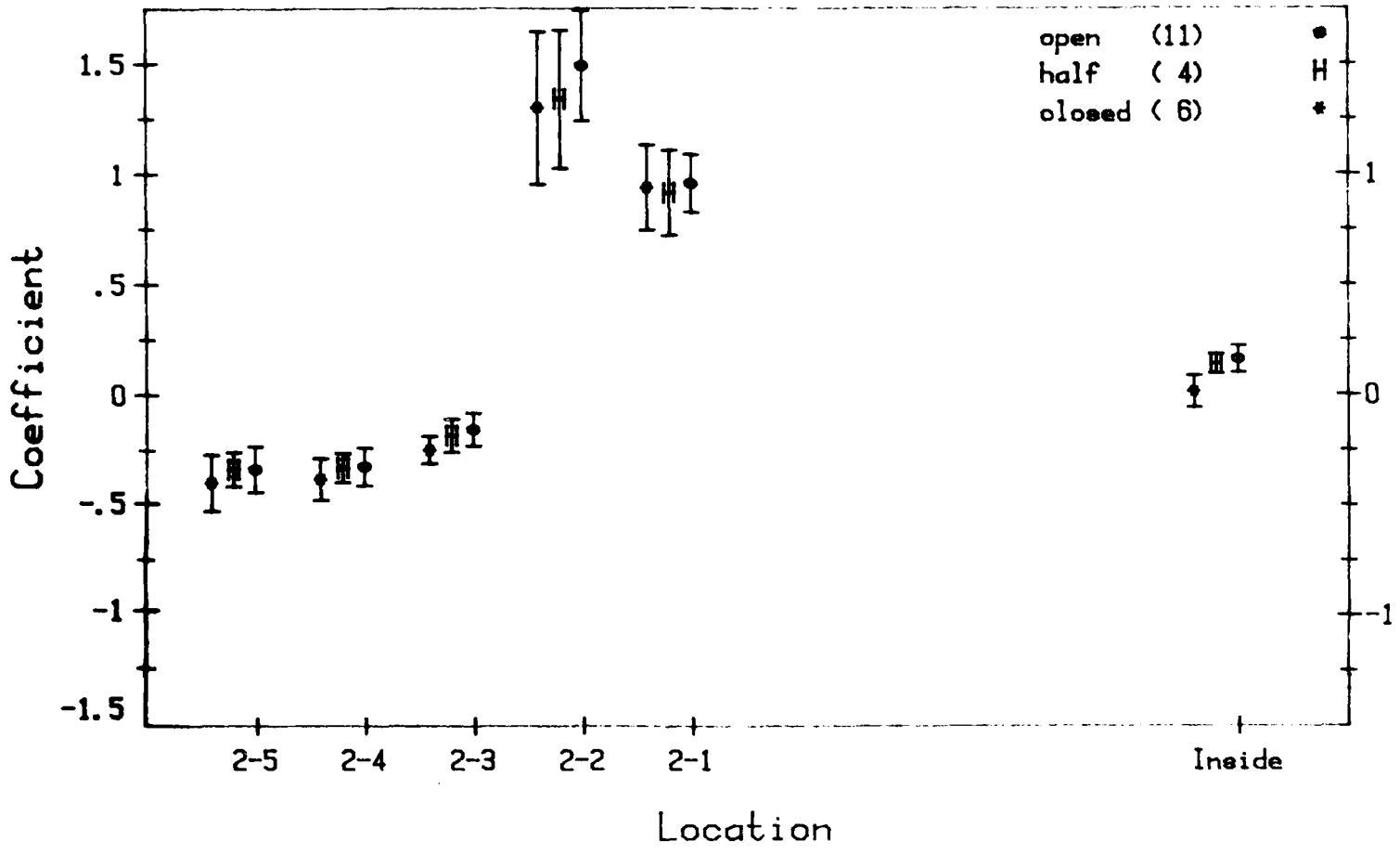

(a) Building No. 3, west apartment, 350-360 degrees.

Figure B-6. The effect on the west apartment of Building No. 3 pressure coefficients due to open windows. Angles are relative to building north. Numbers in parenthesis are points in that angle bin. Ordinate indicators refer to taps in main text.

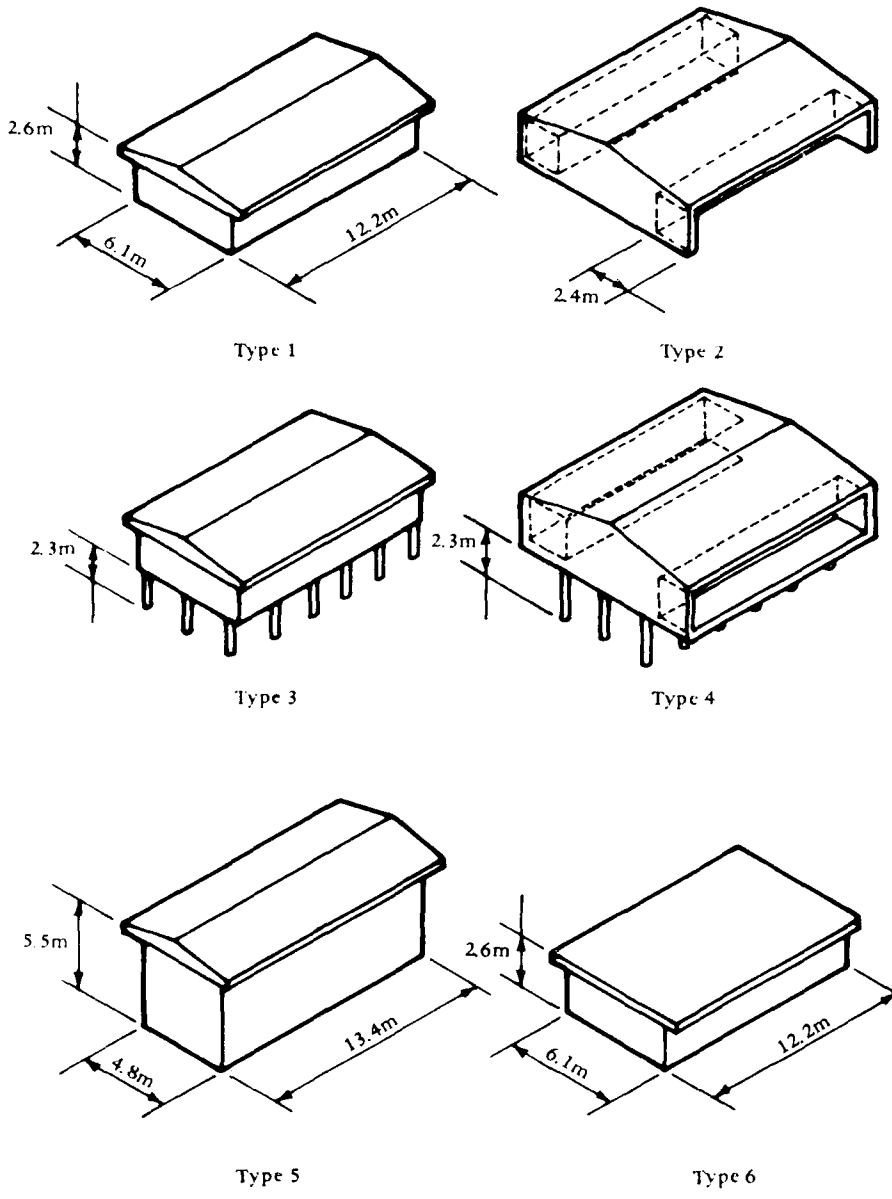

Figure C-1. Wind directions on buildings.

Appendix C

PRESSURE COEFFICIENTS FOR RESIDENTIAL HOUSING
AND COMMERCIAL BUILDINGS
(Ref 17 and 18)

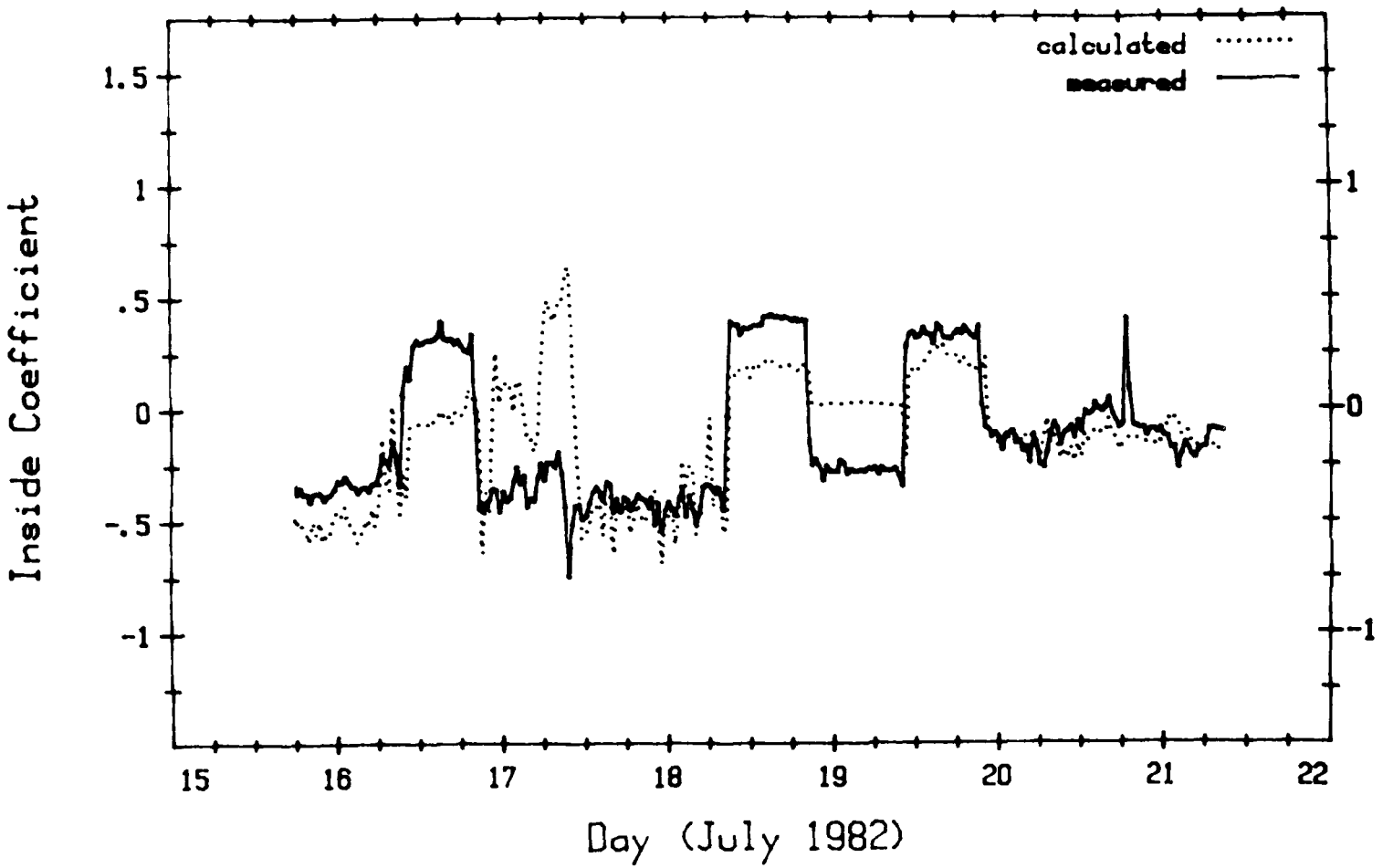

(d) Building No. 3, east apartment.

Figure B-9. Continued.

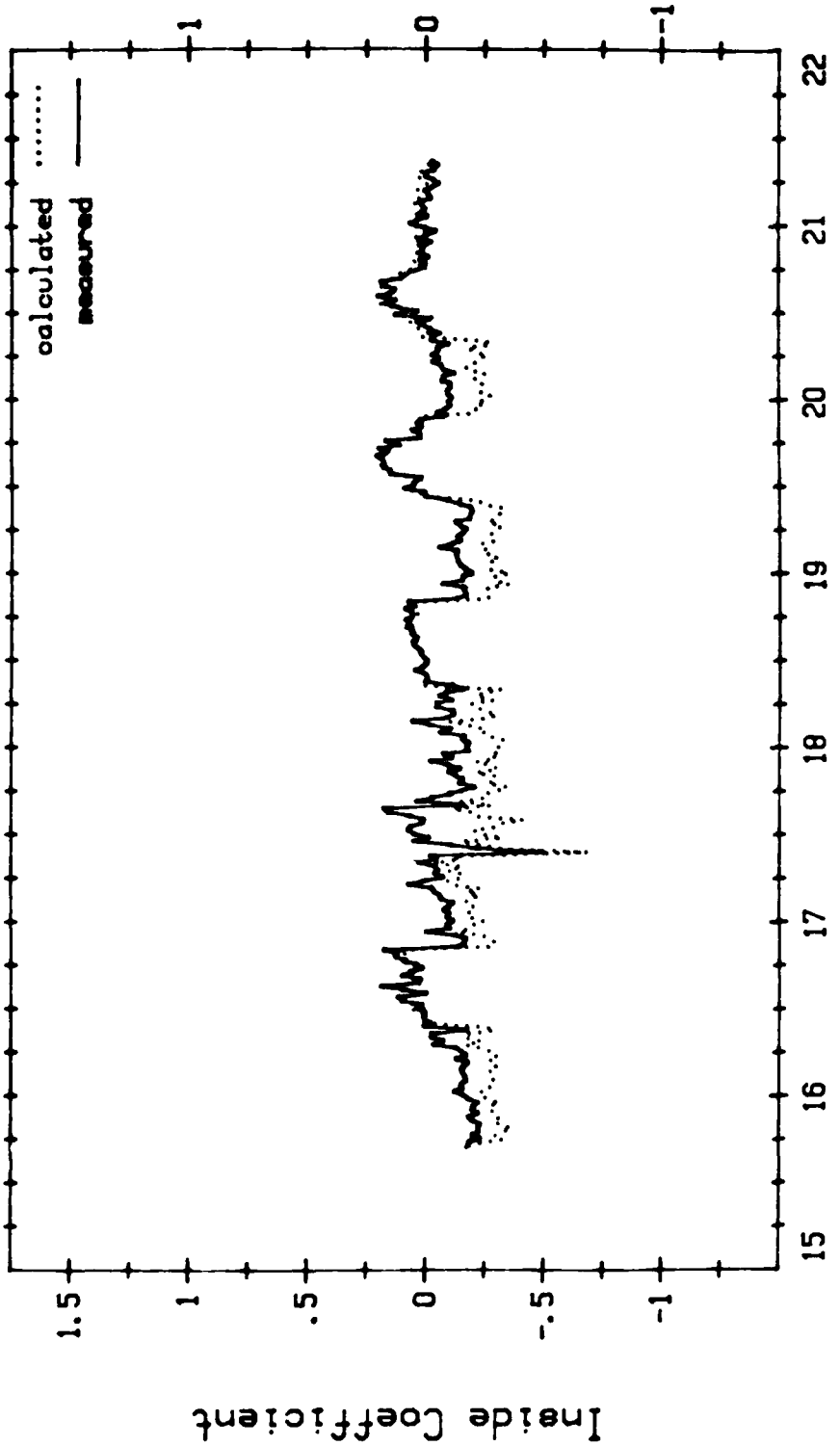

(c) Building No. 3, west apartment.

Figure B-9. Continued.

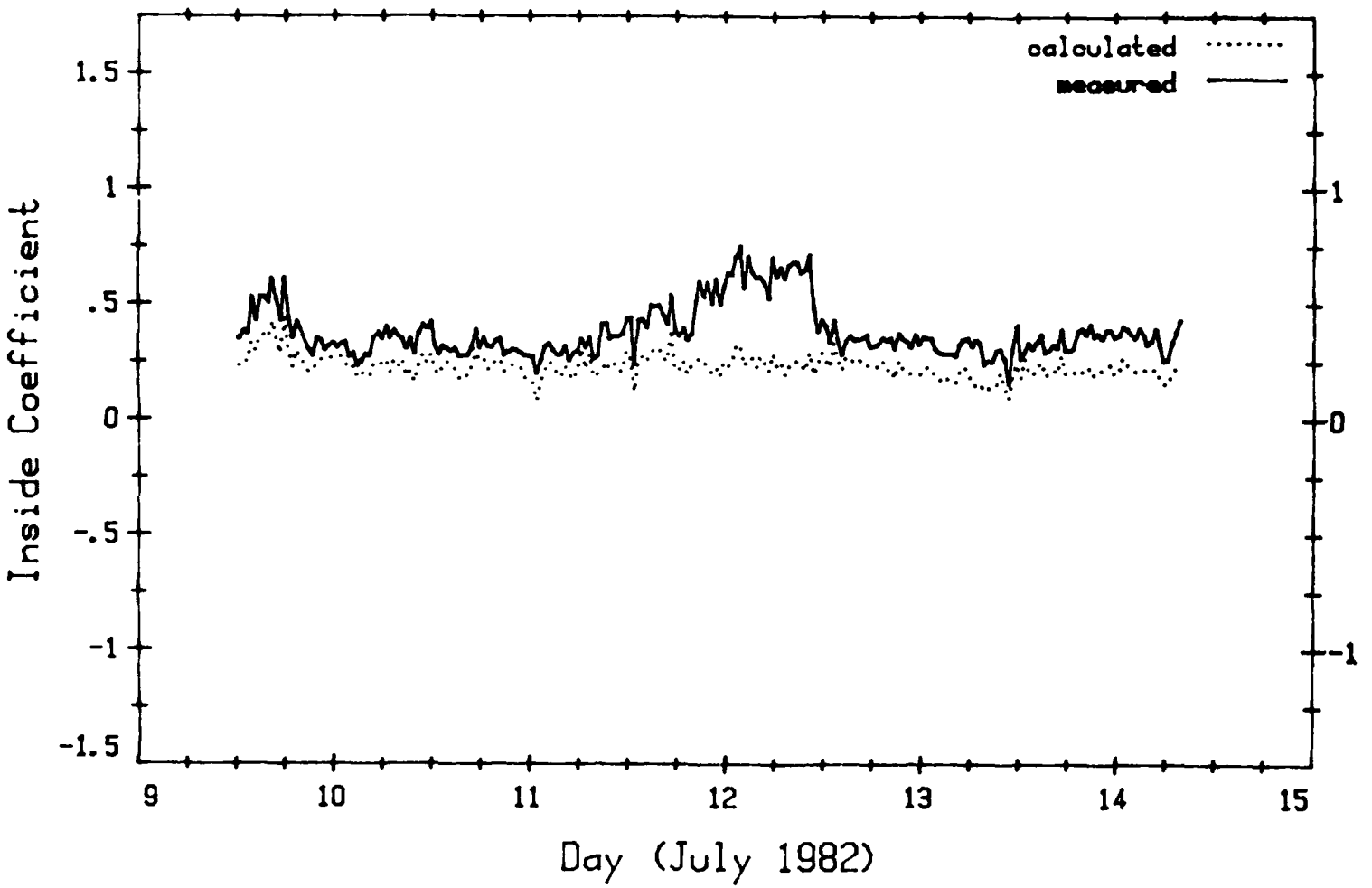

(b) Building No. 2, west side.

Figure B-9. Continued.

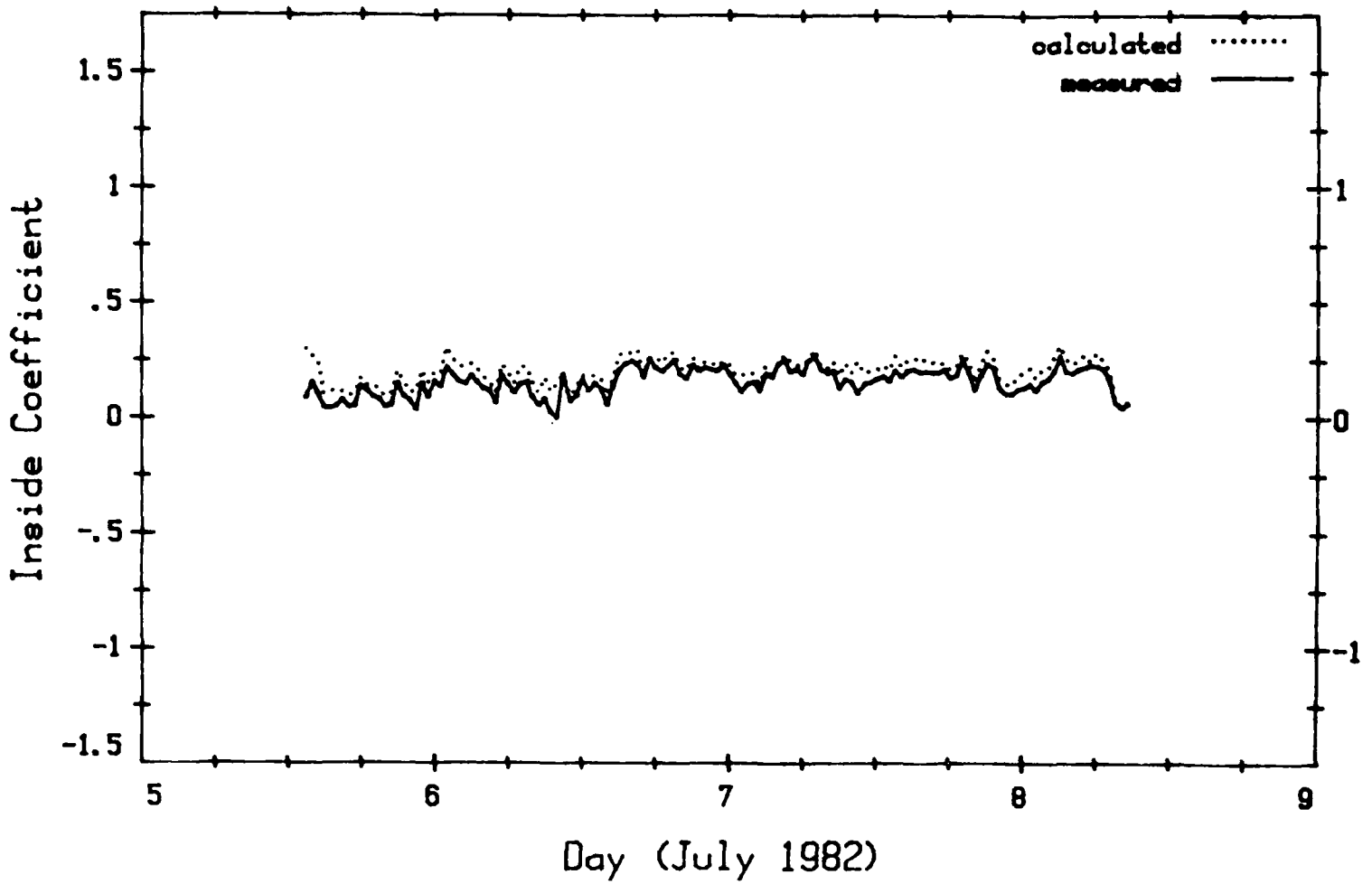

(a) Building No. 1, second story.

Figure B-9. Time series data for both measured and calculated internal pressure coefficients.

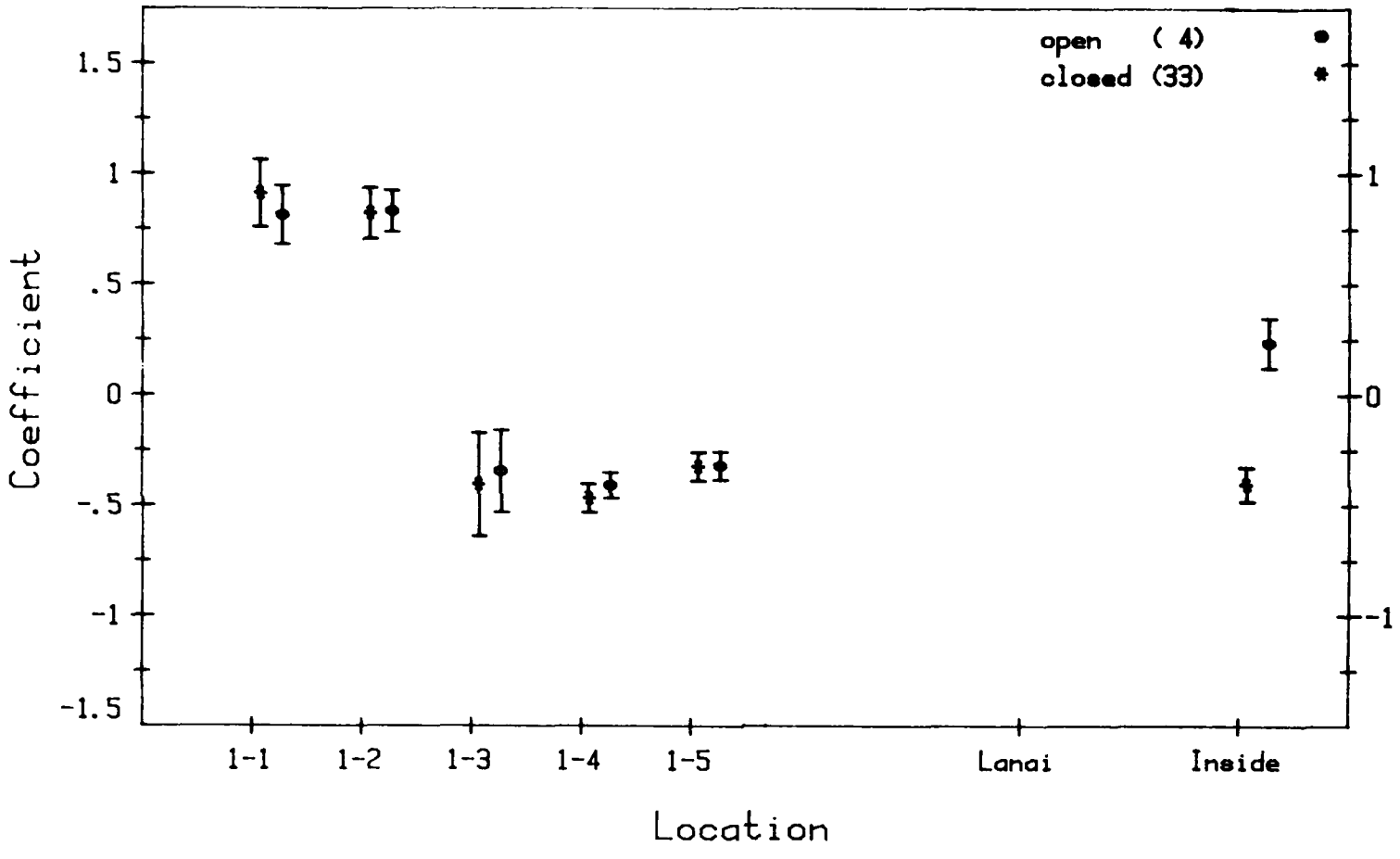

(c) Building No. 3, east apartment (lanai opened) 10-20 degrees.

Figure B-8. Continued.

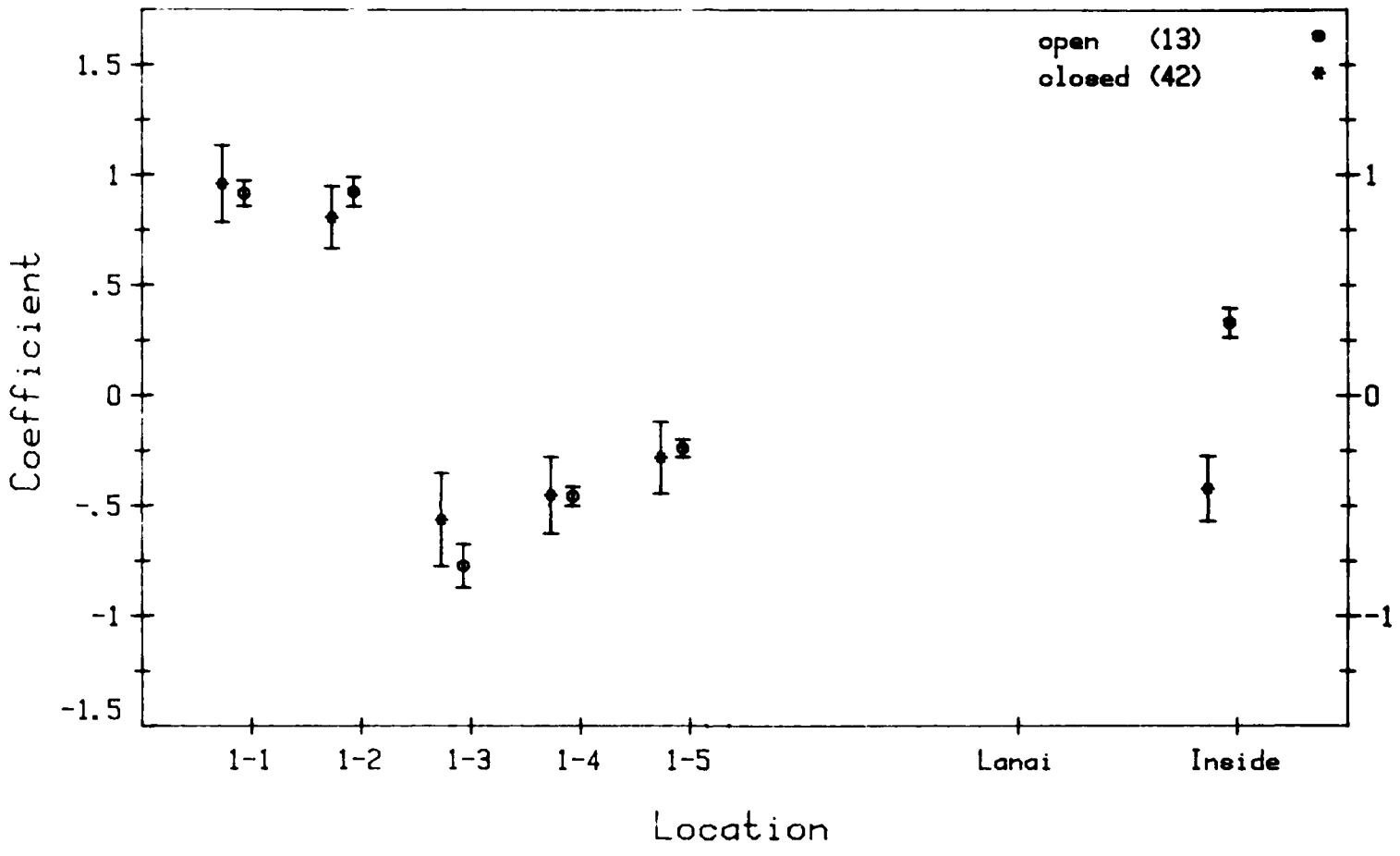

(b) Building No. 3, east apartment (lanai opened) 0-10 degrees.

Figure B-8. Continued.

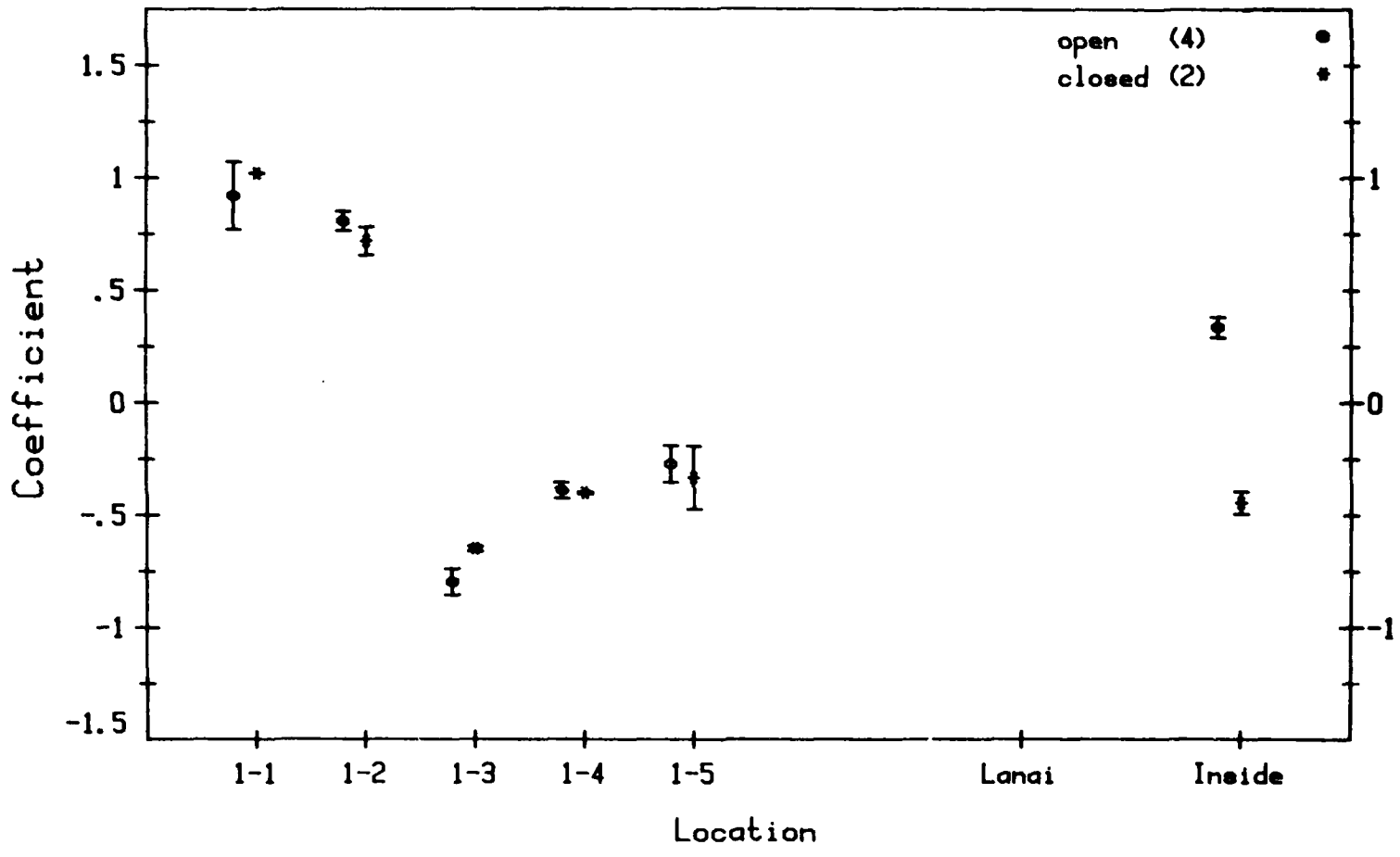

(a) Building No. 3, east apartment (lanai opened) 350-0 degrees.

Figure B-8. The effect on the east apartment of Building No. 3 pressure coefficients due to open windows (lanai opened). Angles are relative to building north. Numbers in parenthesis are points in that angle bin. Ordinate indicators refer to taps in main text.

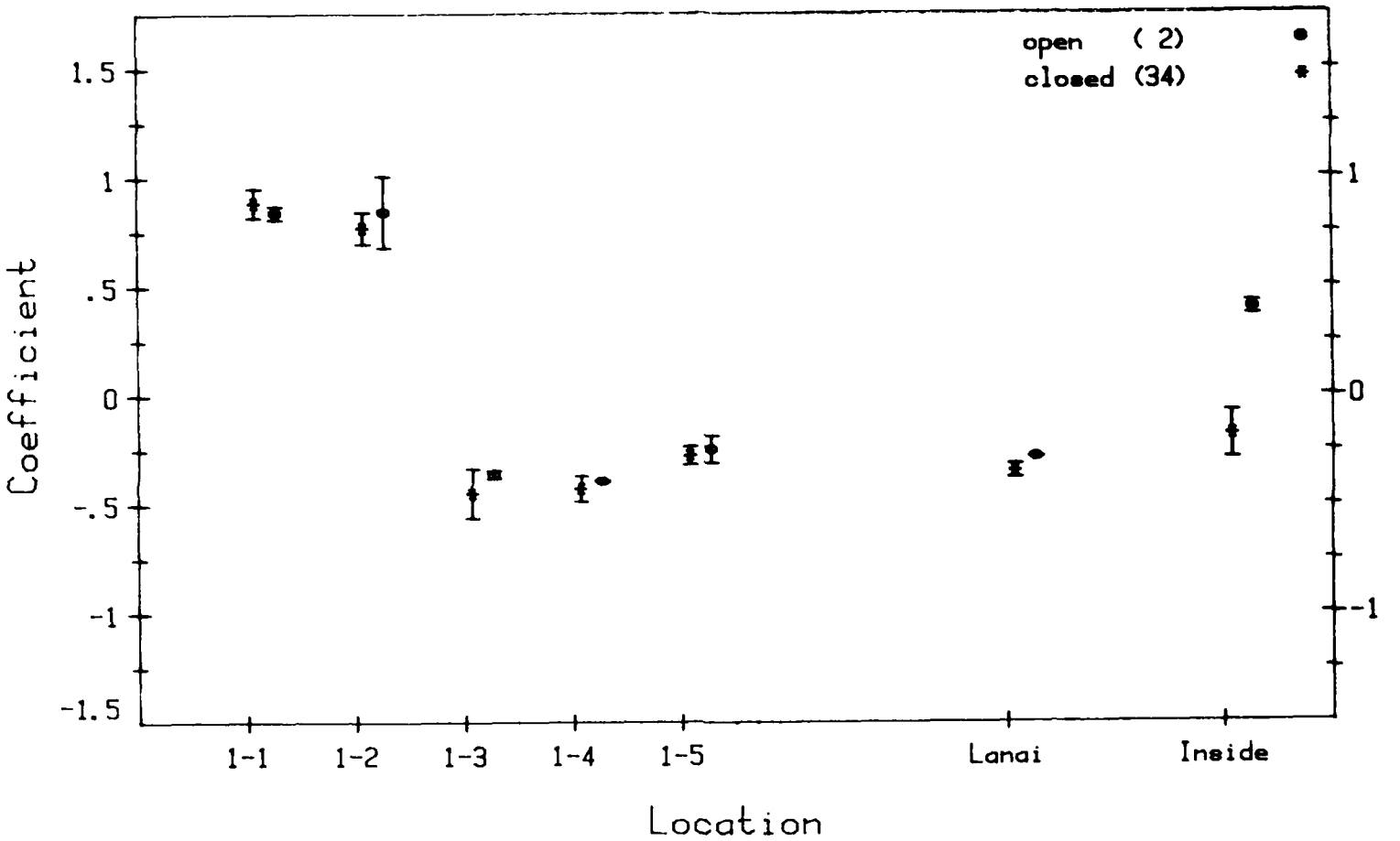

(c) Building No. 3, east apartment (lanai isolated) 10-20 degrees.

Figure B-7. Continued.

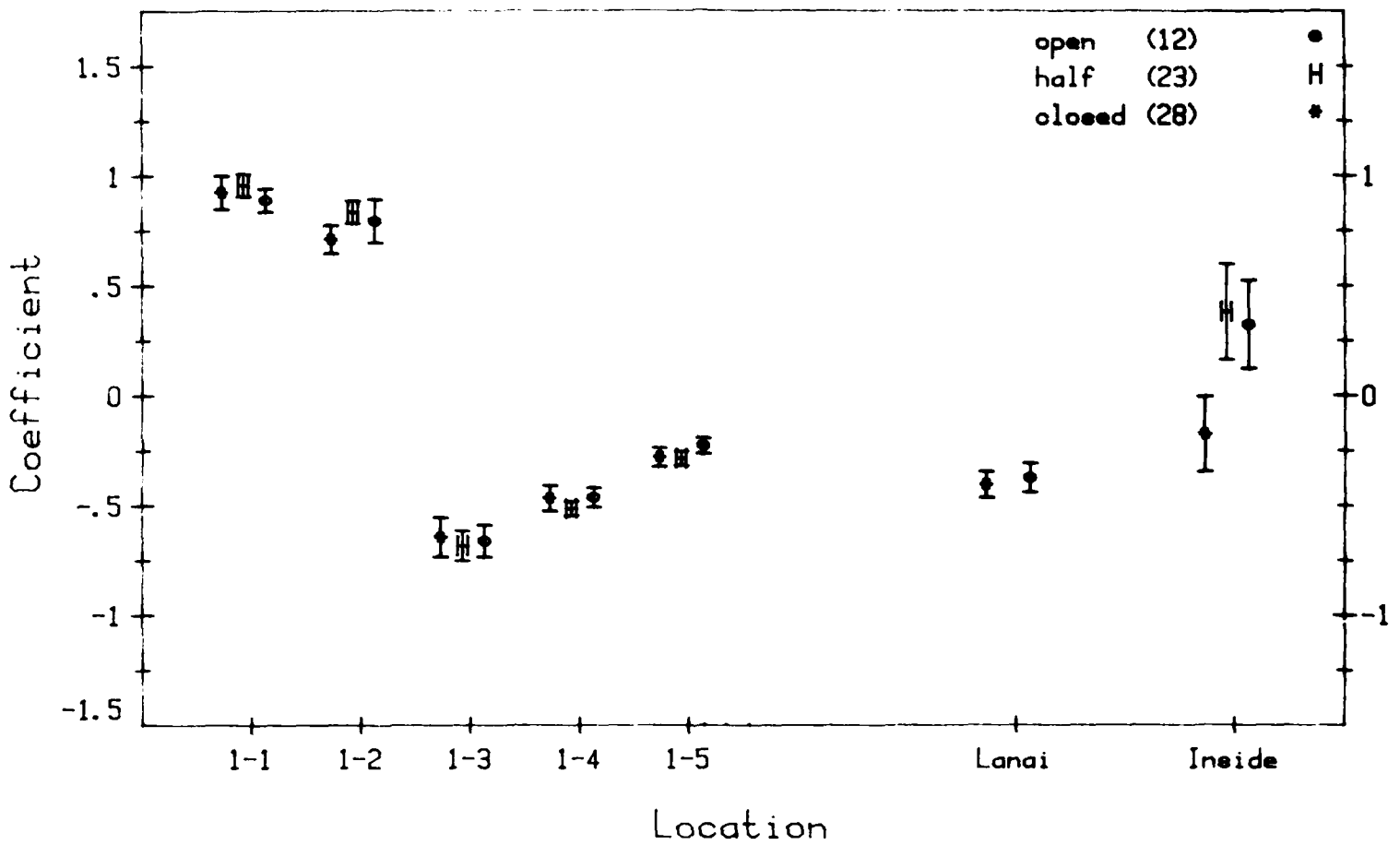

(b) Building No. 3, east apartment (lanai isolated) 0-10 degrees.

Figure B-7. Continued.

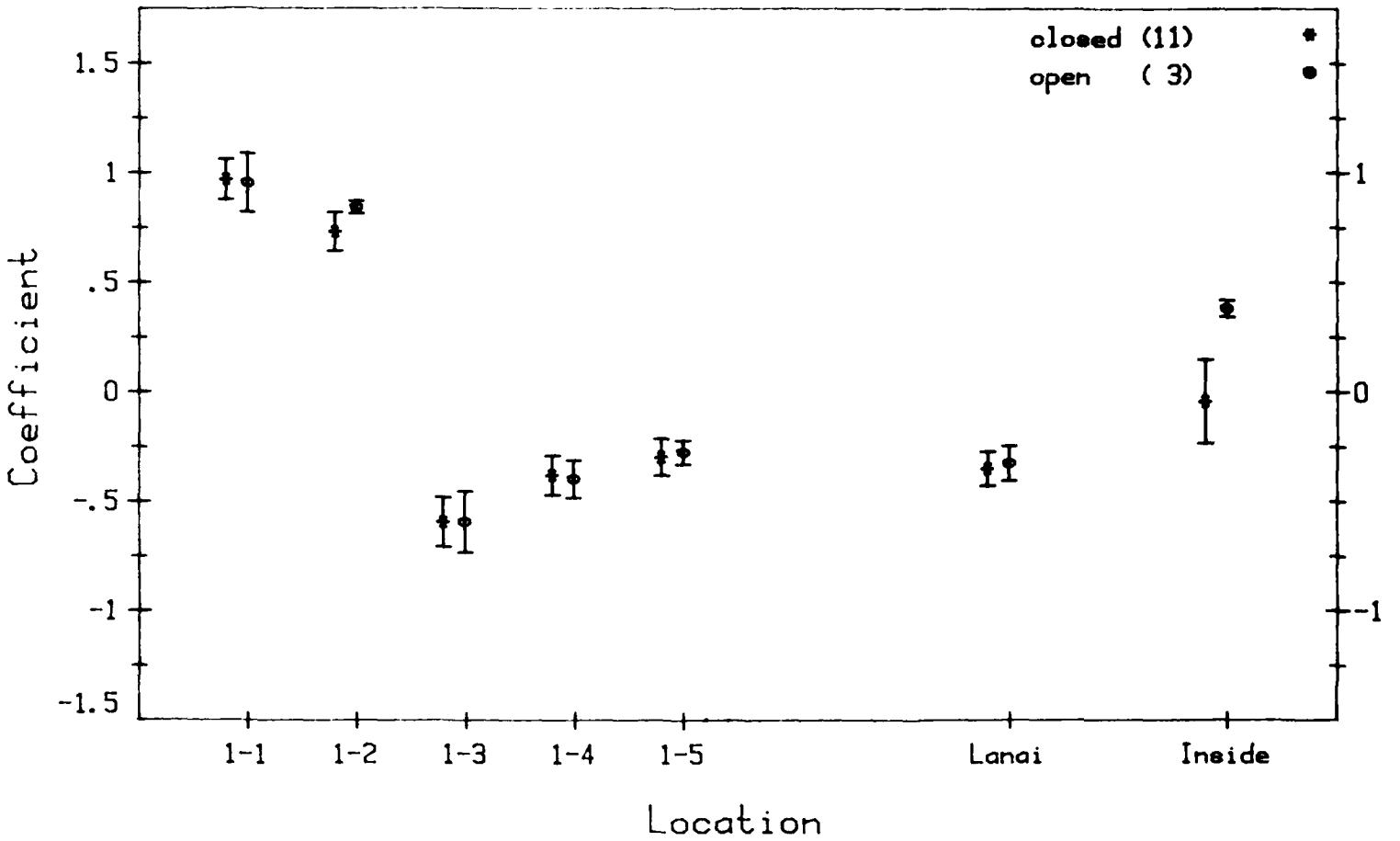

(a) Building No. 3, east apartment (lanai isolated) 350-360 degrees.

Figure B-7. The effect of the east apartment of Building No. 3 pressure coefficients due to open windows (lanai isolated). Angles are relative to building north. Numbers in parenthesis are points in that angle bin. Ordinate indicators refer to taps in main text.

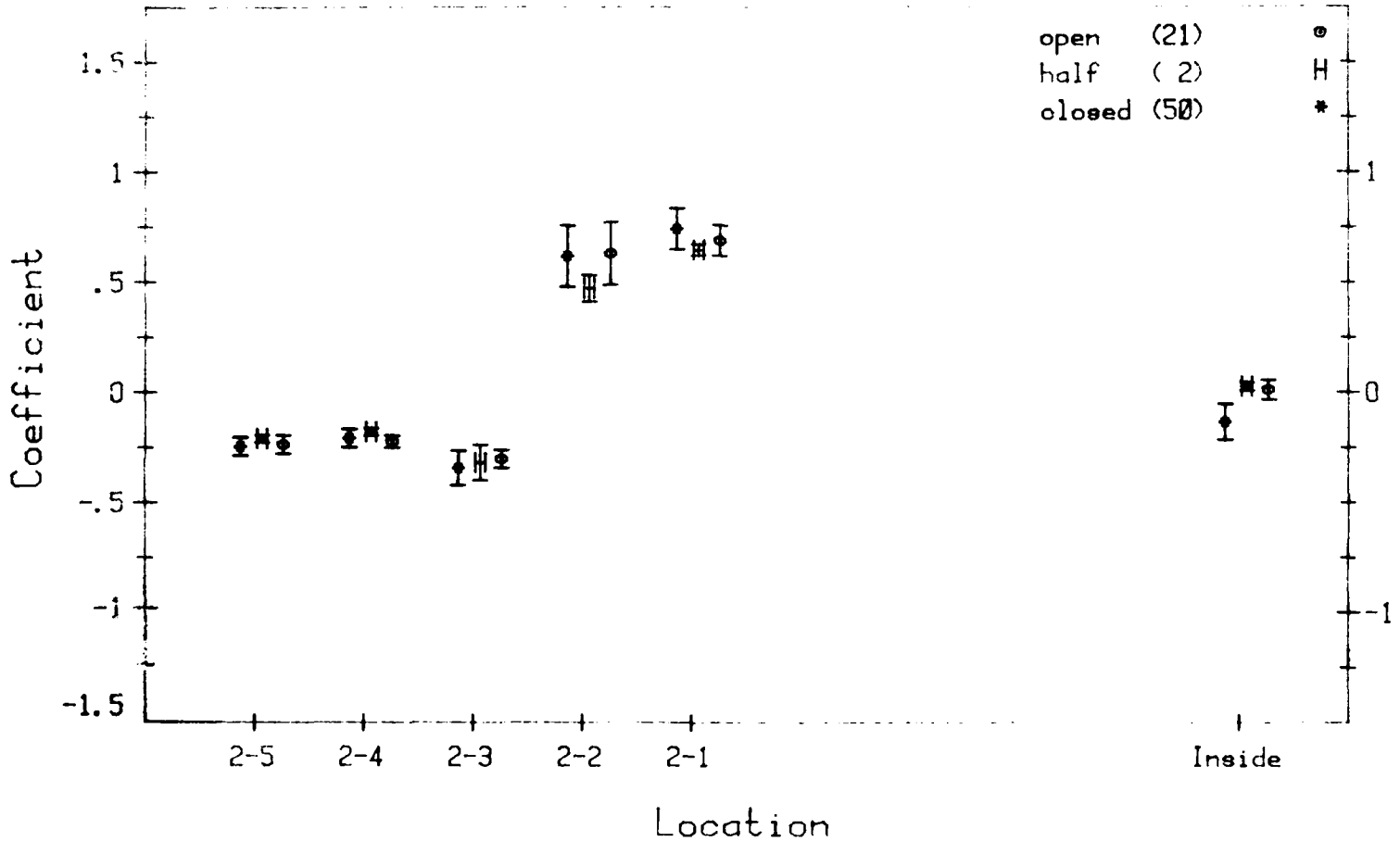

(c) Building No. 3, west apartment, 10-20 degrees.

Figure B-6. Continued.

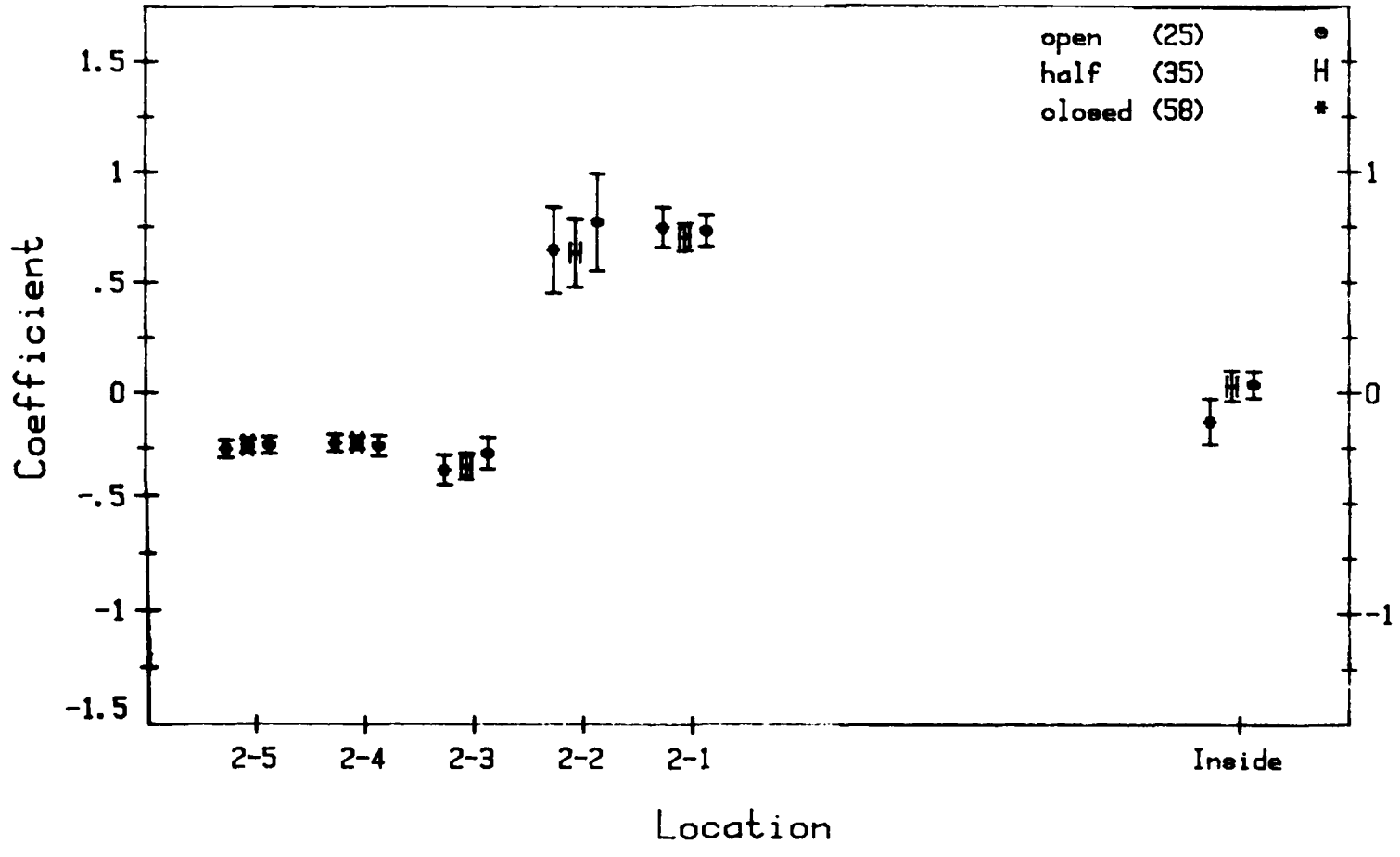

(b) Building No. 3, west apartment 0-10 degrees.

Figure B-6. Continued.

Table C-1. Summary of Wind Pressure Difference Characteristics at Mid-Height of Walls on Six Types of Isolated Models at Wind Incidences, Normal, 30 Degrees and 45 Degrees to Long Walls.

Model Features	Model Type	Overall Ranking Based on Average Pressure Diff. Coefft. Between Long Walls	Incidence to Long Wall (degrees)	Average Pressure Diff. Coefft. Between Long Walls	Maximum Pressure Diff. Coefft. Between Opposite Points on Long Walls	Minimum Pressure Diff. Coefft. Between Opposite Points on Long Walls
Single story on-grade	1	Worst	0	0.49	0.56 C	0.42 BE
			30	0.41	0.67 WE	0.10 LE
			45	0.34	0.71 WE	-0.02 LE
Average				0.41		
Single story on-grade with extended eaves and end walls	2	2nd Best	0	0.51	0.56 C	0.46 BE
			30	0.66	0.71 WE	0.58 LE
			45	0.58	0.63 C	0.52 C
Average				0.58		
Single story elevated above ground	3	3rd Best	0	0.65	0.71 C	0.60 BE
			30	0.58	0.79 WE	0.33 LE
			45	0.43	0.81 WE	0.00 LE
Average				0.55		
Single story elevated above ground with extended verandas and end walls	4	Best	0	0.81	0.85 BE	0.77 C
			30	0.67	0.75 LE	0.50 WE
			45	0.75	0.81 LE	0.73 BE
Average				0.74		
Two story	5	5th Best	0	0.61	0.6 C	0.52 BE
			30	0.33	0.37 C	0.24 WE
			45	0.31	0.42 C	0.12 LE
Average				0.42		
Single story on-grade with flat roof	6	4th Best	0	0.51	0.58 C	0.44 BE
			30	0.42	0.69 WE	0.08 LE
			45	0.35	0.71 WE	0.00 LE
Average				0.43		

C = center one-third of long walls; BE = both ends of long walls; WE = windward ends of long walls; LE = leeward ends of long walls

Table C-2. Wind at 45 Degrees Incidence to a Long Wall.

Model Features	Average Pressure Differential Coefficient Between Mid-Height of Long Walls for Wind at 45 degrees Incidence to a Long Wall (Reference Pressure – Dynamic 10 Meters Above Ground in Wooded Suburban Terrain)
Single story elevated above ground with extended eaves and end walls (Type 4)[a]	0.75
Single story on-grade with extended eaves and end walls (Type 2)[a]	0.58
Single story elevated above ground (Type 3)[a]	0.43
Single story on-grade with flat roof (Type 6)	0.35
Single story on-grade with 10 degree pitch roof (Type 1)	0.34
Two story (Type 5)	0.31

[a]Note that the three highest ranking model types, 4, 2 and 3, at 45 degrees incidence were also highest ranking averaged over wind incidences of 0 degrees, 30 degrees and 45 degrees.

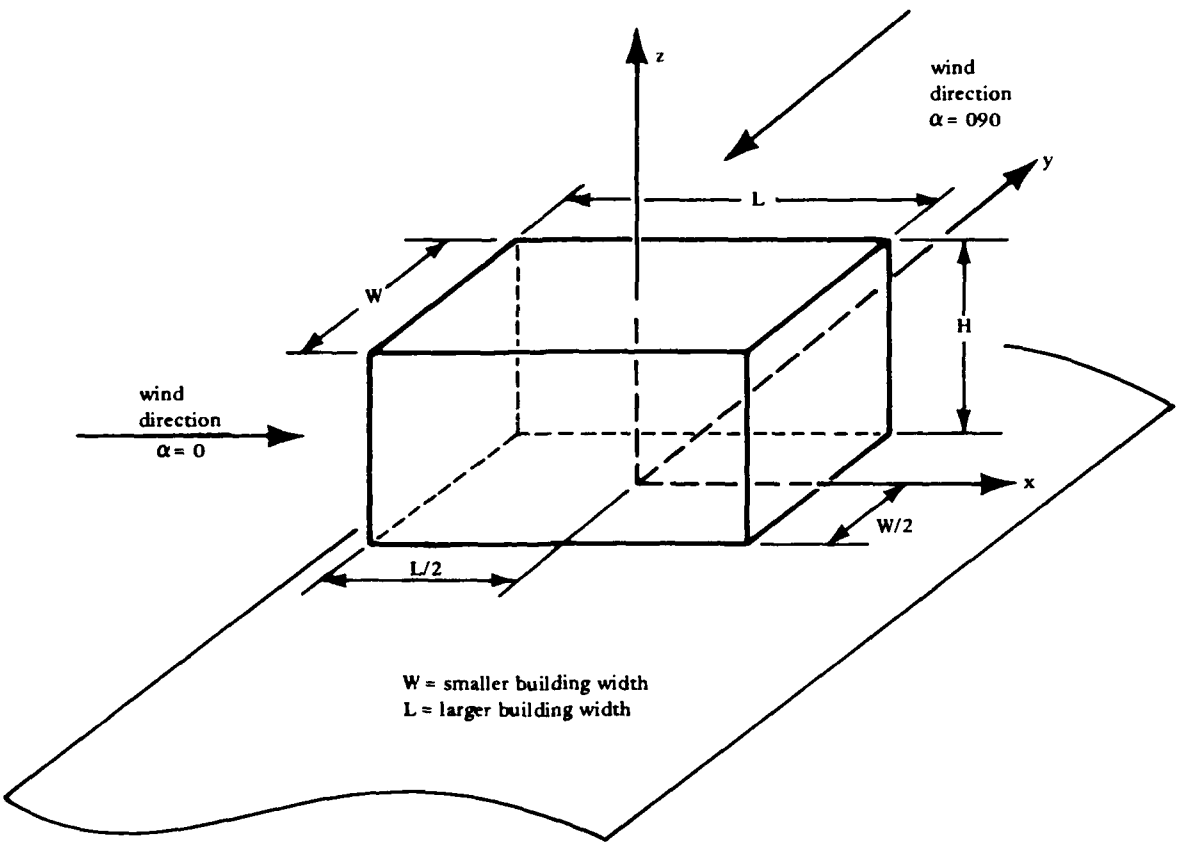

calculate side ratio: $\gamma = \frac{\text{width of building}}{\text{length (larger side) of building}} = \frac{W}{L}$

Figure C-2. Averaged pressure coefficients based on a reference velocity measured at the roof, $\bar{C}_p$, for a side ration of 1.0.

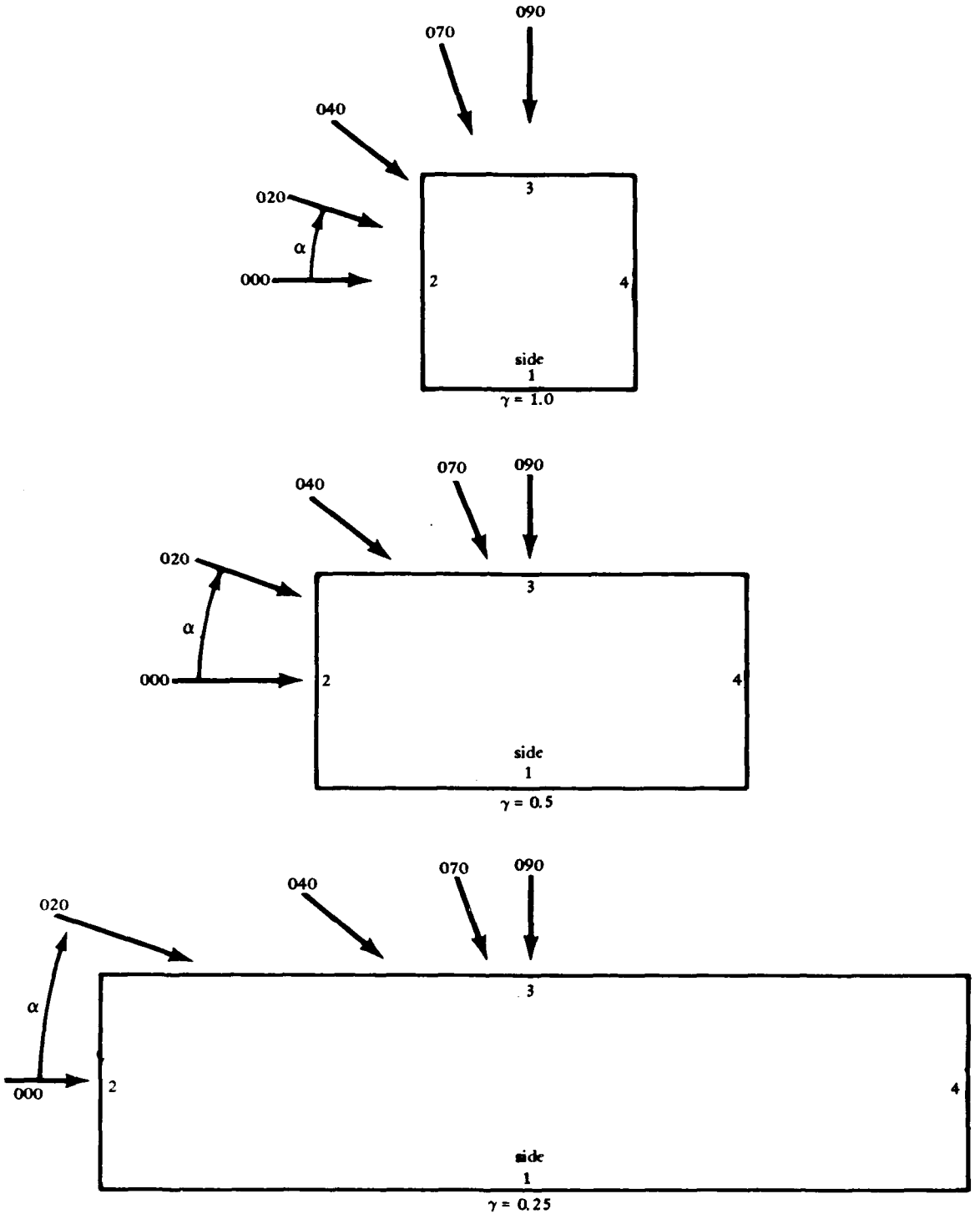

Figure C-3. **Averaged pressure coefficients based on a reference velocity measured at the roof, $\bar{C}_p$, for a side ration of 0.5.**

Graphs: Pressure coefficients for buildings three stories height or less with a single value reference speed, U_r, at building roof height, $\Delta\bar{C}_p = \bar{C}_{p3}$ ($\bar{C}_{p1} = 0$).

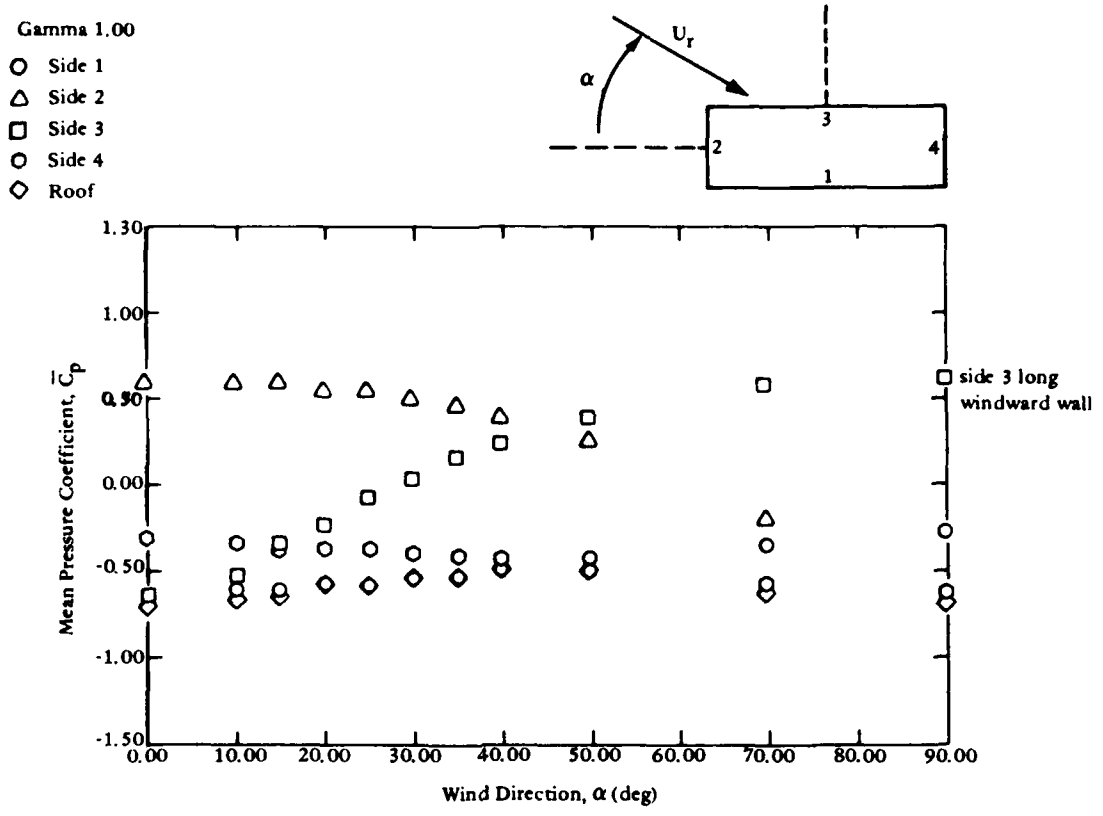

Figure C-4. **Averaged pressure coefficients based on a reference velocity measured at the roof, $\bar{C}_p$, for a side ratio of 0.25.**

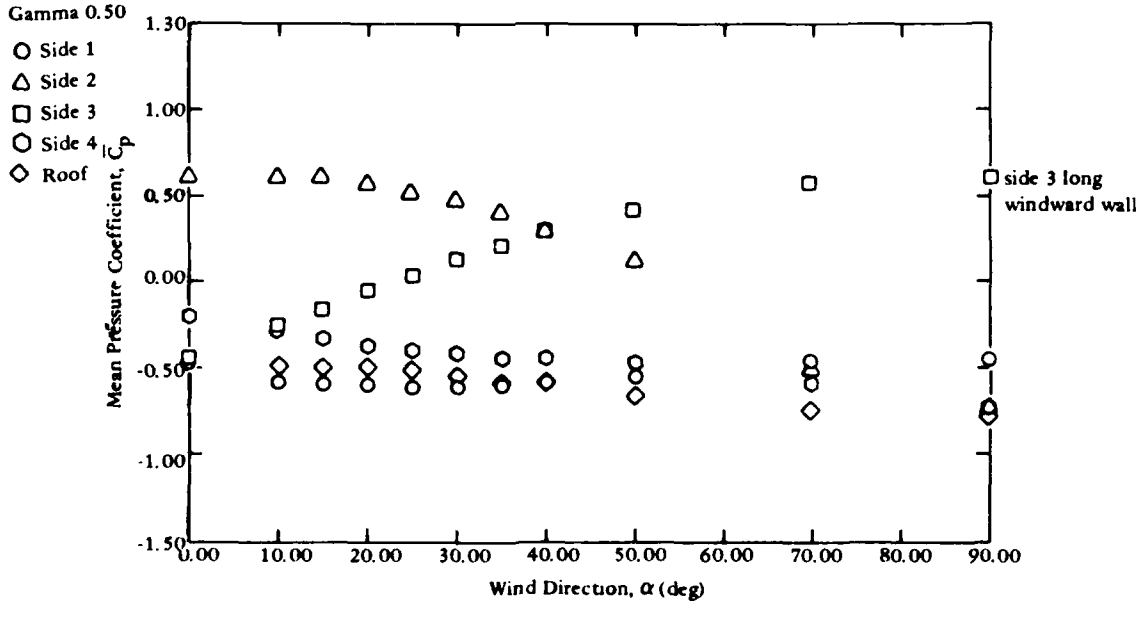

Figure C-5. **Averaged local pressure coefficients, $\bar{C}_p$, for a side ratio of 1.0.**

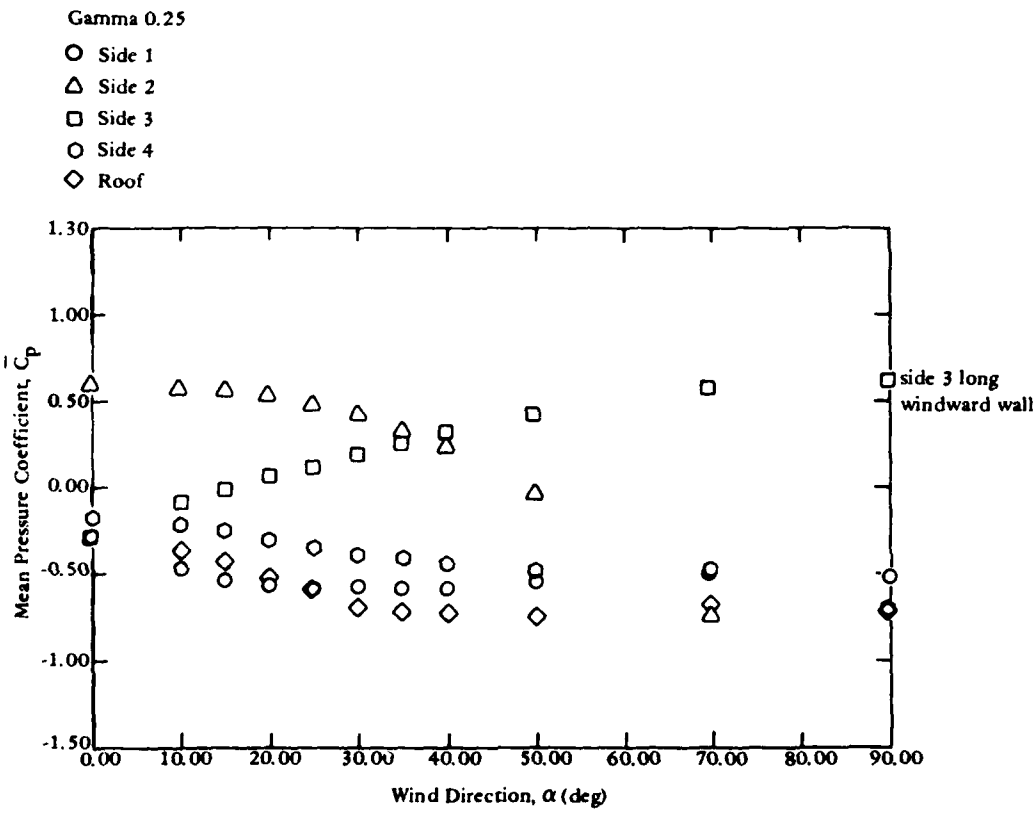

Figure C-6. **Averaged local pressure coefficients, $\bar{C}_p$, for a side ratio of 0.5.**

Graphs Pressure coefficients for tall buildings for multiple values of reference velocity, U_z. $\Delta\bar{C}_p = \bar{C}_{p_3}$.

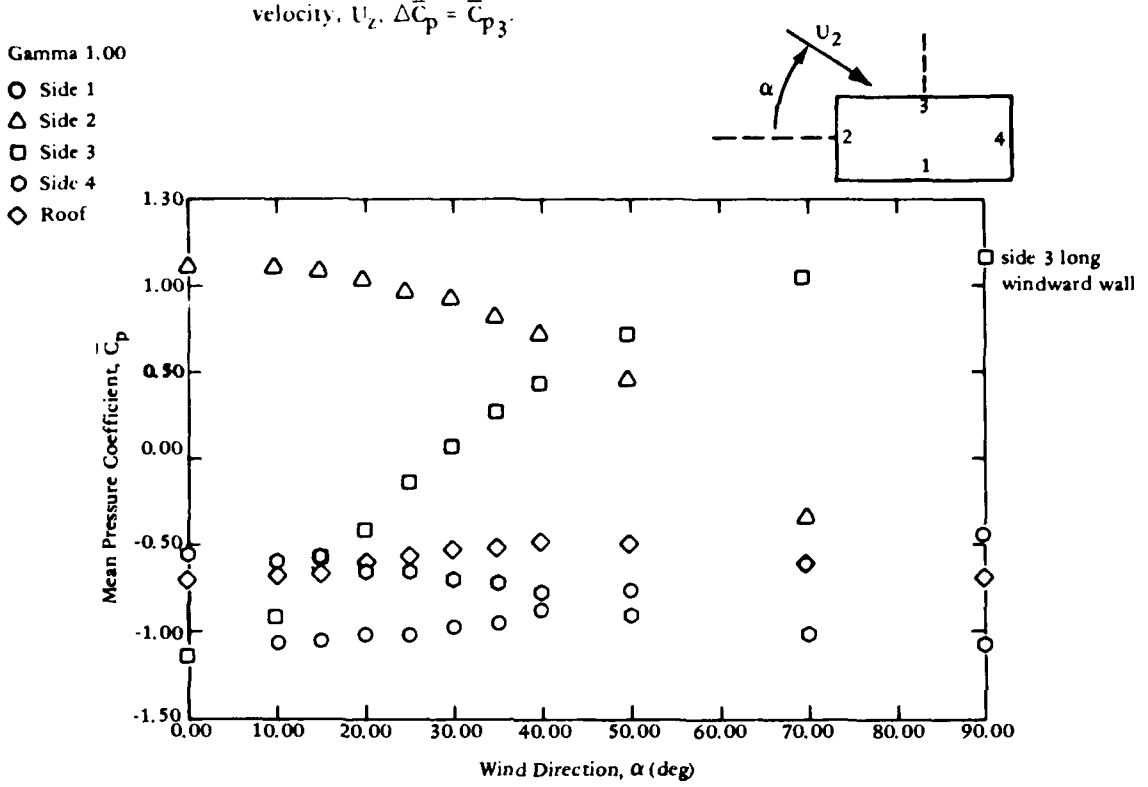

Figure C-7. **Averaged local pressure coefficients, $\bar{C}_p$, for a side ratio of 0.25.**

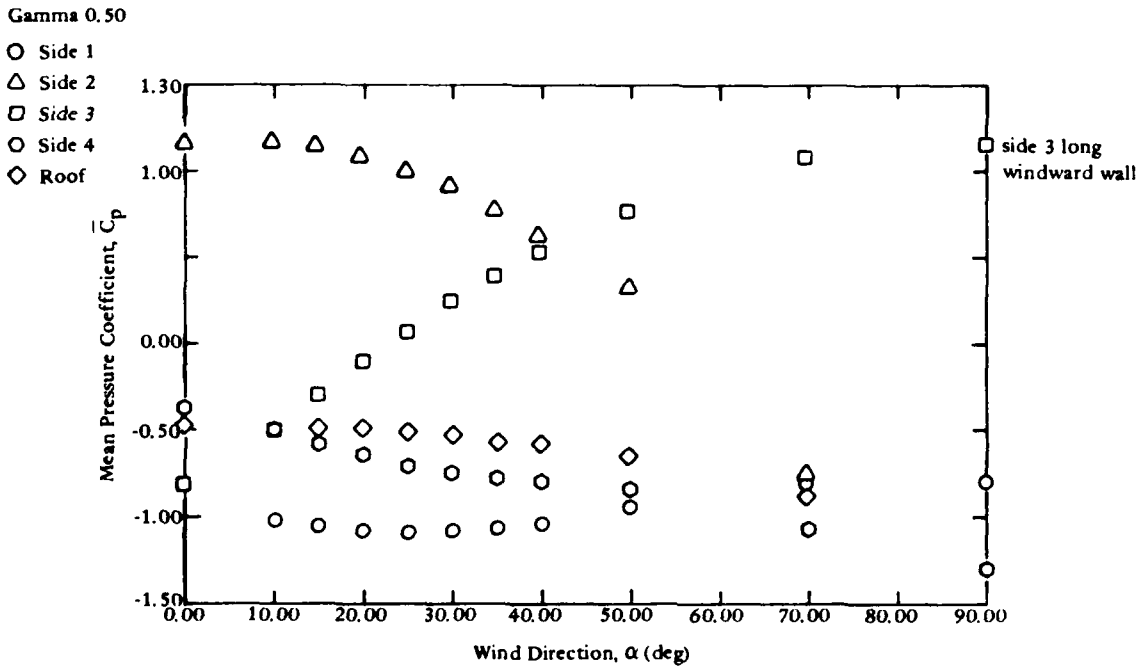

Figure C-8. **Solid model types used in mid-wall height pressure distribution studies.**

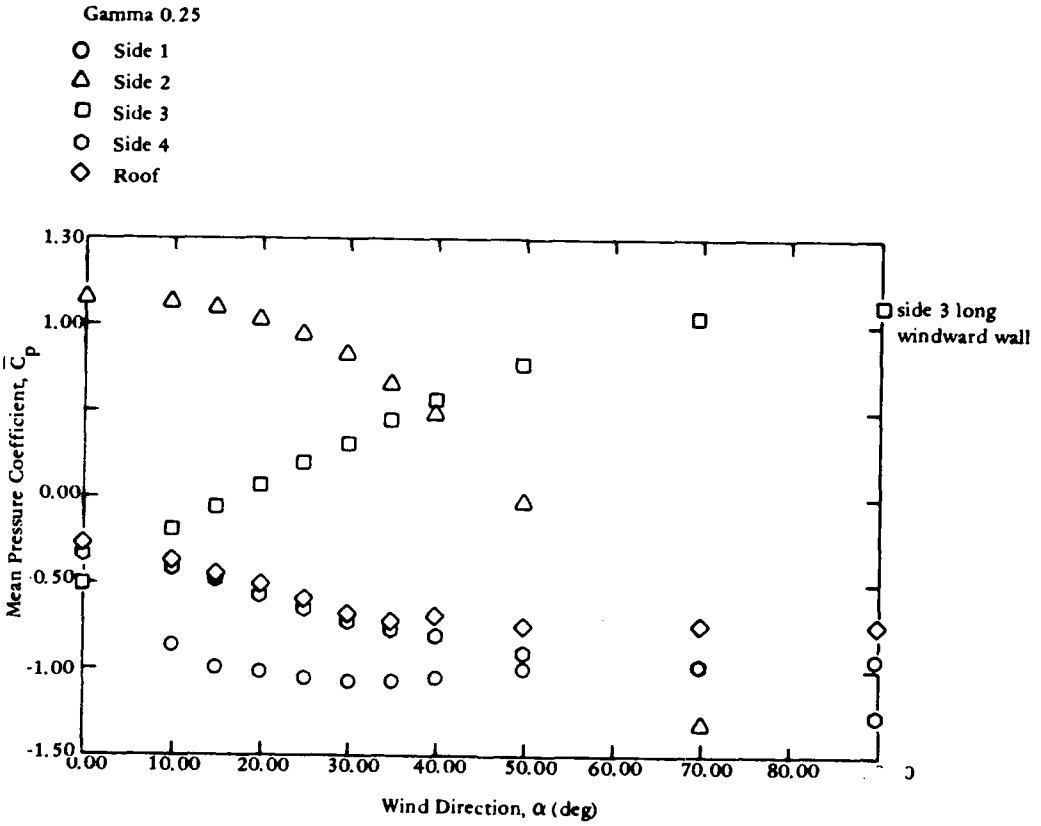

Figure C-9. **Coordinate system of building.**

DISTRIBUTION LIST

AFB 82ABG DEMC, Williams AZ; ABG DEE (F. Nethers), Goodfellow AFB TX; AF Tech Office (Mgt & Ops), Tyndall, FL; HQ MAC DEEE, Scott, IL; SAMSO MNND, Norton AFB CA; Samso Dec (Sauer) Vandenburg, CA; Stinfo Library, Offutt NE

AFESC DEB, Tyndall, FL

ARMY ARRADCOM, Dover, NJ; BMDSC-RE (H. McClellan) Huntsville AL; Contracts - Facs Engr Directorate, Fort Ord, CA; DAEN-CWE-M, Washington DC; DAEN-MPE-D Washington DC; DAEN-MPU, Washington DC; ERADCOM Tech Supp Dir. (DELSD-L) Ft. Monmouth, NJ; Natick R&D Command (Kwoh Hu) Natick MA; Tech. Ref. Div., Fort Huachuca, AZ

ARMY - CERL Library, Champaign IL

ARMY CORPS OF ENGINEERS MRD-Eng. Div., Omaha NE; Seattle Dist. Library, Seattle WA

ARMY CRREL G. Phetteplace Hanover, NH

ARMY ENGR DIST, Library, Portland OR

ARMY ENVIRON. HYGIENE AGCY HSE-EW Water Qual Eng Div Aberdeen Prov Grnd MD

ARMY MATERIALS & MECHANICS RESEARCH CENTER Dr. Lenoe, Watertown MA

ARMY MISSILE R&D CMD SCI Info Cen (DOC) Redstone Arsenal, AL

ARMY MTMC Trans Engr Agency MTT-CE, Newport News, VA

ADMINSUPU PWO, BAHRIAN

ASO PWD (ENS M W Davis), Phildadelphia, PA

BUREAU OF RECLAMATION Code 1512 (C. Selander) Denver CO

CINCLANT CIV ENGR SUPP PLANS OFFR NORFOLK, VA

COMNAVRESFOR Code 473, New Orleans, LA

CNM Code MAT-04, Washington, DC; Code MAT-08E, Washington, DC; NMAT - 044, Washington DC

CNO Code NOP-964, Washington DC; Code OP 987 Washington DC; Code OP-413 Wash, DC; Code OPNAV 09B24 (H); OP987J, Washington, DC

COMFLEACT, OKINAWA PWD - Engr Div, Sasebo, Japan; PWO, Kadena, Okinawa; PWO, Sasebo, Japan

COMNAVMARIANAS Code N4, Guam

COMOCEANSYSLANT PW-FAC MGMNT Off Norfolk, VA

COMOCEANSYSPAC SCE, Pearl Harbor HI

COMSUBDEVGRUONE Operations Offr, San Diego, CA

DEFFUELSUPPCEN DFSC-OWE (Term Engrng) Alexandria, VA; DFSC-OWE, Alexandria VA

DOE Div Ocean Energy Sys Cons Solar Energy Wash DC; INEL Tech. Lib. (Reports Section), Idaho Falls, ID

DTIC Defense Technical Info Ctr Alexandria, VA

DTNSRDC Code 4111 (R. Gierich), Bethesda MD

DTNSRDC Code 522 (Library), Annapolis MD

ENVIRONMENTAL PROTECTION AGENCY Reg. III Library, Philadelphia PA; Reg. VIII, 8M-ASL, Denver CO

FLTCOMBATTRACENLANT PWO, Virginia Bch VA

GIDEP OIC, Corona, CA

GSA Assist Comm Des & Cnst (FAIA) D R Dibner Washington, DC ; Off of Des & Const-PCDP (D Eakin) Washington, DC

HC & RS Tech Pres. Service, Meden, Washington, DC

LIBRARY OF CONGRESS Washington, DC (Sciences & Tech Div)

MARINE CORPS BASE Code 406, Camp Lejeune, NC; Maint Off Camp Pendleton, CA; PWD - Maint. Control Div. Camp Butler, Kawasaki, Japan; PWO Camp Lejeune NC; PWO, Camp Pendleton CA; PWO, Camp S. D. Butler, Kawasaki Japan

MARINE CORPS HQS Code LFF-2, Washington DC

MCAS Facil. Engr. Div. Cherry Point NC; CO, Kaneohe Bay HI; Code S4, Quantico VA; Facs Maint Dept - Operations Div, Cherry Point; PWD - Utilities Div, Iwakuni, Japan; PWO, Iwakuni, Japan; PWO, Yuma AZ

MCDEC NSAP REP, Quantico VA

MCLB B520, Barstow CA; Maintenance Officer, Barstow, CA; PWO, Barstow CA

MCRD SCE, San Diego CA

NAF PWD - Engr Div, Atsugi, Japan; PWO, Atsugi Japan

NALF OINC, San Diego, CA

NARF Code 100, Cherry Point, NC; Code 612, Jax, FL; Code 640, Pensacola FL; SCE Norfolk, VA

NAS CO, Guantanamo Bay Cuba; Code 114, Alameda CA; Code 183 (Fac. Plan BR MGR); Code 18700, Brunswick ME; Code 18U (ENS P.J. Hickey), Corpus Christi TX; Code 8F, Patuxent Riv., MD; Dir of Engrng, PWD, Corpus Christi, TX

NAVSURFWPNCEN R-15 (Dr. J. Ward) White Oak Lab Silver Spring MD

NAVAIRSYSCOM PWD Code 8P (Grover) Patuxent River, MD

NAS Lakehurst, NJ; Lead Chief Petty Offr PW Self Help Div, Beeville TX; PW (J. Maguire), Corpus Christi TX, PWD - Engr Div Dir, Millington, TN; PWD - Engr Div, Gtmo, Cuba; PWD - Engr Div, Oak Harbor, WA, PWD Maint Cont. Dir., Fallon NV, PWD Maint Div , New Orleans, Belle Chasse LA; PWD, Code

1821H (Pfankuch) Miramar, SD CA; PWD, Maintenance Control Dir., Bermuda; PWO Belle Chasse, LA; PWO Chase Field Beeville, TX; PWO Key West FL; PWO Lakehurst, NJ; PWO Sigonella Sicily; PWO Whiting Fld, Milton FL; PWO, Dallas TX; PWO, Glenview IL; PWO, Millington TN; PWO, Miramar, San Diego CA; SCE Norfolk, VA; SCE, Barbers Point HI; SCE, Cubi Point, R.P

NATL RESEARCH COUNCIL Naval Studies Board, Washington DC

NAVACT PWO, London UK

NAVAEROSPREGMEDCEN SCE, Pensacola FL

NAVAIRDEVCEN Chmielewski, Warminster, PA; PWD, Engr Div Mgr, Warminster, PA

NAVAIRPROPTESTCEN CO, Trenton, NJ

NAVCOASTSYSCEN CO, Panama City FL; Code 715 (J Quirk) Panama City, FL; Library Panama City, FL; PWO Panama City, FL

NAVCOMMAREAMSTRSTA PWO, Norfolk VA; SCE Unit 1 Naples Italy; SCE, Wahiawa HI

NAVCOMMSTA Code 401 Nea Makri, Greece; PWD - Maint Control Div, Diego Garcia Is.; PWO, Exmouth, Australia

NAVCONSTRACEN Curriculum Instr. Stds Offr, Gulfport MS

NAVEDTRAPRODEVCEN Technical Library, Pensacola, FL

NAVEDUTRACEN Engr Dept (Code 42) Newport, RI

NAVEODTECHCEN Code 604, Indian Head MD

NAVFAC PWO, Brawdy Wales UK; PWO, Centerville Bch, Ferndale CA; PWO, Point Sur, Big Sur CA

NAVFACENGCOM Alexandria, VA; Code 03 Alexandria, VA; Code 03T (Essoglou) Alexandria, VA; Code 04B3 Alexandria, VA; Code 051A Alexandria, VA; Code 09M54, Tech Lib, Alexandria, VA; Code 100, Alexandria, VA; Code 1113, Alexandria, VA; Code 082, Alexandria, VA

NAVFACENGCOM - CHES DIV, Code 403 Washington DC; FPO-1 Washington, DC; Library, Washington, D.C.

NAVFACENGCOM - LANT DIV, Code 111, Norfolk, VA; Code 403, Norfolk, VA; Eur. BR Deputy Dir, Naples Italy; Library, Norfolk, VA; Code 1112, Norfolk, VA

NAVFACENGCOM - NORTH DIV, Code 04 Philadelphia, PA; Code 04AL, Philadelphia PA; Code 09P Philadelphia PA; Code 111 Philadelphia, PA; ROICC, Contracts, Crane IN

NAVFACENGCOM - PAC DIV, (Kyi) Code 101, Pearl Harbor, HI; CODE 09P PEARL HARBOR HI; Code 402, RDT&E, Pearl Harbor HI; Library, Pearl Harbor, HI

NAVFACENGCOM - SOUTH DIV, Code 403, Gaddy, Charleston, SC; Code 1112, Charleston, SC; Library, Charleston, SC

NAVFACENGCOM - WEST DIV, AROICC, Contracts, Twentynine Palms CA; Code 04B San Bruno, CA; Library, San Bruno, CA; O9P 20 San Bruno, CA; RDT&E LO San Bruno, CA

NAVFACENGCOM CONTRACTS AROICC, NAVSTA Brooklyn, NY; AROICC, Quantico, VA; Contracts, AROICC, Lemoore CA; Dir, Eng. Div., Exmouth, Australia; Eng Div dir, Southwest Pac, Manila, PI; OICC, Southwest Pac, Manila, PI; OICC-ROICC, NAS Oceana, Virginia Beach, VA; OICC ROICC, Balboa Panama Canal; ROICC AF Guam; ROICC Code 495 Portsmouth VA; ROICC Key West FL; ROICC MCAS El Toro; ROICC, Keflavik, Iceland; ROICC, NAS, Corpus Christi, TX; ROICC, Pacific, San Bruno CA; ROICC-OICC-SPA, Norfolk, VA

NAVHOSP PWD - Engr Div, Beaufort, SC

NAVMAG PWD - Engr Div, Guam; SCE, Subic Bay, R.P.

NAVOCEANSYSCEN Code 4473B (Tech Lib) San Diego, CA; Code 523 (Hurley), San Diego, CA; Code 6700, San Diego, CA; Code 811 San Diego, CA

NAVORDMISTESTFAC PWD - Engr Dir, White Sands, NM

NAVORDSTA PWD - Dir, Engr Div, Indian Head, MD; PWO, Louisville KY

NAVPETOFF Code 30, Alexandria VA

NAVPETRES Director, Washington DC

NAVPHIBASE CO, ACB 2 Norfolk, VA; SCE Coronado, SD,CA

NAVREGMEDCEN PWD - Engr Div, Camp Lejeune, NC; PWO, Camp Lejeune, NC

NAVREGMEDCEN PWO, Okinawa, Japan

NAVREGMEDCEN SCE; SCE San Diego, CA; SCE, Camp Pendleton CA; SCE, Guam; SCE, Newport, RI; SCE, Oakland CA

NAVREGMEDCEN SCE, Yokosuka, Japan

NAVSCOLCECOFF C35 Port Hueneme, CA

NAVSCSOL PWO, Athens GA

NAVSEASYSCOM Code 0325, Program Mgr, Washington, DC; SEA 04E (L Kess) Washington, DC

NAVSECGRUACT PWO, Adak AK; PWO, Edzell Scotland; PWO, Puerto Rico; PWO, Torri Sta, Okinawa

NAVSECSTA PWD - Engr Div, Wash., DC

NAVSHIPYD Code 202.4, Long Beach CA; Code 202.5 (Library) Puget Sound, Bremerton WA; Code 380, Portsmouth, VA; Code 382.3, Pearl Harbor, HI; Code 400, Puget Sound; Code 440 Portsmouth NH; Code 440, Norfolk; Code 440, Puget Sound, Bremerton WA; Code 453 (Util. Supr), Vallejo CA; Library, Portsmouth NH; PW Dept, Long Beach, CA; PWD (Code 420) Dir Portsmouth, VA; PWD (Code 450-HD) Portsmouth, VA; PWD (Code 453-HD) SHPO 03, Portsmouth, VA; PWO, Bremerton, WA; PWO, Mare Is.; PWO, Puget Sound; SCE, Pearl Harbor HI

NAVSTA Adak, AK; CO, Brooklyn NY; Code 4, 12 Marine Corps Dist, Treasure Is., San Francisco CA; Dir Engr Div, PWD, Mayport FL; Dir Mech Engr 37WC93 Norfolk, VA; Engr. Dir., Rota Spain; Long Beach,

CA; Maint Cont Div , Guantanamo Bay Cuba; PWD - Engr Dept, Adak, AK; PWD - Engr Div, Midway Is ; PWO, Keflavik Iceland; PWO, Mayport FL; SCE, Guam, Marianas; SCE, Pearl Harbor HI; SCE, San Diego CA; SCE, Subic Bay, R.P.; Utilities Engr Off Rota Spain
NAVSUPPACT CO, Naples, Italy; PWO Naples Italy
NAVSUPPFAC PWD - Maint Control Div, Thurmont, MD
NAVSURFWPNCEN PWO, White Oak, Silver Spring, MD
NAVTECHTRACEN SCE, Pensacola FL
NAVTELCOMMCOM Code 53, Washington, DC
NAVWPNCEN Code 2636 China Lake, PWO (Code 266) China Lake, CA; ROICC (Code 702), China Lake CA
NAVWPNSTA (Clebak) Colts Neck, NJ; Code 092, Concord CA, Code 092A, Seal Beach, CA
NAVWPNSTA PW Office Yorktown, VA
NAVWPNSTA PWD - Maint Control Div., Concord, CA; PWD - Supr Gen Engr, Seal Beach, CA; PWO, Charleston, SC; PWO, Seal Beach CA
NAVWPNSUPPCEN Code 09 Crane IN
NCTC Const. Elec School, Port Hueneme, CA
NCBC Code 10 Davisville, RI; Code 15, Port Hueneme CA; Code 155, Port Hueneme CA; Code 156, Port Hueneme, CA; Code 25111 Port Hueneme, CA; Code 430 (PW Engrng) Gulfport, MS; Code 470.2, Gulfport, MS, Library, Davisville, RI; NEESA Code 252 (P Winters) Port Hueneme, CA; PWO (Code 80) Port Hueneme, CA; PWO, Davisville RI; PWO, Gulfport, MS; Technical Library, Gulfport, MS
NMCB FIVE, Operations Dept; THREE, Operations Off.
NOAA (Mr. Joseph Vadus) Rockville, MD; Library Rockville, MD
NRL Code 5800 Washington, DC
NSC Code 54.1 Norfolk, VA
NSD SCE, Subic Bay, R.P.
NSWSES Code 0150 Port Hueneme, CA
NUSC DET Code 5202 (S. Schady) New London, CT; Code EA123 (R.S. Munn), New London CT; Code SB 331 (Brown), Newport RI
OFFICE SECRETARY OF DEFENSE OASD (MRA&L) Dir. of Energy, Pentagon, Washington, DC
ONR Code 221, Arlington VA; Code 700F Arlington VA
PACMISRANFAC HI Area Bkg Sands, PWO Kekaha, Kauai, HI
PHIBCB 1 P&E, San Diego, CA
PWC ACE Office Norfolk, VA; CO, (Code 10), Oakland, CA; Code 10, Great Lakes, IL; Code 105 Oakland, CA; Code 110, Great Lakes, IL; Code 110, Oakland, CA; Code 121.1, Oakland, CA; Code 154 (Library), Great Lakes, IL; Code 200, Great Lakes IL; Code 400, Great Lakes, IL; Code 400, Pearl Harbor, HI; Code 400, San Diego, CA; Code 420, Great Lakes, IL; Code 420, Oakland, CA; Code 424, Norfolk, VA; Code 500 Norfolk, VA; Code 505A Oakland, CA; Code 600, Great Lakes, IL; Code 610, San Diego Ca; Code 700, Great Lakes, IL; Library, Code 120C, San Diego, CA; Library, Guam; Library, Norfolk, VA; Library, Pearl Harbor, HI; Library, Pensacola, FL; Library, Subic Bay, R.P.; Library, Yokosuka JA; Util Dept (R Pascua) Pearl Harbor, HI; Utilities Officer, Guam
SPCC PWO (Code 120) Mechanicsburg PA
TVA Smelser, Knoxville, Tenn.; Solar Group, Arnold, Knoxville, TN
U.S. MERCHANT MARINE ACADEMY Kings Point, NY (Reprint Custodian)
USAF REGIONAL HOSPITAL Fairchild AFB, WA
USCG G-MMT-4/82 (J Spencer); Library Hqs Washington, DC
USCG R&D CENTER Library New London, CT
USDA Forest Service Reg 3 (R. Brown) Albuquerque, NM
USNA Ch. Mech. Engr. Dept Annapolis MD; ENGRNG Div, PWD, Annapolis MD; Energy-Environ Study Grp, Annapolis, MD; Mech. Engr. Dept. (C. Wu), Annapolis MD
USS FULTON WPNS Rep. Offr (W-3) New York, NY
ARIZONA Kroelinger Tempe, AZ; State Energy Programs Off., Phoenix AZ
AUBURN UNIV. Bldg Sci Dept, Lechner, Auburn, AL
BERKELEY PW Engr Div, Harrison, Berkeley, CA
BONNEVILLE POWER ADMIN Portland OR (Energy Consrv. Off., D. Davey)
BROOKHAVEN NATL LAB M. Steinberg, Upton NY
CALIFORNIA STATE UNIVERSITY LONG BEACH, CA (CHELAPATI)
CONNECTICUT Office of Policy & Mgt, Energy, Div, Hartford, CT
CORNELL UNIVERSITY Ithaca NY (Serials Dept, Engr Lib.)
DAMES & MOORE LIBRARY LOS ANGELES, CA
DRURY COLLEGE Physics Dept, Springfield, MO
FLORIDA ATLANTIC UNIVERSITY Boca Raton, FL (McAllister)
FOREST INST FOR OCEAN & MOUNTAIN Carson City NV (Studies - Library)
GEORGIA INSTITUTE OF TECHNOLOGY (LT R. Johnson) Atlanta, GA; Col. Arch, Benton, Atlanta, GA
HARVARD UNIV. Dept. of Architecture, Dr. Kim, Cambridge, MA
HAWAII STATE DEPT OF PLAN. & ECON DEV. Honolulu HI (Tech Info Ctr)
IOWA STATE UNIVERSITY Dept. Arch, McKrown, Ames, IA
WOODS HOLE OCEANOGRAPHIC INST. Woods Hole MA (Winget)
KEENE STATE COLLEGE Keene NH (Cunningham)

LEHIGH UNIVERSITY Bethlehem PA (Linderman Lib. No.30, Fleecksteiner)
LOUISIANA DIV NATURAL RESOURCES & ENERGY Div OF R&D, Baton Rouge, LA
MAINE OFFICE OF ENERGY RESOURCES Augusta, ME
MISSOURI ENERGY AGENCY Jefferson City MO
MIT Cambridge MA (Rm 10-500, Tech Reports, Engr. Lib.); Cambridge, MA (Harleman)
MONTANA ENERGY OFFICE Anderson, Helena, MT
NATURAL ENERGY LAB Library, Honolulu, HI
NEW HAMPSHIRE Concord NH (Governor's Council on Energy)
NEW MEXICO SOLAR ENERGY INST. Dr. Zwibel Las Cruces NM
NY CITY COMMUNITY COLLEGE BROOKLYN, NY (LIBRARY)
NYS ENERGY OFFICE Library, Albany NY
OAK RIDGE NATL LAB T. Lundy, Oak Ridge, TN
PURDUE UNIVERSITY Lafayette, IN (CE Engr. Lib)
SCRIPPS INSTITUTE OF OCEANOGRAPHY LA JOLLA, CA (ADAMS)
SEATTLE U Prof Schwaegler Seattle WA
SRI INTL Phillips, Chem Engr Lab, Menlo Park, CA
STATE UNIV OF NEW YORK Fort Schuyler, NY (Longobardi)
STATE UNIV OF NY AT BUFFALO School of Medicine, Buffalo, NY
TEXAS A&M UNIVERSITY J.M. Niedzwecki, College Station, TX; W.B. Ledbetter College Station, TX
UNIVERSITY OF CALIFORNIA Energy Engineer, Davis CA; LIVERMORE, CA (LAWRENCE LIVERMORE LAB, TOKARZ); UCSF, Physical Plant, San Francisco, CA
UNIVERSITY OF DELAWARE Newark, DE (Dept of Civil Engineering, Chesson)
UNIVERSITY OF FLORIDA Dept Arch., Morgan, Gainesville, FL
UNIVERSITY OF HAWAII HONOLULU, HI (SCIENCE AND TECH. DIV.)
UNIVERSITY OF ILLINOIS (Hall) Urbana, IL; URBANA, IL (LIBRARY)
UNIVERSITY OF MASSACHUSETTS (Heronemus), ME Dept, Amherst, MA
UNIVERSITY OF NEBRASKA-LINCOLN Lincoln, NE (Ross Ice Shelf Proj.)
UNIVERSITY OF NEW HAMPSHIRE Elec. Engr. Depot, Dr. Murdoch, Durham, N.H.
UNIVERSITY OF TEXAS Inst. Marine Sci (Library), Port Arkansas TX
UNIVERSITY OF TEXAS AT AUSTIN AUSTIN, TX (THOMPSON)
UNIVERSITY OF WASHINGTON Seattle WA (E. Linger)
UNIVERSITY OF WISCONSIN Milwaukee WI (Ctr of Great Lakes Studies)
ARVID GRANT OLYMPIA, WA
ATLANTIC RICHFIELD CO. DALLAS, TX (SMITH)
BECHTEL CORP. SAN FRANCISCO, CA (PHELPS)
BROWN & ROOT Houston TX (D. Ward)
CHEMED CORP Lake Zurich IL (Dearborn Chem. Div.Lib.)
COLUMBIA GULF TRANSMISSION CO. HOUSTON, TX (ENG. LIB.)
DESIGN SERVICES Beck, Ventura, CA
DIXIE DIVING CENTER Decatur, GA
DURLACH, O'NEAL, JENKINS & ASSOC. Columbia SC
GARD INC. Dr. L. Holmes, Niles, IL
LITHONIA LIGHTING Application eng. Dept. (B. Helton), Conyers, GA 30207
MCDONNELL AIRCRAFT CO. (Goff) Sr Engr. Engrng Dept, St. Louis, MO
MEDERMOTT & CO. Diving Division, Harvey, LA
NEWPORT NEWS SHIPBLDG & DRYDOCK CO. Newport News VA (Tech. Lib.)
PACIFIC MARINE TECHNOLOGY (M. Wagner) Duvall, WA
PG&E Library, San Francisco, CA
PORTLAND CEMENT ASSOC. Skokie IL (Rsch & Dev Lab. Lib.)
RAYMOND INTERNATIONAL INC. F. Colle Soil Tech Dept, Pennsauken, NJ
SANDIA LABORATORIES Albuquerque, NM (Vortman); Library Div., Livermore CA
SCHUPACK ASSOC SO. NORWALK, CT (SCHUPACK)
SHELL DEVELOPMENT CO. Houston TX (C. Sellars Jr.)
TEXTRON INC. BUFFALO, NY (RESEARCH CENTER LIB.)
TRW SYSTEMS REDONDO BEACH, CA (DAI)
UNITED TECHNOLOGIES Windsor Locks CT (Hamilton Std Div., Library)
WARD, WOLSTENHOLD ARCHITECTS Sacramento, CA
WESTINGHOUSE ELECTRIC CORP. Annapolis MD (Oceanic Div. Lib. Bryan); Library, Pittsburgh PA
WM CLAPP LABS - BATTELLE DUXBURY, MA (LIBRARY)
FISHER San Diego, Ca
KEITON, BOB Ft Worth, TX
KRUZIC, T.P. Silver Spring, MD
T.W. MERMEL Washington DC
WALTZ Livermore, CA

PLEASE HELP US PUT THE ZIP IN YOUR MAIL! ADD YOUR FOUR NEW ZIP DIGITS TO YOUR LABEL (OR FACSIMILE), STAPLE INSIDE THIS SELF-MAILER, AND RETURN TO US.

(fold here)

DEPARTMENT OF THE NAVY

NAVAL CIVIL ENGINEERING LABORATORY
PORT HUENEME, CALIFORNIA 93043-5003

OFFICIAL BUSINESS
PENALTY FOR PRIVATE USE, $300
1 IND-NCEL 2700/4 (REV 12-79)
0930-LL-L70-0044

POSTAGE AND FEES PAID
DEPARTMENT OF THE NAVY
DOD-316

U.S.MAIL

Commanding Officer
Code L14
Naval Civil Engineering Laboratory
Port Hueneme, California 93043-5003

INSTRUCTIONS

The Naval Civil Engineering Laboratory has revised its primary distribution lists. The bottom of the mailing label has several numbers listed. These numbers correspond to numbers assigned to the list of Subject Categories. Numbers on the label corresponding to those on the list indicate the subject category and type of documents you are presently receiving. If you are satisfied, throw this card away (or file it for later reference).

If you want to change what you are presently receiving:

- Delete - mark off number on bottom of label.
- Add - circle number on list.
- Remove my name from all your lists – check box on list.
- Change my address – line out incorrect line and write in correction (ATTACH MAILING LABEL).
- Number of copies should be entered after the title of the subject categories you select.

Fold on line below and drop in the mail.

Note: Numbers on label but not listed on questionnaire are for NCEL use only, please ignore them.

Fold on line and staple.

DEPARTMENT OF THE NAVY

NAVAL CIVIL ENGINEERING LABORATORY
PORT HUENEME, CALIFORNIA 93043

OFFICIAL BUSINESS
PENALTY FOR PRIVATE USE, $300
1 IND-NCEL-2700/4 (REV. 12-73)
0930-LL-L70-0044

POSTAGE AND FEES PAID
DEPARTMENT OF THE NAVY
DOD-316

Commanding Officer
Code L14
Naval Civil Engineering Laboratory
Port Hueneme, California 93043

DISTRIBUTION QUESTIONNAIRE

The Naval Civil Engineering Laboratory is revising its primary distribution lists.

SUBJECT CATEGORIES

1 **SHORE FACILITIES**
2 Construction methods and materials (including corrosion control, coatings)
3 Waterfront structures (maintenance/deterioration control)
4 Utilities (including power conditioning)
5 Explosives safety
6 Construction equipment and machinery
7 Fire prevention and control
8 Antenna technology
9 Structural analysis and design (including numerical and computer techniques)
10 Protective construction (including hardened shelters, shock and vibration studies)
11 Soil/rock mechanics
13 BEQ
14 Airfields and pavements
15 ADVANCED BASE AND AMPHIBIOUS FACILITIES
16 Base facilities (including shelters, power generation, water supplies)
17 Expedient roads/airfields/bridges
18 Amphibious operations (including breakwaters, wave forces)
19 Over-the-Beach operations (including containerization, materiel transfer, lighterage and cranes)
20 POL storage, transfer and distribution
24 POLAR ENGINEERING
24 Same as Advanced Base and Amphibious Facilities, except limited to cold-region environments
28 ENERGY/POWER GENERATION
29 Thermal conservation (thermal engineering of buildings, HVAC systems, energy loss measurement, power generation)
30 Controls and electrical conservation (electrical systems, energy monitoring and control systems)
31 Fuel flexibility (liquid fuels, coal utilization, energy from solid waste)
32 Alternate energy source (geothermal power, photovoltaic power systems, solar systems, wind systems, energy storage systems)
33 Site data and systems integration (energy resource data, energy consumption data, integrating energy systems)
34 ENVIRONMENTAL PROTECTION
35 Solid waste management
36 Hazardous/toxic materials management
37 Wastewater management and sanitary engineering
38 Oil pollution removal and recovery
39 Air pollution
40 Noise abatement
44 OCEAN ENGINEERING
45 Seafloor soils and foundations
46 Seafloor construction systems and operations (including diver and manipulator tools)
47 Undersea structures and materials
48 Anchors and moorings
49 Undersea power systems, electromechanical cables, and connectors
50 Pressure vessel facilities
51 Physical environment (including site surveying)
52 Ocean-based concrete structures
53 Hyperbaric chambers
54 Undersea cable dynamics

TYPES OF DOCUMENTS

85 Techdata Sheets
86 Technical Reports and Technical Notes
82 NCEL Guide & Updates
( ) None – remove my name
83 Table of Contents & Index to TDS
91 Physical Security

END

FILMED

7-85

DTIC